ISTANBUL TECHNICAL UNIVERSITY ★ GRADUATE SCHOOL OF SCIENCE ENGINEERING AND TECHNOLOGY

MODEL BASED OPTIMAL LONGITUDINAL VEHICLE CONTROL

Ph.D. THESIS

Murat ÖTKÜR

Mechanical Engineering Department

Mechanical Engineering Program

SEPTEMBER 2016

ISTANBUL TECHNICAL UNIVERSITY ★ GRADUATE SCHOOL OF SCIENCE ENGINEERING AND TECHNOLOGY

MODEL BASED OPTIMAL LONGITUDINAL VEHICLE CONTROL

Ph.D. THESIS

Murat ÖTKÜR
(503072032)

Mechanical Engineering Department

Mechanical Engineering Program

Thesis Advisor: Prof. Dr. Murat EREKE
Thesis Co-Advisor: Dr. Orhan ATABAY

SEPTEMBER 2016

İSTANBUL TEKNİK ÜNİVERSİTESİ ★ FEN BİLİMLERİ ENSTİTÜSÜ

MODEL BAZLI OPTİMAL DOĞRUSAL ARAÇ KONTROLÜ

DOKTORA TEZİ

Murat ÖTKÜR
(503072032)

Makina Mühendisliği Anabilim Dalı

Makina Mühendisliği Programı

Tez Danışmanı: Prof. Dr. Murat EREKE
Eş Danışman: Öğr. Göv. Dr. Orhan ATABAY

EYLÜL 2016

Murat Ötkür, a Ph.D. student of İTU Graduate School of Science Engineering and Technology student ID 503072032, successfully defended the thesis/dissertation entitled "MODEL BASED OPTIMAL LONGITUDINAL VEHICLE CONTROL", which he prepared after fulfilling the requirements specified in the associated legislations, before the jury whose signatures are below.

Thesis Advisor : **Prof. Dr. Murat EREKE** ....
İstanbul Technical University

Co-advisor : **Dr. Orhan ATABAY** ....
İstanbul Technical University

Jury Members : **Prof. Dr. İ. Ahmet GÜNEY** ....
İstanbul Technical University

Assoc. Prof. Dr. Özgen AKALIN ....
İstanbul Technical University

Prof. Dr. İrfan YAVAŞLIOL ....
Yıldız Technical University

Prof. Dr. Muammer ÖZKAN ....
Yıldız Technical University

Assoc. Prof. Dr. Tarkan SANDALCI ....
Yıldız Technical University

Date of Submission : 30 May 2016
Date of Defense : 23 September 2016

To my family, wife and daughter…

FOREWORD

This thesis is based on my research on longitudinal vehicle control at İstanbul Technical University vehicle technology laboratory together with Ford Otosan Calibration & Control department between 2008 and 2016. Finalization of my thesis study took more than 8 years and had great contribution my academic and professional carrier.

First of all, I would like to express my gratitude to my advisor, Dr. Orhan Atabay, for providing me outstanding support during the whole thesis period. I really appreciated the close collaboration, and the positive working environment resulting from his trust. I am very grateful to him for his patience, help and valuable contribution to find my own way to the success of this thesis study.

I would also like to my profound respect and gratitude to Prof. Dr. Murat Ereke for the great opportunity to complete this thesis study in his experienced guidance.

I would like to acknowledge Ford Otosan for the facility and resource supply throughout the whole study. I am grateful to Ozan Ayhan, Canan Karadeniz (my supervisors while I am at calibration engineer position) and Alper Bozkurt (my manager while I am calibration supervisor) for their patience during the evolution of the study.

I would like to thank to a very special old friend and colleague Ziya Caba with whom I have walked through the Ph.D. route together. I express my sincere gratitude for his friendship and support throughout the whole thesis period. He had completed his thesis study already and hopefully I will join himself within the upcoming mounts.

I want to thank to TUBITAK for the doctoral grant throughout this study (BIDEB Support 2221).

This thesis owes its existence to the help, support, inspiration and love of my family. I would like to thank my mother, father and sister for their support during my whole education and academic period.

Finally I would like thank the most extraordinary person in my life deserving most of the acknowledgements: my dear wife Kübra Ötkür. Without her support and understanding I would never be eligible to finalize this dissertation. In 2015 she had given me the most important present of my life, my daughter Nazlı and hopefully after finalizing the thesis study I would give all my love and time to compensate the long study durations during which I lost the opportunity to live with them. Once again Kübra, thank you for your endless love and understanding.

September 2016

Murat ÖTKÜR
(Mechanical Engineer, M.Sc.)

TABLE OF CONTENTS

Page

FOREWORD ix
TABLE OF CONTENTS xi
ABBREVIATIONS xiii
LIST OF SYMBOLS AND INDICES xv
LIST OF TABLES xvii
LIST OF FIGURES xix
SUMMARY xxv
ÖZET xxix
1. INTRODUCTION 1
  1.1 Motivation 1
  1.2 Objectives 3
  1.3 Scope 4
  1.4 Contributions 4
  1.5 Structure of the Thesis 5
2. LITERATURE REVIEW 7
  2.1 Powertrain Modelling 9
    2.1.1 Powertrain models without backlash 10
    2.1.2 Powertrain models with backlash 14
      2.1.2.1 Backlash modelling 14
      2.1.2.2 Available powertrain models with backlash 16
    2.1.3 Powertrain modelling with multi-body dynamics and hardware in the loop simulations. 18
  2.2 Engine Brake Torque Estimation 18
  2.3 Driveability Improvement via Engine Torque Control 21
  2.4 Conclusion 25
3. ENGINE TORQUE CONTROL 27
  3.1 Engine Torque Management Control Structures 28
  3.2 Engine Torque Production Control Structures 30
  3.3 Proposed Torque Management Control Module 31
  3.4 Conclusion 34
4. IN CYLINDER PRESSURE BASED ENGINE BRAKE TORQUE MODEL 35
  4.1 Brake Torque Estimation Model 37
  4.2 Indicated Mean Effective Torque Calculation 40
  4.3 In Cylinder Pressure Measurement 43
  4.4 Results and Conclusion 43
    4.4.1 Steady state results 43
    4.4.2 Transient Results 49
  4.5 Conclusion 50
5. DRIVELINE MODELLING 51

5.1 4 Mass Vehicle Model........52
5.2 2 Mass Vehicle Model........55
5.3 3 Mass Vehicle Model........59
5.4 4 Mass Vehicle Model Results........61
5.5 Conclusion........65
6. CONTROLLER DEVELOPMENT FOR DRIVEABILITY........67
6.1 Driveline Control Strategies........67
6.1.1 PID Control........67
6.1.2 H-Infinity Control........68
6.1.3 LQR Control........69
6.2 Model Predictive Control........71
6.3 MPC Parameter Study........79
6.3.1 2 mass vehicle model MPC tuning for 3rd gear........79
6.3.2 2 mass vehicle model MPC tuning for 4th gear........88
6.4 2 Mass Vehicle Model Based Controller Results........95
6.5 3 Mass Vehicle Model Based Controller Results........101
6.6 Conclusion........106
7. CONCLUSION AND RECOMMEDATIONS........107
REFERENCES........111
APPENDICES........115
CURRICULUM VITAE........131

ABBREVIATIONS

ATDC : After Top Dead Centre
BMEP : Break Mean Effective Pressure
BTDC : Before Top Dead Centre
CAE : Computer Aided Engineering
CH : Control Horizon
CVT : Continuously Variable Transmission
DOF : Degree of Freedom
ECU : Engine Control Unit
EGR : Exhaust Gas Recirculation
EGT : Exhaust Gas Temperature
ESP : Electronic Stability Program
FEAD : Front End Accessory Drives
FRG : Final Reduction Gear
FTP : Federal Test Procedure
FWD : Front Wheel Drive
GPOPS : Gauss Pseudo spectral Optimization Software
HGV : Heavy Goods Vehicle
HIL : Hardware in the Loop
HRR : Heat Release Rate
$\mathbf{H}_\infty$: H Infinity
IMEP : Indicated mean Effective Pressure
ICE : Internal Combustion Engine
LTC : Load Transient Correction
LTI : Linear Time Invariant
LQ : Linear Quadratic
LQG : Linear Quadratic Gaussian
LQR : Linear Quadratic Regulator
MAF : Mass Air Flow
MBF50 : Mass Burned Fuel %50
MPC : Model-based Predictive Control
NARX : Nonlinear Auto Regressive with Exogenous
NEDC : New European Driving Cycle
NVH : Noise Vibration Harshness
OBD : On Board Diagnostics
OEM : Original Equipment Manufacturer
PCM : Powertrain Control Module
P : Proportional
PD : Proportional and Derivative
PH : Prediction Horizon
PI : Proportional and Integral
PID : Proportional, Integral and Derivative
PMAX : Maximum in Cylinder Pressure

RWD **:** Rear Wheel Drive
R2S **:** Regulated Two Stage
SAE **:** Society of Automotive Engineers
SPGS : Single Port Gauge Pressure Sensor
TCS **:** Traction Control System
TMAP **:** Manifold Air Pressure and Temperature
TDC **:** Top Dead Centre
Tip-in **:** Press Acceleration Pedal
Tip-out **:** Release Acceleration Pedal
VGT **:** Variable Geometry Turbocharger
WOT **:** Wide Open Throttle
ZV **:** Zero Vibration

SYMBOLS

$\boldsymbol{brTQ}$: Engine brake torque
$\boldsymbol{inTQ}$: Engine indicated torque
$\boldsymbol{J}$: Moment of inertia [kgm^2]
$\boldsymbol{T}$: Torque [Nm]
$\boldsymbol{k}$: Torsional spring coefficient [Nm/rad]
$\boldsymbol{B}$: Torsional damper coefficient [Nm.s/rad]
$\boldsymbol{C_D}$: Drag coefficient [-]
$\boldsymbol{F}$: Force [Nm]
$\boldsymbol{f}$: Fraction of heat added [-]
$\boldsymbol{f_r}$: Rolling coefficient [-]
$\boldsymbol{r}$: Radius [m]
$\boldsymbol{g}$: Gravity [m/s^2]
$\boldsymbol{I}$: Gear ratio [-]
$\boldsymbol{m}$: Mass [kg]
$\boldsymbol{v}$: Velocity [m/s^2]
$\boldsymbol{\theta}$: Crank angle
$\boldsymbol{\theta_0}$: Angle of the start of the heat addition
$\Delta\boldsymbol{\theta}$: Duration of the heat addition (length of burn)
a : Wiebe function coefficient 1
n : Wiebe function coefficient 2
$\boldsymbol{\theta}$: Angular position [rad]
$\boldsymbol{\dot{\theta}}$: Angular velocity [rad/s]
$\boldsymbol{\ddot{\theta}}$: Angular acceleration [rad/s^2]
$\boldsymbol{\rho}$: Density [kg/m^3]
$\boldsymbol{\alpha}$: Road gradient [rad]
$\boldsymbol{\sigma}$: Pacejka tyre model coefficient [Nm/% slip]

LIST OF TABLES

Table 4.1: ECU parameters and variable names used for in cylinder pressure calculation……………….……………………………………..........**38**
Table 4.2 : Simulation parameters for different injection patterns…...……………45
Table 5.1 : Engine and vehicle properties……..…………………………………...**62**
Table 6.1 : Summary of MPC and P controller gain parameters…………..………**90**
Table B.1 : Test Vehicle Specifications……………………………………...**117**
Table C.1 : Driveline model parameters……………………………………..**118**
Table D.1 : Summary of MPC and P controller gain parameters for 3rd gear 3 mass model……………………………………………………..............**119**
Table D.2 : Summary of MPC and P controller gain parameters for 4th gear 3 mass model…..………………………………………………………**119**

LIST OF FIGURES

Figure 2.1 : Vehicle response for a tip-in & tip-out response showing error states; Top sub-figure: Engine brake torque request, Mid sub-figure: Engine speed measurement, Bottom sub-figure: Vehicle longitudinal acceleration measurement. **8**
Figure 2.2 : Relationship of overshoot and rise rate characteristics to subjective ratings for tip-in manoeuvres [4]. **9**
Figure 2.3 : Schematics of vehicle powertrain with an internal combustion engine [5]. **10**
Figure 2.4 : Schematics of a shaft with backlash [8]. **15**
Figure 2.5 : Simplified model of the powertrain with transfer function representation [16]. **17**
Figure 3.1: Engine control module overview within a torque based strategy **28**
Figure 3.2: Load transient correction (LTC) algorithm working principle for tip-in (upper subfigure) and tip-out (lower subfigure) manoeuvres. **30**
Figure 3.3: Proposed torque demand control algorithm with model based control .. **33**
Figure 4.1: In cylinder pressure measurement equipment (Left: AVL Indimicro module, Right: AVL cylinder pressure sensor) [42]. **36**
Figure 4.2: Indicom software in cylinder pressure measurement screen. **36**
Figure 4.3: Airpath model schematics of 2.0 litre diesel bi-turbo engine. **37**
Figure 4.4: General schematic of engine gas air flow system. **38**
Figure 4.5: Volumetric efficiency map used in ECU for 2 lt diesel turbocharger engine. **39**
Figure 4.6: Sample Indicator diagram. **41**
Figure 4.7: Piston Schematics. **41**
Figure 4.8: In cylinder pressure data with 0.5 degree crank angle resolution (upper sub-figure: w.r.t. 720 degree crank angle, lower sub-figure: w.r.t. 42 degree crank angle) **44**
Figure 4.9: Engine mapping points. **45**
Figure 4.10: In cylinder pressure measurement and estimation for 2250 rpm, 240 Nm brake torque point. **46**
Figure 4.11: In cylinder pressure measurement and estimation for 2250 rpm, 240 Nm brake torque point (Zoomed view on injection region). **46**
Figure 4.12: In cylinder pressure measurement and estimation for 2150 rpm, 160 Nm brake torque point. **47**
Figure 4.13: In cylinder pressure measurement and estimation for 3500 rpm, full load torque (392 Nm) point. **48**
Figure 4.14: Indicated torque estimation error. **48**
Figure 4.15: Indicated torque estimation error. **49**
Figure 4.16: Indicated torque estimation error. **50**
Figure 5.1: Components of vehicle driveline for a FWD vehicle. **51**
Figure 5.2: Free body diagram of 4 mass vehicle model with 4 inertias connected by 2 spring damper elements and tyre. **52**

Figure 5.3: MATLAB/Simulink model block of inertial element $J1$ (the total inertia of engine, flywheel and clutch primary side block). **54**
Figure 5.4: MATLAB/Simulink clutch spring & damper simulation block. **55**
Figure 5.5: 4 Mass vehicle MATLAB/Simulink model. **56**
Figure 5.6: Free body diagram of simplified 2 mass vehicle model. **57**
Figure 5.7: MATLAB/Simulink 2 mass vehicle model. **58**
Figure 5.8: Simplified 3 mass vehicle model. **59**
Figure 5.9: 3 Mass vehicle MATLAB/Simulink model. **60**
Figure 5.10: Spring Nonlinear clutch and drive-shaft characteristics. **62**
Figure 5.11: Accelerator pedal position and brake torque request trace for the 3rd and 4th gear tip-in and tip-out manoeuvres. **63**
Figure 5.12: Comparison of vehicle measurements and simulation results for 3rd gear tip-in and tip-out manoeuvre; Top sub-figure: Vehicle longitudinal acceleration, Mid sub-figure: Vehicle speed, Bottom sub-figure: Engine speed. **64**
Figure 5.13: Comparison of vehicle longitudinal acceleration measurement and simulation results for 3rd gear tip-in (left) and tip-out manoeuvres (right). **64**
Figure 5.14: Comparison of vehicle measurements and simulation results for 4th gear tip-in and tip-out manoeuvre; Top sub-figure: Vehicle longitudinal acceleration, Mid sub-figure: Vehicle speed, Bottom sub-figure: Engine speed. **65**
Figure 5.15: Comparison of vehicle acceleration measurement and simulation results for 4th gear tip-in (left) and tip-out manoeuvres (right). **65**
Figure 6.1: Block diagram of a PID controller in a feedback loop [44]. **68**
Figure 6.2: Augmented plant and controller schematics [45]. **69**
Figure 6.3: MPC operation for single input single output system. **73**
Figure 6.4: Basic structure of MPC [49]. **73**
Figure 6.5: MATLAB/Simulink model of the 3 mass model with MPC + P controller. **78**
Figure 6.6: MPC Simulink model blocks. **78**
Figure 6.7: MPC state estimator Simulink block diagram. **79**
Figure 6.8: MPC tuning engine brake torque signal for 3rd gear. **80**
Figure 6.9: Vehicle acceleration response for no controller case for 3rd gear. **81**
Figure 6.10: Vehicle acceleration response for no controller case (Zoomed view at maximum load change manoeuvre) for 3rd gear. **81**
Figure 6.11: MPC structure overview. **82**
Figure 6.12: Vehicle acceleration response for MPC parameters determination for 3rd gear. **83**
Figure 6.13: Vehicle acceleration response for MPC parameters determination (Zoomed view at maximum load change manoeuvre) for 3rd gear. **84**
Figure 6.14: Vehicle acceleration response for MPC parameters determination (Zoomed view at maximum load change tip-in manoeuvre) for 3rd gear. **84**
Figure 6.15: Vehicle acceleration response for MPC parameters determination (Zoomed view at maximum load change tip-out manoeuvre) for 3rd gear. **85**
Figure 6.16: Engine brake torque request for MPC parameters determination for 3rd gear. **86**

Figure 6.17: Engine brake torque request for MPC parameters determination (Zoomed view at maximum load change manoeuvre) for 3rd gear. **86**
Figure 6.18: Engine brake torque request for MPC parameters determination (Zoomed view at maximum load change tip-in manoeuvre) for 3rd gear. **87**
Figure 6.19: Engine brake torque request for MPC parameters determination (Zoomed view at maximum load change tip-in manoeuvre) for 3rd gear. **87**
Figure 6.20: MPC tuning engine brake torque signal for 4th gear. **88**
Figure 6.21: Vehicle acceleration response for no controller case for 4th gear. **89**
Figure 6.22: Vehicle acceleration response for no controller case (Zoomed view at maximum load change manoeuvre) for 4th gear. **89**
Figure 6.23: Vehicle acceleration response for MPC parameters determination for 4th gear. **91**
Figure 6.24: Vehicle acceleration response for MPC parameters determination (Zoomed view at maximum load change manoeuvre) for 4th gear. **91**
Figure 6.25: Vehicle acceleration response for MPC parameters determination (Zoomed view at maximum load change tip-in manoeuvre) for 4th gear. **92**
Figure 6.26: Vehicle acceleration response for MPC parameters determination (Zoomed view at maximum load change tip-out manoeuvre) for 4th gear. **92**
Figure 6.27: Engine brake torque request for MPC parameters determination for 4th gear. **93**
Figure 6.28: Engine brake torque request for MPC parameters determination (Zoomed view at maximum load change manoeuvre) for 4th gear. **94**
Figure 6.29: Engine brake torque request for MPC parameters determination (Zoomed view at maximum load change tip-in manoeuvre) for 4th gear. **94**
Figure 6.30: Engine brake torque request for MPC parameters determination (Zoomed view at maximum load change tip-in manoeuvre) for 4th gear. **95**
Figure 6.31: Comparison of simulation results of no-controller, MPC & MPC + P controller for 3rd gear tip-in and tip-out manoeuvre; Top sub-figure: Vehicle longitudinal acceleration measurement, Mid sub-figure: Vehicle speed, Bottom sub-figure: Engine speed. **96**
Figure 6.32: Comparison of simulation results of no-controller, MPC & MPC + P controller for 3rd gear tip-in manoeuvre. **97**
Figure 6.33: Comparison of simulation results of no-controller, MPC & MPC + P controller for 3rd gear tip-out manoeuvre. **97**
Figure 6.34: Comparison of engine torque for simulation results of no-controller, MPC & MPC + P controller for 3rd gear tip-in and tip-out manoeuvre. **98**
Figure 6.35: Comparison of simulation results of no-controller, MPC & MPC + P controller for 4th gear tip-in and tip-out manoeuvre; Top sub-figure: Vehicle longitudinal acceleration measurement, Mid sub-figure: Vehicle speed, Bottom sub-figure: Engine speed. **99**
Figure 6.36: Comparison of simulation results of no-controller, MPC & MPC + P controller for 4th gear tip-in manoeuvre. **99**
Figure 6.37: Comparison of simulation results of no-controller, MPC & MPC + P controller for 4th gear tip-out manoeuvre. **100**

Figure 6.38: Comparison of engine torque for simulation results of no-controller, MPC & MPC + P controller for 4th gear tip-in and tip-out manoeuvres. **100**
Figure 6.39: Comparison of simulation results of no controller, MPC & MPC + P controller for 3rd gear tip-in and tip-out manoeuvre; Top sub-figure: Vehicle longitudinal acceleration measurement, Mid sub-figure: Vehicle speed, Bottom sub-figure: Engine speed. **102**
Figure 6.40: Comparison of simulation results of no controller, MPC & MPC + P controller for 3rd gear tip-in (left) and tip-out manoeuvres (right). **102**
Figure 6.41: Comparison of simulation results of no controller, MPC & MPC + P controller for 3rd gear tip-out manoeuvre. **103**
Figure 6.42: Comparison of engine torque for simulation results of no controller, MPC & MPC + P controller for 3rd gear tip-in and tip-out manoeuvres. **103**
Figure 6.43: Comparison of simulation results of no-controller, MPC & MPC + P controller for 4th gear tip-in and tip-out manoeuvre; Top sub-figure: Vehicle longitudinal acceleration measurement, Mid sub-figure: Vehicle speed, Bottom sub-figure: Engine speed. **104**
Figure 6.44: Comparison of simulation results of no-controller, MPC & MPC + P controller for 4th gear tip-in manoeuvre. **105**
Figure 6.45: Comparison of simulation results of no-controller, MPC & MPC + P controller for 4th gear tip-out manoeuvre. **105**
Figure 6.46: Comparison of engine torque for simulation results of no-controller, MPC & MPC + P controller for 4th gear tip-in and tip-out manoeuvres. **106**
Figure C.1: 3 mass model vehicle acceleration response for no controller case for 4th gear. **120**
Figure C.2: 3 mass model vehicle acceleration response for no controller case (Zoomed view at maximum load change manoeuvre) for 4th gear. **120**
Figure C.3: 3 mass model vehicle acceleration response for MPC parameters determination for 3rd gear. **121**
Figure C.4: 3 mass model vehicle acceleration response for no controller case (Zoomed view at maximum load change manoeuvre) for 3rd gear. **121**
Figure C.5: 3 mass model vehicle acceleration response for MPC parameters determination (Zoomed view at maximum load change tip-in manoeuvre) for 3rd gear. **122**
Figure C.6: 3 mass model vehicle acceleration response for MPC parameters determination (Zoomed view at maximum load change tip-out manoeuvre) for 3rd gear. **122**
Figure C.7: 3 mass model engine brake torque request for MPC parameters determination for 3rd gear. **123**
Figure C.8: 3 mass model engine brake torque request for MPC parameters determination (Zoomed view at maximum load change manoeuvre) for 3rd gear. **123**
Figure C.9: 3 mass model engine brake torque request for MPC parameters determination (Zoomed view at maximum load change tip-in manoeuvre) for 3rd gear. **124**
Figure C.10: 3 mass model engine brake torque request for MPC parameters determination (Zoomed view at maximum load change tip-in manoeuvre) for 3rd gear. **124**

Figure C.11: 3 mass model vehicle acceleration response for no controller case for 4th gear. **125**
Figure C.12: 3 mass model vehicle acceleration response for no controller case (Zoomed view at maximum load change manoeuvre) for 4th gear. **125**
Figure C.13: 3 mass model vehicle acceleration response for MPC parameters determination for 4th gear.. **126**
Figure C.14: 3 mass model vehicle acceleration response for MPC parameters determination (Zoomed view at maximum load change manoeuvre) for 4th gear. **126**
Figure C.15: 3 mass model vehicle acceleration response for MPC parameters determination (Zoomed view at maximum load change tip-in manoeuvre) for 4th gear... **127**
Figure C.16: 3 mass model vehicle acceleration response for MPC parameters determination (Zoomed view at maximum load change tip-out manoeuvre) for 4th gear... **127**
Figure C.17: 3 mass model engine brake torque request for MPC parameters determination for 4th gear.. **128**
Figure C.18: 3 mass model engine brake torque request for MPC parameters determination (Zoomed view at maximum load change manoeuvre) for 4th gear. **128**
Figure C.19: 3 mass model engine brake torque request for MPC parameters determination (Zoomed view at maximum load change tip-in manoeuvre) for 4th gear... **129**
Figure C.20: 3 mass model engine brake torque request for MPC parameters determination (Zoomed view at maximum load change tip-in manoeuvre) for 4th gear... **129**

MODEL BASED OPTIMAL LONGITUDINAL VEHICLE CONTROL

SUMMARY

Considering the competitive environment in automotive industry, original equipment manufacturers (OEMs) in this industry are in a challenging competition with each other to offer their customers more attractive vehicles. Cost, emissions, fuel economy, noise vibration & harshness (NVH), durability, performance and driveability properties make a product able to distinguish from its competitors' products. Each of these attributes has a major contribution of forming a perception of the customers' choosiness. New technologies as a result of the research and developments activities in electronics resulted with complex electro-mechanical systems in automobiles. With the addition of recent developments in materials and manufacturing processes on top of it, especially in diesel fuelled internal combustion engines (ICE), torque and power delivery had almost doubled with respect to the conventional engines developed not more than two decades ago. Additionally as a result of latest developments at air path and gas exchange systems control, torque build up rate had significantly increased enabling the vehicles to be more agile and reactive to load change request manoeuvres. As a result of all these capability improvements, vehicle response characteristics to high torque and power capacity engines changed extremely altering the necessity of proper and robust driveability calibration requirements. Driveability properties of the vehicles had gained significant importance in terms of customer satisfaction. This dissertation focuses on improving vehicle driveability properties taking advantage of simulation tools and model based control. The overall profit of this thesis is providing improved driveability via using engine torque production and vehicle models and controllers at the same time.

Torque transmission from the vehicle's power unit to the road surface via tires is a complex structure which should be handled with extreme care considering the overall driveability performance of the vehicle. An agile throttle response of the vehicle is aimed without error modes like acceleration initial kick, bump, response delay, stumble or shuffle. However considering the nonlinearities resulting from the complex structures at the drivetrain of the vehicle, this requirement becomes significantly challenging. Despite mechanical control at longitudinal motion in conventional vehicles, modern vehicles are equipped with electromechanical systems. Thanks to technological developments in the automotive industry that current capability of the vehicles enables us to develop better platforms for improving driveability characteristics. Modern engine control units (ECUs) have the capability of processing thousands of signals in a less than tens of milliseconds and as a result regulate numerous actuators which results with displacement of the vehicle complying all regulative requirements and customer expectations. Acceleration throttle pedal input signal is recorded by electronic control unit, processed and finally used to control the parameters for the combustion systems. In terms of driveability control, automotive manufacturers' engine control algorithms

employ input shaping or simple filtering algorithms. These algorithms use look-up tables and main control strategy is to slew the pedal oriented torque request for the tip-in and tip-out manoeuvres in an open loop control methodology especially in backlash transition region of the driveline. Considering the fact that there is no close loop control and these features become subjective calibration methodologies and outcome becomes strongly dependant on calibrator's capability and performance. Moreover filling look-up tables for all gear, engine speed and pedal position combinations requires significant amount of calibration development time. Taking into consideration all of these obstacles of the current driveability features, the subject of automated torque control for improved driveability is a state of the art research topic both within automotive manufacturers and academic researchers as it can be described as an optimization problem dealing with performance and comfort counter measures.

Knowledge of the instantaneous produced torque by the engine is a key item with respect to satisfying above stated attributes in vehicle longitudinal motion control. Currently common approach for combustion management is the usage of look-up table based structures with the drawback of poor conformity of the produced torque. Look-up tables define air and fuel quantity setpoints in order to produce requested indicated torque without feedback of the produced torque. These look-up tables are filled at engine dynamometer test benches at normal ambient conditions. In general fuel and air quantity setpoint maps have the axes of engine speed and indicated torque and requested amount of desired variable is filled to the corresponding point of the look-up table. In real world driving conditions fuel quantity control is robust however especially with turbocharged systems; requested air quantities may deviate from the setpoint values especially when considering transient manoeuvres. This phenomenon is called "turbo/boost lag" and significantly affects the produced torque. The situation is much worse for non-standard conditions, extreme hot and cold and altitude. In the literature most of the proposed vehicle longitudinal motion control related engine torque control algorithms base on the fact that requested torque will be generated immediately from the diesel engine. However as explained above this is not the case in real life applications. Therefore engine characteristic is either not included or covered with a simple filtering algorithm in conventional vehicle longitudinal motion related engine torque control methodologies. Engine brake torque model combined driveability control algorithm proposed in this thesis is differentiated from the previous studies in the literature within this perspective. Proposed "In cylinder pressured based engine brake torque model algorithm" works in harmony with the driveability control structure and improves overall vehicle response characteristics.

Within the scope of this study a 4 degree of freedom powertrain model consisting of 4 inertias, 2 set of spring and damper elements with tyre characteristics, is built in MATLAB/Simulink environment. Model validation considering longitudinal vehicle dynamics is performed with employing vehicle level tests using a tip-in followed by a tip-out acceleration pedal signal input load change manoeuvres. Comparison of simulation results and measured vehicle test data shows that proposed model is capable of capturing vehicle acceleration profile revealing unintended error states for the specified input signals.

Considering the driveability control perspective, a Model Predictive Control (MPC) algorithm employed to manipulate the pedal map oriented torque demand signal in an automotive powertrain application in order attenuate the powertrain oscillations in

longitudinal vehicle motion control. 4 mass model could not be employed at with the MPC algorithm due to very high level of nonlinearity. Therefore two simplified versions of 2 and 3 mass models have been developed. It has been verified that both 2 and 3 mass vehicle models are accurate enough to employ the MPC torque control algorithm. As the aim of this study is to develop a close loop driveability algorithm for real world applications, the 4 mass vehicle model is used as replacement environment for the subjected vehicle in order to employ 2 and 3 mass vehicle model based control algorithm. MPC algorithms via using both models showed good capability, however smoothness of the driving profile with the 2 mass vehicle model is slightly better than the 3 mass model. Moreover to further improve the powertrain oscillations without compromising from overall system response speed, an additional anti-shuffle control element, basically a P controller based on the speed difference of engine and vehicle speeds, has been implemented to the MPC control algorithm. Literature review about the engine torque control for improved driveability show that all the researcher use MPC alone. Proposed MPC with additional P controller is a new contribution to the literature in the subjected area of research.

MODEL BAZLI OPTİMAL DOĞRUSAL ARAÇ KONTROLÜ

ÖZET

Otomotiv sektöründeki zorlu rekabet ortamı göz önüne alındığında, otomotiv üreticileri müşterilerine daha çekici ve fonksiyonel araçlar sunabilmak için birbirleri ile sürekli bir yarış halindelerdir. Maliyet, emisyon, yakıt ekonomisi, gürültü ve titreşim, dayanıklılık, performans ve araç sürüş özellikleri gibi kriterlerde yapılan iyileştirmeler sayesinde üreticiler rakip firmaların araçlarına göre daha avantajlı bir yere gelmeyi hedeflerler. Bu özelliklerin her biri müşterilerin kullandığı / kullacağı araç için olumlu bir algı oluşturulmasında önemli katkısı vardır. Bilişim ve elektronik sektöründeki araştırma ve gelişmeler faaliyetleri sonucunda elde edilen yeni teknolojiler ışığında otomobil mimarisindeki elektro-mekanik istemlerin kullanımı oldukça artmıştır. Buna ek olarak malzeme bilimi ve üretim teknolojisinde gelişmeler ışığında dizel yakıtlı içten yanmalı motorlarun tork ve güç eğrileri 20 yıl önce üretilen motorlardaki tork ve güç seviyelerine göre neredeyse 2 katına çıkmıştır. Ayrıca araçların ivmelenme manevralarındaki hızlanma tepki seviyeleri de özellikle hava yolu kontrolündeki yenilik ve gelişmeler doğrultusunda oldukça artmıştır ve araçları çok daha çevik ve sürücülerin gaz pedalı hareketine bağlı isteklerine çok daha fazla duyarlı hale getirmiştir. Motor tork ve güç kapasitelerindeki gelişmeler doğrultusunda araçların gaz pedalı tepkileri ciddi oranda değişmiş ve iyi bir araç sürüş özellikleri kalibrasyonuna ihtiyaç doğmuştur. Tüm gelişmelerin neticesinde araç sürüş özellikleri, müşteri memnuiyeti kriterleri arasında önemli bir paya sahip olmuştur. Bu tez çalışması araç sürüş üzellikleri simulasyon programları ve model bazlı kontrol algoritmaları kullanarak iyileştirmeyi amaçlamaktadır.

Aracın güç ünitesi olan motorlardan tekerlekler vasıtasıyla yola olan tork ve kuvvet iletimi son derece karmaşık bir yapıya sahiptir ve araç sürüş özellikleri düşünüldüğünde dikkatli bir şekilde ele alınmalıdır. Aracın gaz pedalı hareketine olan tepkisi gecikme içermemeli, yeteri kadar hızlı ve seri olmalı aynı zamanda vurma, sarsıntı, salınım ve yığılma gibi hata modları içermemelidir. Bununla birlikte araç aktarma organları bileşenlerindeki doğrusal olmayan sistemler düşünüldüğünde, yukarıda bahsedilen araç sürüş özellikleri beklentilerini karşılamak son derece zorlu bir hal almaktadır. Eski araçlardaki gaz pedalı ve kelebeği arasındaki bağlantı teli vasıtasıyla sağlanan mekanik araç doğrusal ekseni kontrolünden farklı olarak, günümüzün modern araçları elektromekanik sistemler ile donatılmıştır. Motor kontrol üniteleri araç dorusal ekseni hareketini regülatif ve müşteri beklentileri ile uyumlu şekilde sağlamak için onlarca sensör sinyalini algıladıkdan sonra milisaniyeler içersinde işleyerek, motor ve araç aktüatörlerinin kontrolü için uygun sinyalleri üretirler. Araç sürüş özellikleri algoritmları düşünüldüğünde otomobil üreticileri gaz pedalı deplasmanına bağlı sürücü tork isteğini yumuşatan veya filtreleyen algorithmalar kullanırlar. Bu algoritmalar genellikle harita bazlıdırlar ve ana misyonları özellikle araç aktarma organlarındaki dişli mekanizmalarındaki boşluklardan geçerken geçerken tork artış ve azalma hızlarını limitleyerek araç sürüş özelliklerini iyileştirmektir. Sistem herhangi bir kapalı döngü içermediği için, bu

algoritmalar subjectif kalibrasyon yöntemleri olarak tanımlanabilirler ve sistemin doğru çalışması, bu haritaları kalibre edem kalibrasyon mühendisinin hislerine ve yeteneğine bağlıdır. Ayrıca bu haritalardaki araç hızı, pedal pozisyonu ve vitese bağlı kombinasyonlar içerirler ve tüm olası koşulları içeren bir kalibrasyon yapılması oldukça zaman almaktadır. Mevcut kalibrasyon yapısının yukarıda bahsedilen kusurları göz önüne alındığında; araç sürüş özelliklerinin iyileştirilmesi için performans ve konfor gibi birbirleriye çelişen isteklerin optimizasyonunu barındıran gelişmiş tork kontrolü, otomobil üreticileri ve akademik dünyada son derece ilgi çeken bir konu haline gelmiştir.

Araç doğrusal ekseni hareket kontrolü algoritmalarının başarılı bir şekilde kullanılabilmesi için motorun anlık olarak ürettiği torkun bilinmesi oldukça önemlidir. Günümüz araçlarının yanma kontrolü incelendiğinde, mevcut yapının harita bazlı olduğu görülür ve bu yapıda üretilen torkun doğrulaması yapılmamaktadır. Bu haritalar motor test dinamometrelerinde normal hava koşulları için (25 derece sıcaklık ve deniz seviyesi irtifa) doldurulurlar. Genellikle bu haritaların eksenleri motor hızı ve istenilen indike tork şeklinde olup, haritanın içeriğini ise istenilen yanma parametresinin belirtilen motor hızı ve indike torktaki değeri oluşturur. Bu yapı araçlarda kullanılırken bazı sıkıntılar yaratabilir. Motorlarda yanmayı oluşturan yakıt yolu parametreleri kontrolü çok daha hassas bir şekilde yapılırken (istenilen yakıt özellikleri: basınç, zamanlama ve miktar), gecici rejim manevraları düşünüldüğünde hava yolu parametreleri özellikle turbo şarj içeren dizel motor motorlarda istenilen değerden sapma gösterebilir. Bu durum “turbo gecikmesi” olarak adlandırılır ve üretilen torku ciddi şekilde etkiler. Aşırı sıcak yada soğuk ve yüksek irtifa koşulları düşünüldüğünde üretilen torktaki sapmalar çok daha fazla olur. Literature incelendiğinde araç eksenel doğrultusu için geliştirilen motor tork kontrol algoritmaları bakımından istenilen anlık torkun motor tarafından verildiği düşünülür. Fakat yukarıda belirtilen nedenlerden dolayı bu durum gerçekleşemez. Bu yüzden literaturde belirtilen araç doğrulsal ekseni için geliştirilen motor tork kontrolü algoritmalarında motor tork karakteristiği ya hiç düşünülmemiştir yada bazı temel gecikme ve filtrele fonksiyonları ile modellenmiştir. Tüm bu anlatılanlar düşünüldüğünde bu tez çalışmasının temelini oluşturan motor tork modeli içeren araç doğrusal ekseni kontrol algoritması literatürdeki diğer çalışmaşlarda ayrışır. Önerilen “Silindir için basınç öngörümlü motor tork kontrol modeli algoritması” araç sürüş özellikleri kontrol yapısı ile uyumlu bir şekilde çalışarak araç tepki karakterini iyileştirir.

Bu çalışma kapsamında MATLAB/Similink modelle ortamında, 4 atalet kütlesi, 2 set yay ve sönüm elemanı ve lastik karakteristiği içeren, 4 serbbestlik dereceli bir aktarma organları modeli oluşturulmuştur. Sadece araç doğrusal ekseni araç dinamiğini içeren model validasyonu, gaz basma ve gazdan çekme gibi yük değişimi manevralarını içeren araç seviyesi tesler ile yürütülmüştür. Test ölçüm sonuçları ve model çıktıları karşılaştırıldığında geliştirilen aktarma organları modelinin araç doğrusal ekseni hızlanma profili için karşılaşılan hata modlarını da içerecek şekilde yansıttığı görülmüştür.

Son olarak araç aktarma organları uygulaması düşünüldüğünde, araç sürüş özelliklerini iyileştirme için sürücü talebi doğrultusunda oluşan tork isteğini araç doğrulsal ekseni hareketinde oluşabilecek salınımları engelleyen model bazlı öngörümlü tork kontrol algoritması geliştirilmiştir. Bu algoritmada 4 serbestlik dereceli model, içerdiği doğrusal olmama durumu yüzünden kullanılamamıştır. Bu yüzden basitleştirilmiş 2 ve 3 serbestlik dereceli araç aktarma organları modelleri oluşturulmuştur. Yapılan çalışmalar doğrultusunda hem 2 hem de 3 serbestlik dereceli modellerin, model bazlı öngörümlü tork kontrol algoritmasını düzgün şekilde çalıştırabilmek için yeterli doğruluk ve çözünürlükde olduğu görülmüştür. Bu çalışmanın amacı kapalı devre bir araç sürüş özellikleri algoritması ortaya çıkarmak olduğu için ve geliştirilen algoritma teknik nedenler dolayısıyla araçta denenemediği için, 4 serbestlik dereceli motor aktarma organları modeli, 2 ve 3 serbestlik dereceli motor aktarma organları modelli içeren model bazlı öngörümlü tork kontrol algoritmalarını çalıştırmak üzere kullanılmıştır. Geliştirilen 2 ve 3 serbestlik dereceli modellerin araç sürüş özellikleri önemli derecede iyileştirdiği görülmüştür. Özellkile ivmelenme profilinin düzgünlüğü ve neden olusan sistem gecikmesi düşünüldüğünde 2 serbestlik dereceli aktarma organları modeli bazlı kontrol algoritmasnın daha iyi sonuç verdiği görülmüştür. Geliştirilen tork kontrol modelli aktarma organları bazlı araç salınımları ciddi oranda azaltsada, tamamen ortadan kaldırmadığı görülmüştür. Bu doğrultuda araç ivmelenme karakteristiğinden minimum seviyede ödün vererek, oluşan salınımları daha da azaltmak ve ivmelenme profilini daha düzgün hale getirmek için temel olarak motor ve araç hızı farkını elimine etme prensibine dayanan bir doğrulsal (P) kontrolcü, model bazlı öngürümlü tork kontrol algoritmasına eklenmiştir. Literatürde bu konuda yapılan çalışmalar incelendiğinde tüm araçtırmacıların model bazlı öngürümlü algoritmayı tek başına kullandıkları görükmektedir ve bu çalışmada önerilen doğrusal kontrolcü eklenmiş model bazlı öngörümlü tork kontrol algoritması bir yenilik olarak mevcut literatür içeriğine eklenmiştir.

1. INTRODUCTION

This thesis study is on the subject of improving driveability and hence it commences with a description of the term “driveability”. In the automotive terminology driveability is described as the sum of the vehicle’s driving traits and mannerisms. The extensive dictionary meaning can be summarized as the general qualitative appraisal of a vehicle drive train's operating qualities, including cold and hot starting, idle smoothness, power delivery, throttle response and tolerance for altitude changes. Vehicle driveability is an important aspect when evaluating vehicle performance. However the essential focus of the driveability is the power delivery and the acceleration pedal response of the vehicle for most of drivers. Considering power and torque increase of the modern engines in the last decades, the importance of the driveability properties has become of vital importance. Moreover additional user driving modes “Comfort, Economy & Performance” capability has been added to the vehicle specification in order to attract different customer expectations. Response time and amplitude of the vehicle to throttle pedal input, differentiates between such modes but the overall expectation of the customer is a smooth driving profile without excessive jerks, shuffles and discontinuities in power delivery.

1.1 Motivation

World automotive industry has changed dramatically in the recent years. New technologies as a result of the research and developments activities in electronics resulted with complex electro-mechanical systems in automobiles in order to cope with regulatory requirements and customer expectation. Every year, with invention of new technologies, complexity of the automotive systems alters especially considering emissions systems and driver aid features. Main purpose of driving aid mechanisms is to deliver a safe and comfortable driving to the customers. Driver aid systems can be classified as active such as proximity detection systems, rear view camera systems, active steering headlights and high beams, cruise control / adaptive cruise control, blind spot monitoring, collision mitigation systems, lane-monitoring

& lane-keep assistance systems; passive systems such as driveability improvement systems.

Unlike the conventional automobiles where acceleration throttle input is mechanically connected to a fuel valve, modern vehicles are equipped with electromechanical systems where acceleration throttle pedal input signal is recorded by electronic control unit, processed and finally used to control the parameters for the combustion systems. This capability ensures a drive profile according to different customer expectations (smooth for gentle driving and agile for performance indexed driving habits) without error states.

Torque transmission from the vehicle's power unit to the tires is a complex structure which should be handled with extreme care considering the overall driveability performance of the vehicle. An agile throttle response of the vehicle is aimed without error modes like acceleration initial kick, bump, response delay, stumble or shuffle. However considering the nonlinearities resulting from the complex structures at the drivetrain of the vehicle, this requirement becomes fairly challenging. Automotive manufactures generates significant amount of research on the subject during the development periods of the vehicles. Additionally this subject attracts interest of many researchers as it can be described as an optimization problem dealing with performance and smoothness counter measures.

Thanks to technological developments in the automotive industry that current capability of the vehicles enables us to develop better platforms for improving driveability characteristics. Modern engine control units have the capability of processing thousands of signals in a less than tens of milliseconds and as a result regulate numerous actuators which results with displacement of the vehicle complying all regulative requirements and customer expectations. No more than twenty years ago quality of driveability of the vehicles was much more primitive considering today's modern vehicles. There was no signal processing between the driver's acceleration pedal input and vehicle response which generates a system prone to error states. In the last decade driveability modules have been developed but still a full autonomous driveability control system is not available.

Current torque management structures in modern vehicles operate without any driveability feed-back signals from vehicle apart from some stability modules like ESP or TCS. Control structure is totally open loop and generally works using look-up table based structures from the acceleration pedal position, engine speed, estimated torque and gear inputs. On a general aspect, certain amount of torque is requested and generated via combustion however effect of generated torque on vehicle motion is not evaluated within the engine control module especially considering driveability perspectives. There are some simple feed forward torque correction algorithms (within driveability modules) which modulate torque request like “anti-jerk” and “anti-shuffle” algorithms in order to minimize the jerk effects and the damp the first order natural frequency oscillation however lack of a close loop control, prevents vehicle from being an error free system in terms of driveability features.

As there is no “closed loop control” which can improve driveability considerably via eliminating the error states, in automotive companies for every vehicle program, it takes significant amount of time for the calibration process of torque management structures with manual methods on the vehicles. Moreover, the driveability calibration is performed with subjective evaluation (very few attributes can be objectively evaluated) and is strongly depended to the capabilities of the calibrator.

With the aid of close loop control systems, it is possible to obtain an error free driveability behaviour from a vehicle without any additional system requirements as current vehicle capability provides all the necessary inputs for a close loop driveability control system. Implementation of such systems will not only fulfil customer expectations but also reduce the development time spend on calibrating driveability features on vehicles.

1.2 Objectives

On the basis of lack of close loop systems in vehicle driveability control systems, longitudinal vehicle motion control is always prone to error states. Therefore, an improved methodology is required for vehicle motion control in order to fulfil customer expectations. This dissertation with the title “Model Based Optimal Longitudinal Vehicle Control” focuses on improving vehicle driveability features of a passenger vehicle considering initial acceleration and deceleration responses (tip-in / tip-out) taking advantage of simulation tools and model based predictive control. Overall profit of the thesis will be improved driveability via using engine torque production and vehicle models together with close loop vehicle throttle response controller. Proposed system will not only ensure that vehicle response is optimum without error states but also decrease development times spend on driveability calibration physically on vehicle.

1.3 Scope

This thesis study focuses on improving vehicle driveability taking advantage of simulation tools and model based control and hence contains development of a model based vehicle longitudinal motion control structure with a closed loop feedback. In this structure, an engine brake torque estimation model (based on in-cylinder pressure estimation) and a vehicle driveline model including fundamental powertrain structures like engine, flywheel, clutch, transmission, final drive (differential), side shafts and wheels are generated. Using the developed model's motion response simulation of the vehicle to the driver requested torque; an automatic closed loop torque correction is applied for obtaining performance & driving smoothness without error states. In this study an engine generated brake torque based model predictive control (MPC) algorithm with an additional anti-shuffle control element is developed.

1.4 Contributions

As a result of recent improvements at engine control structures and computational capability developments during the last decades, the idea of using generated brake torque control had been a state of the art research topic among academic researchers and original equipment manufacturers (OEMs). There are a large number of studies reported in the area of automated engine torque control. Due to the inertial behaviour of the airpath components, transient torque response of a diesel engine (especially turbocharged) is different to the steady state torque generation behaviour. For a load change manoeuvre boost pressure build up and discharge takes some amount of time mainly due to the "boost lag" phenomenon. With modern engine air path control algorithms and sophisticated hardware like variable geometry turbocharger (VGT) or 2-Stage turbocharging, boost response of the diesel engine significantly improved. However due to above explained facts, in reality torque reporting error on transient manoeuvres is still inevitable. In the literature most of the proposed engine control algorithms base on the fact that requested torque will be generated immediately from the diesel engine. Therefore engine characteristic is either not included or cover with a simple filtering algorithm. Engine brake torque model combined driveability control algorithm proposed in this thesis is differentiated from the previous studies in the literature. Proposed “In cylinder pressured based engine brake torque model algorithm” works in harmony with the driveability control structure and improves overall vehicle response righteousness.

Within the scope of this study a MPC algorithm employed to attenuate the powertrain oscillations in longitudinal vehicle motion control. In order to further improve the powertrain oscillations without compromising from overall system response speed, an additional anti-shuffle control element, basically a P controller based on the speed difference of engine and vehicle speeds, has been implemented to the MPC control algorithm. Literature review about the engine torque control for improved driveability show that all the researcher use MPC alone. Proposed MPC with additional P controller is a new contribution to the literature in the subjected area of research.

1.5 Structure of the Thesis

Thesis report starts with the literature review section containing a revision of the previous academic research study about powertrain modelling, engine brake torque estimation and driveability improvement via engine torque control. Chapter 3 basically explains engine torque control structure in modern electronically controlled vehicles and refers to the possible improvement opportunity which is explained in the upcoming chapters of the thesis. The later 3 chapters are “in cylinder pressure based engine brake torque control”, “driveline modelling” and “controller development for driveability”; and form the heart of the thesis study and contains explanations of the developed engine and vehicle models and controllers. The conclusion section summaries the performed work and states the contributions of the study to the literature.

2. LITERATURE REVIEW

Latest research and developments activities in electronic and automotive industries resulted complex electro-mechanical systems equipped automobiles in order to cope with not only regulatory requirements but also elevated customer expectations. Correspondingly, power and torque delivery capability of the modern engines increased significantly in the last decades. Conventional automobiles had longitudinal vehicle control employing an acceleration pedal, which is mechanically connected to a fuel/air throttle valve. Controversially modern vehicles are equipped with complex mechatronics systems such as Engine Control Unit (ECU) with various sensors and actuators. Acceleration throttle pedal input signal is recorded and processed in order to control the produced the parameters for the combustion system and hence produced torque. When engine and driveline components are triggered with a high amount of torque/load change manoeuvre as a result of acceleration pedal response, low frequency oscillations occur if the driveability calibration of the powertrain is inadequate. Figure 2.1 shows a B class front wheel drive (FWD) passenger vehicle response at second gear to an acceleration input pedal change request. Lower subfigure clearly indicates that sudden brake torque change results with acceleration overshoot / undershoot followed by decaying low frequency oscillations for tip-in and tip-out manoeuvres respectively. These low frequency oscillations correspond to the first resonance frequency of the driveline and typical resonance frequencies are 2-8 Hz depending on gear for manual transmission passenger vehicles [1]. Considering that whole body vibration at 2 Hz and above can cause discomfort and injury [2], elimination of these low frequency oscillations is of vital importance for achieving comfortable drive characteristics.

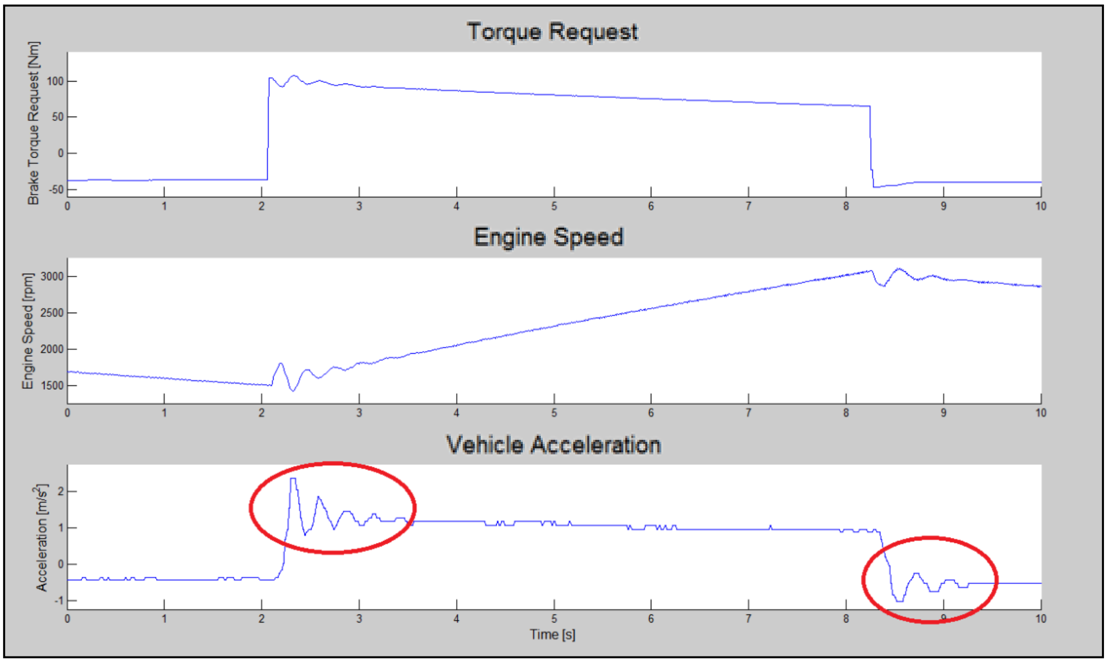

Figure 2.1 : Vehicle response for a tip-in & tip-out response showing error states; Top sub-figure: Engine brake torque request, Mid sub-figure: Engine speed measurement, Bottom sub-figure: Vehicle longitudinal acceleration measurement.

According to AVL-DRIVE (a well-known driveability analysis and development tool for the objective assessment) driveability assessment analysis, tip-in and tip-out manoeuvres have 9% and 10% weights respectively over the whole driveability evaluation [3]. Considering the tip-in manoeuvre, the following error states with the specified weightings are used to form the final assessment result of a tip-in response rating:

- Jerks (18%)
- Kick (15%)
- Initial bump (15%)
- Response delay (12%)
- Stumble (10%)
- Torque build-up (10%)
- Torque smoothness (5%)
- Absolute torque (5%)
- Vibrations (5%)
- Noise (5%)

As can be easily understood from the above analysis, tip-in and tip-out driveability is a very complex phenomenon that should be handled with extreme care. Within this scope, Dorey and Holmes developed a subjective vehicle evaluation methodology [4]. For the tip-in and tip-out manoeuvres the most important characteristics that effects driver's impression of vehicle driveability are overshoot and rise rate. These metrics are inversely related to the subjective evaluation rating (Figure 2.2). Similarly, considering decaying oscillations, damping ratio and natural frequency are the other metrics that effect overall driveability score. Rapid reduction and decay of oscillations in acceleration response is the desired response from a typical vehicle.

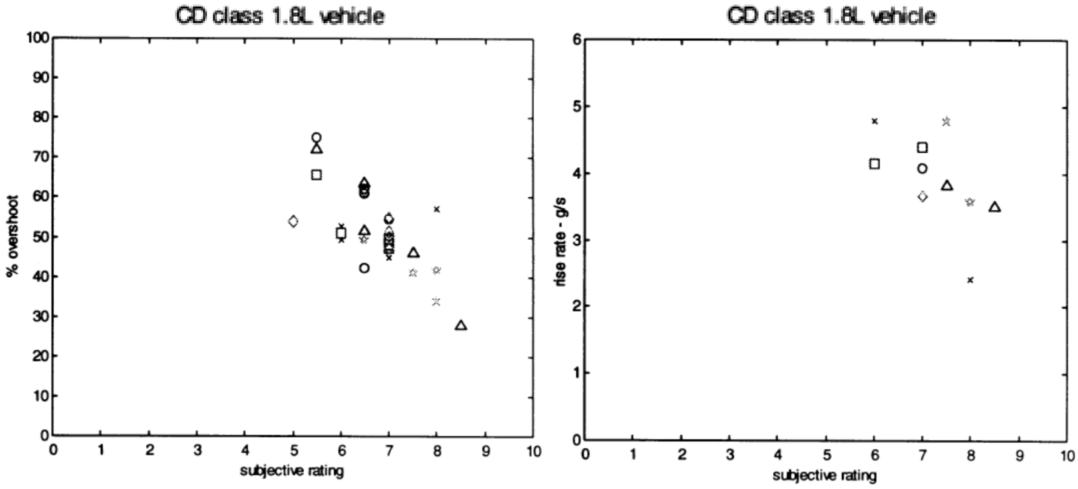

Figure 2.2 : Relationship of overshoot and rise rate characteristics to subjective ratings for tip-in manoeuvres [4].

2.1 Powertrain Modelling

Model based driveability control is a state of the art topic within academic world and automotive industry. In order to employ a model based driveability control feature, powertrain modelling is a necessity. In the literature, vehicle driveline models are already available and frequently used. This subsection will briefly summarize the content of the available models and procure a comparison of the models.

Powertrain modelling has been an important analytical and computer aided engineering (CAE) tool in vehicle development process. It not only enhances great opportunities over vehicle driveability but also reduces vehicle development durations. Powertrain modelling covers the components: engine, clutch, gearbox, propeller shaft, differential, drive shafts, wheels and tires (Figure 2.3, [5]). All these components have major contributions to vehicle longitudinal motion properties and must be taken into consideration for powertrain modelling. Each of the components has complex structures and there are many parameters that should be taken into account during modelling which alters the complexity of the models.

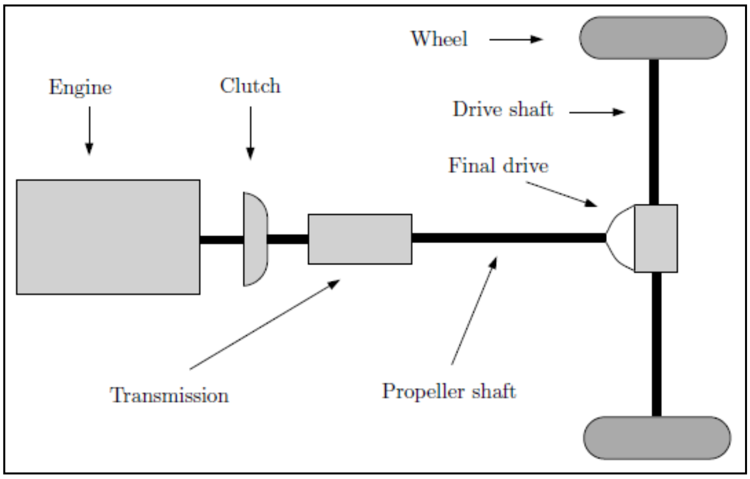

Figure 2.3 : Schematics of vehicle powertrain with an internal combustion engine [5].

Driveability modelling can be used for hardware selection in the development phase of the vehicle. Abuasaker and Sorniotti presented linear and non-linear driveline models for Heavy Goods Vehicles (HGVs) in order to evaluate the main parameters for optimal tuning, when considering the driveability [6]. The implemented models consider the linear and non-linear driveline dynamics, including the effect of the engine inertia, the clutch damper, the propeller shaft, the half shafts and the tires. Sensitivity analyses are carried out for each driveline component during tip-in manoeuvres. The major outcomes are as follows. The first natural frequency of the drivetrain increases as a function of the half-shaft stiffness and the gear number, and the overall damping decreases as a function of the longitudinal slip stiffness of the tire. The vehicle payload has a significant effect not only on the steady-state acceleration, but also on the overall system dynamics (frequencies and damping).

2.1.1 Powertrain models without backlash

Although backlash phenomenon has great influence at the vehicle such as reducing the system performance and destabilizing the control system, due to its complexity and extreme computational requirement some researcher excluded backlash in their powertrain models.

Kiencke and Nielsen developed a very detailed model of a rear wheel drive (RWD) vehicle powertrain containing all major components, and after deriving the necessary equations for each component, form the vehicle longitudinal motion equations [5]. The models are combinations of rotating inertias connected by damped shaft flexibilities. The generalized Newton's second law is used to derive the motion equations.

Sorniotti performed a very detailed study about powertrain modelling for a FWD vehicle [7]. The author generated 5 different powertrain models (with increasing complexity). Model # 1 can be described as a 2 degree of freedom (DOF) model (2 set of inertias connected by a spring & damper elements characterized by the stiffness of the driveshafts. Model # 2 is very similar to the first one with change of using clutch as the flexible element instead of the driveshafts. Model # 3 is contains the flexibility characteristics of both clutch and driveshafts therefore can be defined as a 3 DOF model (3 set of inertias connected by 2 sets of spring 6 damper elements). Model # 4 advances the predecessor model via addition of tire dynamics which is characterized with a tire equivalent damper. Models # 1 to 4 were only capturing torsional driveline characteristics and vertical and pitch motions of the vehicle were not included. Model # 5 includes the full dynamics of the powertrain, the dynamics of the unsprung masses, the dynamics of the sprung mass, the dynamics of the engine, the gearbox and the dynamics the differential induced by their mounting system on the vehicle body. The subjected study concluded with an evaluation of the main parameters (such as stiffness and damping coefficients of the main components) for optimal tuning of the driveline of a passenger vehicle.

Hayat et al. developed a lumped powertrain and vehicle model in AMEsim simulation environment in order to simulate and evaluate the customer driveability requirements [8]. The superiorities of the lumped parameter model can be described as with the following aspects: its relative simplicity, transient capabilities and parametric possibilities. Proposed global powertrain and vehicle model consists of below components: driveline, tyres and body. Global model is validated with vehicle level experiments comparison with tip-in, take-off and gearshift manoeuvres. Due to complexity of the model and possible restrictions in real time usage, authors developed 2 simplified models via using "Model Order Reduction Algorithm". The first one considers vehicle body, powertrain and unsprung weight dynamics in the longitudinal plane extracting high frequency driveline phenomena. The driveline model takes into account: flywheel rotational inertia and friction phenomena, clutch dry friction model, gearbox equivalent rotational inertia, clutch stiffness, drive shaft stiffness and tyre dynamics. In the second model least active driveline stiffness elements were eliminated, forming a third order transfer function. This model uses only the rotational properties of the components in the driveline to simulate the vehicle dynamics.

Balfour et al. developed a multi (15) degree of freedom vehicle driveline lumped parameter model in MATLAB/Simulink environment [9]. The model covers all the powertrain elements starting from the engine to the wheels. The model is for a FWD application and individual characteristics of the right and left side shafts are taken into consideration. Vertical movement of the vehicle is also covered via suspension modelling. The model has been extensively validated considering the cases: engine decoupled from the driveline, engine coupled to the driveline with varying load and engine coupled to the driveline with varying inertia.

Models of powertrain can be configured in many ways combining different sets of combinations of powertrain components. However, as much as the developed models becomes complex, the burden on model result calculation speed increases. Therefore most of the researchers preferred simplified models that are able to represent powertrain characteristics within a good level of accuracy. Within this scope Fredriksson et al. developed a third order powertrain model with 2 inertias as flywheel (mainly representing the engine inertia) and sum of the inertias of wheels and vehicle weight. Flexibility of the driveshafts is characterized via adding spring and damper properties. In fact the damping properties of the driveshaft partially characterize the longitudinal dynamics of the tires.

Similarly Baumann et al. used a simplified 2 mass model in his studies [10]. It is assumed that all rotating and oscillating masses inside the engine can be combined to a single mass. Clutch is assumed to be always engaged and therefore it is modelled assuming no friction, and mass moment of inertia is neglected. The propeller shaft is assumed to be stiff and the transmission, the final drive is modelled by two rotating inertias. The drive shaft is modelled as a damped torsional flexibility, with spring and damping characteristics. Different than the previously stated models Baumann added damping characteristics to the transmission and final drive components. Proposed model is represented within a state space form. The parameters of the state space model of the drivetrain are identified by measured data. As a measure of oscillations in the driveline the difference between engine speed and wheel speed is used. The drivetrain of a test car was excited with tip-in and tip-out at different engine speeds and the requested torque and the resulting speed difference between engine and wheel were measured.

The community of the mentioned models is clutch is assumed to be always engaged. However in real life clutch engagement status can be as follows: disengaged, engaged and transition between these modes. The complex friction phenomenon during engagement of the clutch alters the importance of the power transmission through the clutch for vehicles. The engagement and disengagement mechanisms are effective during launch and shifting manoeuvres. Additionally springs are used on the clutches for the purpose of reducing the transmission of the combustion vibrations to the powertrain. The main function of an engaging clutch is to transmit the torque gradually so that then the engine is connected to the rest of the powertrain, high accelerations and jerks are avoided. Dassen generated a dynamic model of the clutch and simulated the engagement process and evaluated the performance [11]. Serrarens et al. analysed the dynamic behaviour and control of an automotive dry clutch [12]. Considering three modelling techniques (Lagrange using reduced matrices, state space formulation and the Karnopp approach), the authors preferred to use the Karnopp approach, the authors embedded a straightforward model of the clutch within a dynamic model of an automotive powertrain composing of an internal combustion engine, drivetrain and wheels moving a vehicle through tire-road adhesion. Moreover they adopted a decoupling controller from literature and compared the closed and open loop results with the proposed simulation model. Finally a modified controller is proposed and analysed that improves the controllability over the vehicle's drive comfort.

Dolcini et al. developed a simple driveline model, with four state variables which is capable of capturing the essential part of the dynamic behaviour of the driveline, for clutch performance optimization for automated manual transmission boxes [13]. Clutch comfort is analysed for standing start and gear shifting manoeuvres. Clutch comfort is described with three rationales: overall duration of the operation (clutch slipping time); ease with which a torque target is met; and oscillations of the driveline after synchronization. For standing start all of these rationales are considered and for gear shift only the first and the third are considered as the driver has no acceleration target. The perceived clutch comfort is mainly affected by two elements: the total length of the engagement and the amplitude of the driveline oscillations following the synchronization. With introduction of an active element in the clutch control system, the possibility of several innovative solutions for improving the clutch comfort through a careful control of this additional degree of freedom is investigated. The experimental results obtained on a prototype vehicle equipped with an automated manual transmission have shown the actual comfort increase induced by this strategy.

2.1.2 Powertrain models with backlash

The deficiency of mentioned models in the chapter 2.1.1 can be summarized as the lack of backlash mechanism at the powertrain. Backlash is mainly caused by the play that exists between the teeth in the different gear components such as transmission and final drive. Also the clutch and the flywheel (especially dual mass flywheel) have minor amount of backlash, introduced in order to reduce vibrations. The drawback of backlash existence at the powertrain components is formation of high impact force when the direction of torque transfer changed: from engine to wheels as in the case for tip-in manoeuvre from wheels to engine as in the case for tip-out manoeuvre. The influence of backlash on the properties of the vehicle can be summarized as negative effect on noise emissions, driveability and quality impression.

2.1.2.1 Backlash modelling

There are a couple of backlash models available in the literature. Lagerberg summarised possible model structures as follows: dead zone model, simplified dead zone model, modified dead zone model and physical model [14]. The backlash models will be described using a shaft illustration. In figure 2.4, backlash is the described as the play within the shaft and quantized as $\pm \alpha$. Total travel of the shaft is 2α.

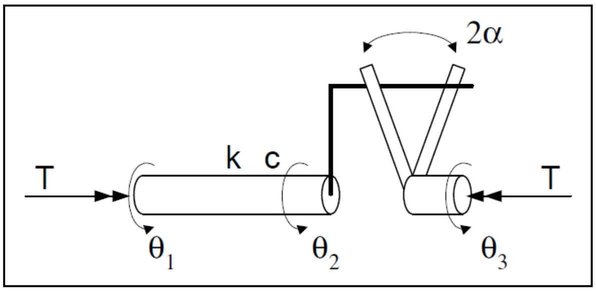

Figure 2.4 : Schematics of a shaft with backlash [8].

Dead zone model

Dead zone model fundamental relies on the fact that torque transmission is not valid during backlash crossing. Stiffness and damping of the shaft are described as k and c respectively and angular position of the shaft is defined at three points θ_1, θ_2 and θ_3. θ_1 and θ_3 are the input and output locations respectively where as θ_2 is defined as the location just before the fictitious backlash phenomenon. Total displacement of the shaft and transmitted torque are defined as equation 2.1 and 2.2 respectively.

$$\theta_d = \theta_1 - \theta_3 \tag{2.1}$$

$$T_{dz} = \begin{cases} k.(\theta_d - \alpha) + c.\dot{\theta}_d & \theta_d > \alpha \\ 0 & |\theta_d| < \alpha \\ k.(\theta_d + \alpha) + c.\dot{\theta}_d & \theta_d < -\alpha \end{cases} \tag{2.2}$$

Simplified dead zone model

In the case of no damping and the stiffness coefficient of the shaft is very big, the dead zone model can be simplified. In this case the system will switch between two distinct modes: contact mode and backlash mode where only one total mass and two unconnected mass exists respectively.

Modified dead zone model

In the modified dead zone model no torque is no torque is allowed from the damping term for the case of the rotation is in the inward direction. Using if-else condition transmitted torque is described at equation 2.3 using T_{dz} from equation 2.2.

$$T = \begin{cases} 0 & if\ T_{dz} < 0\ and\ \theta_d > 0\ or\ if\ T_{dz} > 0\ and\ \theta_d < 0 \\ T_{dz} & 0 \end{cases} \tag{2.3}$$

Physical model

The superiority of the physical model is that it includes one extra state variable (the position in backlash) resulting with the possibility of modelling both the backlash angle and the remaining twist of the shaft. The total displacement of the shaft, the position in the backlash and shaft twist are defined with the equations 2.4 and 2.5 respectively.

$$\theta_b = \theta_2 - \theta_3 \tag{2.4}$$

$$\theta_d - \theta_b = \theta_1 - \theta_2 \tag{2.5}$$

This model also contains the damping properties and the transmitted torque is stated as below:

$$T = k.(\theta_d - \theta_{b)} + c.(\dot{\theta}_d - \dot{\theta}_b) \tag{2.6}$$

where $\dot{\theta}_b$is defined with the following equation.

$$\dot{\theta}_b = \begin{cases} max\left(0, \dot{\theta}_d + \frac{k}{c}.(\theta_d - \theta_b)\right) & \theta_b = -\alpha \\ \dot{\theta}_d + \frac{k}{c}.(\theta_d - \theta_b) & |\theta_b| < \alpha \\ min\left(0, \dot{\theta}_d + \frac{k}{c}.(\theta_d - \theta_b)\right) & \theta_b = \alpha \end{cases} \tag{2.7}$$

2.1.2.2 Available powertrain models with backlash

In order to capture the shunt and shuffle phenomenon in vehicle drivelines Templin proposed powertrain model with backlash and tyre slip [15]. The model captures the drivetrain’s first order eigen frequency. The aim of the researcher was to use this introduced model at powertrain oscillations control therefore the easiness of model parameters determination was important. Author demonstrated that the model parameters, including the backlash size, can be estimated without using more than the existing engine torque signal and engine and vehicle speed measurements. Vehicle level experiments proved out the capability of the model with good correlation of simulations and vehicle level results considering driveline dynamics.

One of the recent models developed with backlash is for a continuously variable transmission (CVT) developed by Caruntu et al. [16] at MATLAB/Simulink environment. Modelled powertrain involves following components: engine, CVT, final reduction gear (FGR), flexible drive shafts and driving wheel. The backlash nonlinearities are considered between the flexible shafts and the wheel. Developed model is validated by via using Honda 1.6i ES CVT test vehicle and showed good correspondence.

Similarly Berriri et al. used a simplified model of the powertrain in order to cope with the high order powertrain systems nonlinearities [17]. Proposed model consisted of 2 inertias (1 representing engine flywheel and the other as vehicle mass) and 1 flexible shaft (only containing spring characteristics without damper properties) with backlash. Different to the previous studies, the authors represented all the powertrain characteristics within transfer function format (figure 2.5). System frictions of the engine and vehicle are represented with c_{eng} and c_{veh}. Additionally it is assumed that clutch is always engaged and the differential is locked (right and left driveshaft are turning with the same shaft speed). The inertias of gearbox, driveshaft and the wheels are neglected. The numerical values of the powertrain model are derived from the experimental data analysis and from the information provided by the manufacturer, in order to fit the Citroen Picasso.

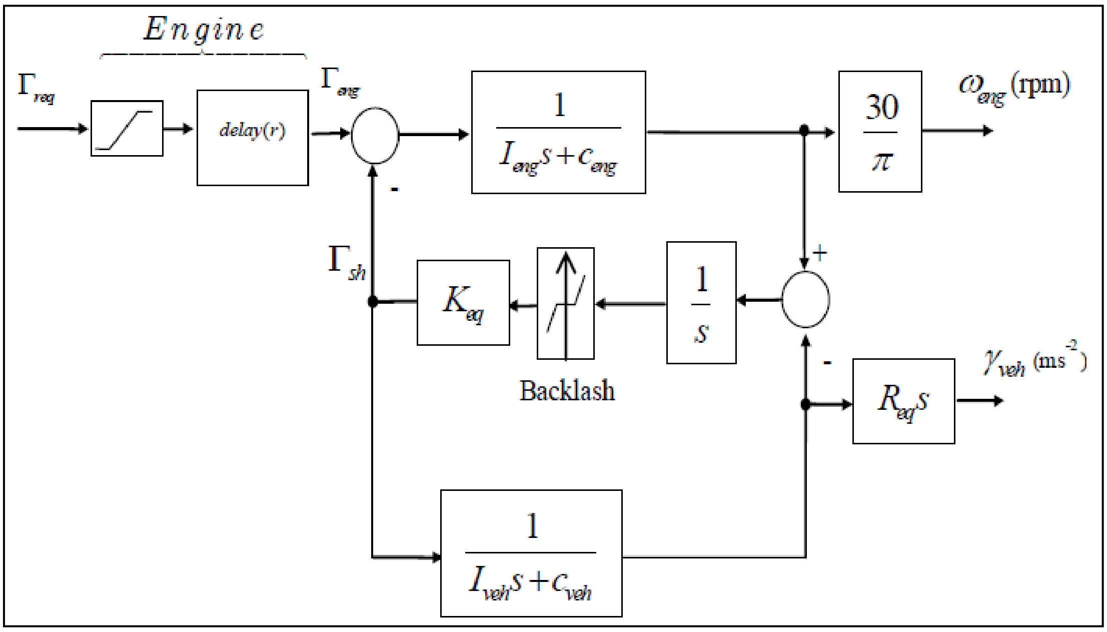

Figure 2.5 : Simplified model of the powertrain with transfer function representation [17].

2.1.3 Powertrain modelling with multi-body dynamics and hardware in the loop simulations.

Simulation of the powertrain components using multi-body simulation programs is also another important point of interest for researchers. Gotoh and Yakoub developed a high fidelity full multibody dynamics vehicle model using LMS commercial multibody code and investigated its use in virtual design and troubleshooting of a vehicle response to throttle input [18]. The model is then used to simulate different transient driveability events such as tip-in / tip-out and Wide Open Throttle (WOT) acceleration. Tiller et al. developed a detailed vehicle model in Modelica, consisting of the 3D vehicle chassis, engine, automatic gearbox and hydraulics to control the gearbox performed the simulations of these models using Dymola [19].

Hardware in the Loop (HIL) simulations allows vehicle systems and models to be tested in a simulation environment. Engines, vehicles, and other components that the engine control unit normally controls are replaced by high-fidelity models executed on a real-time computer system. Some of the vehicle or engine components may also be tested and evaluated in accordance with the models of the other components using the HIL systems. The method brings out several advantages over real component testing such as preventing damage to the components in case of extreme excitations due to uncalibrated control parameters or decreasing the development times via model based tuning as many control parameters may be tried with in loops of simulations. A HIL environment allows strong interaction between the modelling, hardware, control law development, and implementation issues in a realistic repeatable test laboratory [20].

2.2 Engine Brake Torque Estimation

Key parameter for engine control is the knowledge of the instantaneous torque developed, or its underlying cause, the in-cylinder pressure developed in each cylinder by the combustion process. In the absence of real-time torque measurement, torque estimation is usually achieved through look-up tables or empirical models (Current strategy in modern ECUs). However given the increase in engine operating parameters as well as engine operating regimes as a result of emission control and exhaust aftertreatment technologies, accurate torque estimation has become more challenging as well as necessary. Methods using real sensors give more accurate results but due to cost and durability issues could not attracted the desired attention from automotive manufacturers. As an alternative “virtual sensors” method is used for instantaneous torque estimation. The fact that virtual sensors do not have piece cost other than development expenses and have no durability issues, makes them favourable for mass production vehicles. However robustness issue is the substantial drawback of the method.

Brahma et al. developed a virtual sensor predicting torque based on a first law used regression model for estimating mean value engine torque on-board a diesel engine [21]. With a large number of parameters affecting torque; influenced from multiple injections, complex turbo machinery, high rates of exhaust gas recirculation (EGR), multiple combustion modes and extremely high rail pressures; it is challenging to make completely empirical models to be robust enough. The approach in the work is to not using engine parameters but to use the already existing measurements of flows, temperatures and pressures across the engine block control volume to perform an approximate energy balance based regression to estimate torque.

Catania et al. developed an innovative zero-dimensional predictive combustion model for Heat Release Rate (HRR) and in-cylinder pressure estimation. Starting from the injection parameters, the profile of the injection rate is calculated, which in turn allows the chemical energy release to be estimated [22]. This approach is based on the assumption that HRR is proportional to the energy associated with the accumulated mass of fuel within the combustion chamber at each time instant. The model is applied to each multiple-injection pulse separately, and a proper ignition delay is taken into account.

The inputs to the model are either quantities that are set by the ECU (Boost pressure & temperature, injection quantities) or parameters that are calculated from physically consistent correlations derived from a wide data set of engine working conditions, for different engines.

The main model outputs, in addition to the pressure traces, are: HRR, MFB50 (Mass Fraction Fuel Burn %50), PMAX (Maximum in Cylinder Pressure), IMEP (Indicated Mean Effective Pressure). The model was applied to a sample of steady state diesel combustion processes at different engine loads and speeds and for various EGR rates on different engine prototypes with CRs of 16.5, 15.5 and 15. Very good results were obtained in terms of MFB50, PMAX, IMEP and the pressure trace simulation, showing the capability of the model to properly capture the physics of in-cylinder processes.

Ponti et al. identified a zero-dimensional combustion model as the proper tool to observe the effects of the intake and injection pattern characteristics on the combustion process [23]. Each combustion phase is considered separately and modelled using the well-known Wiebe function. The energy release process therefore can be reconstructed using a proper combination of Wiebe functions, each of them characterized by a certain set of parameters.

The combustion model has been obtained using a linear combination of Wiebe functions and allows for extracting information related to each combustion (pre-mixed and diffusive) associated with each injection performed. This allowed for interpreting experimental data obtained by varying the injection pattern configuration in order to observe the influence of Pilot and Pre injections on combustion.

Filipi and Assanis developed a transient, single-cylinder, engine simulation module using steady-state zero-dimensional model as the foundation for the development [24]. Transient extension has involved the implementation of instantaneous engine torque and engine dynamics models on a crank-angle basis. Subsequently, the transient simulation has been validated against experimental results from a single-cylinder engine, and selected parametric studies have been performed to illustrate the model’s capabilities.

Katsumata et al. developed an engine torque estimation model via integrating physical and statistical combustion models [25]. Wiebe function is utilized to calculate the heat release rate in Gasoline engines in order to decrease modelling time and retain model accuracy. The combination of a heat release rate model (capable of estimating the heat release rate for various driving conditions and satisfies requirements for high accuracy and reduction of calibration points and development time) and an intake air estimation model is used to calculate the torque for each cycle from cylinder pressure. The torque estimation model is developed using testing data at steady state conditions. However transient response of the engine is validated using the proposed model. The model can calculate the cylinder pressure of the each cycle well and consequently the torque.

2.3 Driveability Improvement via Engine Torque Control

Vehicle driveability had become one of the major aspects of product quality and driveability refinement plays a key role in product differentiation in automotive world. Unrefined driveability calibration definitely results with undesired jerk motions and low frequency oscillations of the vehicle. The easiest method to reduce these low frequency oscillations is input torque filtering and rate shaping, however it results with vehicle performance degradation. Park et al. proposed Zero Vibration (ZV) input shaping method based on vehicle model resulted oscillation damping and period values on a manual transmission front wheel drive vehicle [26]. Authors compared ZV input shaping with input filtering and concluded that ZV input shaping is superior to input filtering as shock-jerk is reduced to %25 with the same delay time.

Automotive manufacturers’ engine control algorithms employ a similar input shaping and filtering method: so-called anti-jerk feature. Anti-jerk algorithms use look-up tables and main control strategy is to slew the pedal oriented torque request in an open loop control methodology especially in backlash transition region. Taking in to consideration the fact that there is no close loop control and anti-jerk feature is a subjective calibration methodology, outcome becomes strongly dependant on calibrator’s performance. Moreover filling look-up tables for all gear, engine speed and pedal position combinations requires significant amount of development time. Taking into consideration of these obstacles of the current driveability features, the subject of automated torque control for improved driveability is a state of the art research topic both within automotive manufacturers and academic researchers as it can be described as an optimization problem dealing with performance and comfort counter measures. There are a large number of studies reported in the area of automated engine torque control.

Richard et al. was one of the first researchers that employed the idea of using engine as an actuator in order to actively damp the powertrain oscillations [27]. The authors proposed a pole placement control design with a methodical choice of the closed loop poles location using a simplified linear model with time delay as the plant model. Similarly Lagerberg and Egardt evaluated for different controllers for powertrains with backlash: Simple PID controller, PID controller with torque compensator, simple active switching controller and modified switching controller.

[28]. The first two of the proposed controllers were linear. PID controller was relatively conservatively tuned to avoid too large jerk levels from the backlash impact and on the latter one shaft torque compensator was added to further reduce powertrain oscillations however could not be completely eliminated. The 3rd and the 4th controllers are switching between two modes: Contact and backlash modes. In contact mode, the controllers follow driver’s request acceleration setpoint and in backlash mode the engine side of the backlash is controlled towards contact with the wheel side in the appropriate direction. The controller is called active switching controller as it tries to get out of the backlash region. Models were only evaluated in simulation environment and ıt is concluded that linear models are robust but on the other side slower than the switching controllers. Similarly torque compensator improves controller performance with drawback of sensitivity to noise. Best performance is achieved with active controllers but more works needs to be done considering the robustness of the controllers.

Fredriksson et al. studied different linear controllers such as PID, “Pole Placement” and “LQG/LTR” (Linear Quadratic Gaussian / Loop Transfer Recovery) [29]. These were assessed using criteria like transient performance, parameters and noise sensitivity. The proposed “LQG/LTR” controller is evaluated as the most suitable of the investigated controllers as it is easy to tune, works satisfactory both in simulations as well as in real field trials. Bruce et al. proposed the concept of using a feedforward controller in combination with an LQ (Linear Quadratic) feedback [30]. Given the fact that engine torque capacity is limited for transient response, while calculating the reference signal for the feedforward algorithm, rate limiting and the reference governor methods were implemented. Proposed algorithms were validated in simulation environment with ideal model and an on purpose parameter error introduced cases. Baumann et al. developed two different control methodologies for anti-jerk control: A $H\infty$ controller using mixed sensitivity approach [10] and a model based predictive controller using Smith predictor approach to cover the system inherent dead-time [31], where controller gains were determined using root locus method. At both studies speed difference is used as the input variable output variable of the controller is corrective torque. Controller performance comparison with respect to a classical PD (Proportional and Derivative) controller has been drawn and superiority of the proposed methodology is demonstrated on the latter study.

Similarly Pettersson and Nielsen proposed a speed-control strategy including behaviour of the driveline in the control scheme [32]. The model based state-feedback controller calculates fuel amount reducing the low frequency driveline oscillations also hen facing nonlinear torque limitations from maximum torque and diesel smoke limitation algorithms. Berriri et al. developed a partial torque compensator in order to actively damp powertrain oscillations [17]. In similarity with the previous studies, developed controller uses engine speed measurement as input to the controller to calculate the corrective torque that will oppose to the shuffle phenomenon. Diversity of the proposed methodology from previous studies is that the control synthesis is more or less independent of the driveline characteristics and non linearities, as it is employing a simplified model of the engine without the precise characteristics of the driveline. Superiority of the methodology is that it may be tuned directly on the vehicle, considering the fact that post design tuning parameters are few and with clear meanings, the overall benefit over the previous approaches is a reduced cost and time for development. Webersinke et al. proposed two linear quadratic controllers: a comfort controller, which damps the driveline oscillations and a dynamic controller which guarantees a high dynamical performance [33]. Both control algorithms show improvement on system performance: enhanced driving comfort with reduced driveline resonances without loss of dynamics. Templin et al. developed an LQR (Linear Quadratic Regulator) formulation of a driveline anti-jerk controller which acts as a torque compensator and does not require any state reference trajectories [34]. The time derivative of the driveshaft torque is used as a virtual system output and regulated to zero resulting no need for reference variable. The controller output torque demand acts like a tuning factor for the driver’s torque request and asymptotically tracks original signal. The proposed methodology is extended with an optimization based handling of the backlash transition that limits the shunt phenomenon [35]. At both of the studies, results were verified by measurements in a heavy duty truck and show good improvement with respect to non-controller case. As a discrepancy to the previous studies, He et al. established a torque-based nonlinear predictive control approach with an additional torque load estimation component based on a mean value model of the internal combustion engine [36]. A proportional-integral observer is employed to estimate the torque load of the powertrain and a torque-based nonlinear predictive controller is designed by use of iterative optimization. One of the latest studies on the subject topic is held by Fang et al. [37]. Subjected study involves a new model reference approach using engine speed as a control objective letting the engine speed output follow the referred speed at any time by forcing the plant transfer function. A comparison of the used methodology with classical state space and PID (Proportional, Integral and Derivative) controllers shows that the proposed controller had better performance on speed, acceleration and torque control aspects.

Considering the superior properties of Model Predictive Control such as input/output constraints and capability to cope with measured and unmeasured disturbance, control strategy has gained significant interest recently in powertrain vehicle control applications. Lagerberg and Egardt proposed a MPC controller with constraints on input torque as maximum and minimum limitations and input torque rate and achieved promising performance results [38]. The authors compared the achievement with the theoretically optimal open loop performance with feedback controller and obtained similar performance. On the order than the authors also commented that due to the high computation requirement of the MPC algorithms, they need do made some simplifications on the model such that delays are ignored and all the state variables are measured. Xiaohui et al. employed MPC algorithm with a simplified 2 mass vehicle model without backlash with physical constraints of the driveline system mechanism, the maximum frequency response of the engine as actuator is restricted, it cannot provide a high drive torque or make the drive torque low very quickly [39]. Simulation results show that that the designed controller can deal with the contradictive requirements very well such as it not only improve driving comfort, but also guarantee fast dynamic response. Finally, the robustness of the controller against uncertainties is proved by the simulations with different settings. Similarly Yoon et al. proposed a MPC algorithm for vehicle longitudinal motion control with comfortability and acceleration power counter measures [40]. The authors used a simplified 2 mass vehicle model with flexible elements assumed at the driveshafts and developed a discrete form with varying sampling time and inherent input dead-segment. Control variables for the MPC scheme is chosen as the torsion as torsion angle of the driveshaft and its rate. Because of the essential process noise and measurement disturbance, the authors employed a Kalman filter to estimate the full state variables in the observer model. Model validation is performed at simulation environment and a comparison to direct P controller for torsion angle reduction is done. Balau and Lazar developed a MPC algorithm for dual-clutch powershift automatic transmissions with dry clutches using a state-space piecewise affine drivetrain model [41]. The proposed horizon-1 predictive controller based on flexible Lyapunov functions was tested in MATLAB/Simulink and proved good results and outperforms controllers obtained using typical methods such as PID control.

2.4 Conclusion

Powertrain first natural frequency originated oscillations introduce significant discomfort to vehicle characteristics for sudden load change manoeuvres and needs to be eliminated for good driveability attributes. Within this perspective automotive manufacturers and academic researchers developed several algorithms to damp these oscillations with the intent of without comprising for performance metrics. In general although many complex control structures has been demonstrated within the academic world, automotive manufacturers preferred to use simpler methods like input torque shaping or filtering without closed loop control, considering stability problems for the complex control algorithms and ECU capabilities. In order to employ control structures, simple or detailed powertrain modelling is required. Within the literature there are many work performed within this area, however in general 2 or 3 degree of freedom (mass models) are the most common one considering the simplicity of the model to work in alignment with the control structures.

Engine brake torque is used as the output signal in the control structures. However there is no guarantee that engine will provide the requested torque especially considering very fast torque change requests coming from the controller algorithms. Engine brake torque estimation is an important enabler considering the wellness of the driveability control algorithms. Within the literature there are many ways t estimate engine brake torque like zero or one dimensional models. But all off them rely on the steady state engine torque data obtained at normal ambient conditions. Therefore for accurate engine brake torque estimation, in cylinder pressure based combustion analysis is a state of the art topic.

Researched used many different control methodologies for active damping of the powertrain oscillations such as PID, H infinity, LGR and MPC controller. Among the others MPC has superiorities like coping with constrains and predicted and unpredicted disturbances. Thanks to recent developments in the MATLAB MPC control toolbox, using MPC algorithms has become considerable favourable in control problems.

3. ENGINE TORQUE CONTROL

Despite the mechanical control in conventional vehicles, due to stricter emission requirements, elevated customer expectations concerning driveability and fuel economy and reliability; motion control in modern vehicles operates electronically via Powertrain Control Modules (PCM). PCM receives several input signals from sensors like acceleration, clutch and brake pedal positions, vehicle speed, gear position, temperatures at various locations like intake air, coolant, oil, etc. and battery and state of charge of battery. Using these signals PCM governs actuators like fuel pumps, injectors, gas exchange system actuators (such as exhaust gas recirculation valve, variable geometry nozzle position, and electronic throttle body) in order to control the produced torque or engine and vehicle system actuators (such as electronic thermostat, alternator, active grill shutter in order to control the auxiliary functions.

Several function blocks are employed in state of the art engine control architectures however considering vehicle propulsion they can be classified into two main blocks: Engine torque demand and engine torque production control (Figure 3.1). These structures will be explained in the upcoming subsections. Briefly engine torque management control retrieves various torque demands like driver, cruise control, esp, hardware protection, driveability modules and apparently defines the instantaneous torque that will be generated from the internal combustion engine. Considering torque producing mechanism for a turbocharged diesel engines, right amount of air with the specified pressure and EGR ratio is compressed inside the cylinder via the reciprocating upwards movement of the cylinder piston to the cylinder head and near TDC (Top Dead Centre) the specified amount of pressurized fuel is injected into combustion chamber. As a result self-ignition occurs resulting combustion and consequently torque production.

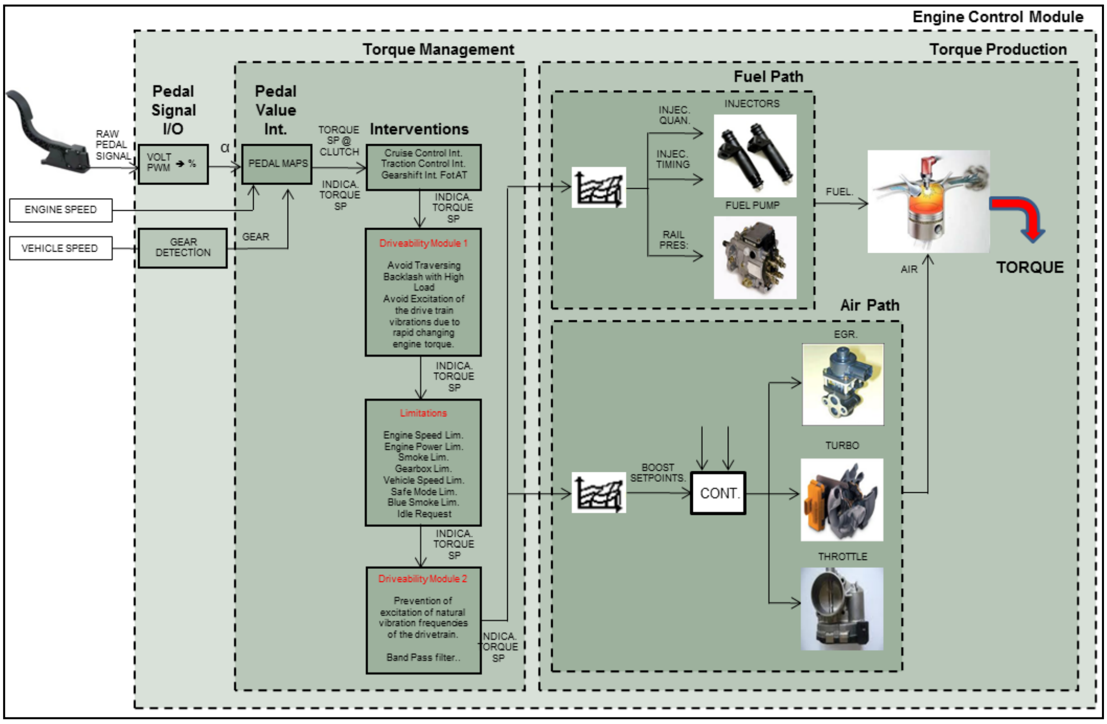
Engine Control Module
Torque Management
Torque Production
Pedal Signal I/O
Pedal Value Int.
Interventions
RAW PEDAL SIGNAL
VOLT PWM ➔ %
α
PEDAL MAPS
TORQUE SP @ CLUTCH
Cruise Control Int.
Traction Control Int.
Gearshift Int. FotAT
INDICA. TORQUE SP
ENGINE SPEED
VEHICLE SPEED
GEAR DETECTION
GEAR
Driveability Module 1
Avoid Traversing Backlash with High Load
Avoid Excitation of the drive train vibrations due to rapid changing engine torque.
Limitations
Engine Speed Lim.
Engine Power Lim.
Smoke Lim.
Gearbox Lim.
Vehicle Speed Lim.
Safe Mode Lim.
Blue Smoke Lim.
Idle Request
Driveability Module 2
Prevention of excitation of natural vibration frequencies of the drivetrain.
Band Pass filter..
Fuel Path
INJEC. QUAN.
INJEC. TIMING
RAIL PRES.
INJECTORS
FUEL PUMP
FUEL
AIR
TORQUE
Air Path
BOOST SETPOINTS
CONT.
EGR.
TURBO
THROTTLE

Figure 3.1 : Engine control module overview within a torque based strategy.

3.1 Engine Torque Management Control Structures

Conventional electronically controlled engine management strategies controls the fuel and air path quantities individually. As a result of the ever-growing number of interacting electronic vehicle control systems requirements, new control algorithms for the purpose of managing the increasing system complexity are generated. Torque based engine control architecture which uses a central torque demand variable to control all the combustion regulating qualities, is a very common and popular approach employed by several car manufacturer companies. The final torque demand variable is the result of the coordination of all torque requests and interventions from different subsystems such as driveability, hardware protection, electronic stability or transmission control modules.

In order to understand torque management structure, a systematic categorization of the block can be structured as flows:

1. Pedal Value Interpretation: The main functionality of the torque management structure is requesting the amount of torque that should be produced in the ideal case via the combustion from the torque production blocks. Considering the engine requirements at the instant of interest torque management modules interprets the

driver request from the pedals signals (clutch, brake, acceleration) and shift positions and converts it to a torque setpoint.

2. Interventions & Limitations: Previously obtained torque setpoint (can be indicated torque at the combustion chamber of the real brake torque at the output of the engine, clutch) is further processed by several modules such as external interventions (for example cruise and traction control, automatic gearbox), and limitations (such as engine speed and power, gearbox, smoke, vehicle speed, blue smoke and safe mode).

3. Driveability: Further processing of the previously obtained torque setpoint via the driveability modules generates a final torque setpoint (generally indicated) value that is fed to the torque production module. Driveability modules aim to deliver the driver requested torque as fast as possible without the error conditions stated during the driveability assessment section at the introduction part of this document. The common approach is to avoid excitation of the drivetrain vibrations due to rapid changing engine torque and traversing backlash with high load. In figure 3.2 torque slew algorithm for the load transition correction are shown for tip-in and tip-out manoeuvres. For the tip-in manoeuvre actual torque request is increased rapidly following the driver request up to a threshold point which is define with respect to engine speed and gear using 2D look up based maps. Afterward actual torque request is limitedly incremented again using 2D look up based maps with torque and engine speed inputs. There are separate maps for each gear. The common approach is to increase the torque rapidly up to a point close to backlash entrance, traverse the backlash with a low increment rate and afterwards increase the increment rate. For the tip-out manoeuvre similar to the tip-in one, torque is reduced rapidly following the driver request down to the threshold point which is define with respect to engine speed and gear using 2D look up based maps. Diversely there is a second threshold again defined with 2D map structure and torque decrement rate between these two thresholds are defined via using 2D look up based maps with torque and engine speed inputs for each gear individually. Once the torque request is below the second threshold, indicated torque is reduced to 0 immediately. Additionally prevention of the excitation of the natural vibration frequencies of the drivetrain is a major goal of the driveability modules which is issue with the anti-shuffle algorithm. Basically

oscillations are detected by high pass filtering of the deviation in engine speed with respect to vehicle speed.

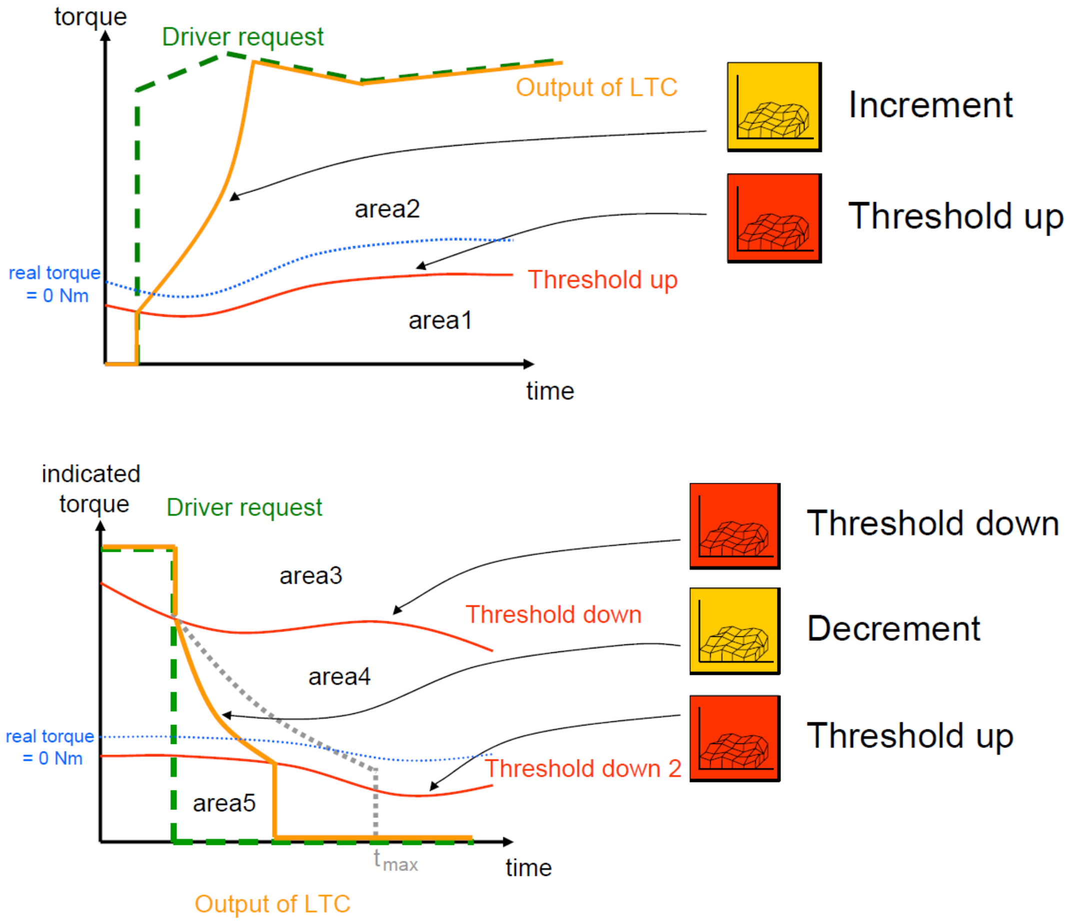
torque
Driver request
Output of LTC
Increment
area2
Threshold up
real torque
= 0 Nm
Threshold up
area1
time
indicated
torque
Driver request
Threshold down
area3
Threshold down
Decrement
area4
real torque
= 0 Nm
Threshold up
Threshold down 2
area5
t_{max}
time
Output of LTC

Figure 3.2 : Load transient correction (LTC) algorithm working principle for tip-in (upper subfigure) and tip-out (lower subfigure) manoeuvres.

3.2 Engine Torque Production Control Structures

Torque production module operates the several actuators in harmony using the inputs from the engine sensors in order to deliver the requested torque from the torque management module. In diesel engines the torque production module is generally categorized into two sections: Fuel and Air Paths. In order to deliver torque via the combustion process within the emissions and hardware requirements, inside the combustion chamber the correct amount of fuel should be met with the correct amount of air at the right timing. The air path aims to supply the requested air quantity and content (Fresh air and exhaust gas ratio) at the demanded pressure using the actuators like turbocharger boost pressure actuators, air intake throttles and EGR valves. The fuel path is responsible for delivering the requested amount of fuel at the correct fuel pressure within the desired injection pattern (number of minor injections and the timing between the minor injections). Thanks to the modern injection architecture and the common rail systems, injection pattern up to 5 or 6 minor injections and fuel pressures up to 2000 bar can be easily achieved in the current diesel engines. The properties of the air and fuel are defined considering the emission requirements, engine stability conditions and the hardware limits.

The common approach for the combustion management is the usage of look up table based strategy. Most of the look up tables in combustion control uses the engine speed and indicated torque setpoint values as the inputs, and defines the quantity of the control variable. Such a structure is very robust as it does not have any controller which may cause instabilities depending on the performance of the controller. Look up tables are filled with air and fuel quantity setpoints in which the required data is maintained with engine dynamometers test generally at steady state conditions and normal ambient conditions. For different environmental temperature and altitude conditions some correction algorithms are applied, however validation of these algorithms is subjected to very limited amount of test data. Considering the look up tables based structure the drawback of the current torque production strategy is lack of conformity of the produced torque, especially at transient conditions or at different operating points that the normal ambient conditions. Current algorithms in engine control modules do not use a torque feedback control strategy using direct or indirect torque measurement sensors. The obstacle behind the issue is the high cost of sensors considering production vehicles and the robustness problems as such kind of sensor are very fragile for deterioration after long operating hours. Only for on board diagnosis (OBD) purposes some primitive engine speed related torque estimation algorithms are employed.

3.3 Proposed Torque Management Control Module

Conventional torque management structures in modern vehicles operate without any driveability feed-back signals from vehicle apart from some stability modules like ESP or TCS. Control structure is totally open loop and is generally based on look up table based structures from the acceleration pedal position, engine speed and gear inputs in section. On a general aspect certain amount of torque is requested and generated via combustion however the effect of generated torque on vehicle motion is not evaluated within the engine control module especially considering driveability perspectives. There are some simple feed forward torque correction algorithms (within driveability modules) which modulate torque request like “anti-shuffle” and “torque slewing” algorithms in order to minimize the jerk effects and the damp the first order natural frequency oscillation.

As there is no closed loop control which can improve driveability considerably via eliminating the error states, in automotive companies for every vehicle program, it takes significant amount of time for the calibration process of torque management structures. Moreover the driveability calibration is performed with subjective evaluation (very few attributes can be objectively evaluated) and is strongly depended to the capabilities of the calibrator. Finally a production representative vehicle is essential for the calibration process otherwise hardware and software changes in the program will require re-performing the driveability.

This study contains development of a model based vehicle longitudinal motion control structure. Proposed torque demand control algorithm with MPC algorithm is depicted at figure 3.3. In this structure an engine model and vehicle model including drivetrain are constructed. Using the developed models, motion response of the vehicle to the predicted torque input is estimated and an automatic torque correction process based on MPC and proportional control is applied for obtaining driving smoothness and eliminating error states. Such an approach definitely improves driveability of the vehicle and decrease the amount of time spent on driveability calibration. Another benefit of the automated process is elimination of the subjective calibration development and evaluation. The brand DNA of the company within the driveability perspective can be applied to all vehicles lines in production easily. Moreover driveability calibration can be constituted even without having a production representative vehicle as further changes can be easily implemented via model based calibration. Additionally such an approach will foresee many possible problems in terms of driveability during hardware selection prevent occurrence.

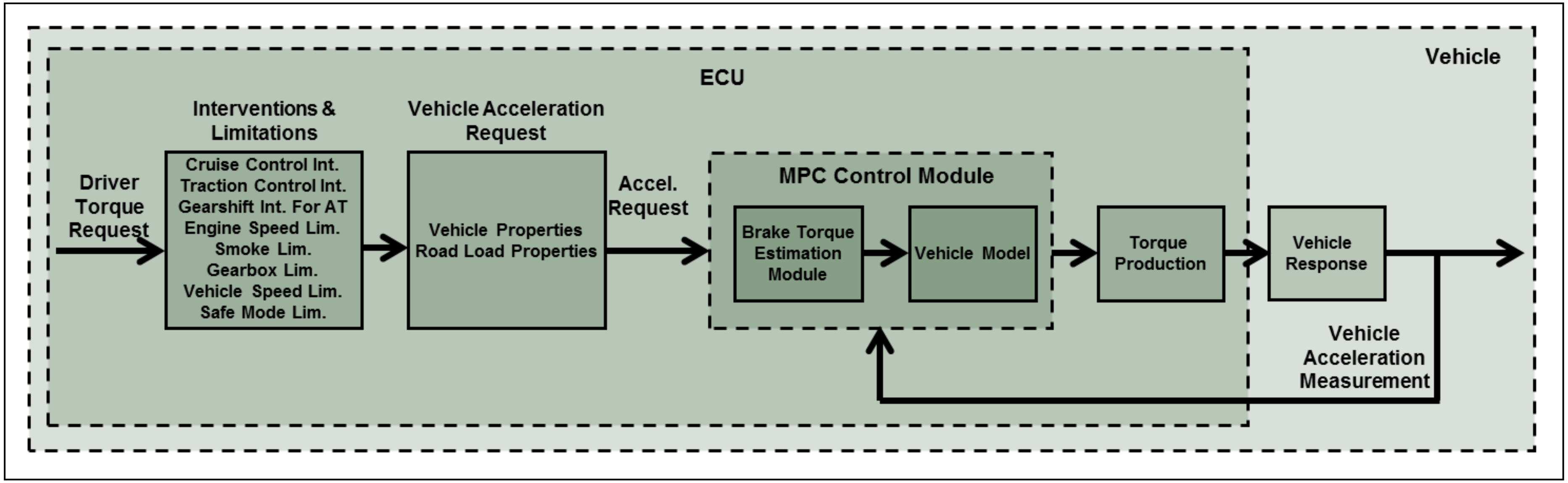
Vehicle
ECU
Interventions & Limitations
Vehicle Acceleration Request
Driver Torque Request
Cruise Control Int.
Traction Control Int.
Gearshift Int. For AT
Engine Speed Lim.
Smoke Lim.
Gearbox Lim.
Vehicle Speed Lim.
Safe Mode Lim.
Vehicle Properties
Road Load Properties
Accel. Request
MPC Control Module
Brake Torque Estimation Module
Vehicle Model
Torque Production
Vehicle Response
Vehicle Acceleration Measurement

Figure 3.3 : Proposed torque demand control algorithm with model based control.

3.4 Conclusion

Thanks to the recent technological developments in electronics industry that automobiles are equipped with complex electro mechanical structures enabling control of several combustion related engine and vehicle functions like producing torque or driveability control consequently. Modern ECUs are capable of possessing thousands of signals within tens of milliseconds and producing the control signals for the related actuators. Combustion process is generally controlled with look up table based structures considering the easiness and stability of the process resulting lack of accuracy especially for transient manoeuvres and different environmental conditions. Considering the importance of driveability characteristics, several algorithms are employed with ECU for vehicle longitudinal motion control. Due to possible stability problems, automotive manufacturers prefer to use simple input shaping and filtering algorithms with the perspective of driveability control. The idea behind the logic is damp rise and fall rates of the engine produced torque request and tempering the resulted jerk motions. However this results with compromising from vehicle performance. Additionally due to lack of closed loop feedback, current driveability algorithms cannot guarantee successful results at all conditions. Proposed methodology within this thesis is to use an in cylinder based engine brake torque model with an MPC controller in order to actively damp the powertrain oscillations without compromising from vehicle performance.

4. IN CYLINDER PRESSURE BASED ENGINE BRAKE TORQUE MODEL

In turbocharged diesel engines the intake air is pressurized using the exhaust energy of the combustion gases. A turbine at the exhaust side of the engine is used to rotate the close-coupled shaft of the compressor at the intake side for the purpose of pressurizing the intake air. However due to the nature of turbocharger, the turbo lag effect deteriorates the performance of the boost build up process especially at transient acceleration manoeuvres. Modern engines try to overcome this phenomenon via using variable geometry turbo wanes or smart waste-gates. Using such actuators smaller turbochargers can be selected which reduces turbo lag issues and do not over-speed at high engine speed, consequently exhaust flow rate conditions. Combined with the transient combustion effects, turbo lag significantly deteriorates torque production. For a moderate transient cycle such as FTP-75 (Federal Test Procedure 75: Cycle used for emission homologation at U.S.) the turbocharger lag resulted torque deficiency can be as much as 10 to 15%. Considering the above stated vehicle control algorithms such an error is almost intolerable. Therefore transient torque estimation algorithm is essential for the sake of model based vehicle driveability control.

Within the scope of this study, a brake torque estimation model is generated using basic PCM signals like air pressure and quantity, fuel quantity and timings, rail pressure, etc… based on simple heat release assumptions. An airpath model for inlet manifold gas properties is generated using the vehicle sensors and estimation outputs from ECU (Mass airflow sensor output at the air box, the manifold pressure sensor output upstream of the EGR mixture tube, exhaust manifold pressure estimation based on exhaust model and turbocharger turbine efficiency mapping data). Additionally EGR rate is calculated again using mass airflow data and vehicle volumetric efficiency information. Afterwards a stochastic heat release and in-cylinder pressure model is developed depending on air and fuel properties at the combustion chamber. Wiebe function is used to for each combustion event while estimating in cylinder pressure pattern. Cylinder pressure model parameters are tuned for steady state conditions. In cylinder pressure model is verified with real measurements on the engine using pressure sensors and indicating software with AVL Indimicro in cylinder pressure measurement equipment (Figure 4.1). Indicated torque is calculated from in cylinder pressure data. Figure 4.2 shows a typical AVL Indicom software cylinder pressure measurement data. The knowledge of friction and accessory torque losses is essential for brake torque determination from indicated torque estimation. Fortunately ECU torque loss structure already has this capability.

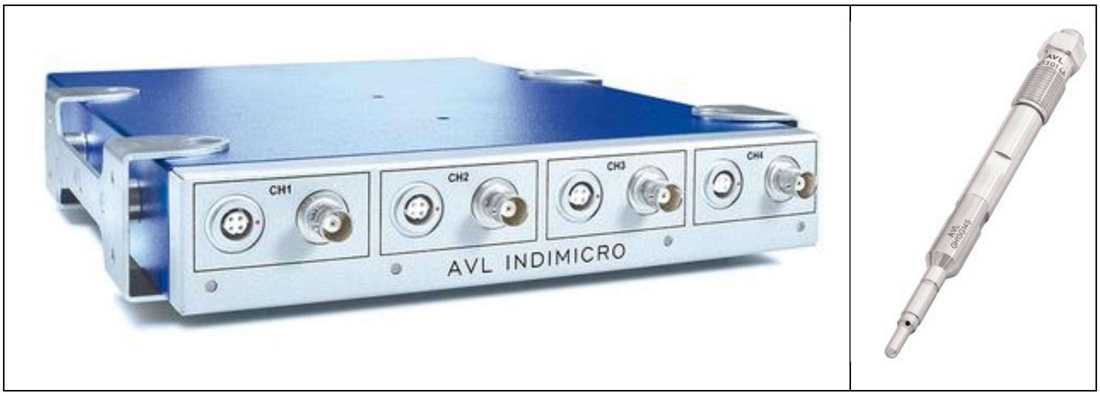
CH1
CH2
CH3
CH4
AVL INDIMICRO
AVL

Figure 4.1 : In cylinder pressure measurement equipment (Left: AVL Indimicro module, Right: AVL cylinder pressure sensor) [42].

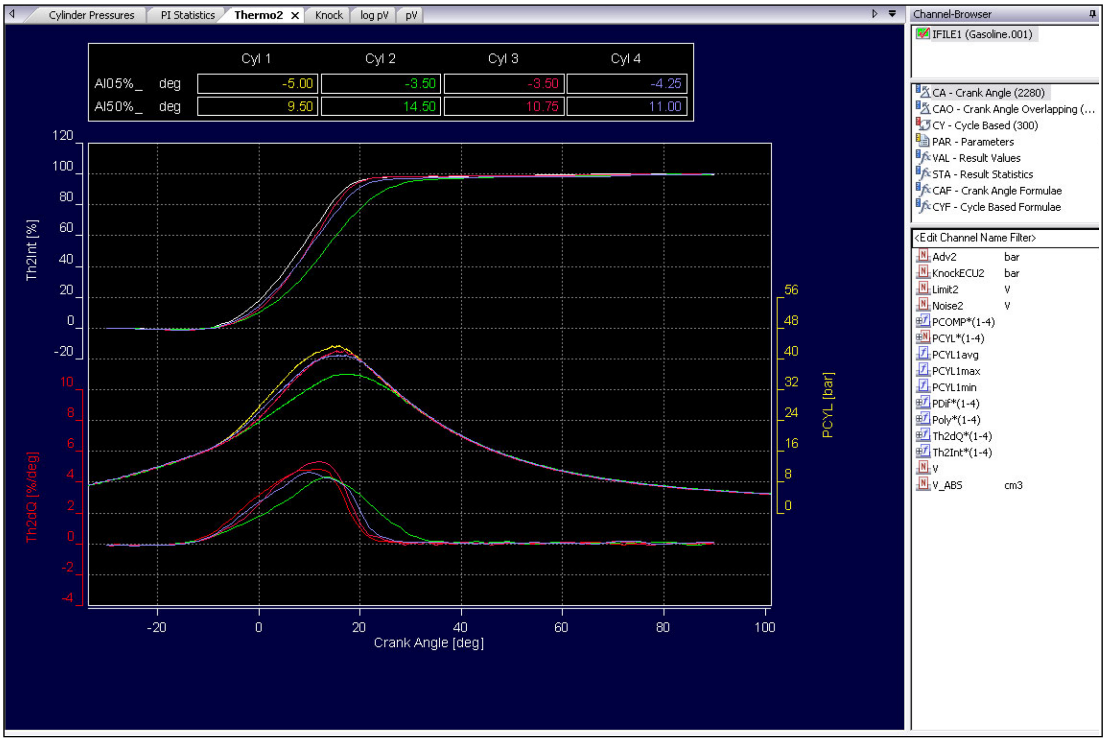
Cylinder Pressures
PI Statistics
Thermo2
Knock
log pV
pV
Channel-Browser
Th2Int [%]
Th2dQ [%/deg]
PCYL [bar]
Crank Angle [deg]
120
100
80
60
40
20
0
-20
10
8
6
4
2
0
-2
-4
56
48
40
32
24
16
8
0
-20
0
20
40
60
80
100

		Cyl 1	Cyl 2	Cyl 3	Cyl 4
AI05%_	deg	-5.00	-3.50	-3.50	-4.25
AI50%_	deg	9.50	14.50	10.75	11.00

IFILE1 (Gasoline.001)

CA - Crank Angle (2280)
CAO - Crank Angle Overlapping (...
CY - Cycle Based (300)
PAR - Parameters
VAL - Result Values
STA - Result Statistics
CAF - Crank Angle Formulae
CYF - Cycle Based Formulae

<Edit Channel Name Filter>

Adv2	bar
KnockECU2	bar
Limit2	V
Noise2	V
PCOMP*(1-4)	
PCYL*(1-4)	
PCYL1avg	
PCYL1max	
PCYL1min	
PDif*(1-4)	
Poly*(1-4)	
Th2dQ*(1-4)	
Th2Int*(1-4)	
V	
V_ABS	cm3

Figure 4.2 : Indicom software in cylinder pressure measurement screen.

4.1 Brake Torque Estimation Model

The brake torque estimation model in this study is based on predicting in cylinder pressure with respect to crank angle. Basic ECU parameters like injection quantities and start of injections, rail pressure, inlet and exhaust manifold properties are used. Prototype two litre inline 4 cylinder turbocharged diesel engine used in the model validation which has EGR flow with EGR cooler component. The engine is equipped with a high pressure common rail system with maximum pressure up to 2000 bar. Fuel system is capable of up to 6 interrupted injections in one stroke depending on rail pressure and engine speed. Current ECU software is equipped with MAF (Mass Air Flow), TMAP (Manifold Air Pressure and Temperature), SPGS (Single Port Gauge Pressure Sensor) for exhaust manifold pressure, EGT (Exhaust Gas Temperature) and engine coolant temperature sensors (Figure 4.3).

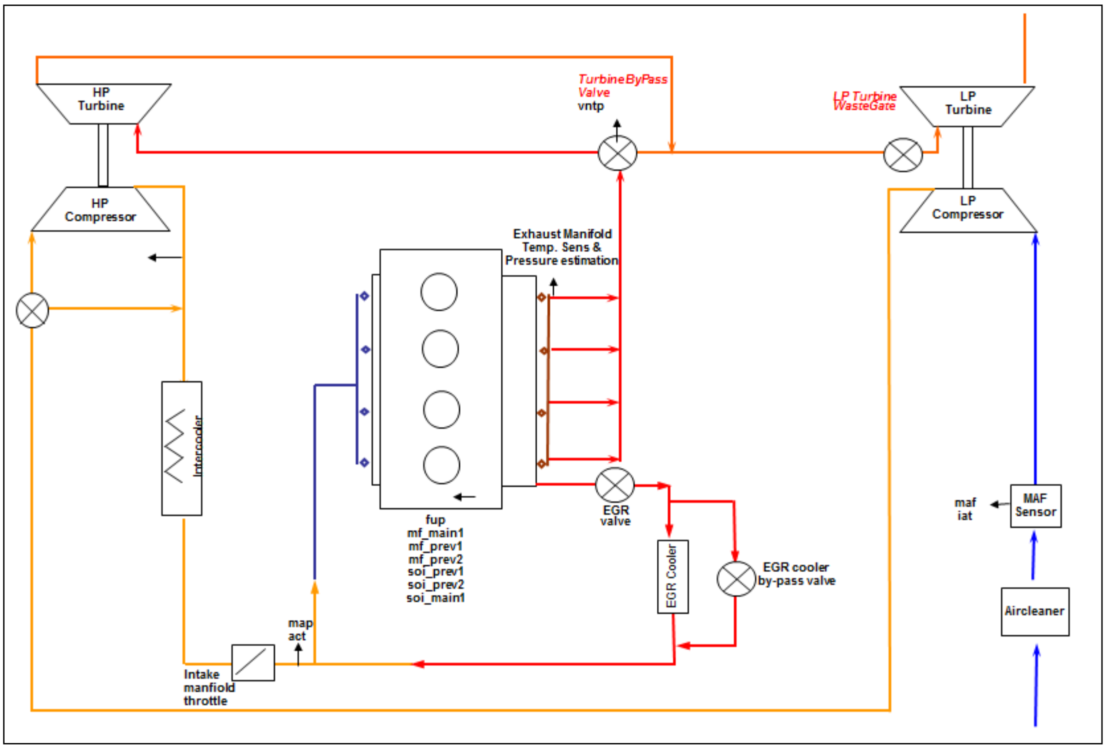
HP
Turbine
TurbineByPass
Valve
vntp
LP Turbine
WasteGate
LP
Turbine
HP
Compressor
LP
Compressor
Exhaust Manifold
Temp. Sens &
Pressure estimation
Intercooler
fup
mf_main1
mf_prev1
mf_prev2
soi_prev1
soi_prev2
soi_main1
EGR
valve
EGR Cooler
EGR cooler
by-pass valve
maf
iat
MAF
Sensor
Aircleaner
map
act
Intake
manfiold
throttle

Figure 4.3 : Airpath model schematics of 2.0 litre diesel bi-turbo engine.

Exhaust gas properties are very well known for all conditions; however intake air properties are not known for EGR (Exhaust Gas Recirculation) flow enabled conditions. A simple airpath model was generated for calculating intake manifold air temperature (Figure 4.4). For this purpose already built-in ECU feature volumetric efficiency map is used for total charge capacity (Figure 4.5). As fresh air mass flow is measured with sensor, EGR flow is calculated via subtraction fresh air from total air flow.

$$m_{egr} = m_{charge} - m_{maf} \tag{4.1}$$

Table 4.1 : ECU parameters and variable names used for in cylinder pressure calculation.

Parameter	ECU Variable
Engine Speed	Epm_nEng
Airflow Through Air box	Afs_dm
Inlet Manifold Pressure	Air_pIntkVUs
Inlet Manifold Temperature	Air_tCACDs
Exhaust Manifold Pressure	ASMod_pExhMnfUs
Exhaust Manifold Temperature	ASMod_tExhMnfUs
Fuel Pressure	RailP_pFlt
Total Injection Quantity	InjCrv_qSetUnBal
Main Injection Quantity	InjCrv_qMI1Des
Pilot 1 Injection Quantity	InjCrv_qPi2Des
Pilot 2 Injection Quantity	InjCrv_qPi2Des
Main Injection Timing	InjCrv_phiMI1Des
Pilot 1 Injection Timing	InjCrv_phiPi1Des
Pilot 2 Injection Timing	InjCrv_phiPi2Des

EGR cooler downstream temperature is calculated via using EGR cooler efficiency curve with respect to EGR flow provided by the supplier.

$$T_{egr} = T_{exh}\ \epsilon_{egrcooler}(T_{exh} - T_{coolant}) \tag{4.2}$$

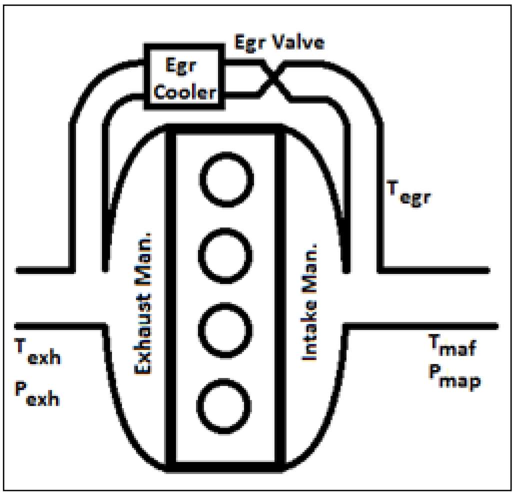

Figure 4.4 : General schematic of engine gas air flow system.

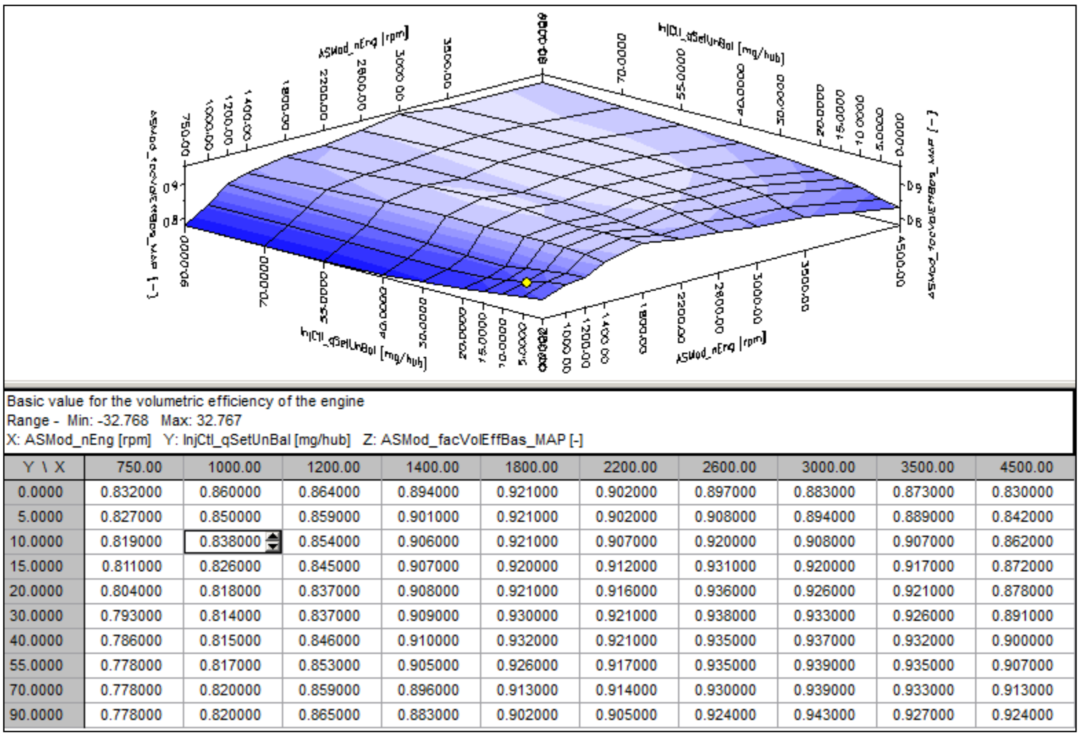
ASMod_nEng [rpm]
750.00
1000.00
1200.00
1400.00
1800.00
2200.00
2600.00
3000.00
3500.00
4500.00
InjCtl_qSetUnBal [mg/hub]
90.0000
70.0000
55.0000
40.0000
30.0000
20.0000
15.0000
10.0000
5.0000
0.0000
0.9
0.8
ASMod_facVolEffBas_MAP [-]

Basic value for the volumetric efficiency of the engine
Range - Min: -32.768 Max: 32.767
X: ASMod_nEng [rpm] Y: InjCtl_qSetUnBal [mg/hub] Z: ASMod_facVolEffBas_MAP [-]

Y \ X	750.00	1000.00	1200.00	1400.00	1800.00	2200.00	2600.00	3000.00	3500.00	4500.00
0.0000	0.832000	0.860000	0.864000	0.894000	0.921000	0.902000	0.897000	0.883000	0.873000	0.830000
5.0000	0.827000	0.850000	0.859000	0.901000	0.921000	0.902000	0.908000	0.894000	0.889000	0.842000
10.0000	0.819000	0.838000	0.854000	0.906000	0.921000	0.907000	0.920000	0.908000	0.907000	0.862000
15.0000	0.811000	0.826000	0.845000	0.907000	0.920000	0.912000	0.931000	0.920000	0.917000	0.872000
20.0000	0.804000	0.818000	0.837000	0.908000	0.921000	0.916000	0.936000	0.926000	0.921000	0.878000
30.0000	0.793000	0.814000	0.837000	0.909000	0.930000	0.921000	0.938000	0.933000	0.926000	0.891000
40.0000	0.786000	0.815000	0.846000	0.910000	0.932000	0.921000	0.935000	0.937000	0.932000	0.900000
55.0000	0.778000	0.817000	0.853000	0.905000	0.926000	0.917000	0.935000	0.939000	0.935000	0.907000
70.0000	0.778000	0.820000	0.859000	0.896000	0.913000	0.914000	0.930000	0.939000	0.933000	0.913000
90.0000	0.778000	0.820000	0.865000	0.883000	0.902000	0.905000	0.924000	0.943000	0.927000	0.924000

Figure 4.5 : Volumetric efficiency map used in ECU for 2 lt diesel turbocharger engine.

Residual gas pressure in the combustion chamber is calculated according to the below empiric formula where N is the engine speed.

$$P_r = P_{exh}\,(1 + A\,N/1\,e^{-4}) \tag{4.3}$$

Similar formula is used for intake stroke in cylinder pressure.

$$P_i = P_{man}\,(1 + B\,N/1\,e^{-4}) \tag{4.4}$$

A & B coefficients are determined experimentally for each speed and load condition. For the compression stroke till start of combustion, in cylinder pressure curve is calculated according the polytrophic compression. As reference pressure and volume conditions at bottom death centre is taken into account.

$$p\,V^k = p_0\,{V_0}^k = C \tag{4.5}$$

The differential first law for this model for a small crank angle change, dQ, is:

$$dQ - dW = dU \tag{4.6}$$

Using the following definitions, Q : heat release , $dW = P\ dV$ and , $dU = m\ \ c_v\ dT$, $R = \ C_p - C_v$ and $k = \ {}^{c_p}/_{c_v}$, and differentiating according to crank angle θ energy equation becomes as follows:

$$\frac{dP}{dQ} = \frac{k-1}{V}\frac{\partial Q}{\partial \theta} - k\ \frac{P}{V}\frac{dV}{d\theta} \tag{4.7}$$

For heat release term, $\frac{dQ}{d\theta}$, Wiebe function for the burn fraction is used.

$$f\ = 1 - exp\left[-a\left(\frac{\theta - \theta_0}{\Delta\theta}\right)^n\right] \tag{4.8}$$

where:

f = fraction of heat added

θ = crank angle

θ_0 = angle of the start of the heat addition

$\Delta\theta$ = duration of the heat addition (length of burn)

a = Wiebe function coefficient 1

n = Wiebe function coefficient 2

Heat release, ∂Q, over the crank angle change, $d\theta$, is:

$$\frac{\partial Q}{d\theta} = Q_{in}\frac{df}{d\theta} \tag{4.9}$$

where Q_{in} is the total heat for the particular injection calculated from the quantity of the injection and specific heat value.

4.2 Indicated Mean Effective Torque Calculation

An indicator diagram plots cylinder pressure versus combustion chamber volume (Figure 4.5), and clearly indicates the work as the area encircled clockwise by the trajectory. The area which is encircled clockwise represents the positive work produced by combustion. The very narrow area which is encircled counter clockwise represents the work required to pump gases through the cylinder.

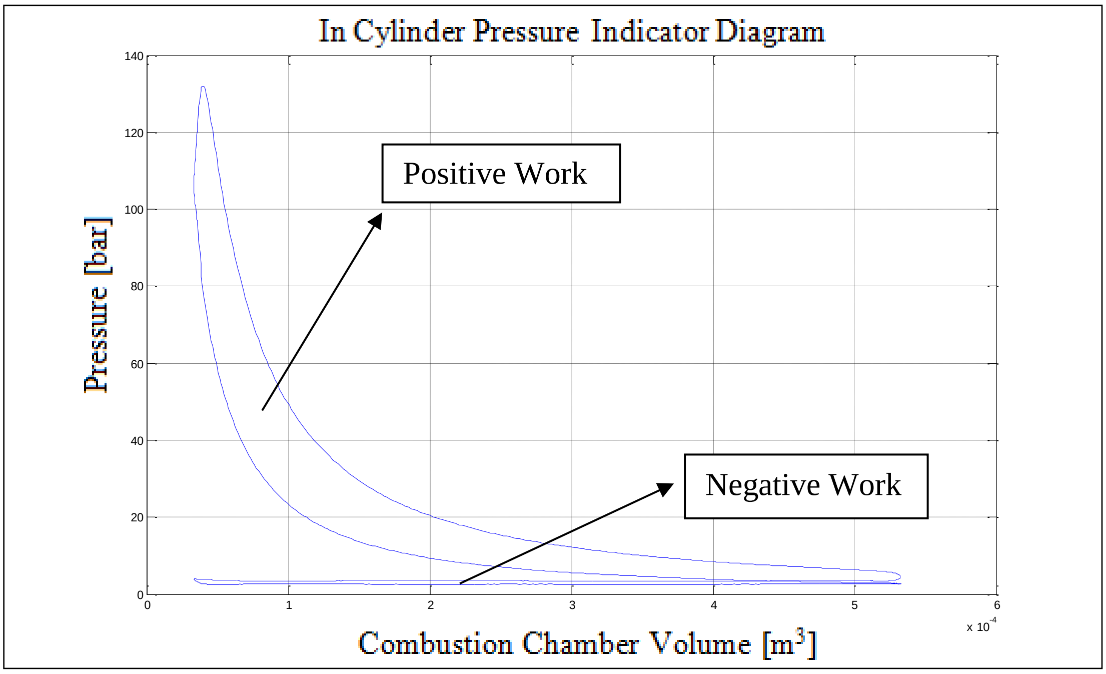

Figure 4.6 : Sample Indicator diagram.

In order to calculate work done in the indicator diagram combustion chamber volume with respect to crank angle should be calculated. The basic geometry of a reciprocating internal-combustion engine is shown in figure 4.6. The figure includes cylinder, piston, crank shaft, and connecting rod, and most geometric and kinematic properties of the engine can be derived from the below simple schematics. Below equations are derived using basic kinematics crank & rod mechanism.

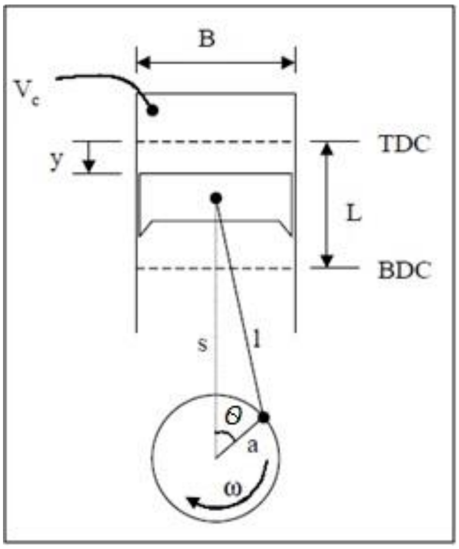

Figure 4.7 : Piston Schematics.

Where *B* = Bore, *L* = Stroke, *l* = Connecting rod length, V_c = Clearance volume, a = Crank radius, and θ = Crank angle.

The vertical position of the piston is completely determined by the crank angle θ. Cosine theorem can be applied to the triangle formed by the connecting rod, the crank, and the vertical line connecting the piston bolt and the centre of the crank shaft.

$$l^2 = s^2 + a^2 - 2\, a\, s \cos(\theta) \tag{4.10}$$

Vertical piston position relative to the TDC can be expressed as

$$z = l + a - s \tag{4.11}$$

After making necessary arrangements, piston position is obtained as follows.

$$z(\theta) = l + a\,(1 - \cos(\theta)) - (l^2 - a^2 \sin^2(\theta))^{1/2} \tag{4.12}$$

At TDC, the volume of the combustion chamber is the clearance volume, V_c. For any other crank position, the combustion chamber volume is the sum of the clearance volume and a cylindrical volume with diameter B and height y. So, the combustion chamber volume can be expressed as a function of the crank angle

$$V(\theta) = V_c + \frac{\pi\, B^2}{4} z(\theta) \tag{4.13}$$

The mechanical work transferred from the cylinder gases to the piston during the course of one thermodynamic cycle is called the indicated work, and is given by

$$W_{c,i} = \int_{\theta=-2\pi}^{\theta=2\pi} p(\theta)\, dV(\theta) \tag{4.14}$$

Calculation of in cylinder pressure was given in the previous section. Indicated torque is calculated using the below equation, where n_c is number of cylinders.

$$InTQ = W_{c,i}\, \frac{n_c}{4\pi} \tag{4.15}$$

Brake torque is calculated via subtraction the friction and front end accessory drive (FEAD) losses from the indicated torque values.

$$brTQ = InTQ - T_{Loss.Fric} - T_{Loss.Fead} \tag{4.16}$$

4.3 In Cylinder Pressure Measurement

In order to validate the brake torque estimation model for steady state conditions, in cylinder pressure measurements is carried out on the prototype engine. In cylinder pressure measurement is performed using special high frequency pressure transducers. The transducers are placed instead of the glow plugs using special adapters. High frequency engine speed measurement is performed using a speed encoder mounted on the crank pulley. AVL Indicom indicating software is used for data acquisition. Integrated system is capable of having pressure date with 0.5 degree crank angle resolution (Figure 4.7). Indicom measurements consist of 100 consecutive 4 stroke engine revolutions. Mean value of all measurements for all cylinders are used for the analysis used in this study.

4.4 Results and Conclusion

4.4.1 Steady state results

Engine mapping data is taken between 1000 rpm to 4500 rpm with 250 rpm interval and 0 Nm to 450 Nm (limited with full load curve) with 16 Nm (1 BMEP) interval (Figure 4.8). Oil and coolant temperatures are conditioned to 90℃ and maximum boost temperature is set to 50℃. 3 different injection strategies are applied for the whole engine mapping process: Main only, Pilot2 + Main and Pilot1 + Pilot2 + Main. Table 4.2 summarizes the operating points speed and torque values and fuel and air parameters quantities at these operating points. 3 detailed simulations are visualized where the injection patterns are twin pilot + main, single pilot + main and main only covering whole injection pattern.

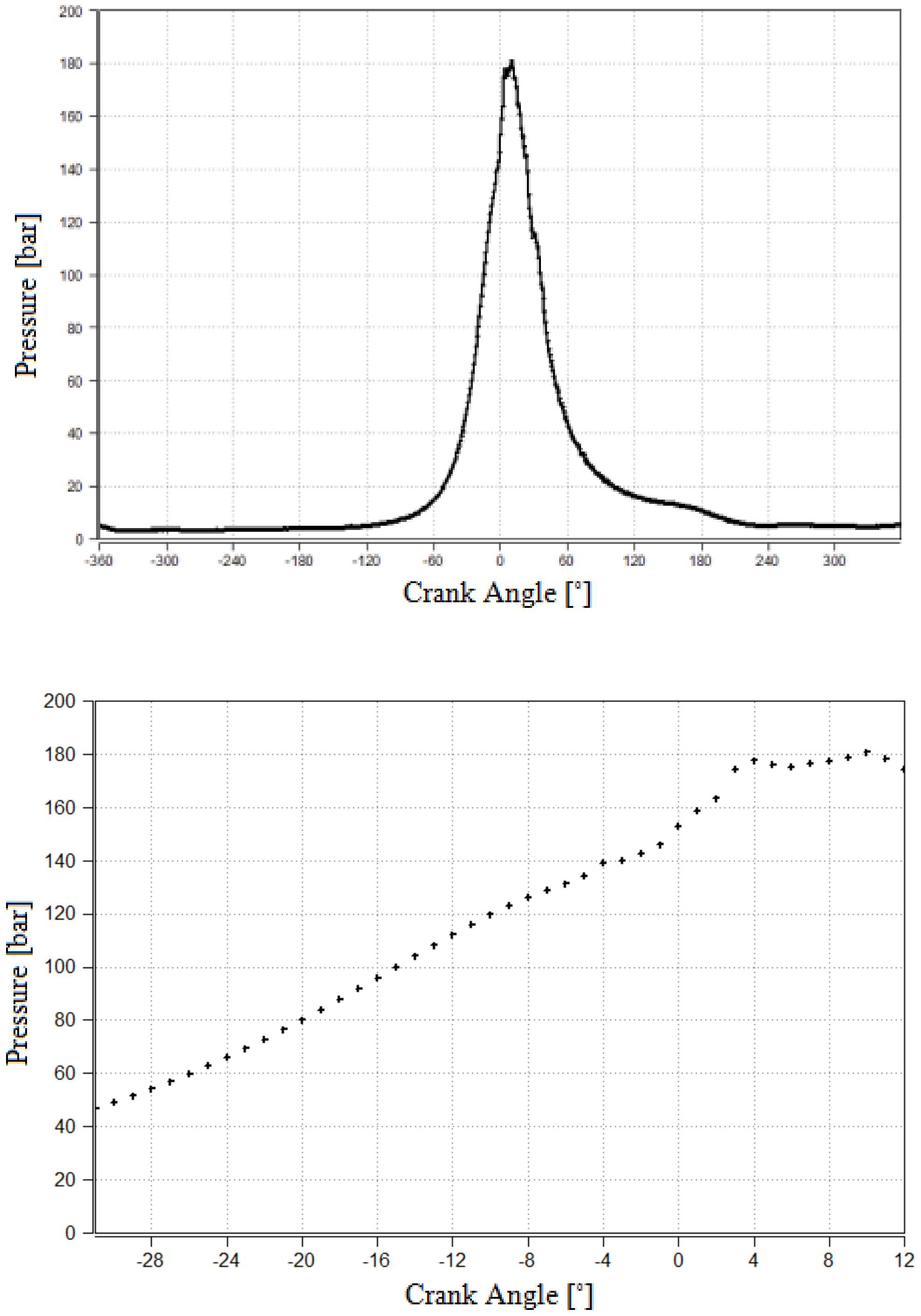

Figure 4.8 : In cylinder pressure data with 0.5 degree crank angle resolution (upper sub-figure: w.r.t. 720 degree crank angle, lower sub-figure: w.r.t. 42 degree crank angle)

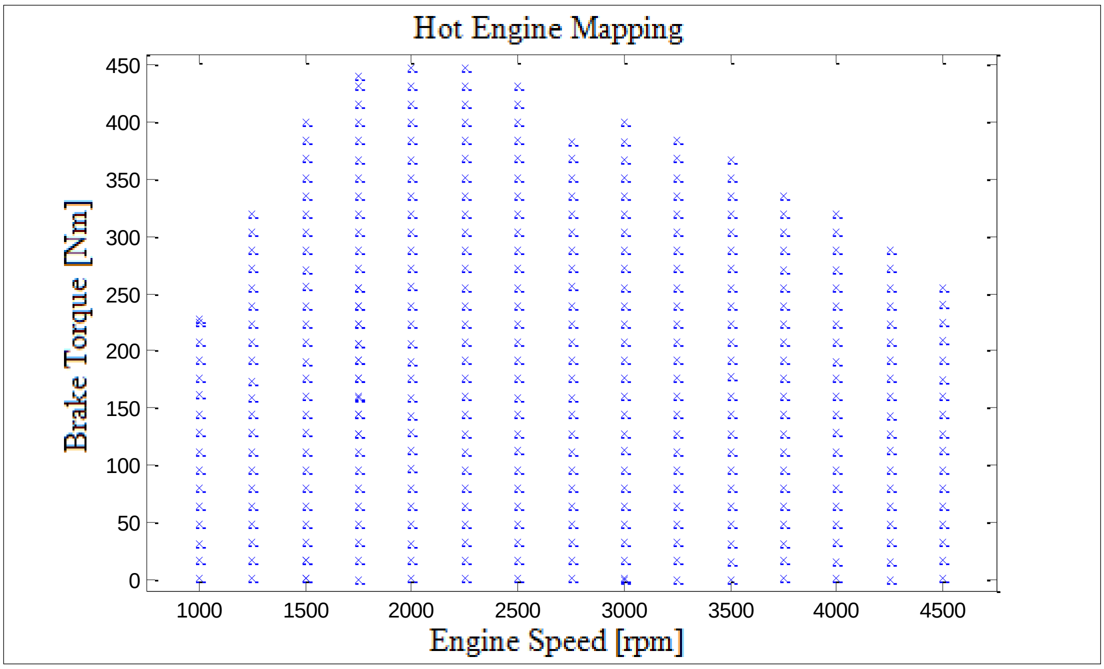

Figure 4.9 : Engine mapping points.

Table 4.2 : Simulation parameters for different injection patterns.

	Simulation 1	Simulation 2	Simulation 3
Engine Speed	2250	2150 rpm	3500 rpm
Torque	240 Nm	160 Nm	391.5 Nm
Airflow Through Air box	281 kg/h	281 kg/h	617 kg/h
Inlet Manifold Pressure	2580 mbar	2225 mbar	2940 mbar
Exhaust Manifold Pressure	3390 mbar	3010 mbar	2900 mbar
Fuel Pressure	1550 bar	1200 bar	2000 bar
Total Injection Quantity	43.2 mg/str	27.9 mg/str	77.9 mg/str
Pilot 1 Injection Quantity	1.5 mg/str	1.6 mg/str	0 mg/str
Pilot 2 Injection Quantity	1.7 mg/str	0 mg/str	0 mg/str
Main Injection Quantity	40 mg/str	26.35 mg/str	77.91 mg/str
Pilot 1 Injection Timing	22.1 ˚ (BTDC)	12.47 ˚(BTDC)	0 ˚ (BTDC)
Pilot 2 Injection Timing	11.6 ˚ (BTDC)	0 ˚(BTDC)	0 ˚ (BTDC)
Main Injection Timing	3.3 ˚ (ATDC)	1.1˚ (BTDC)	13.5 ˚ (BTDC)

Below figures (4.10 & 4.11) belongs to data point 2250 rpm and 240 Nm Torque point. Results show that in cylinder pressure estimations are in good correlation with measurement.

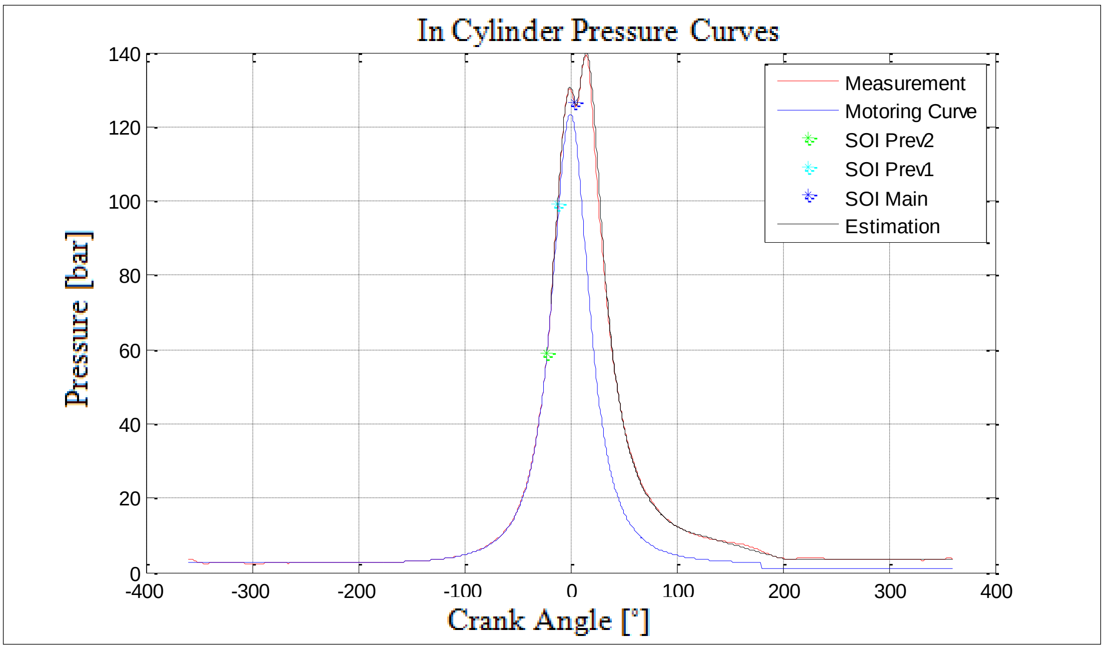

Figure 4.10 : In cylinder pressure measurement and estimation for 2250 rpm, 240 Nm brake torque point.

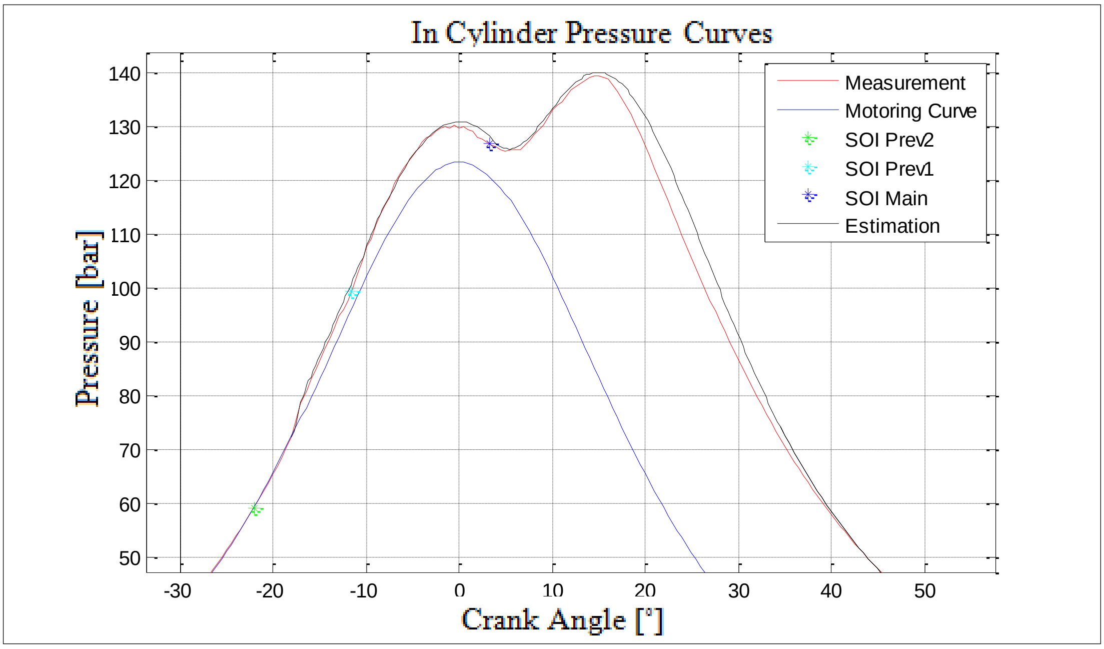

Figure 4.11 : In cylinder pressure measurement and estimation for 2250 rpm, 240 Nm brake torque point (Zoomed view on injection region).

Figure 4.12 refers to the simulation point 2, 2150 rpm 160 Nm brake torque which belongs to NEDC (New European Driving Cycle) 100 – 120 Nm acceleration peak torque value. EGR is enabled at this condition. Single pilot injection is carried out. Last simulation point is full load at 3500 rpm engine speed without EGR and with main only injection strategy (Figure 4.13). Considering in cylinder pressure measurements and simulation results, it can be concluded that simulation results are in good correlation with the measurement data.

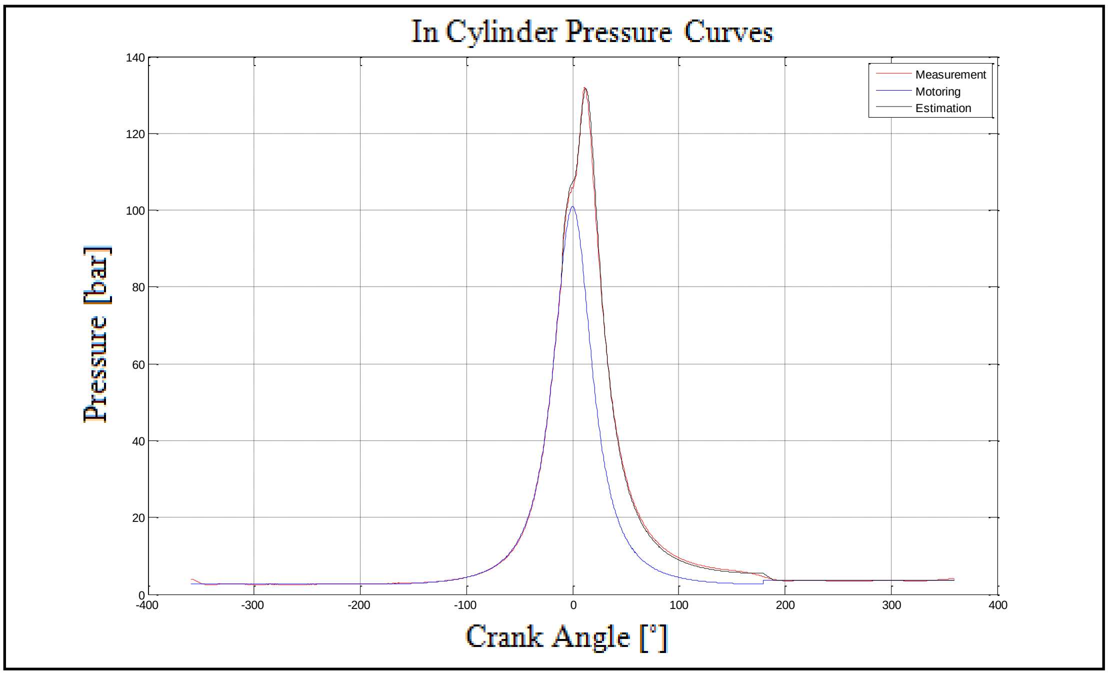

Figure 4.12 : In cylinder pressure measurement and estimation for 2150 rpm, 160 Nm brake torque point.

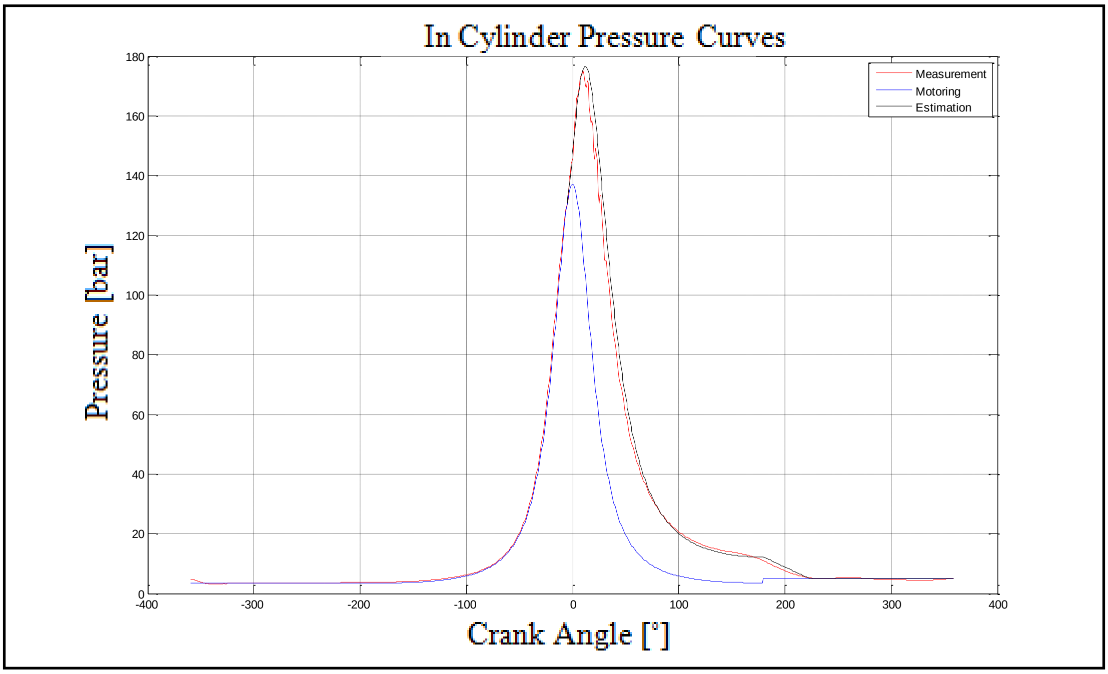

Figure 4.13 : In cylinder pressure measurement and estimation for 3500 rpm, full load torque (392 Nm) point.

Figure 4.14 shows the indicated torque estimation error over whole engine mapping points. Maximum and minimum errors are 28.78 Nm and -24.48 Nm subsequently and in %10 error band for low torque values.

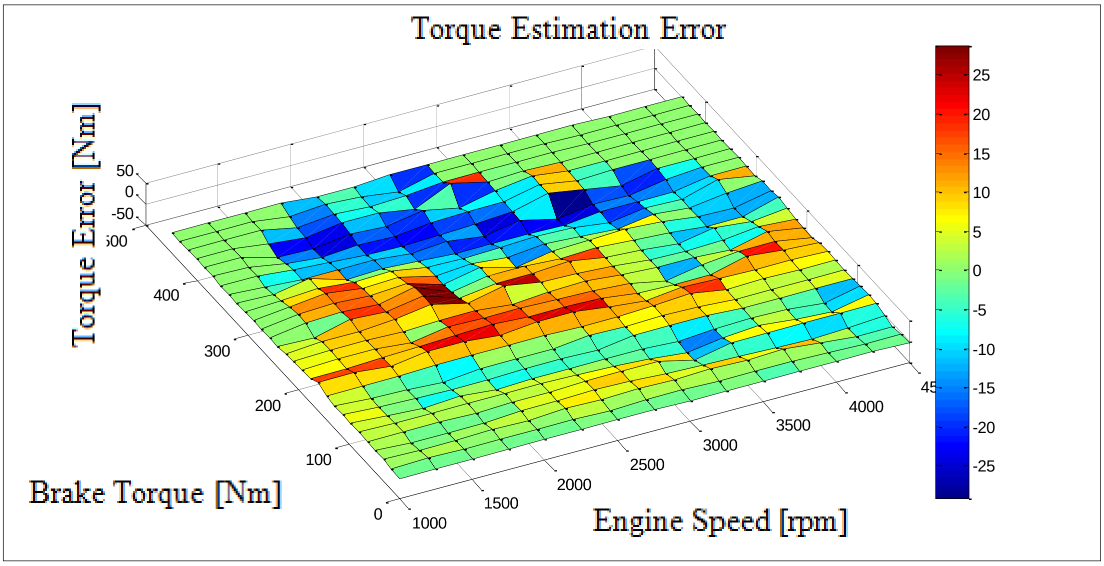

Figure 4.14 : Indicated torque estimation error.

4.4.2 Transient Results

A load change manoeuvre with the following steps has been done on vehicle. ECU record speed and indicated torque profile has been converted to an engine dynamometer test sequence. Figures 4.15 and 4.16 clear shows that introduced transient torque model is capable of estimating engine produced torque within ± 30 Nm accuracy range.

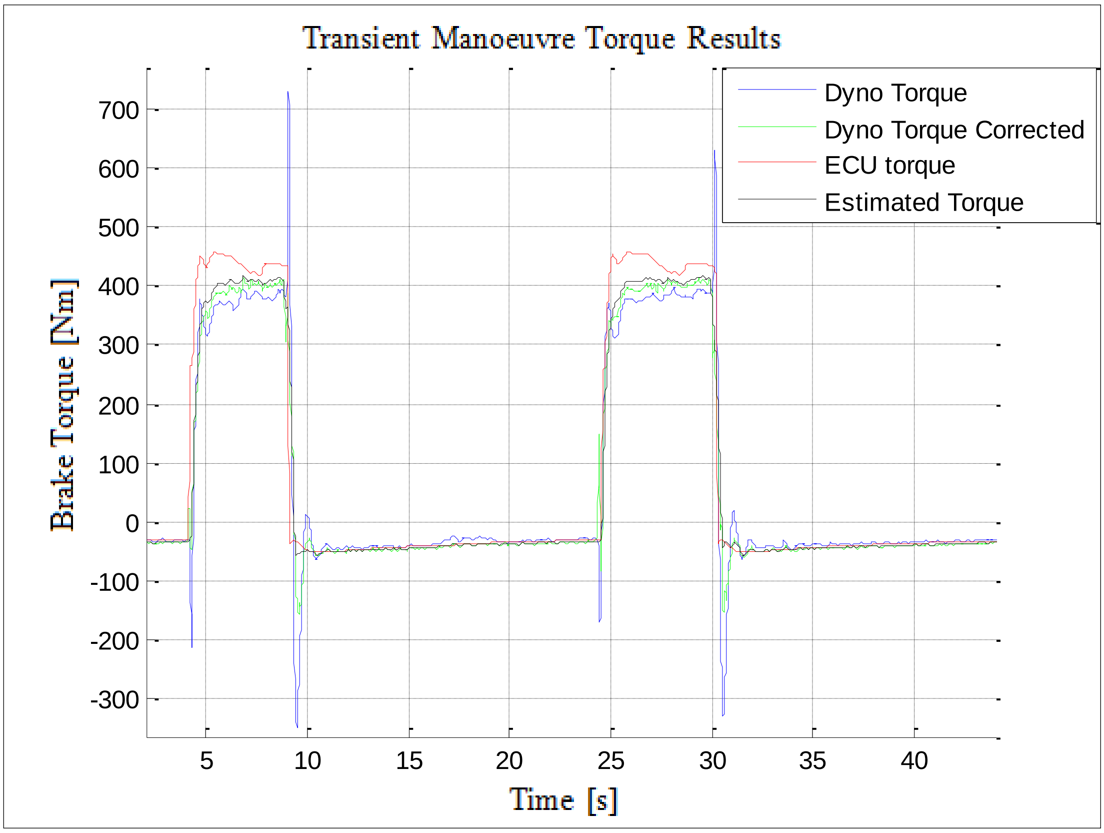

Figure 4.15 : Fourth gear engine torque comparison.

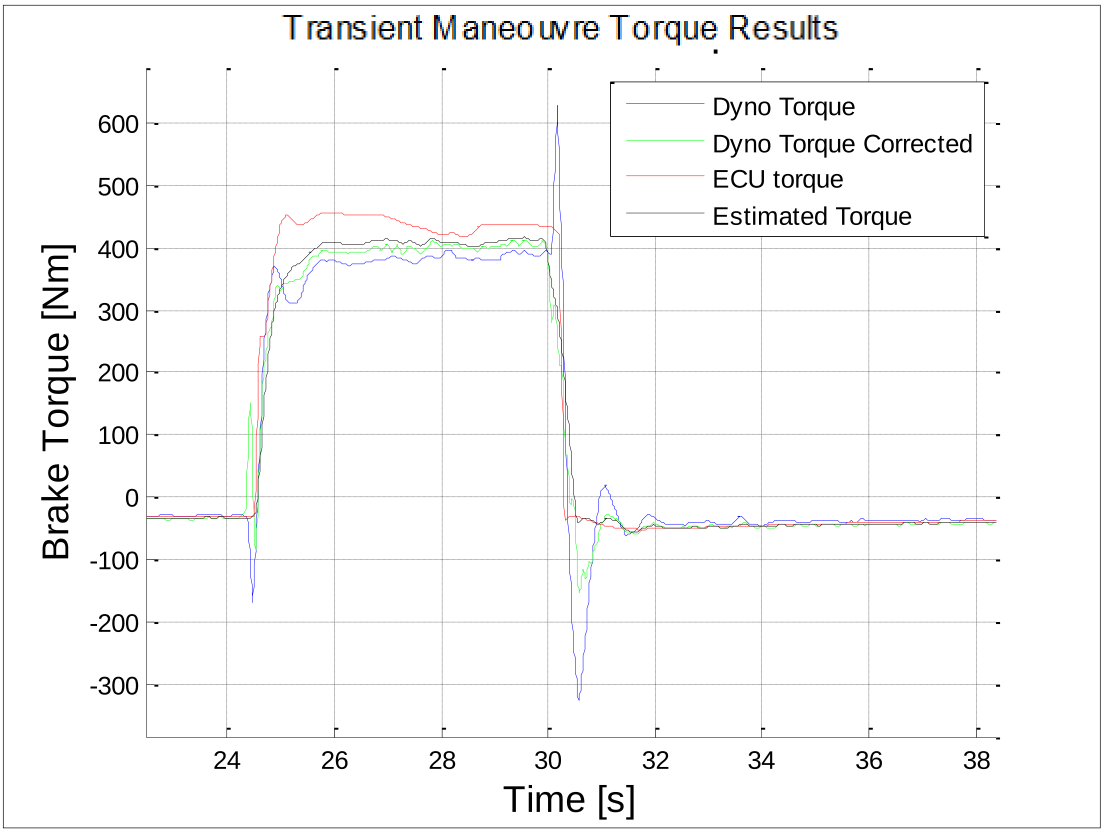

Figure 4.16 : Fourth gear engine torque comparison (zoomed view).

4.5 Conclusion

Within the scope of this study, an in cylinder pressure estimation model is generated for turbocharged diesel engines. The model works in crank angle base and general combustion parameters like fuel and air properties are used as they are already available within the ECU network. Combustion charge temperature is calculated via employing a simple thermodynamic model for EGR cooler. Pressure estimation is based on Wiebe function usage and it is basically used for heat release calculation individually for each injection. Once the pressure within the combustion chamber is achieved, indicated torque is calculated integrating the pressure curve. Indicated to brake torque conversion is permed using friction curves and accessory devices torque loss information which is already available at the ECU network. Obtained engine brake torque results are in good correlation with the real measurement on the engine dynamometer.

5. DRIVELINE MODELLING

Within the scope of this study driveline model of a front wheel drive vehicle is generated. In FWD vehicles traction is available only at the front wheels and power is transmitted from the engine to the tires over the below components: flywheel, clutch, transmission, final drive, driveshafts and wheels (Figure 5.1).

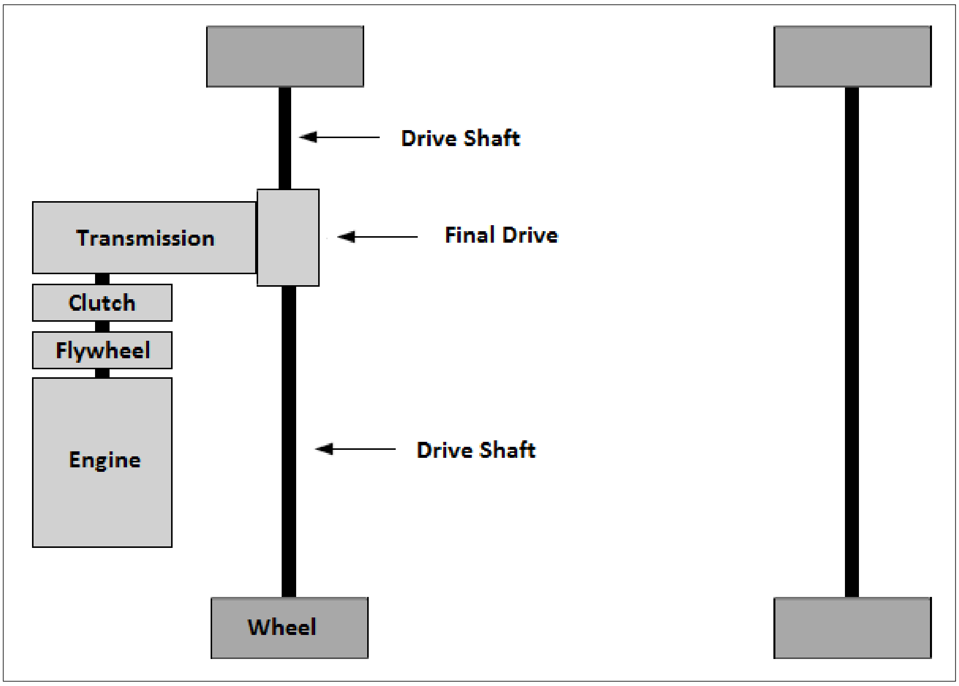

Figure 5.1 : Components of vehicle driveline for a FWD vehicle.

Elasticity of the various driveline components and backlash originated from gear reduction mechanisms and fasteners causes torsional vibrations resulting unintended shunt and shuffle behaviours, when a vehicle is subjected to an acceleration change request. In order to eliminate these vibrations driveline parameters and engine generated brake torque should be handled carefully. As an objective of this thesis the idea is to use a closed loop controller vehicle plant model to actively damp the powertrain oscillation.

Within this scope a simplified 4 mass powertrain model is built and model validation considering longitudinal vehicle dynamics is performed with vehicle level tests using a tip-in followed by a back-out acceleration pedal signal input manoeuvre. Comparison of simulation results and vehicle test data shows that simplified model is capable of capturing vehicle acceleration profile revealing unintended error states for the specified input signals.

5.1 4 Mass Vehicle Model

When studying driveline of a front wheel drive vehicle, clutch and drive shafts are subjected to relatively highest torsional deformation resulting possibility for oscillations. In order to capture longitudinal vehicle dynamics characteristics these components should be modelled with flexible elements (Figure 5.2).

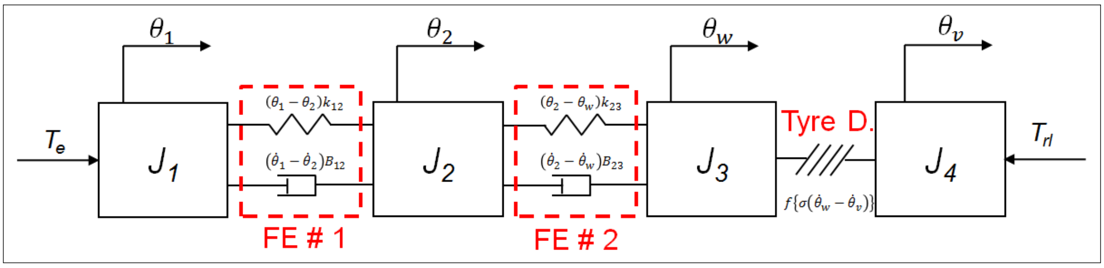
θ_1
θ_2
θ_w
θ_v
T_e
J_1
$(\theta_1-\theta_2)k_{12}$
$(\dot{\theta}_1-\dot{\theta}_2)B_{12}$
FE # 1
J_2
$(\theta_2-\theta_w)k_{23}$
$(\dot{\theta}_2-\dot{\theta}_w)B_{23}$
FE # 2
J_3
Tyre D.
$f\{\sigma(\dot{\theta}_w-\dot{\theta}_v)\}$
J_4
T_{rl}

Figure 5.2 : Free body diagram of 4 mass vehicle model with 4 inertias connected by 2 spring damper elements and tyre.

4 mass vehicle model consists of the components below:

- Integrated inertia node 1 (J_1): Engine, flywheel, clutch primary side
- Flexible element # 1: Clutch
- Integrated inertia node 2 (J_2): Clutch secondary side, transmission, final drive
- Flexible element # 2: Drive shafts
- Wheel and tyre inertia, node 3 (J_3)
- Tyre dynamics
- Vehicle inertia, node 4 (J_4)

Applying Newton’s second law to each of the inertia components results with below differential equations.

$$J_1\ddot{\theta}_1 = T_e - (\theta_1 - \theta_2)k_{12} - (\dot{\theta}_1 - \dot{\theta}_2)B_{12} \tag{5.1}$$

$$J_2\ddot{\theta}_2 = (\theta_1 - \theta_2)k_{12} + (\dot{\theta}_1 - \dot{\theta}_2)B_{12} - (\theta_2 - \theta_w)k_{23} - (\dot{\theta}_2 - \dot{\theta}_w)B_{23} \tag{5.2}$$

$$J_3\ddot{\theta}_w = (\theta_2 - \theta_w)k_{23} + (\dot{\theta}_2 - \dot{\theta}_w)B_{23} - f\{\sigma(\dot{\theta}_w - \dot{\theta}_v)\} \tag{5.3}$$

$$J_4\ddot{\theta}_v = f\{\sigma(\dot{\theta}_w - \dot{\theta}_v)\} - T_{rl} \tag{5.4}$$

where

- θ_x, $\dot{\theta}_x$and $\ddot{\theta}_x$are the angular position, velocity and acceleration of the xth node respectively,
- k_{xy} and B_{xy} are the stiffness and damping coefficients of the spring damper elements between xth and yth nodes respectively.
- T_e is the generated engine brake torque at crankshaft level,
- Road load is modelled as the sum of the aerodynamic, rolling and grade resistance forces as below (x),

  $$T_{rl} = \mathrm{r_w}.\left(\mathrm{F_{aero}} + \mathrm{F_{rr}} + \mathrm{F_g}\right) \tag{5.5}$$

  where

  - $F_{aero} = \frac{1}{2}.\rho_{air}.C_D.v^2 \qquad (5.6)$
  - $F_{rr} = m_{tot}.g.cos(\alpha).f_r \qquad (5.7)$
  - $F_g = m_{tot}.g.sin(\alpha) \qquad (5.8)$

- $f\{\sigma\}$ is the tyre/road friction force function,
- J_1 is the total inertia of engine, flywheel and clutch primary side,

  $$J_1 = J_e + J_{fw} + J_{cp} \tag{5.9}$$

- J_2 is the total inertia of clutch secondary side, transmission, final drive and drive shafts,

$$J_2 = J_{cs} + \frac{J_t}{i_t^2} + \frac{J_{fd}}{i_t^2 . i_f^2} + \frac{J_{ds}}{i_t^2 . i_f^2} \tag{5.10}$$

where

  - i_t is the reduction ratio of the selected gear
  - i_f is the reduction ratio of the final gear

- J_3 is the total inertia of wheels including tyres at crankshaft level

$$\mathrm{J}_3 = 4\frac{\mathrm{J_w}}{\mathrm{i}_t^2 . \mathrm{i}_f^2} \tag{5.11}$$

- J_4 is the total inertia of the vehicle mass at crankshaft level

$$\mathrm{J}_4 = \mathrm{m_{tot}} . \left(\frac{\mathrm{r_w}}{\mathrm{i}_t^2 . \mathrm{i}_f^2}\right)^2 \tag{5.12}$$

Rotational inertia block receives all positives torques as input # 1and all feedback torques as input # 2. The difference between these values is divided by the rotational inertia of the component modelled using the gain block. Two integrators, initial conditions of the first one is determined using the initial engine speed defined as input # 3 and the second one is determined as initial angular displacement (Set as 0), calculate angular velocity and angular position for the object modelled. “MATLAB / Simulink” model of inertial element J_1 is shown at Figure 5.3.

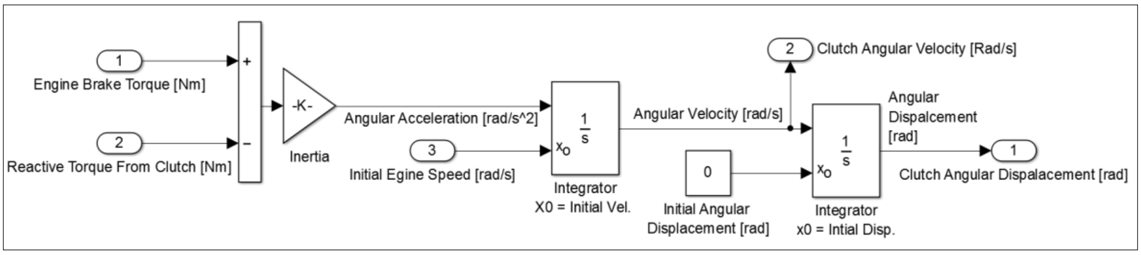
1
Engine Brake Torque [Nm]
2
Reactive Torque From Clutch [Nm]
+
-
-K-
Inertia
Angular Acceleration [rad/s^2]
3
Initial Egine Speed [rad/s]
1/s
x0
Integrator
X0 = Initial Vel.
Angular Velocity [rad/s]
2
Clutch Angular Velocity [Rad/s]
0
Initial Angular Displacement [rad]
1/s
x0
Integrator
x0 = Intial Disp.
Angular Dispalcement [rad]
1
Clutch Angular Dispalacement [rad]

Figure 5.3 : MATLAB/Simulink model block of inertial element $\boldsymbol{J_1}$ (the total inertia of engine, flywheel and clutch primary side block).

Flexible elements (clutch and drive shafts) in the vehicle model were modelled using spring/damper simulation block. The aim of this block is to accurately calculate the reactive torque generated when a torsional displacement occurs on either side. Block accepts angular position and velocity for two inertias connected to each side. For components which are not in rotational domain (i.e. chassis, vehicle, etc.) the equivalent angular position and velocity of their inertias have to be calculated. In this block, both stiffness and damping torques are embedded in lookup tables. Although the stiffness output is a function of torsion generated on the component, the damping torque is set to zero when the stiffness torque is zero. This has been implemented to model the backlash, where the damping forces disappear. “MATLAB / Simulink” model of clutch is shown at Figure 5.4.

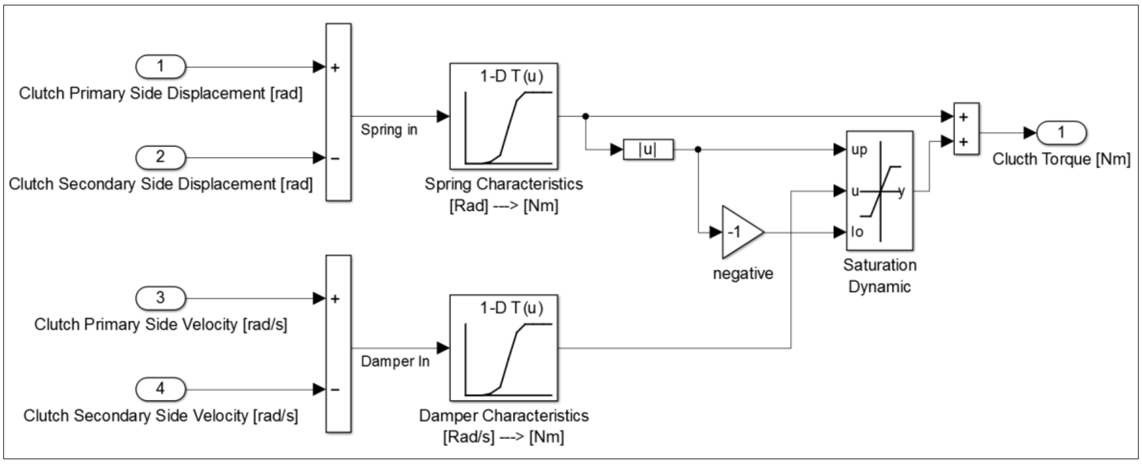
1
Clutch Primary Side Displacement [rad]
2
Clutch Secondary Side Displacement [rad]
+
−
Spring in
1-D T(u)
Spring Characteristics
[Rad] ---> [Nm]
|u|
-1
negative
up
u
y
lo
Saturation
Dynamic
+
+
1
Clucth Torque [Nm]
3
Clutch Primary Side Velocity [rad/s]
4
Clutch Secondary Side Velocity [rad/s]
+
−
Damper In
1-D T(u)
Damper Characteristics
[Rad/s] ---> [Nm]

Figure 5.4 : MATLAB/Simulink clutch spring & damper simulation block.

Tyre dynamics is simulated using the well-known Pacejka's magic tyre formula [43]. Tyre slip is calculated via dividing the speed delta between the tyre circumference and the vehicle with absolute vehicle speed. The coefficient of friction within the tyre-road interface is obtained from a lookup table and used to calculate the tractive effort. MATLAB/Simulink representation of the 4 mass vehicle model is shown at figure 5.5.

5.2 2 Mass Vehicle Model

Due to high level of nonlinearities at the 4 mass vehicle model, model predictive control algorithm cannot be operated successfully. Therefore a simplified 2 mass vehicle model with road load component has been developed for the model predictive controller plant usage. Driveshafts have been assumed as the main source for the elasticity, resulting a 2 mass system combined with a spring / damper element (Figure 5.6).

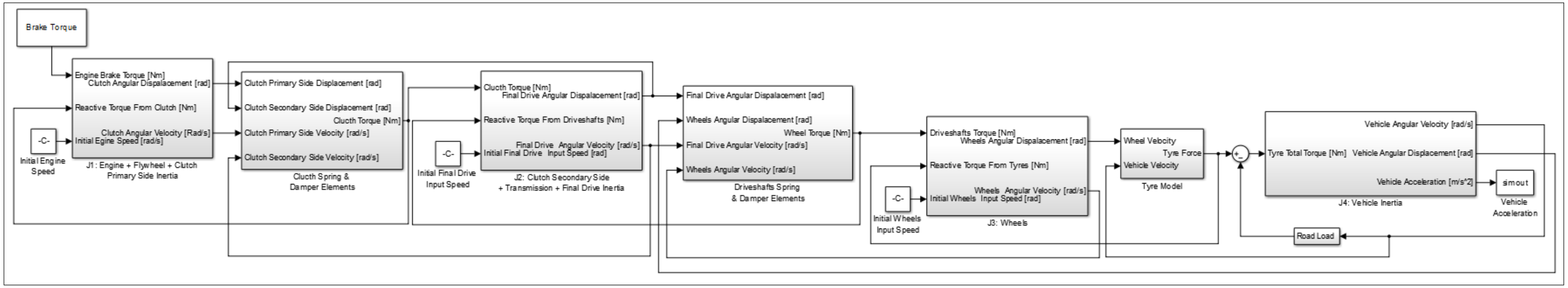
Brake Torque
Engine Brake Torque [Nm]
Clutch Angular Dispalacement [rad]
Reactive Torque From Clutch [Nm]
Clutch Angular Velocity [Rad/s]
Initial Egine Speed [rad/s]
-C-
Initial Engine Speed
J1 : Engine + Flywheel + Clutch Primary Side Inertia
Clutch Primary Side Displacement [rad]
Clutch Secondary Side Displacement [rad]
Clucth Torque [Nm]
Clutch Primary Side Velocity [rad/s]
Clutch Secondary Side Velocity [rad/s]
Clucth Spring & Damper Elements
-C-
Initial Final Drive Input Speed
Clucth Torque [Nm]
Final Drive Angular Dispalacement [rad]
Reactive Torque From Driveshafts [Nm]
Final Drive Angular Velocity [rad/s]
Initial Final Drive Input Speed [rad]
J2: Clutch Secondary Side + Transmission + Final Drive Inertia
Final Drive Angular Dispalacement [rad]
Wheels Angular Dispalacement [rad]
Wheel Torque [Nm]
Final Drive Angular Velocity [rad/s]
Wheels Angular Velocity [rad/s]
Driveshafts Spring & Damper Elements
Driveshafts Torque [Nm]
Wheels Angular Dispalacement [rad]
Reactive Torque From Tyres [Nm]
Wheels Angular Velocity [rad/s]
Initial Wheels Input Speed [rad]
-C-
Initial Wheels Input Speed
J3: Wheels
Wheel Velocity
Tyre Force
Vehicle Velocity
Tyre Model
+
_
Tyre Total Torque [Nm]
Vehicle Angular Velocity [rad/s]
Vehicle Angular Displacement [rad]
Vehicle Acceleration [m/s^2]
J4: Vehicle Inertia
simout
Vehicle Acceleration
Road Load

Figure 5.5 : 4 Mass vehicle MATLAB/Simulink model.

2 mass vehicle model consists of components below:

Integrated inertia node 1 (J_1): Engine, flywheel, clutch primary & secondary sides, transmission and final drive

Flexible element # 1: Driveshafts

Integrated inertia node 2 (J_2): Wheels, tyres and vehicle

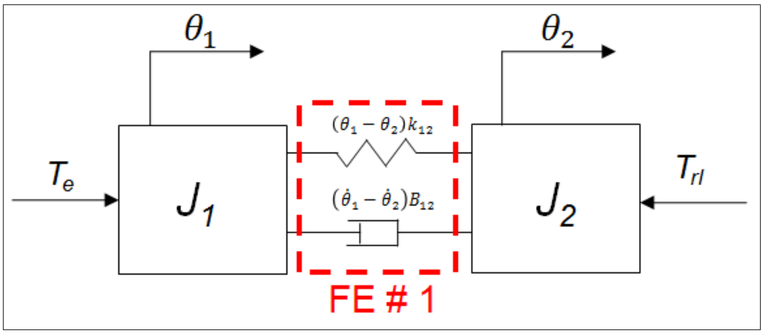
θ_1
θ_2
$(\theta_1 - \theta_2)k_{12}$
$(\dot{\theta}_1 - \dot{\theta}_2)B_{12}$
T_e
J_1
J_2
T_{rl}
FE # 1

Figure 5.6 : Free body diagram of simplified 2 mass vehicle model.

Applying Newton’s second law to each of the inertia components results with below differential equations.

$$J_1 \cdot \ddot{\theta}_1 = T_e - (\theta_1 - \theta_2).k_{12} - (\dot{\theta}_1 - \dot{\theta}_2).B_{12} \tag{5.13}$$

$$J_2 \cdot \ddot{\theta}_2 = (\theta_1 - \theta_2).k_{12} + (\dot{\theta}_1 - \dot{\theta}_2).B_{12} \tag{5.14}$$

where

θ_x, $\dot{\theta}_x$ and $\ddot{\theta}_x$ are the angular position, velocity and acceleration of the x^{th} node respectively,

k_{12} and B_{12} are the stiffness and damping coefficients of modelled the spring-damper elements of the drive shafts respectively,

T_e and T_{rl} are engine brake torque and road load resistive torque calculated at crankshaft level respectively,

J_1 is the total inertia of engine, flywheel, clutch primary & secondary sides, transmission, final drive

$$J_1 = J_e + J_{fw} + J_{cp} + J_{cs} + \frac{J_t}{i_t^2} + \frac{J_{fd}}{i_t^2 . i_f^2} \tag{5.15}$$

J_2 is the total inertia of drive shafts, wheels, tyres and vehicle mass

$$J_2 = \frac{J_{ds}}{i_t^2 . i_f^2} + 4. \frac{J_w}{i_t^2 . i_f^2} + m_{tot} . \left(\frac{r_w}{i_t^2 . i_f^2} \right)^2 \tag{5.16}$$

State space representation of the 2 mass vehicle model is defined in equations 5.17 to 5.19. Drive shaft torsional angle, angular speed of the engine and angular speed of the driveshaft are defined as the state variables:

$$\begin{aligned} x_1 &= \frac{\theta_1}{i_t i_f} - \theta_2 \\ x_2 &= \dot{\theta}_1 \\ x_3 &= \dot{\theta}_2 \end{aligned} \tag{5.17}$$

The state space model formed as follows:

$$\begin{aligned} \dot{\mathrm{x}}(t) &= \mathrm{A}\, x(t) + \mathrm{B}\, u(t) + H\, T_{rl} \\ y(t) &= C^T \mathrm{x}(t) \end{aligned} \tag{5.18}$$

Consisting of the following system matrices.

$$\mathrm{A} = \begin{pmatrix} 0 & \frac{1}{i_t i_f} & -1 \\ -\frac{k_{12}}{i_t i_f . J_1} & -\frac{\frac{B_{12}}{\left(i_t i_f\right)^2}}{J_1} & \frac{B_{12}}{i_t i_f . J_1} \\ \frac{k_{12}}{J_2} & \frac{B_{12}}{i . J_2} & -\frac{B_{12}}{J_2} \end{pmatrix}, \mathrm{B} = \begin{pmatrix} 0 \\ \frac{1}{J_1} \\ 0 \end{pmatrix}, \mathrm{C^T} = \begin{pmatrix} 0 & \frac{1}{i_t i_f} & -1 \end{pmatrix} \tag{5.19}$$

MATLAB/Simulink model of the 2 mass vehicle model is shown at figure 5.7. 2 inertias were combined with spring damper element. Nonlinear spring and damper characteristics of the driveshafts were embedded in look up tables.

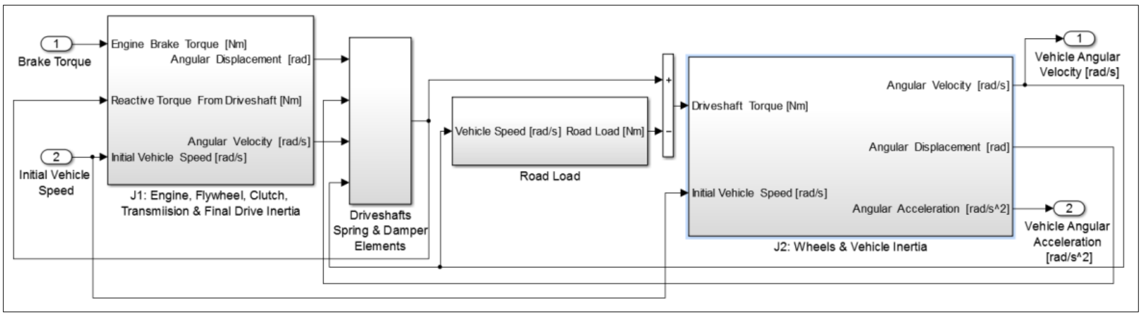
1
Brake Torque
2
Initial Vehicle Speed
Engine Brake Torque [Nm]
Angular Displacement [rad]
Reactive Torque From Driveshaft [Nm]
Angular Velocity [rad/s]
Initial Vehicle Speed [rad/s]
J1: Engine, Flywheel, Clutch, Transmiision & Final Drive Inertia
Driveshafts Spring & Damper Elements
Vehicle Speed [rad/s] Road Load [Nm]
Road Load
+
-
Driveshaft Torque [Nm]
Angular Velocity [rad/s]
Angular Displacement [rad]
Initial Vehicle Speed [rad/s]
Angular Acceleration [rad/s^2]
J2: Wheels & Vehicle Inertia
1
Vehicle Angular Velocity [rad/s]
2
Vehicle Angular Acceleration [rad/s^2]

Figure 5.7 : MATLAB/Simulink 2 mass vehicle model.

5.3 3 Mass Vehicle Model

Due to fact that tire dynamics alter nonlinearity of the model significantly, in order to simplify MPC control model linearization, tire dynamics was removed from the vehicle model resulting to a simplified 3 mass vehicle model with road load component (Figure 5.8).

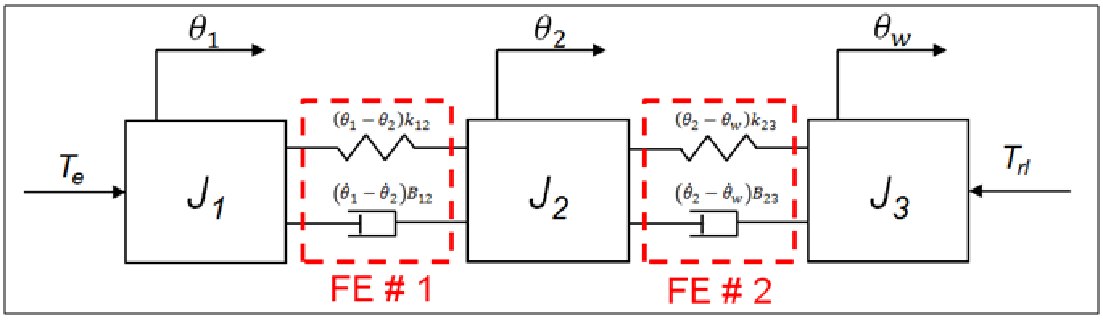
θ_1
θ_2
θ_w
T_e
J_1
$(\theta_1-\theta_2)k_{12}$
$(\dot\theta_1-\dot\theta_2)B_{12}$
J_2
$(\theta_2-\theta_w)k_{23}$
$(\dot\theta_2-\dot\theta_w)B_{23}$
J_3
T_{rl}
FE # 1
FE # 2

Figure 5.8 : Simplified 3 mass vehicle model.

Equation 5.3 has been modified as below and vehicle inertia has been added to J_3. MATLAB/Simulink representation of the 3 mass vehicle model is shown at figure 5.9.

$$J_3\ddot\theta_w=(\theta_2-\theta_w)k_{23}+(\dot\theta_2-\dot\theta_w)B_{23}-T_{rl} \tag{5.20}$$

$$J_3 = 4\frac{J_w}{i_t^2\, i_f^2}+m_{tot}\left(\frac{r_w}{i_t^2\, i_f^2}\right)^2 \tag{5.21}$$

Drive shaft torsional angle, angular speed of the engine and angular speed of the driveshaft are defined as the state variables:

$$\begin{gathered}x_1=\theta_1-\theta_2.i_t\\ x_2=\frac{\theta_2}{i_f}-\theta_w\\ x_3=\dot\theta_1\\ x_4=\dot\theta_2\\ x_5=\dot\theta_w\end{gathered} \tag{5.22}$$

The state space model formed as follows:

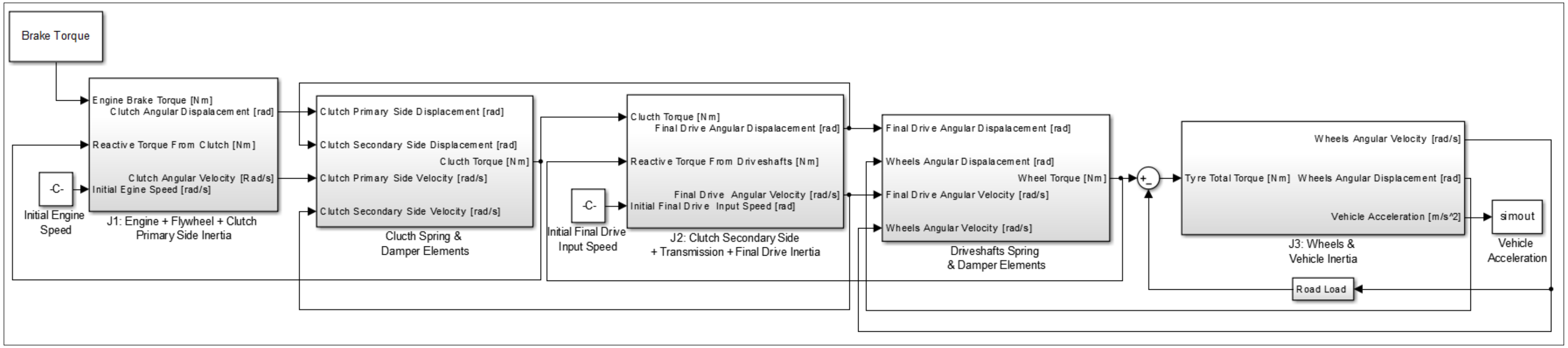
Brake Torque
Engine Brake Torque [Nm]
Clutch Angular Dispalacement [rad]
Reactive Torque From Clutch [Nm]
Clutch Angular Velocity [Rad/s]
Initial Egine Speed [rad/s]
-C-
Initial Engine Speed
J1: Engine + Flywheel + Clutch Primary Side Inertia
Clutch Primary Side Displacement [rad]
Clutch Secondary Side Displacement [rad]
Clucth Torque [Nm]
Clutch Primary Side Velocity [rad/s]
Clutch Secondary Side Velocity [rad/s]
Clucth Spring & Damper Elements
Clucth Torque [Nm]
Final Drive Angular Dispalacement [rad]
Reactive Torque From Driveshafts [Nm]
Final Drive Angular Velocity [rad/s]
Initial Final Drive Input Speed [rad]
-C-
Initial Final Drive Input Speed
J2: Clutch Secondary Side + Transmission + Final Drive Inertia
Final Drive Angular Dispalacement [rad]
Wheels Angular Dispalacement [rad]
Wheel Torque [Nm]
Final Drive Angular Velocity [rad/s]
Wheels Angular Velocity [rad/s]
Driveshafts Spring & Damper Elements
+
-
Tyre Total Torque [Nm]
Wheels Angular Velocity [rad/s]
Wheels Angular Displacement [rad]
Vehicle Acceleration [m/s^2]
J3: Wheels & Vehicle Inertia
simout
Vehicle Acceleration
Road Load

Figure 5.9 : 3 Mass vehicle MATLAB/Simulink model.

$$\dot{\mathrm{x}}(t) = \mathrm{A}\,x(t) + \mathrm{B}\,u(t) + H\,T_{rl}$$
$$y(t) = H\mathrm{x}(t) \tag{5.23}$$

Consisting of the following system matrices:

$$\mathrm{A} = \begin{pmatrix} 0 & 0 & 1 & -i_t & 0 \\ 0 & 0 & 0 & 1/i_f & -1 \\ -k_{12}/J_1 & 0 & -B_{12}/J_1 & B_{12}i_t/J_1 & 0 \\ k_{12}i_t/J_2 & -k_{23}/i_f J_2 & B_{12}i_t/J_2 & -\left(B_{12}i_t^2 + B_{23}/i_f^2\right)/J_2 & B_{23}/i_f J_2 \\ 0 & k_{23}/J_3 & 0 & B_{23}/i_f J_3 & -B_{23}/J_3 \end{pmatrix}$$
$$\mathrm{B} = \begin{pmatrix} 0 \\ 0 \\ 1/J_1 \\ 0 \\ 0 \end{pmatrix}, H = \begin{pmatrix} 0 \\ 0 \\ 0 \\ 0 \\ -1/J_2 \end{pmatrix} \tag{5.24}$$

5.4 4 Mass Vehicle Model Results

4 Mass vehicle model validation was performed via experiments carried out on a CD class front wheel drive (FWD) passenger vehicle equipped with a diesel engine. The engine had a regulated 2 stage (R2S) turbocharger system. Vehicle had a 6 speed dual clutch transmission and test weight was approximately 2125 kg. Engine and vehicle properties are summarized in Table 5.1. Spring and damping coefficients for clutch and drive shafts are shown on Figure 5.10. Backlash of the whole powertrain system is defined with a zero torque transmitting region at the driveshaft spring force coefficient characteristics. Test were performed at manual mode of transmission and acceleration pedal kick-down function – which downshifts automatically if the accelerator brake pedal is pressed more than a certain position (close to maximum) very rapidly - had been disable in order to reach maximum torque without downshifting during the wide open throttle (WOT) manoeuvre. Subjected gearbox had torque truncation protection in low gears; therefore test manoeuvres were done at 3rd and 4th gears where maximum allowed torque values are 400 Nm and 450 Nm respectively. Test manoeuvre consists of a stabilized deceleration with zero accelerator pedal position from 2400 rpm to 2000 rpm engine speed followed by sudden tip-in to 100% pedal position with engine speed acceleration up to 3000 rpm. Manoeuvre is finalized a quick tip-out of the accelerator pedal to 0% and stabilized deceleration to 2500 rpm engine speed (Figure 5.11).

All ECU driveability features such as anti-jerk and anti-shuffle were disabled in order to get a direct torque request from the pedal input (Driver torque demand). Black smoke limitation feature was not turned off as disabling this feature will provide erroneous torque values such that injected fuel will not burn completely due to lack of combustion air. Engine speed, vehicle speed, vehicle acceleration and ECU estimated brake torque signals were captured with an online data acquisition system via direct A7 connection to ECU.

Table 5.1 : Engine and vehicle properties.

Engine Displacement	2.0 lt
Number of Cylinder	4
Rated Power	210PS (3750 rpm)
Rated Torque	450 Nm (2000-2500 rpm)
Transmission	6 Speed Automatic
Torque Truncation at 3rd Gear	400 Nm
Drive Wheel Configuration	Front Wheel Drive
Final Drive Ratio	3.55
Tire Dimensions	245/50R17
Test Weight	2125 kg

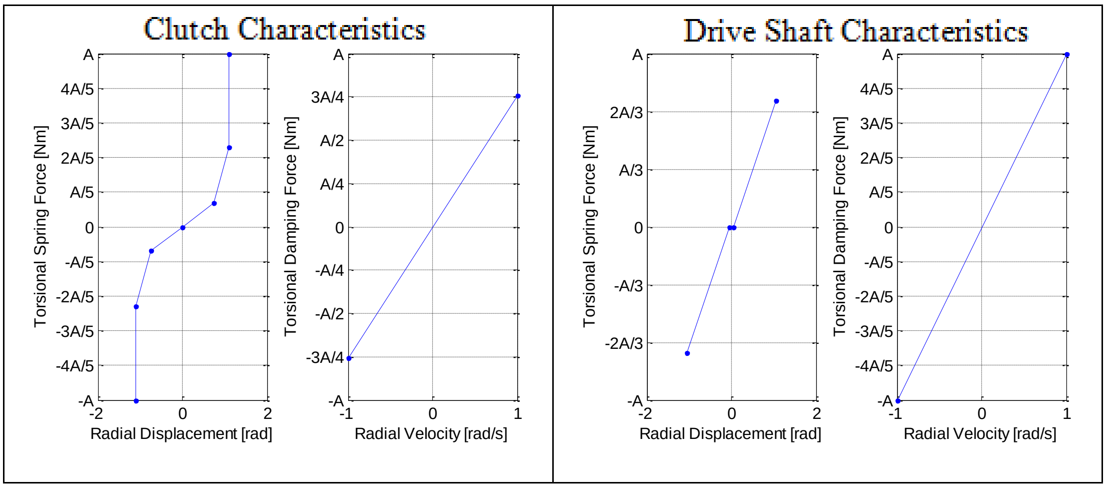

Figure 5.10 : Spring Nonlinear clutch and drive-shaft characteristics.

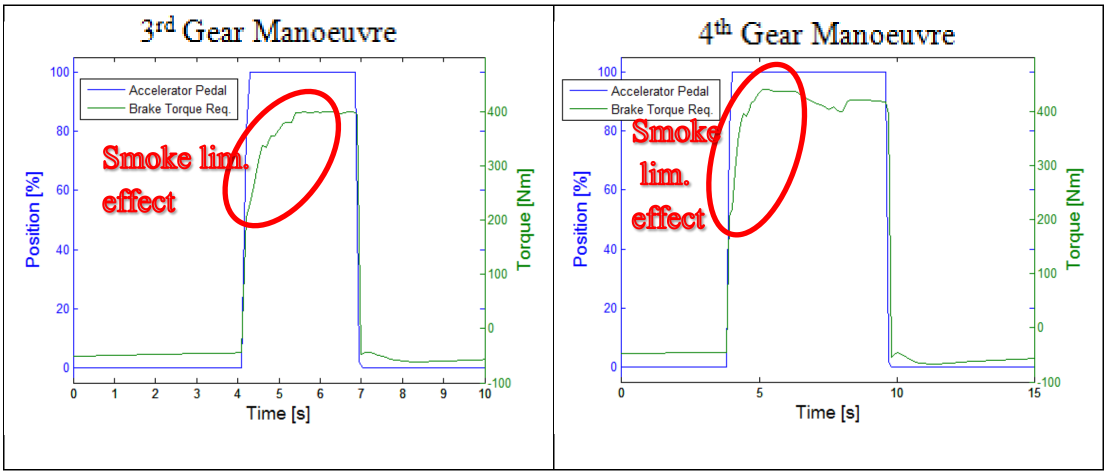

Figure 5.11 : Accelerator pedal position and brake torque request trace for the 3rd and 4th gear tip-in and tip-out manoeuvres.

Comparison of simulation results with vehicle measurements clearly indicates that proposed 4 mass vehicle model is capable of simulating vehicle initial acceleration / deceleration characteristics for 3rd and 4th gears considering tip-in and tip-out manoeuvres respectively (Figures 5.12 & 5.14). Acceleration axis has been normalized in terms of securing intellectual properties. Zoomed view of vehicle longitudinal acceleration comparison for tip-in and tip-out manoeuvres ensures that proposed vehicle model successfully captures powertrain characterization as amplitude and frequency of the oscillation are in good alignment (Figures 5.13 & 5.15).

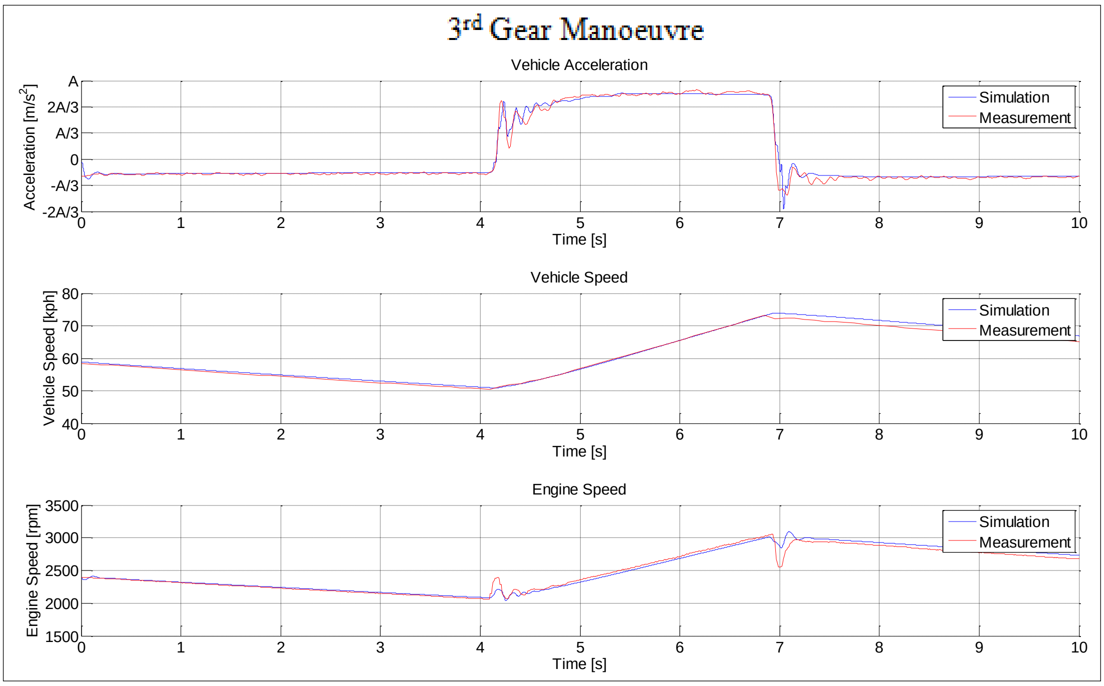

Figure 5.12 : Comparison of vehicle measurements and simulation results for 3rd gear tip-in and tip-out manoeuvre; Top sub-figure: Vehicle longitudinal acceleration, Mid sub-figure: Vehicle speed, Bottom sub-figure: Engine speed.

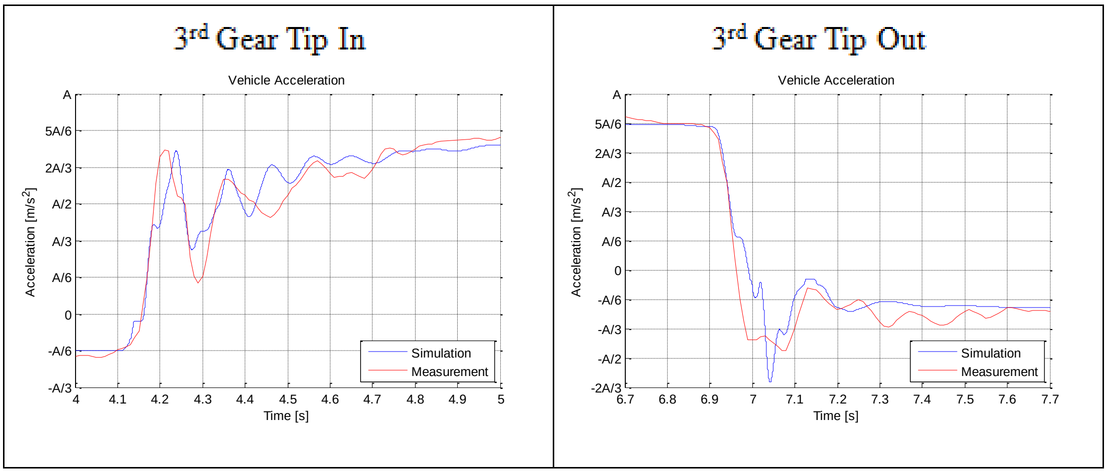

Figure 5.13 : Comparison of vehicle longitudinal acceleration measurement and simulation results for 3rd gear tip-in (left) and tip-out manoeuvres (right).

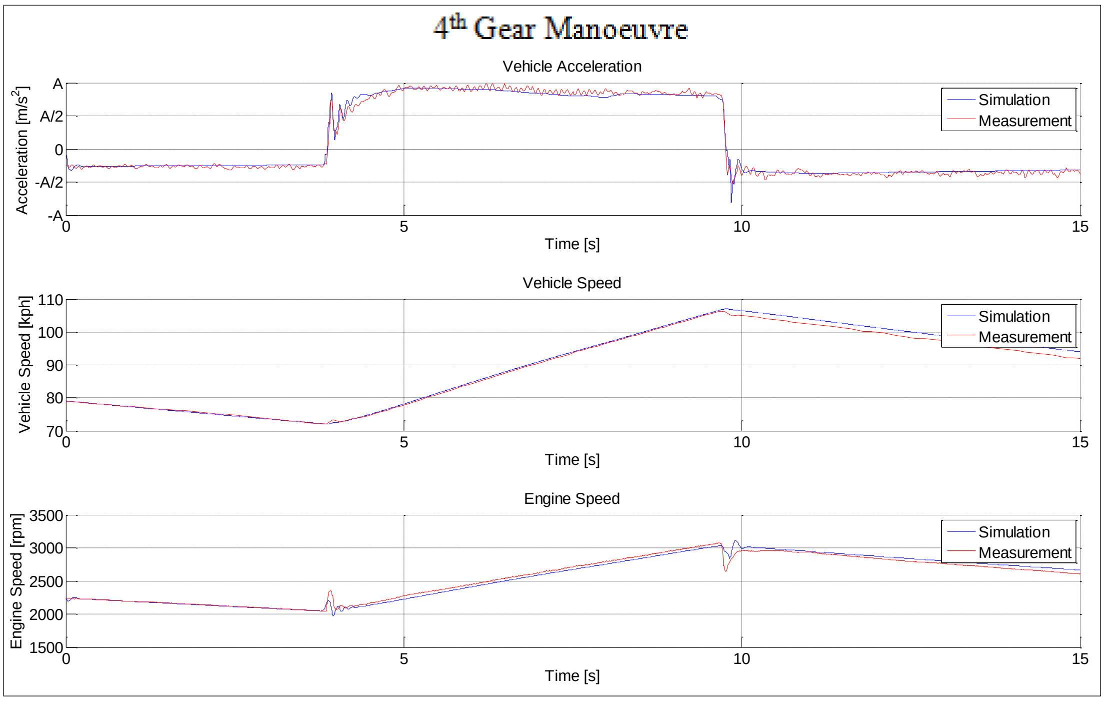

Figure 5.14 : Comparison of vehicle measurements and simulation results for 4th gear tip-in and tip-out manoeuvre; Top sub-figure: Vehicle longitudinal acceleration, Mid sub-figure: Vehicle speed, Bottom sub-figure: Engine speed.

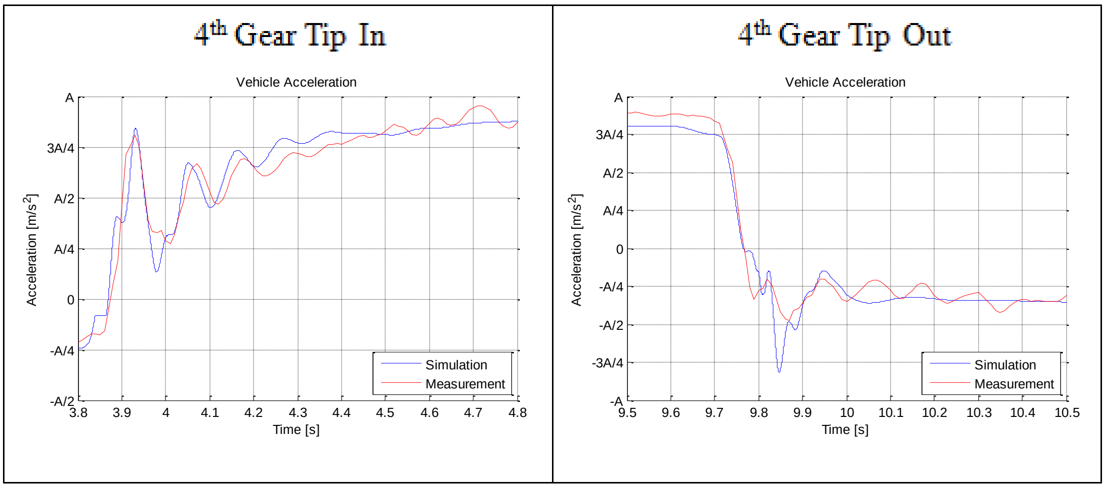

Figure 5.15 : Comparison of vehicle acceleration measurement and simulation results for 4th gear tip-in (left) and tip-out manoeuvres (right).

5.5 Conclusion

Accurate driveline modelling is required for driveability control algorithms. However complexity of the models should be simple enough in order to enable working with the control structures. Within this perspective 3 different powertrain models are generated: 2 mass, 3 mass and 4 mass models. In 2 mass model driveshafts are considered as the flexible elements and the engine, flywheel, clutch, transmission and final drive unit is lumped as the first inertia and wheels and vehicle mass is lumped as the second inertia. 3 mass model has 2 flexible elements: clutch and driveshafts. Engine, flywheel and primary side of the clutch is defined as the first inertia and secondary side of the clutch, transmission and final drive unit is characterized as the second inertia and finally wheels and vehicle mass is lumped as the third inertia.4 mass vehicle model is similar to 3 mass model with the addition of tyre characteristics using simple Pacejka tyre model. 2 and 3 mass models is used with MPC controller and 4 mass vehicle model is used as the simulation environment for the vehicle considering MPC controller functionality.

6. CONTROLLER DEVELOPMENT FOR DRIVEABILITY

Once the model of the vehicle / powertrain has been developed, with the aid of proper control strategy, vehicle longitudinal control satisfying desired performance is achievable. In the literature review section different control strategies used by the researchers are explained briefly. In this section, a basic review of the different control strategies will be explained.

6.1 Driveline Control Strategies

Automotive powertrain longitudinal control has attracted many researchers. Not only simple control algorithms like PID, capable of improving driveability, employed in the previous studies but also complex control algorithms like linear quadratic control (LQR) control and MPC had showed good applicability.

6.1.1 PID Control

PID controller has many uses cases in industrial control. PID controller has superiority over the simple control algorithms like (On/Off, P, PI, PD, etc…) of manipulating the process inputs based on the history and rate of change of the signal improving the accuracy and stability of the control. A PID controller continuously calculates an error value as the difference between a desired setpoint and a measured process variable. The controller attempts to minimize the error over time by adjustment of a control variable to a new value determined by a weighted sum of the proportional ($\mathrm{K_P}$), integral ($\mathrm{K_i}$) and derivative ($\mathrm{K_D}$) terms as follows [44]:

$$u(t) = K_P . e(t) + K_I \int_0^t e(\,t). dt + K_D \frac{de(t)}{dt} \tag{6.1}$$

Block diagram representation of PID controller is shown at figure 6.1. The proportional term responds immediately to the current error, the integral value yields zero steady-state error in tracking a constant setpoint, and the derivative term determines the reaction based on the rate at which the error has been changing. The control element uses the weighted sum of these three actions in order to adjust the process. As a PID controller relies only on the measurement process variable, not on the knowledge of the underlying process, it is does not require a plant model for the controller utilization.

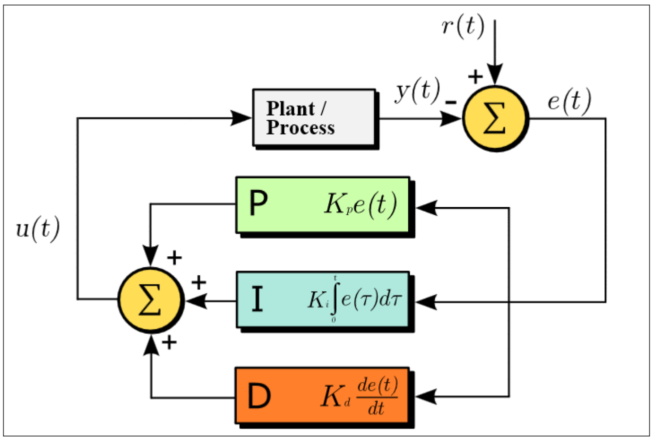

Figure 6.1 : Block diagram of a PID controller in a feedback loop [44].

6.1.2 H-Infinity Control

A fundamental problem in control theory is the design of robust controller that perform well not only for a single plant and under know inputs but also for group of plants and under various type of conditions and disturbances [10]. H-infinity (H_∞) control is developed within this perspective and its methods are used in the control theory to synthesize controller achieving stabilization with guaranteed performance under all circumstances even for the worst external input condition. H_∞ techniques have the advantage over classical control techniques in that they are readily applicable to problems involving multivariate systems with cross-coupling between channels; disadvantages of H_∞ techniques include the level of mathematical understanding needed to apply them successfully and the need for a reasonably good model of the system to be controlled [45]. It is important to keep in mind that the resulting controller is only optimal with respect to the prescribed cost function and does not necessarily represent the best controller in terms of the usual performance measures used to evaluate controllers such as settling time, energy expended, etc. Also, non-linear constraints such as saturation are generally not well-handled.

Problem formulation is as follows. Considering a general block diagram of a control system (Figure 6.2), the plant has 2 inputs: the exogenous input w that includes reference signal and disturbances and the manipulated variables. There are two outputs: the error signal z that is wanted to be minimized and the measured variable y that is used to control the system.

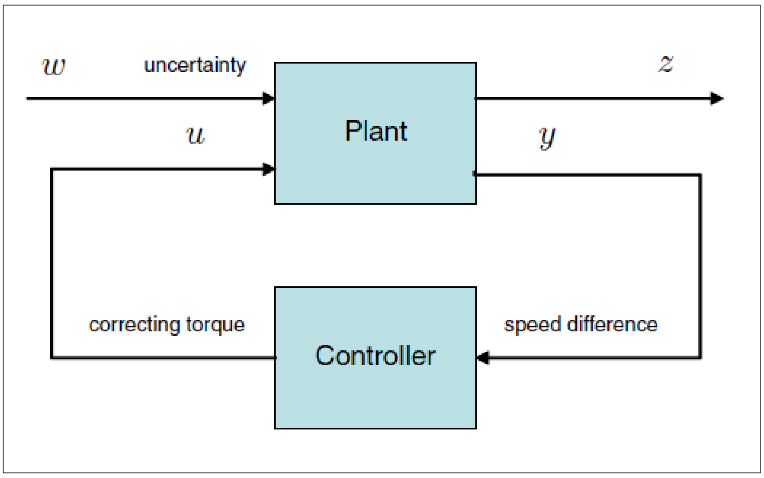

Figure 6.2 : Augmented plant and controller schematics [45].

The design aim is to synthesize a controller that will keep the size of the performance variable z small in the presence of exogenous signals w. In other words, the disturbance rejection performance depends on the size of the closed-loop transfer function from w to z, denoted by $T_{zw}(s)$. The necessity to quantify the size of the transfer function and minimize the peak value of the disturbance has given birth to the idea of H_∞ norm and singular values. It physically says that the target of the control system design is to seek a controller that minimizes the maximum over all disturbances w ($\neq 0$) of the amount of energy coming out of system to the amount of energy going into the system.

6.1.3 LQR Control

Every system can be linearized around a specific operating point with some assumption such as linear time invariant (LTI) system theory. The defining properties of any LTI systems are linearity and time invariance [46]. Linearity means that the relation between the input and the output of the system is a linear map. If a linear system is tested with the signals $u_1(t)$, $u_2(t)$,…, $u_n(t)$, the corresponding responses are $y_1(t)$, $y_2(t)$,…, $y_n(t)$, the response to a signal which can be expressed as a linear combination of the tested input signals:

$$u(t) = \alpha_1 u_1(t) + \alpha_2 u_2(t) + \cdots + \alpha_n u_n(t) \tag{6.2}$$

is

$$y(t) = \alpha_1 y_1(t) + \alpha_2 y_2(t) + \cdots + \alpha_n y(t) \tag{6.3}$$

Time invariance means that whether we apply an input to the system now or k seconds later, the output will be identical except for a time delay of k seconds such that if the output due to input $u(t)$ is $y(t)$, the output due to input $u(t-k)$ is $y(t-k)$. Hence, the system is time invariant because the output does not depend on the particular time the input is applied.

Optimal control theory deals with operating a dynamic system at a minimum cost. Linear quadratic (LQ) problem is the case where the system dynamics are described by a set of differential equations and the cost function is described by a quadratic function. For such a case a feedback controller named linear-quadratic regulator (LQR) is one of the solutions. The cost function is often defined as a sum of the deviations of key measurements. The algorithm finds those controller settings that minimize undesired deviations. The LQR algorithm reduces the amount of the work that is required to optimize the controller but still needs determining of the cost function parameters. LQR controllers are optimal state feedback controllers for LTI systems. Below formulation is retrieved from the source [47].

For a continuous time linear system, defined on $t \in [t_0, t_1]$, described by

$$\dot{x} = Ax + Bu \tag{6.4}$$

with a quadratic cost function defined as follows.

$$J = \frac{1}{2} x^T(t_1)\, F(t_1)\, x(t_1) + \int_{t_0}^{t_1} (x^T Q_x + u^T R\, u + 2x^T N\, u)\, dt \tag{6.5}$$

the feed back control law that minimizes the value of the cost is

$$u = -K\, x \tag{6.6}$$

where K is defined by

$$K = R^{-1}(B^T\, P(t) + N^T) \tag{6.7}$$

and P is found by solving the continuous time Riccati differential equation.

$$A^T P(t) + P(t)A - (P(t)B + N)R^{-1}(B^T P(t) + N^T) + Q = -\dot{P}(t) \tag{6.8}$$

with the boundary condition

$$P(t_1) = F(T_1) \tag{6.9}$$

For an infinite horizon (t ➔ ∞), the cost function becomes

$$J = \int_{t_0}^{t_\infty} (x^T Q_x + u^T R\, u + 2x^T N\, u)\, dt \tag{6.10}$$

and K becomes

$$K = R^{-1}(B^T\, P + N^T) \tag{6.11}$$

and P is found by solving the continuous time Riccati differential equation.

$$A^T P + PA - (PB + N)R^{-1}(B^T P + N^T) + Q = 0 \tag{6.12}$$

The Riccati equation can be written as follows:

$$\alpha^T P + P\alpha - PBR^{-1}B^T P + \vartheta = 0 \tag{6.13}$$

with

$$\alpha = A - BR^{-1}N^T \text{ and } \vartheta = Q - NR^{-1}N^T \tag{6.14}$$

When the feedback control law shown in equation 6.6 is applied with the steady state value of P, the resulting closed loop system is stable enabling to eliminate the stability concerns.

6.2 Model Predictive Control

MPC originated in the late seventies and has been considerably developed in terms of capability and usage area. In fact MPC does not refer to a specific control methodology, instead a wide range of control methodologies that has an explicit use of a model of the process to obtain the desired control signal by minimizing an objective function. The core of all model predictive controllers is to optimize forecasts of the process behaviour via manipulation the plant inputs. The methodology of all the controllers at the MPC family can be summarized as below [48]:

- The future outputs for a determined horizon N, called the prediction horizon, are predicted at each instant t using the process model (Figure 6.3). These predicted outputs $y\ (t+k|t)$ for $k\ =\ 1\ \ldots\ N$ depend on the known values up to instant t (past inputs and outputs) and on the future control signals $u\ (t+k|t)$, $k\ =\ 0\ \ldots\ N$ – 1, which are those to be sent to the system and to be calculated.
- The set of future control signals is calculated by optimizing a determined criterion in order to keep the process as close as possible to the reference trajectory $r(t+k)$. This criterion usually takes the form of a quadratic function of errors between the predicted output signal and the predicted reference trajectory. The control effort is included in the objective function in most cases. An explicit solution can be obtained if the criterion is quadratic, the model is linear and there are no constraints, otherwise an iterative optimization method has to be used.
- The control signal $u\ (t|t)$ is sent to the process whilst the next control signals calculated are rejected, because at the next sampling instant $y(t+1)$ is already known and 1st step is repeated with this new value and all the sequences are brought up to date. Thus the $u\ (t+1|t+1)$ is calculated (which in principle will be different to the $u\ (t+1|t)$ because of the new information available) using the receding horizon concept.

Figure 6.4 depicts the basic structure of the MPC algorithm. A model is used to predict the plant outputs, based on past and current values and on the proposed optimal future control actions. These actions are calculated by the optimizer taking into account the cost function as well as the constraints.

All the MPC algorithms possess common elements as follows: prediction model, objective function, obtaining control law. Prediction model is kind of heart of the MPC algorithm therefore it needs to be complete enough to fully capture the process dynamics. In general prediction model consists of process and disturbance models. The use of the process model is determined by the necessity to calculate the predicted output at the future instants $y\ (t+k|t)$. Process model can be in different forms depending on the complexity of the plant itself. Some of the most common forms are as follows: Impulse response models, step response models, transfer function models, state space models, and nonlinear models.

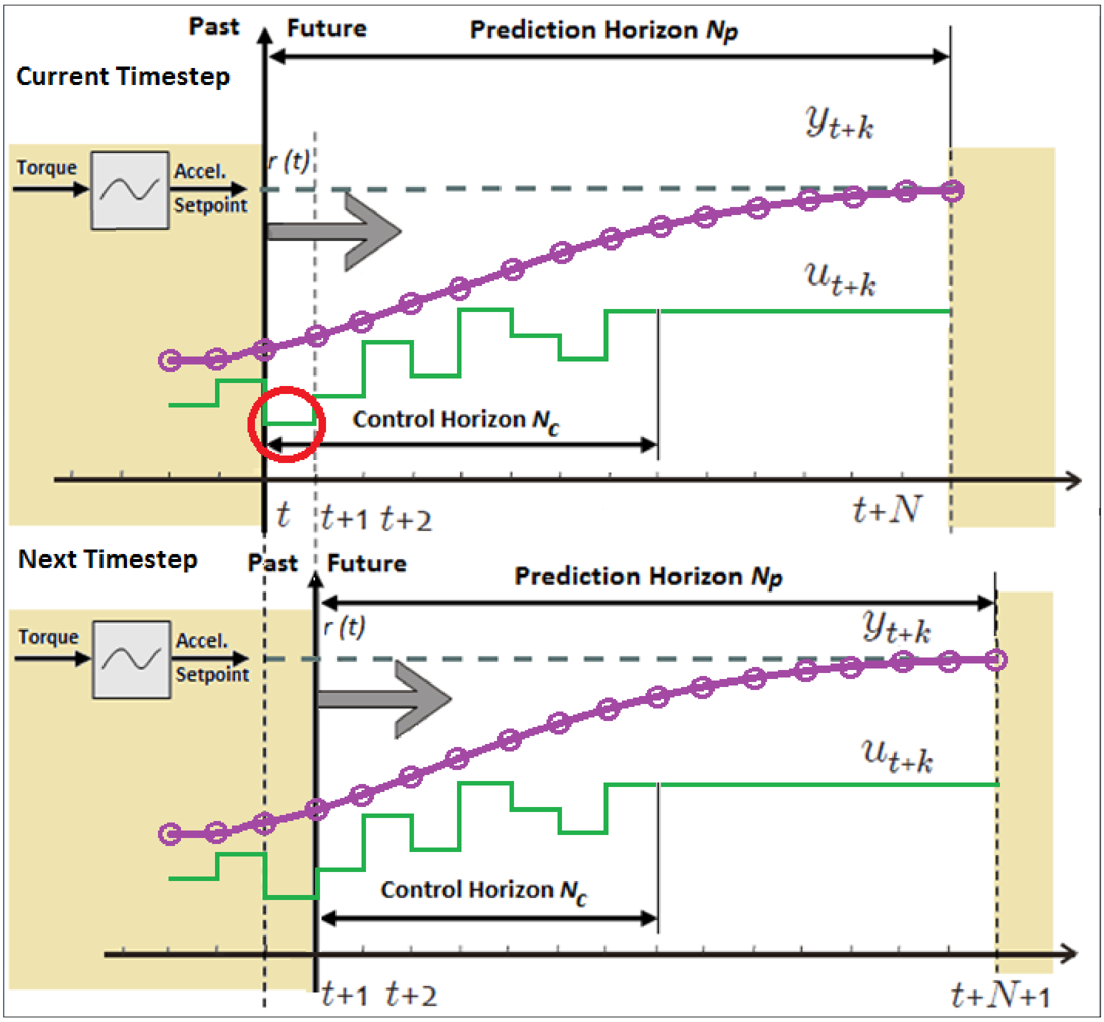
Past
Future
Prediction Horizon Np
Current Timestep
y_{t+k}
Torque
Accel.
Setpoint
r (t)
u_{t+k}
Control Horizon N_c
t
$t+1$
$t+2$
$t+N$
Next Timestep
Past
Future
Prediction Horizon Np
Torque
Accel.
Setpoint
r (t)
y_{t+k}
u_{t+k}
Control Horizon N_c
$t+1$
$t+2$
$t+N+1$

Figure 6.3 : MPC operation for single input single output system.

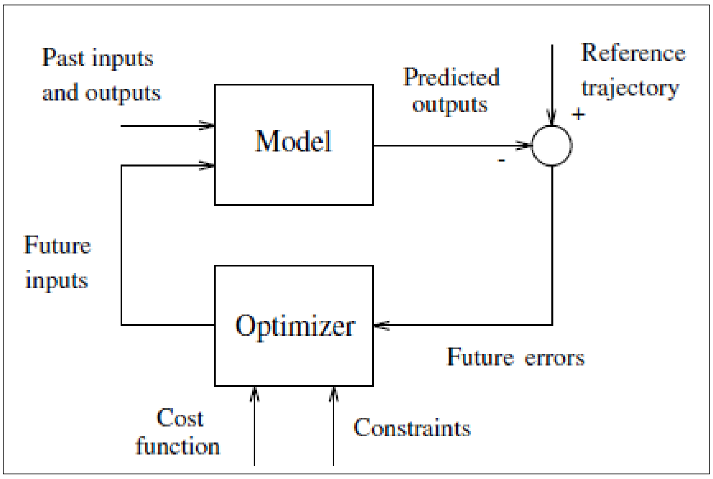
Past inputs
and outputs
Model
Predicted
outputs
Reference
trajectory
+
-
Future
inputs
Optimizer
Future errors
Cost
function
Constraints

Figure 6.4 : Basic structure of MPC [49].

Many processes are nonlinear to varying degrees of severity. In many situations the process will be operating in the neighbourhood of a steady state, and therefore a linear representation will be adequate. A major mathematical obstacle is the lack of superposition principle for nonlinear models, resulting to the fact that the determination of models from process input/output data becomes a very difficult task. If the deviation from linearity is not too large, some approximations can be made, which acknowledge that certain system characteristics change from the operating point to operating point, but it assumes linearity in the neighbourhood of a specific point. It is possible to linearize the model around several operating points and afterwards use with the linear MPC strategy as the process moves from one operating point to the other. Another method is the extended linear MPC in which a basic linear model is used in combination with an explicit model which captures nonlinearities. Different approaches exist that use Wiener models, artificial neural networks, Volterra models, Hammerstein models, NARX models, fuzzy models, etc. which are more appropriate when the nonlinearities are more severe. Within this thesis study nonlinear model structure is used. Plant model containing both vehicle and engine models contain nonlinear elements. Therefore within the MPC toolbox, nonlinear plant model is linearized using Hammerstein-Wiener models.

Objective function is the second element of the MPC algorithms. Various MPC algorithms propose different cost functions for obtaining the control law. The general aim is that the future output (y) on the considered horizon should follow a determined reference signal (r) via calculating the control effort (Δu). The generalized expression for such an objective function is as follows:

$$J(N_1, N_2, N_u) = \begin{array}{c} \sum_{j=N_1}^{N_2} \delta(j)[y(t+j|t) - r(t+j)]^2 + \\ \sum_{j=1}^{N_u} \gamma(j)[\Delta u(t+j-1)]^2 \end{array} \tag{6.15}$$

where N_1 and N_2 are the minimum and the maximum cost horizons and N_u is the control horizon. The meanings of N_1 and N_2 is, they mark the limits of the instants in which it is desirable for the output to follow the reference. Thus, is a high value of N_1 is taken, it will mean that the errors in the first instant for the overall control process is not important. In longitudinal vehicle control applications the first instants are significantly important therefore N_1 is taken as 0. The coefficients $\delta(j)$ and $\gamma(j)$ are the sequences that consider the future behaviour, usually constant values or exponential sequences are considered.

In practice all processes are subjected to constraints. The actuators have a limited field of action as well as a determined slew rate. Considering these limitations, the introduction of constraints is necessary. Normally bounds in the amplitude and the slew rate of the control signal and limits in the outputs will be considered as follows:

$$\begin{aligned} u_{min} &\leq u(t) \leq u_{max} \\ du_{min} &\leq u(t) - u(t-1) \leq du_{max} \qquad (6.16) \\ y_{min} &\leq y(t) \leq y_{max} \end{aligned}$$

By adding these constraints to the objective function the minimization becomes more complex so that the solution cannot be obtained explicitly as in the unconstraint case. Considering the longitudinal vehicle motion, the control element is the produced torque itself. Therefore it is absolutely necessary to define the constraints. The full load torque curve and friction torque curves should be feed to the system as the operating rate of the control signal. Additional derivative of the torque curve should also be taken into considerations especially for the torque build up case. Within this perspective, in this study torque request from the engine as control signal is constrained.

In order to calculate the values $u\,(t+k|t)$, it is necessary to minimize the objective function equation 6.15, via calculating the values of the predicted outputs $y\,(t+k|t)$as a function of past values of the inputs and outputs and of future control signals. An analytic solution can be obtained if the model is linear and there are not constraints, otherwise an iterative method of optimization should be employed. Considering the fact that there will be $N_2 - N_1 + 1$ independent variables which can be in the order of 30 ~ 50, the control structure is imposed by the use of the control horizon concept (N_u). The main logic is as follows, after a certain interval $N_u < N_2$ there is no variation on the control signals which is equivalent to giving infinite weights to the changes in the control from a certain instant.

$$\Delta u(t+j-1)=0 \qquad j>N_u \tag{6.17}$$

As stated earlier, MPC can be used for vehicle longitudinal motion control due to its ability to handle actuator and sensor constraints under finite horizon constrained optimal control framework. There are several advantages of using MPC:

- Intuitive controller concept and relatively easy tuning procedure,
- Engine brake torque absolute and torque increase / decrease rate limits suits well with the MPC control signal constrains concept,
- It includes feed forward control that acts against measured disturbances.

Based on the receding horizon control concept, the linear MPC problem can be formulated by using the discrete time model.

$$\begin{aligned} x_{t+1} &= Ax_t + Bu_t \\ y_t &= Cx_t \end{aligned} \tag{6.18}$$

where *x* is the state vector and *u* is the input vector (mainly indicated as manipulated variables) calculated after solving the optimal control problem. A general formulation of the cost function used at the optimizer of the MPC used in this thesis can be described as follows:

$$\underset{u_t,\ldots,u_{t+N-1}}{min} \quad \left\{\sum_{k=0}^{N-1} \|y_{t+k}-r(t)\|^2+\rho\|u_{t+k}-u_r(t)\|^2\right\} \tag{6.19}$$

subjected to

$$\begin{gathered} x_{t+k+1}=f(x_{t+k},u_{t+k}) \\ y_{t+k}=g(x_{t+k},u_{t+k}) \\ u_{min}\le u_{t+k}\le u_{max} \\ y_{min}\le y_{t+k}\le y_{max} \\ x_t=x(t), k=0,\ldots,N-1 \end{gathered} \tag{6.20}$$

Where u_{min} and u_{max} are the plant input constrains, for the subjected problem friction torque and maximum available torque, similarly y_{min} and y_{max} are the minimum and maximum acceleration quantities for that specific gear. Constraining inputs is definitely required due to the fact that MPC controller can result with a higher torque request that the engine can deliver which will definitely degrade the performance of the controller. The input vector U includes the N_c future input changes. In MPC terminology, N_c is called the control horizon (CH). CH is basically the number of samples that are necessary to capture future control inputs. N_p is the size of the predicted states and output and is called the Prediction Horizon (PH). CH and PH are the main tuning parameters in MPC.

MPC can be used for longitudinal vehicle torque control due to its ability to handle input and output constraints under finite horizon constrained optimal control framework. Once plant model is defined accurately, tuning of the MPC is easy due to intuitive controller concept. Moreover MPC includes feed forward control that acts against measured disturbances such as accessory losses like alternator and air conditioning in automotive applications; however accessory losses are not subjected within the content of this study.

For the proposed study MPC setup parameters are defined as follows:

- Control interval: 0.01s
- Predicted horizon intervals: 100
- Control horizon intervals: 40

MATLAB/Simulink model of the 3 mass model with controller is shown at figure 6.5. Road load resistant force at crankshaft level is subtracted from the driver acceleration pedal request torque and multiplied by 1/total inertia value in order to achieve the vehicle acceleration request which is used as the reference setpoint value for the MPC controller. Modelled vehicle acceleration value is taken as the input to the controller with engine brake torque values as the control variable. Additional P controller using engine and vehicle speed difference value as input variable generates an anti-shuffle torque which is subtracted from the MPC controller output value.

Content of the MPC algorithm block model is showed at figure 6.6. Generally MATLAB/Simulink MPC algorithm consists of three main blocks: reference and modelled disturbance, state estimator and optimizer block. Reference and modelled disturbance and optimizer block consists of S-functions. State estimator block content is showed at figure 6.7. In general, the controller states are unmeasured and must be estimated. By default, the controller uses a steady state Kalman filter that derives from the state observer.

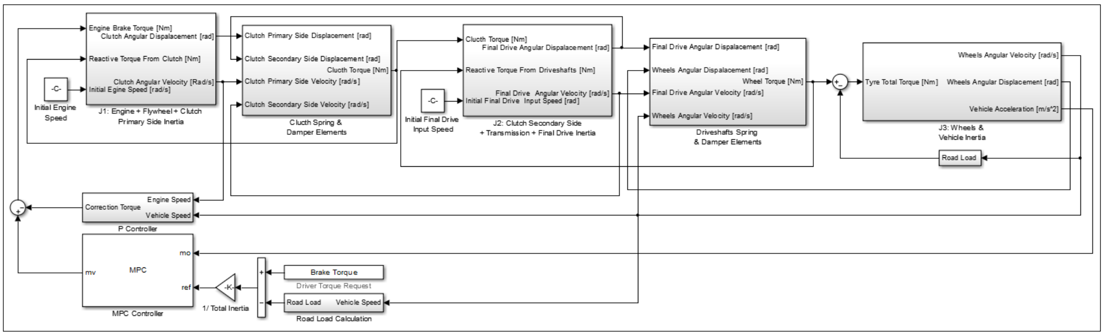
Engine Brake Torque [Nm]
Clutch Angular Dispalacement [rad]
Reactive Torque From Clutch [Nm]
Clutch Angular Velocity [Rad/s]
Initial Egine Speed [rad/s]
-C-
Initial Engine Speed
J1: Engine + Flywheel + Clutch Primary Side Inertia
Clutch Primary Side Displacement [rad]
Clutch Secondary Side Displacement [rad]
Clucth Torque [Nm]
Clutch Primary Side Velocity [rad/s]
Clutch Secondary Side Velocity [rad/s]
Clucth Spring & Damper Elements
Clucth Torque [Nm]
Final Drive Angular Dispalacement [rad]
Reactive Torque From Driveshafts [Nm]
Final Drive Angular Velocity [rad/s]
Initial Final Drive Input Speed [rad]
-C-
Initial Final Drive Input Speed
J2: Clutch Secondary Side + Transmission + Final Drive Inertia
Final Drive Angular Dispalacement [rad]
Wheels Angular Dispalacement [rad]
Wheel Torque [Nm]
Final Drive Angular Velocity [rad/s]
Wheels Angular Velocity [rad/s]
Driveshafts Spring & Damper Elements
Tyre Total Torque [Nm]
Wheels Angular Velocity [rad/s]
Wheels Angular Displacement [rad]
Vehicle Acceleration [m/s^2]
J3: Wheels & Vehicle Inertia
Road Load
Correction Torque
Engine Speed
Vehicle Speed
P Controller
mv
MPC
mo
ref
MPC Controller
-K-
1/ Total Inertia
Brake Torque
Driver Torque Request
Road Load
Vehicle Speed
Road Load Calculation

Figure 6.5 : MATLAB/Simulink model of the 3 mass model with MPC + P controller.

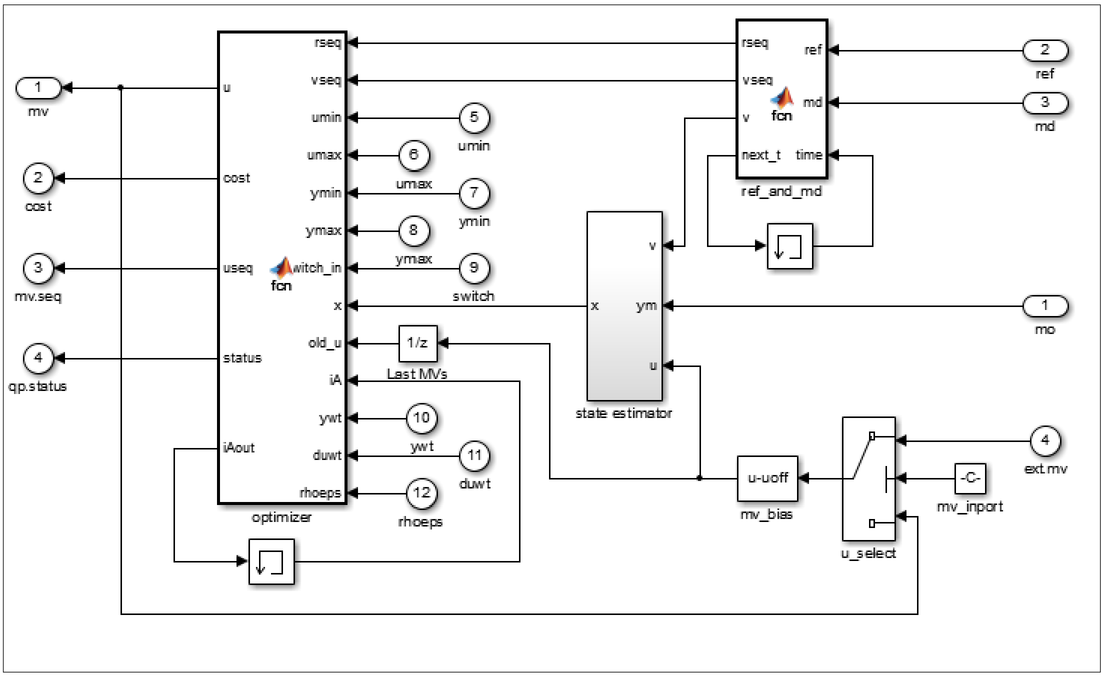
1
mv
2
cost
3
mv.seq
4
qp.status
u
cost
useq
status
iAout
rseq
vseq
umin
umax
ymin
ymax
switch_in
fcn
x
old_u
iA
ywt
duwt
rhoeps
optimizer
5
umin
6
umax
7
ymin
8
ymax
9
switch
1/z
Last MVs
10
ywt
11
duwt
12
rhoeps
v
x
ym
u
state estimator
rseq
vseq
v
next_t
ref
md
time
fcn
ref_and_md
2
ref
3
md
1
mo
u-uoff
mv_bias
u_select
-C-
mv_inport
4
ext.mv

Figure 6.6 : MPC Simulink model blocks.

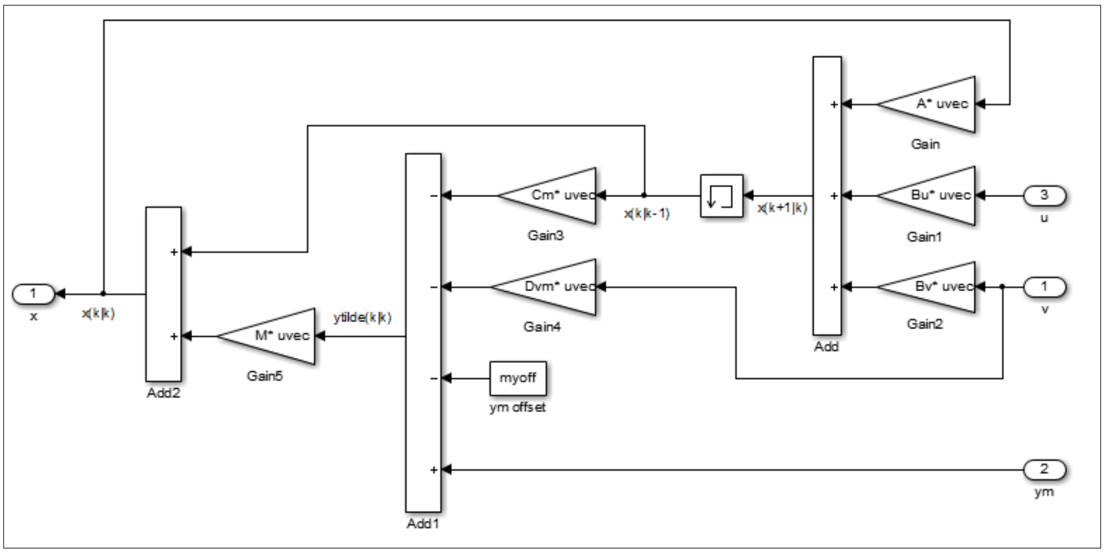
A* uvec
Gain
Bu* uvec
Gain1
Bv* uvec
Gain2
Add
3
u
1
v
2
ym
x(k+1|k)
x(k|k-1)
Cm* uvec
Gain3
Dvm* uvec
Gain4
myoff
ym offset
Add1
ytilde(k|k)
M* uvec
Gain5
Add2
x(k|k)
1
x

Figure 6.7 : MPC state estimator Simulink block diagram.

6.3 MPC Parameter Study

This section deals with MPC algorithm tuning parameters determination. Both for the 2 and 3 mass powertrain models, MPC parameters were tuned for each gear. On the other hand in this section, MPC controller tuning only for 2 mass vehicle model for 3rd and 4th gears will be explained. MPC controller tuning tables and figures for 3 mass model for 3rd and 4th gears are appendix C section.

6.3.1 2 mass vehicle model MPC tuning for 3rd gear

MPC controller uses the vehicle acceleration request as the reference variable. MPC block takes input from the following driver input, and vehicle measurement components and supplies the engine brake torque signal. Engine brake torque signal that is fed to the vehicle model is the manipulated variable. Vehicle acceleration simulation is the measured variable. Engine brake signal fed to the engine and vehicle model is the control variable. In order to tune the MPC, a custom made engine brake torque request signal, which contains load change manoeuvres within the maximum torque range that the engine is capable of delivery, is generated as shown on figure 6.8. Due to gearbox based torque limitation maximum torque is restricted to 400 Nm.

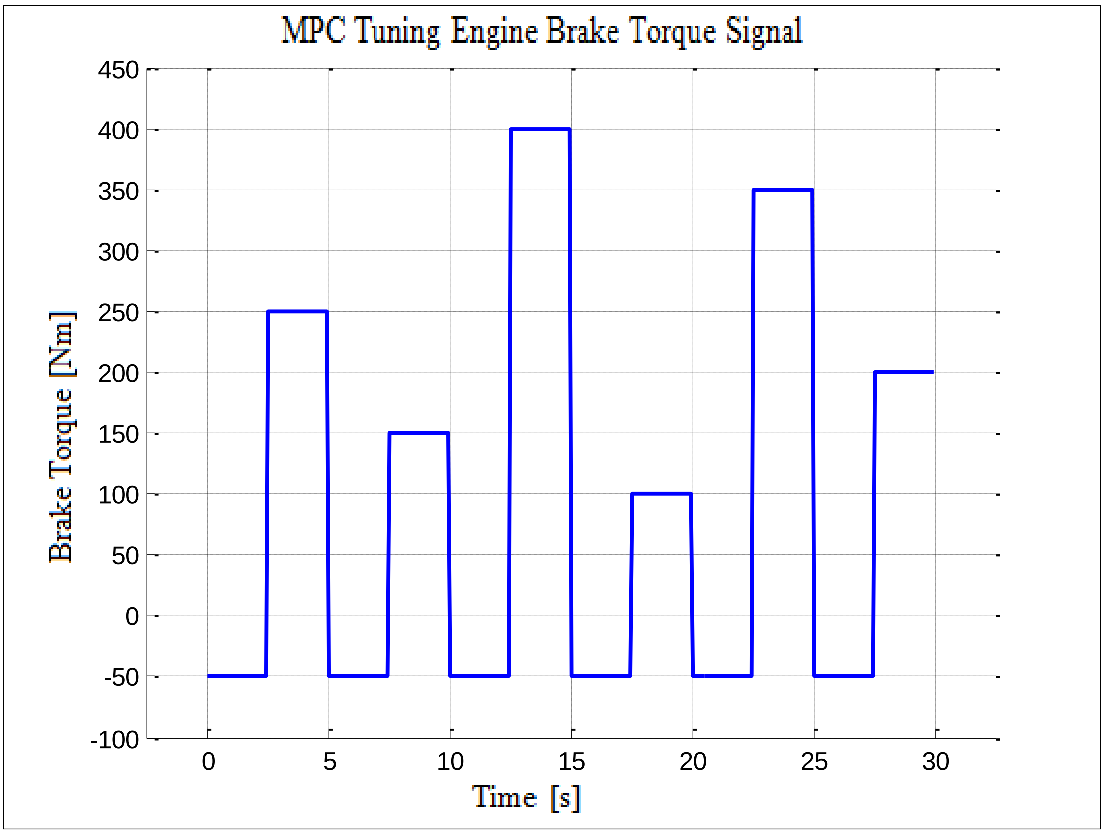

Figure 6.8 : MPC tuning engine brake torque signal for 3rd gear.

Afterwards the generated torque signal is converted to the vehicle acceleration request using the total vehicle inertia including all the rotating components in that specified gear. Comparison of the vehicle acceleration request and vehicle response to the torque request signal without any controller using the developed vehicle model is showed at figures 6.9 and 6.10.

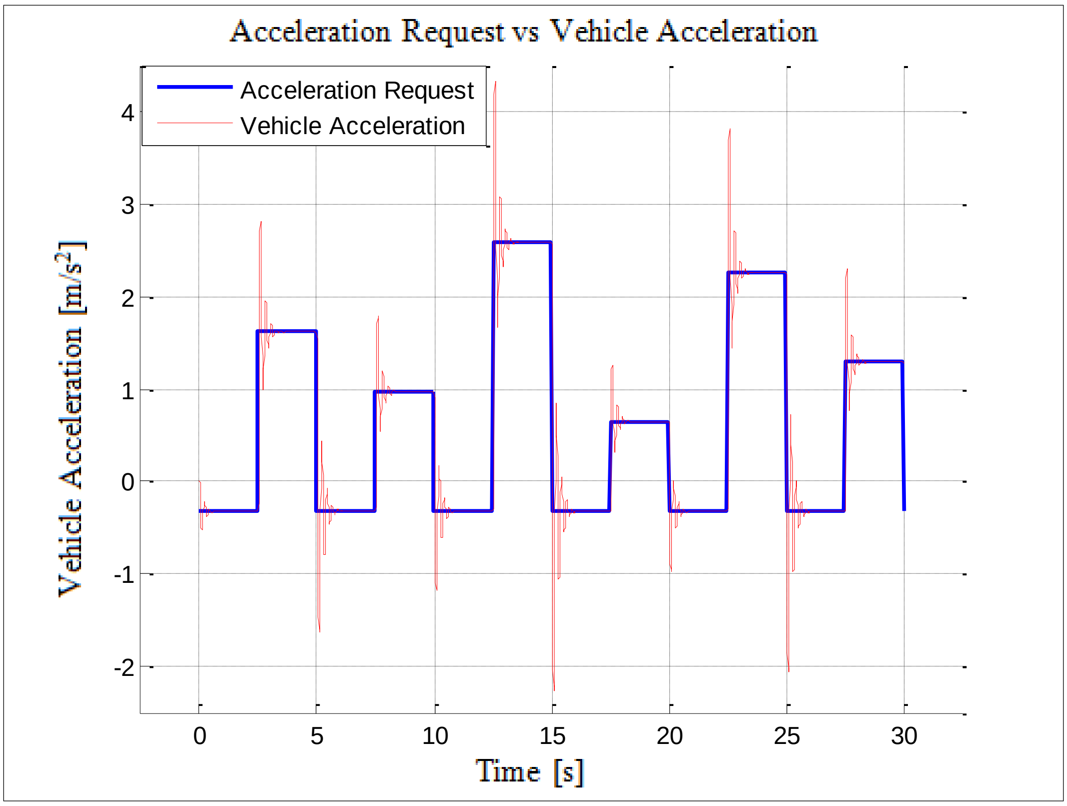

Figure 6.9 : Vehicle acceleration response for no controller case for 3rd gear.

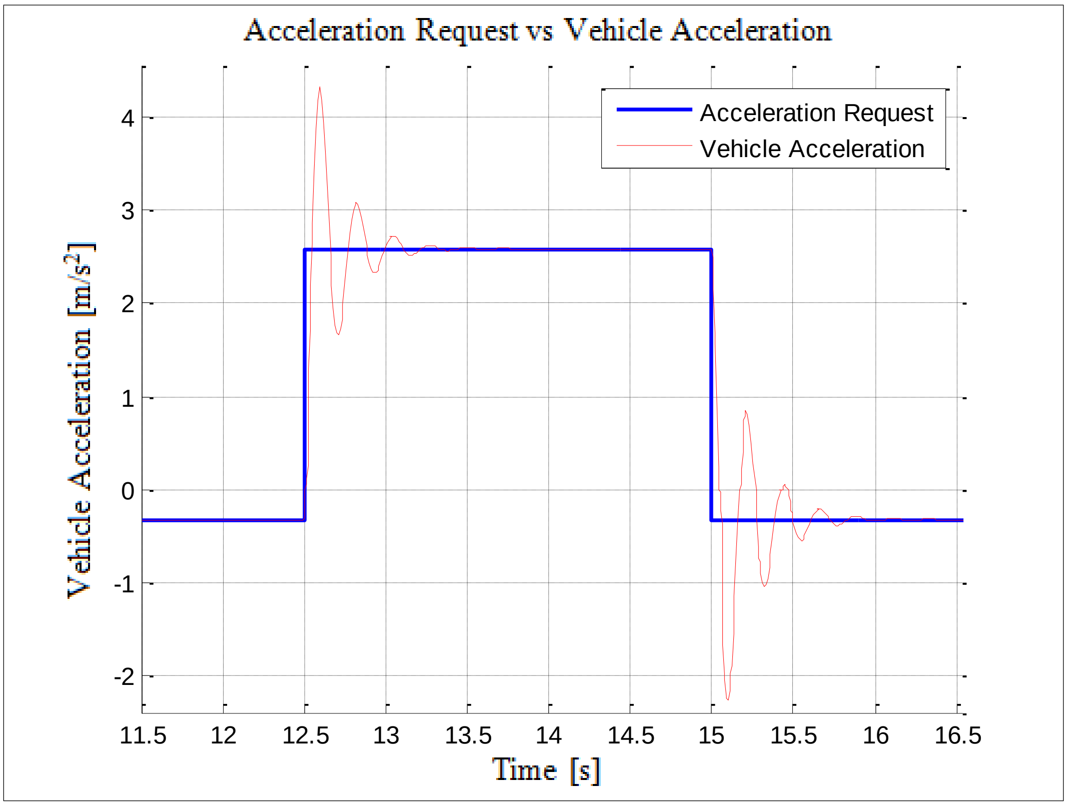

Figure 6.10 : Vehicle acceleration response for no controller case (Zoomed view at maximum load change manoeuvre) for 3rd gear.

MATLAB/Simulink 2012b MPC controller toolbox is a very powerful and user-friendly toolbox. Optional in-ports like measured disturbances, input and output limits and out-ports like optimal cost, optimization status and optimal control sequence are not selected. Input and output limitations were defined within the toolbox however for ECU implementation the limitations lime maximum and minimum available torque should be supplied externally. MPC structure overview is shown at figure 6.11. MPC toolbox automatically linearizes the plant model. Discrete time state space model structure for the 2 mass model at 3rd gear is as follows:

$$\begin{array}{ccc} a= & x1 & x2 \\ x1 & 0.8955 & 0.1045 \\ x2 & 0.002701 & 0.9973 \end{array}$$
$$\begin{array}{cc} b= & u1 \\ x1 & 0.03488 \\ x2 & 5.07e^{-5} \end{array} \tag{6.21}$$
$$\begin{array}{ccc} c= & x1 & x2 \\ y1 & 0.0199 & -0.0199 \end{array}$$
$$\begin{array}{cc} d= & u1 \\ y1 & 0 \end{array}$$

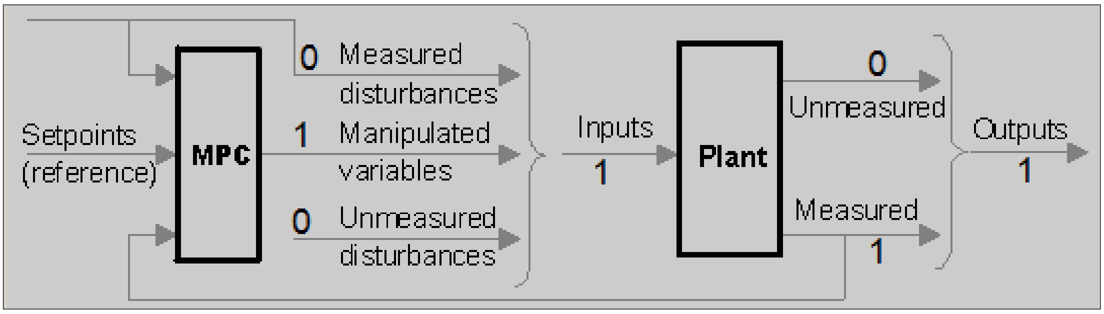

Figure 6.11 : MPC structure overview.

Constraints on manipulated variables are defined according to engine specifications. Minimum engine motoring friction torque is 50Nm at 4500 rpm and maximum engine torque is restricted to 400 Nm at 3rd gear. Therefore minimum and maximum manipulated variable is defined as 50Nm and 400Nm respectively. For the tip-out manoeuvre engine brake torque is almost limitless, so it is defined as 5000 Nm/s. For the tip-in manoeuvre knee torque obtained from time to torque analysis is 200 Nm achieved within 0.2s. Therefore maximum increase rate of manipulated variable is defined as 1000 Nm/s. Three different MPC controller gains are defined as low, medium and high. Although they are defined with overall weight tuning factor, in table 6.1 input rate weight ad output weights are shown separately. P gain controller gain has been defined as 10 and 20 for normal and high gain configuration respectively.

Table 6.1 : Summary of MPC and P controller gain parameters for 3rd gear 2 mass model.

Controller Type	MPC Gain Input Rate Weight	MPC Gain Output Weight	P Controller Gain
Low Gain MPC	0.14918	0.67032	0
Medium Gain MPC	0.101	1.02	0
Medium Gain MPC + P Controller	0.101	1.02	2.5
High Gain MPC	0.081872	1.2214	0
High Gain MPC + P Controller	0.081872	1.2214	2.5
High Gain MPC + P Controller High Gain	0.081872	1.2214	5

2 mass model at 3rd gear vehicle acceleration responses for all configurations are showed at figure 6.12. Detailed view focusing on the maximum load part is showed at figure 6.13 with tip-in and tip-out zooms at figures 6.14 and 6.15 respectively.

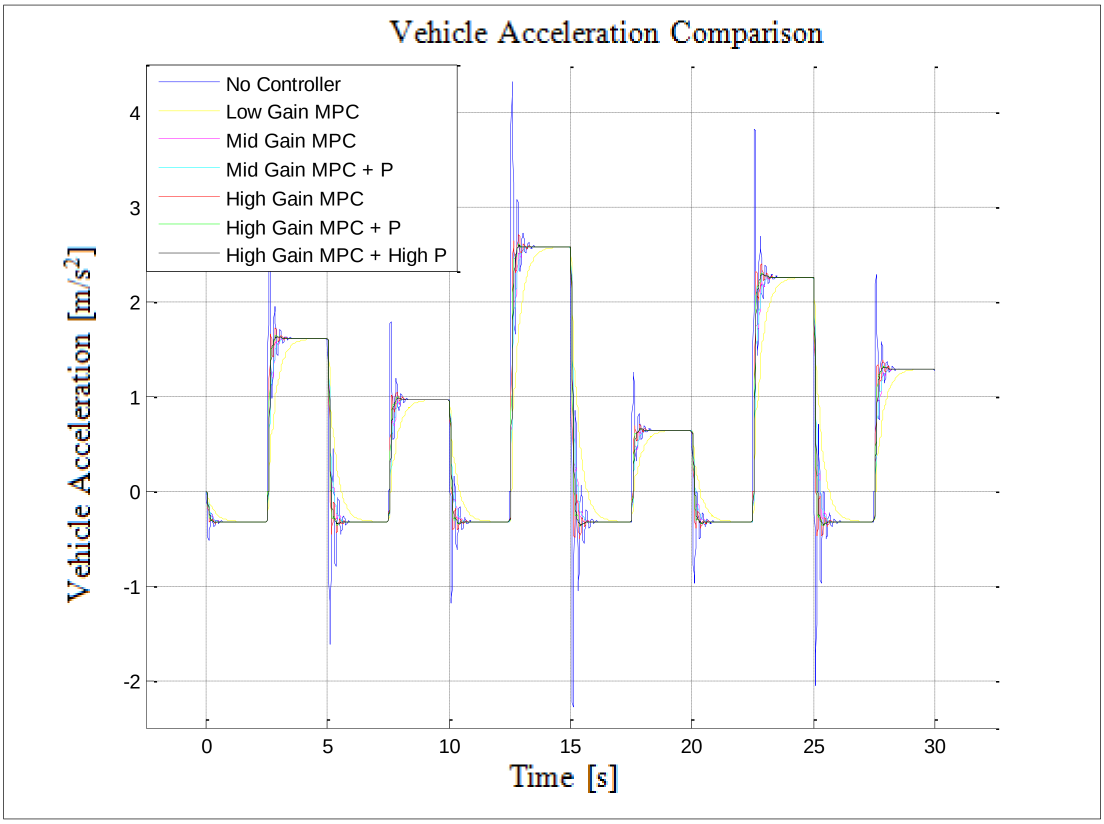

Figure 6.12 : Vehicle acceleration response for MPC parameters determination for 3rd gear.

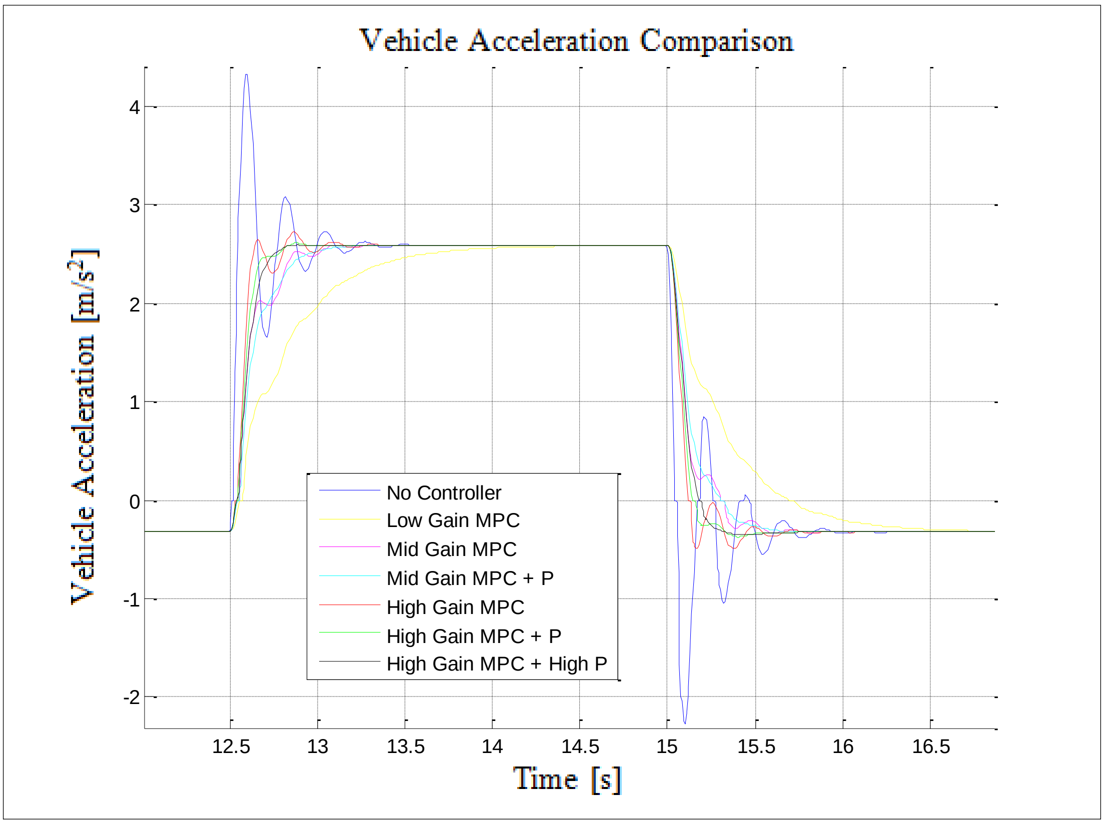

Figure 6.13 : Vehicle acceleration response for MPC parameters determination (Zoomed view at maximum load change manoeuvre) for 3rd gear.

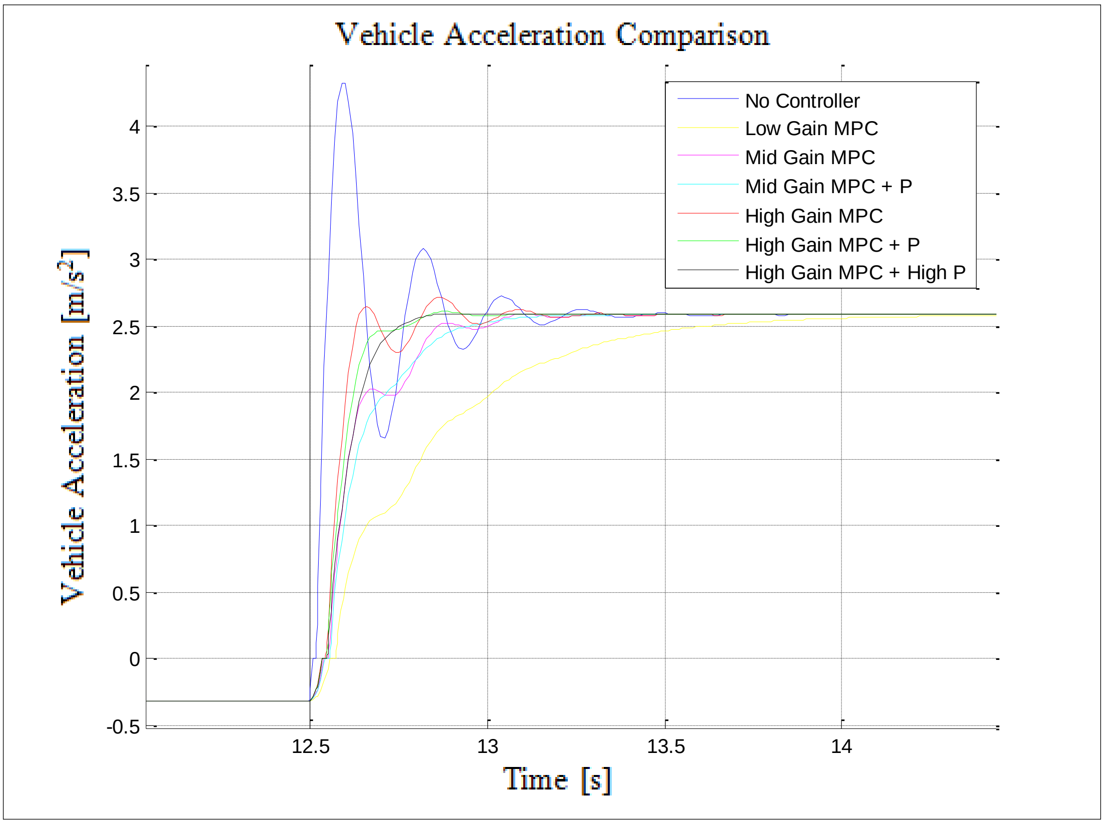

Figure 6.14 : Vehicle acceleration response for MPC parameters determination (Zoomed view at maximum load change tip-in manoeuvre) for 3rd gear.

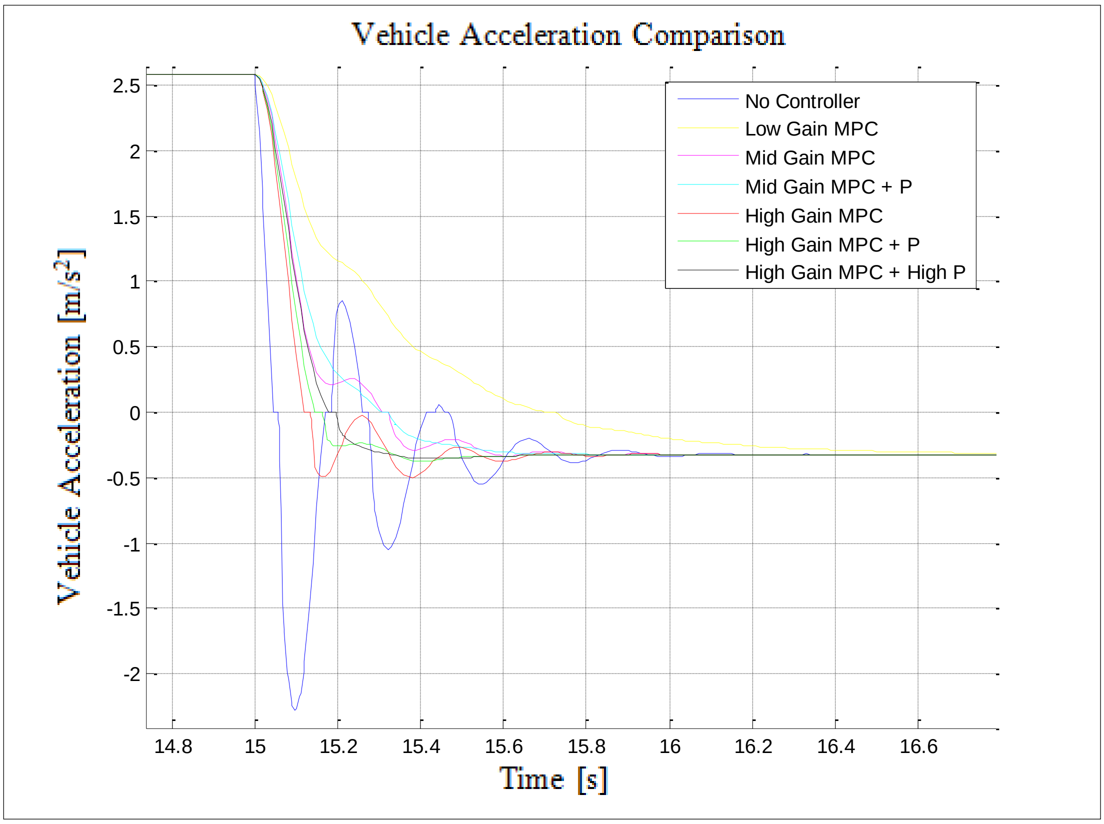

Figure 6.15 : Vehicle acceleration response for MPC parameters determination (Zoomed view at maximum load change tip-out manoeuvre) for 3rd gear.

MPC controller manipulated variable (engine brake torque) signals for all different gain combinations are showed at figure 6.16. Detailed view focusing on the maximum load part is showed at figure 6.17 with tip-in and tip-out zooms at figures 6.18 and 6.19 respectively. Analysis of the results show that MPC controller gain configuration high MPC gain with moderate P controller gain gives the best result as the rise times are 0.2 and 0.15 seconds for the tip-in and tip-out manoeuvres respectively and overshoot values is less than %1 percent.

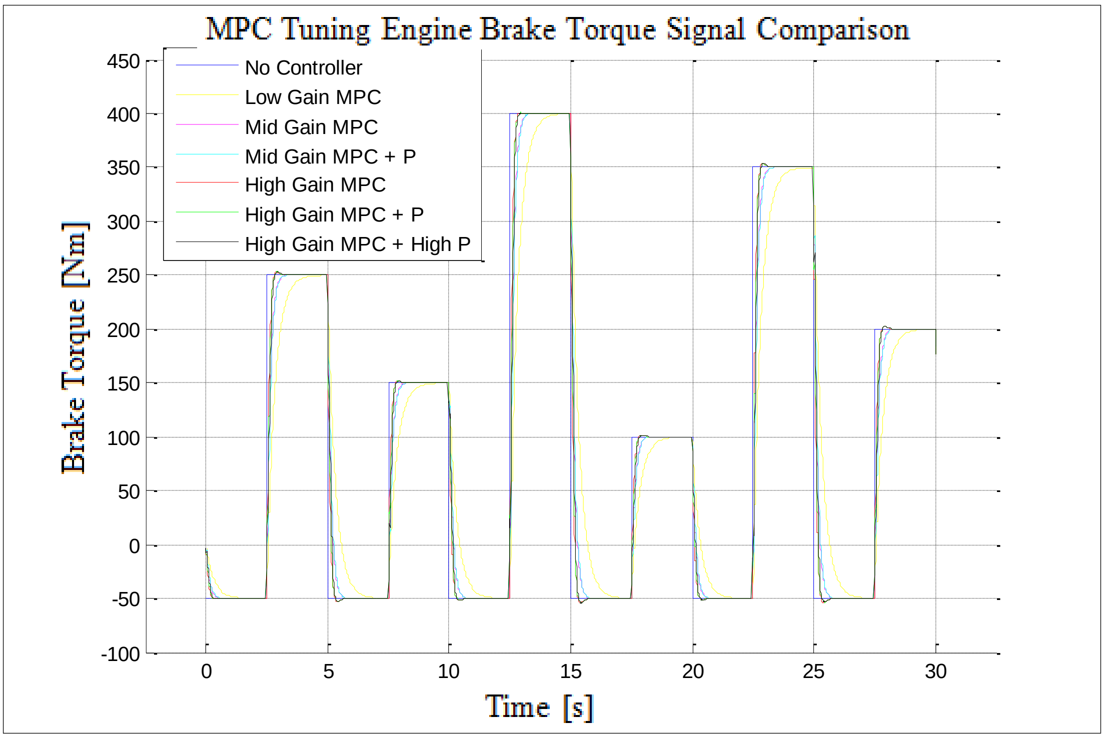

Figure 6.16 : Engine brake torque request for MPC parameters determination for 3rd gear.

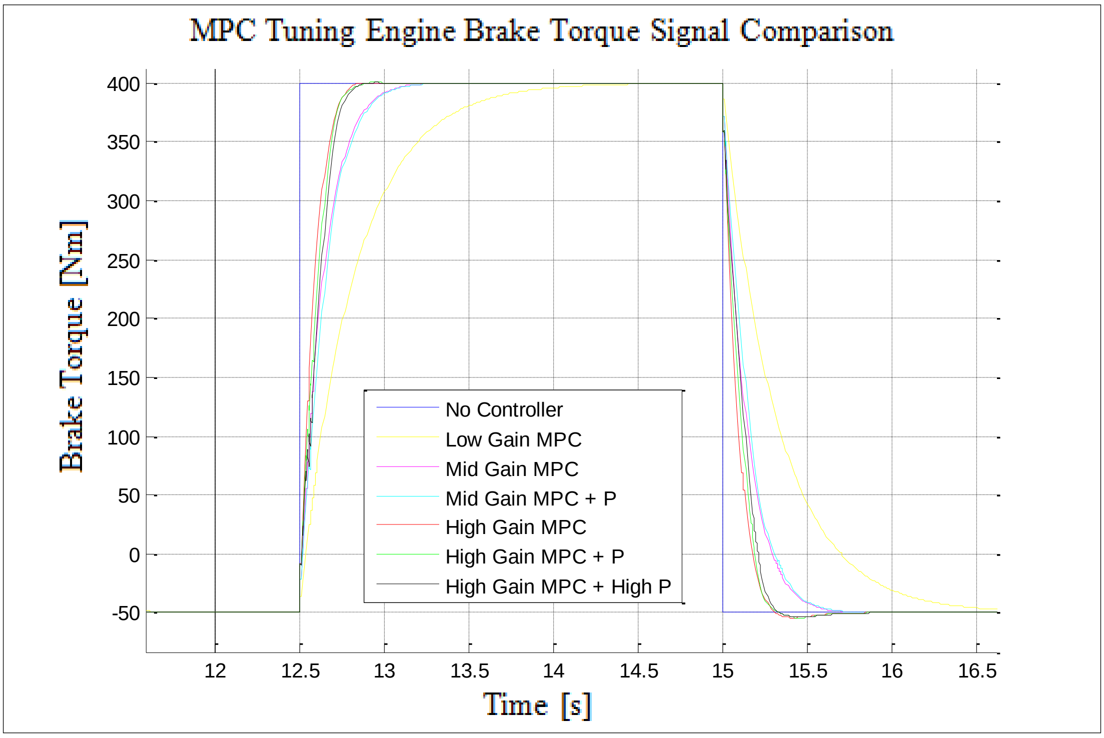

Figure 6.17 : Engine brake torque request for MPC parameters determination (Zoomed view at maximum load change manoeuvre) for 3rd gear.

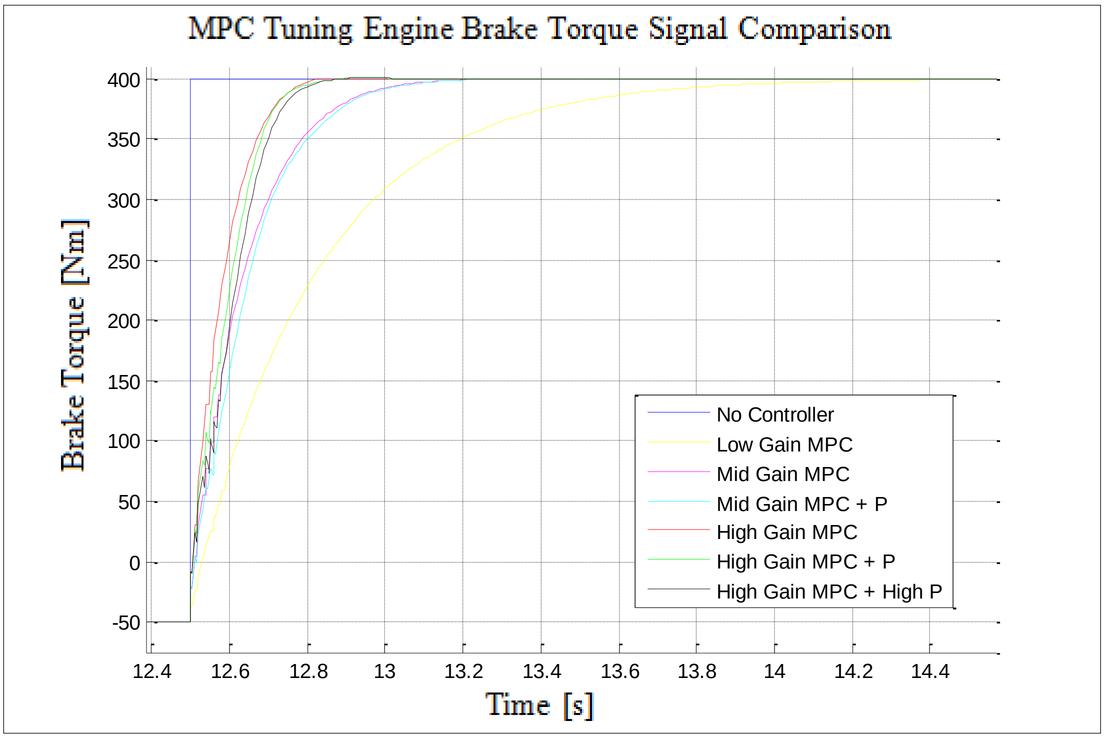

Figure 6.18 : Engine brake torque request for MPC parameters determination (Zoomed view at maximum load change tip-in manoeuvre) for 3rd gear.

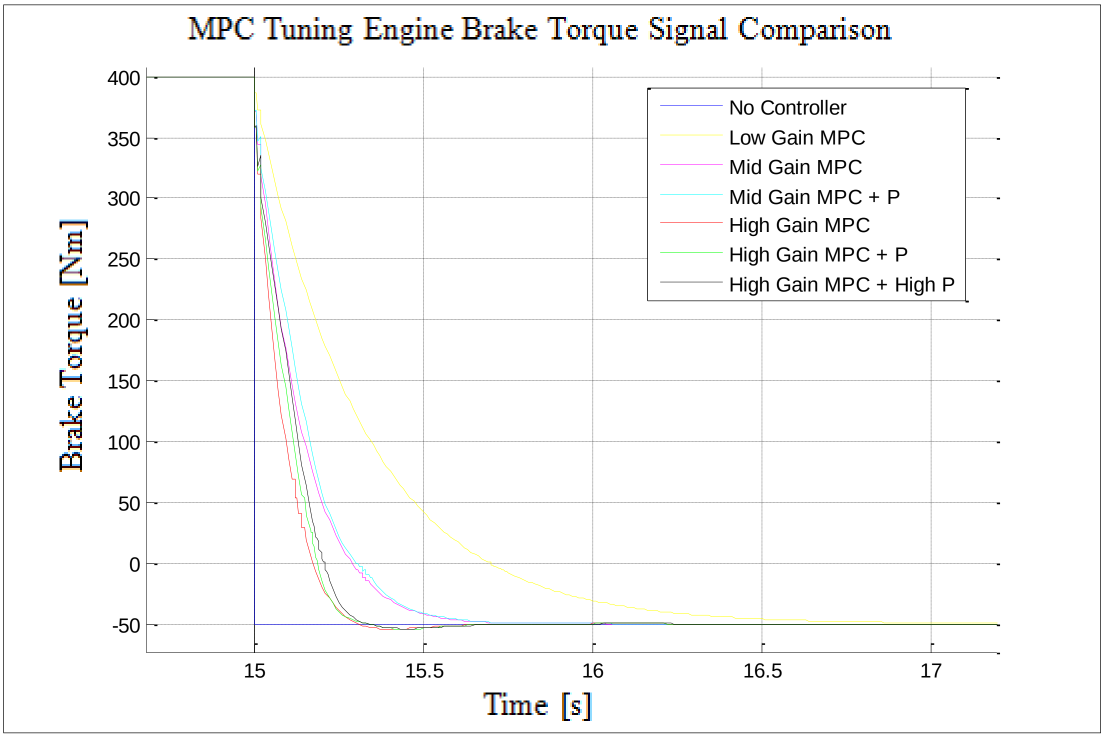

Figure 6.19 : Engine brake torque request for MPC parameters determination (Zoomed view at maximum load change tip-in manoeuvre) for 3rd gear.

6.3.2 2 mass vehicle model MPC tuning for 4th gear

Similarly to the 3rd gear tuning of the MPC controller, a custom made engine brake torque request signal is generated as shown on figure 6.20. Due to there is no gearbox torque limitation at 4th gear, maximum engine torque of the generated signal is takes as 450 Nm.

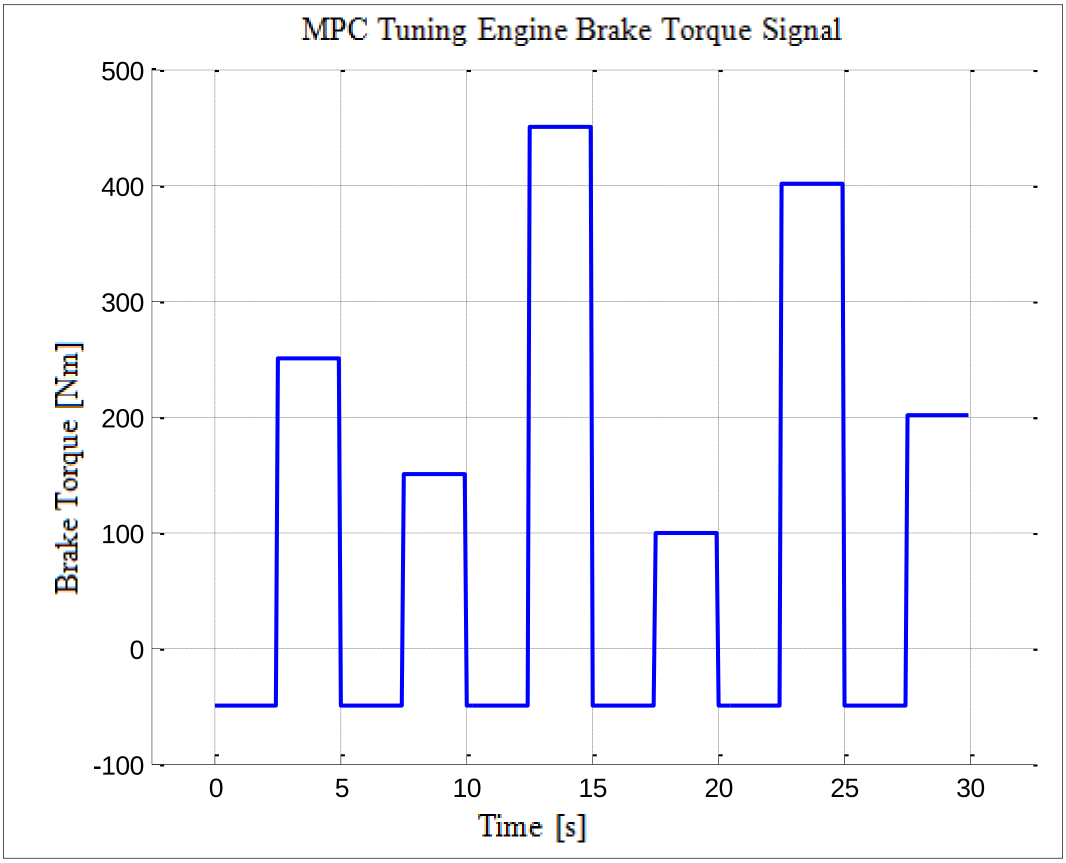

Figure 6.20 : MPC tuning engine brake torque signal for 4th gear.

Afterwards the generated torque signal is converted to the vehicle acceleration request using the total vehicle inertia including all the rotating components in that specified gear. Comparison of the vehicle acceleration request and vehicle response to the torque request signal without any controller using the developed vehicle model is showed at figures 6.21 and 6.22.

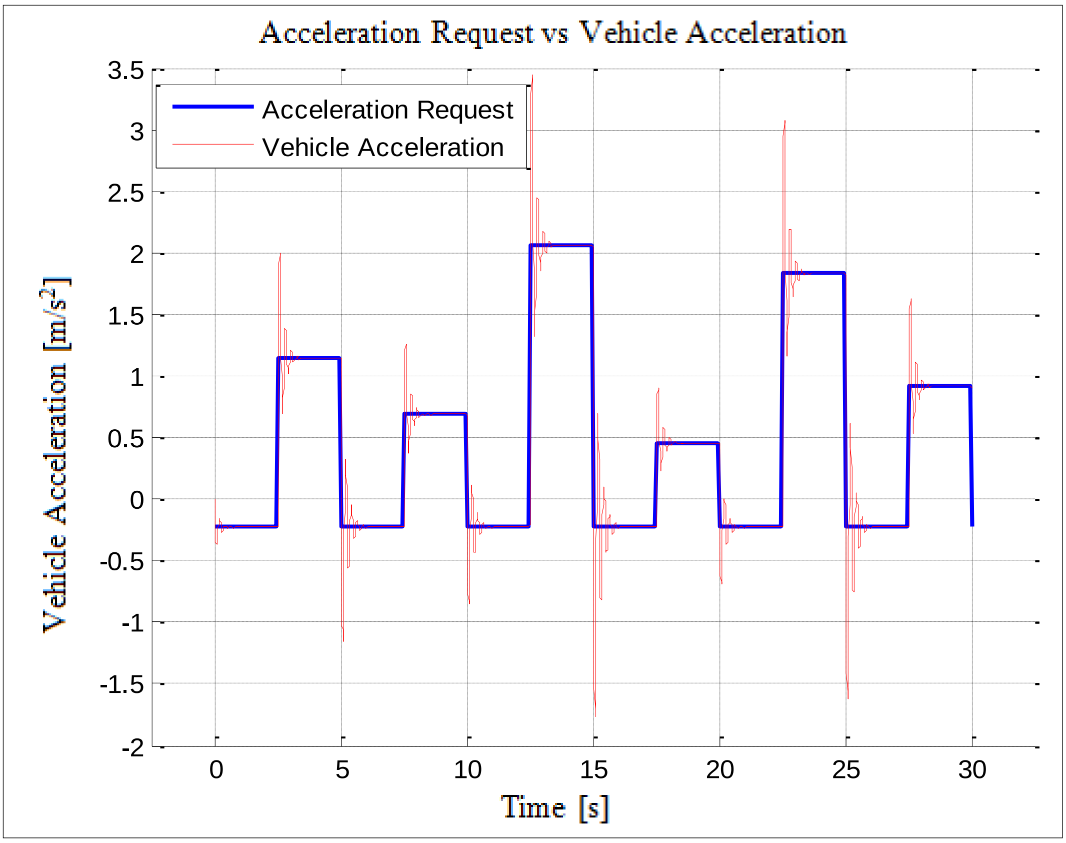

Figure 6.21 : Vehicle acceleration response for no controller case for 4th gear.

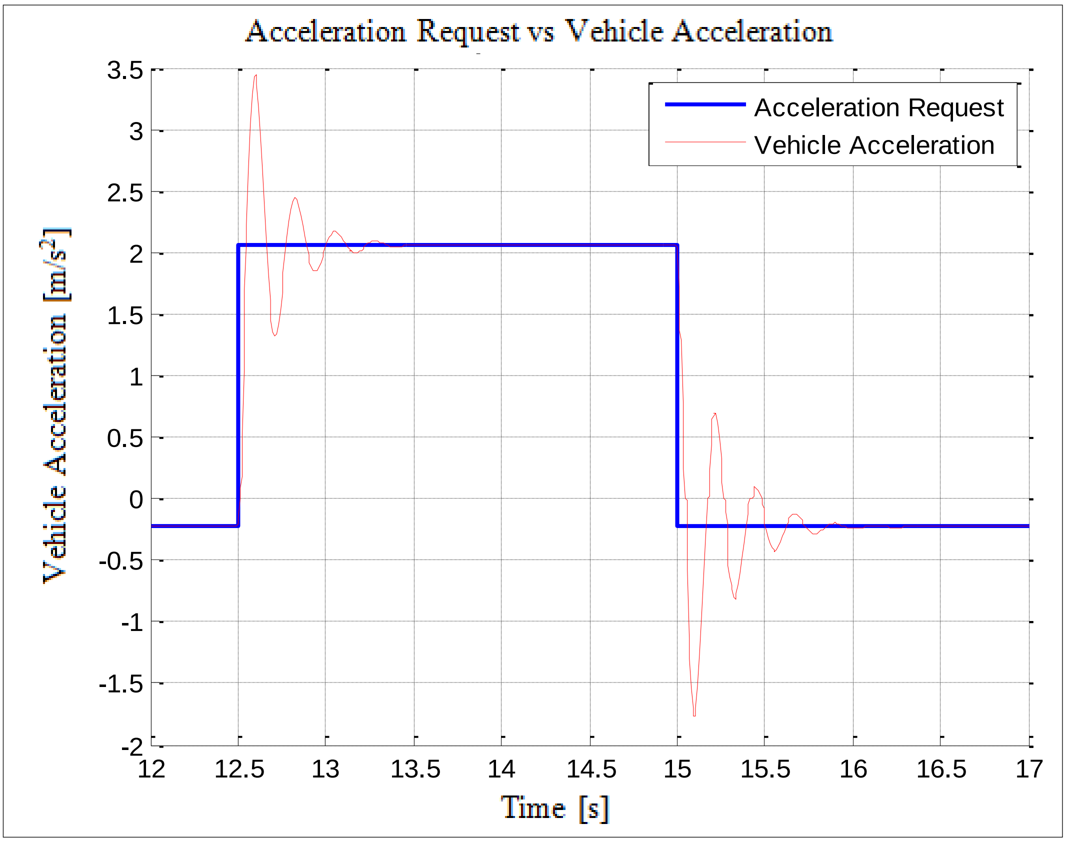

Figure 6.22 : Vehicle acceleration response for no controller case (Zoomed view at maximum load change manoeuvre) for 4th gear.

Discrete time state space model structure for the 2 mass model at 4th gear is as follows:

$$
\begin{array}{ccc} a = & x1 & x2 \\ x1 & 0.8975 & 0.1025 \\ x2 & 0.001321 & 0.9987 \end{array}
$$

$$
\begin{array}{cc} b = & u1 \\ x1 & 0.03418 \\ x2 & 2.426e^{-5} \end{array} \tag{6.21}
$$

$$
\begin{array}{ccc} c = & x1 & x2 \\ y1 & 0.0139 & -0.0139 \end{array}
$$

$$
\begin{array}{cc} d = & u1 \\ y1 & 0 \end{array}
$$

Constraints on manipulated variables are defined similarly to 3rd gear MPC tuning. The only difference is as there is no gearbox limitation at 4th gear, maximum engine torque is set to 450 Nm. Three different MPC controller gains are defined as low, medium and high. Although they are defined with overall weight tuning factor, in table 6.2 input rate weight ad output weights are shown separately. P gain controller gain has been defined as 10 and 20 for normal and high gain configuration respectively.

Table 6.2 : Summary of MPC and P controller gain parameters for 4th gear 2 mass model.

Controller Type	**MPC Gain Input Rate Weight**	**MPC Gain Output Weight**	**P Controller Gain**
Low Gain MPC	0.097886	0.6671	0
Medium Gain MPC	0.067031	1.4918	0
Medium Gain MPC + P Controller	0.067031	1.4918	10
High Gain MPC	0.044932	2.2255	0
High Gain MPC + P Controller	0.044932	2.2255	10
High Gain MPC + P Controller High Gain	0.044932	2.2255	20

2 mass model at 4th gear vehicle acceleration responses for all configurations are showed at figure 6.23. Detailed view focusing on the maximum load part is showed at figure 6.24 with tip-in and tip-out zooms at figures 6.25 and 6.26 respectively.

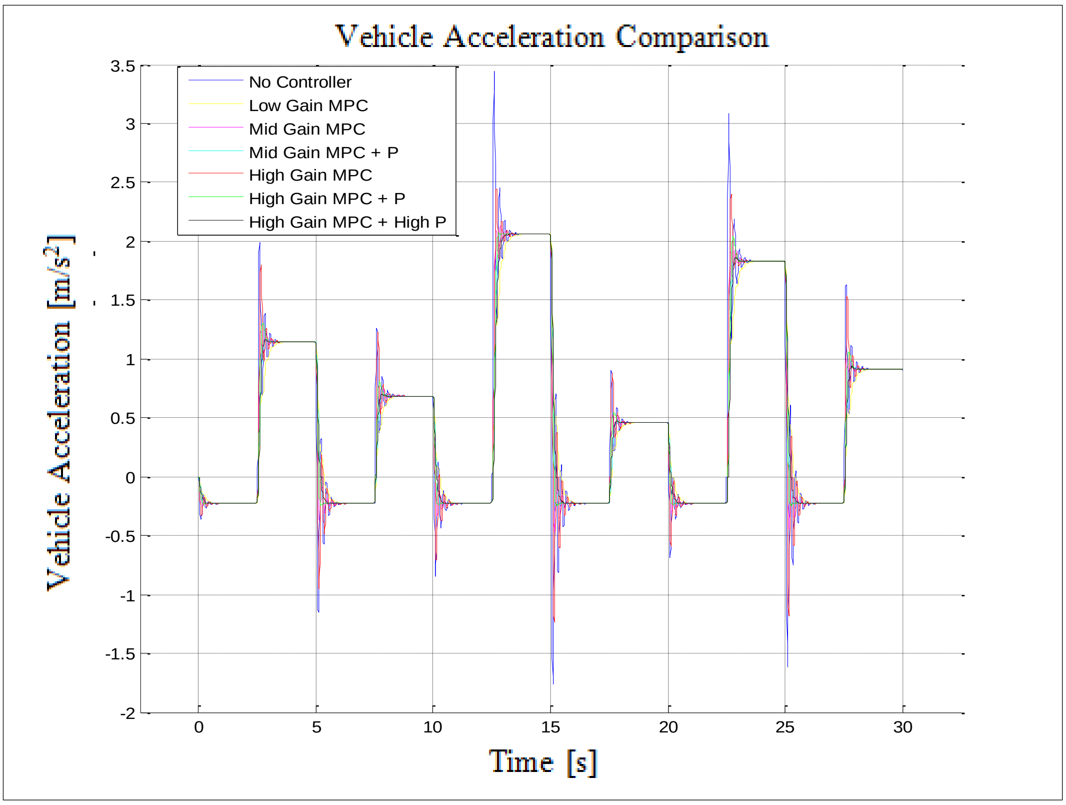

Figure 6.23 : Vehicle acceleration response for MPC parameters determination for 4th gear.

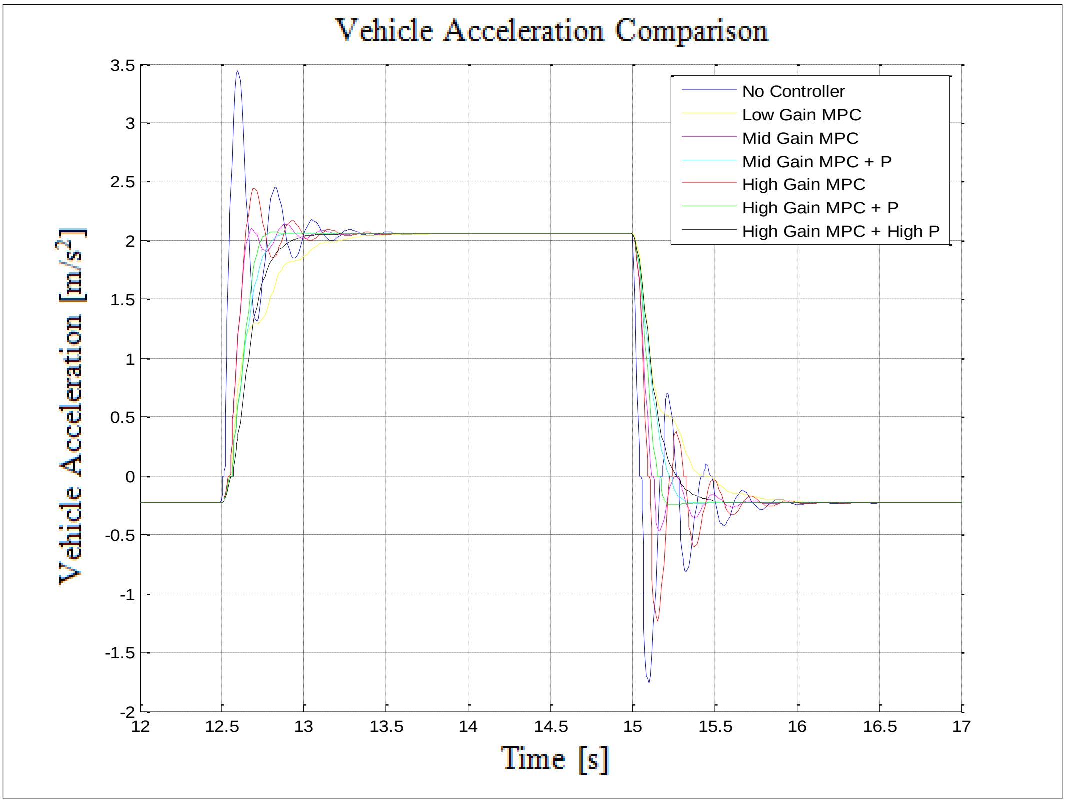

Figure 6.24 : Vehicle acceleration response for MPC parameters determination (Zoomed view at maximum load change manoeuvre) for 4th gear.

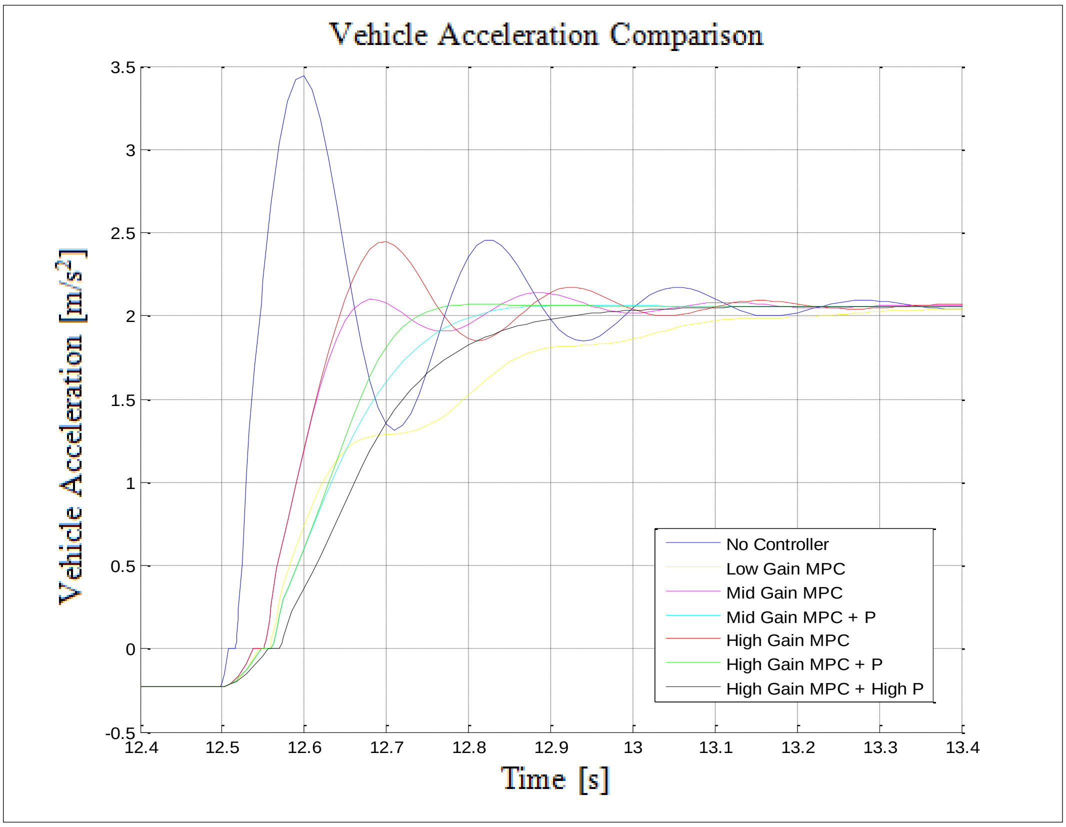

Figure 6.25 : Vehicle acceleration response for MPC parameters determination (Zoomed view at maximum load change tip-in manoeuvre) for 4th gear.

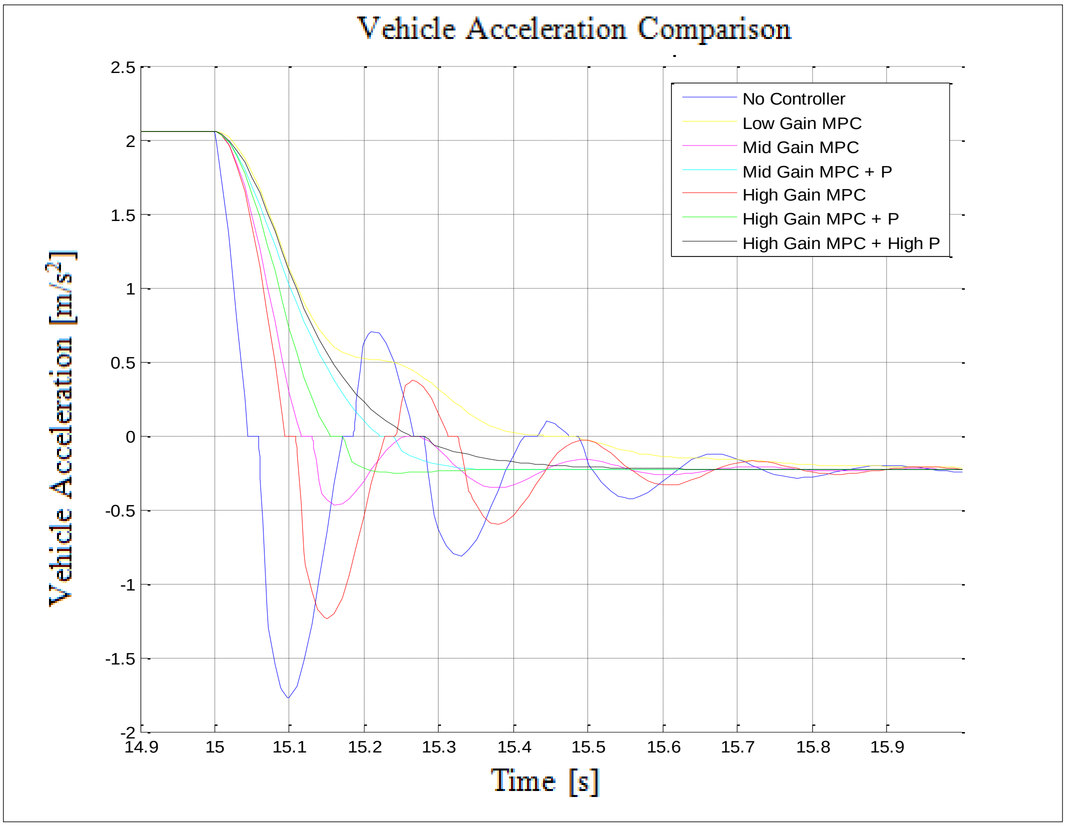

Figure 6.26 : Vehicle acceleration response for MPC parameters determination (Zoomed view at maximum load change tip-out manoeuvre) for 4th gear.

MPC controller manipulated variable (engine brake torque) signals for all different gain combinations are showed at figure 6.27. Detailed view focusing on the maximum load part is showed at figure 6.28 with tip-in and tip-out zooms at figures 6.29 and 6.30 respectively. Analysis of the results show that MPC controller gain configuration high MPC gain with moderate P controller gain gives the best result as the rise times are 0.2 and 0.15 seconds for the tip-in and tip-out manoeuvres respectively and overshoot values is less than %1 percent.

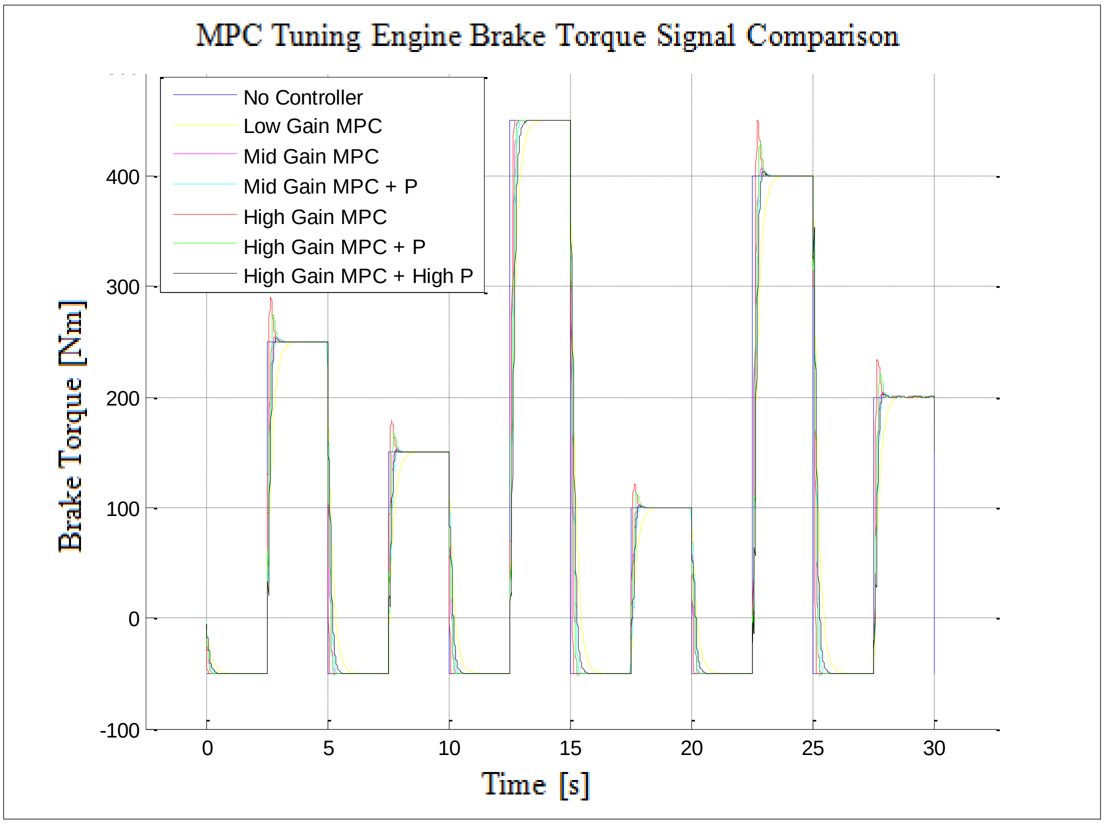

Figure 6.27 : Engine brake torque request for MPC parameters determination for 4th gear.

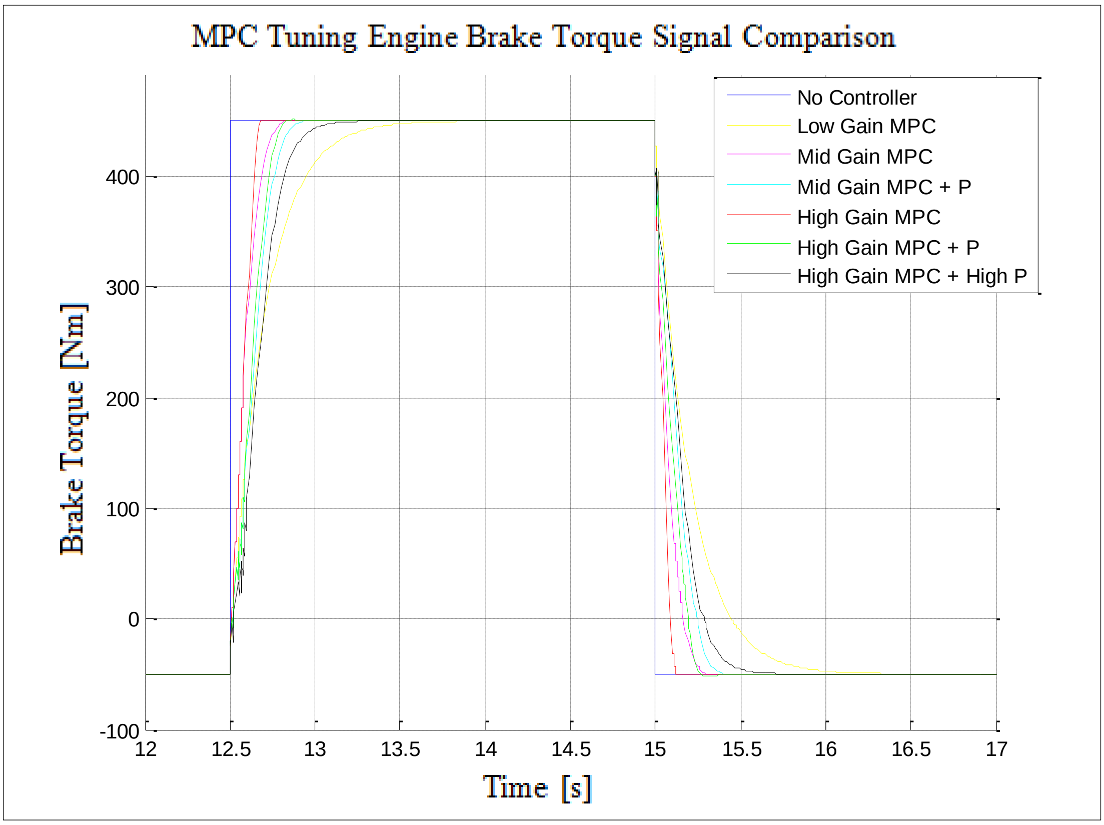

Figure 6.28 : Engine brake torque request for MPC parameters determination (Zoomed view at maximum load change manoeuvre) for 4th gear.

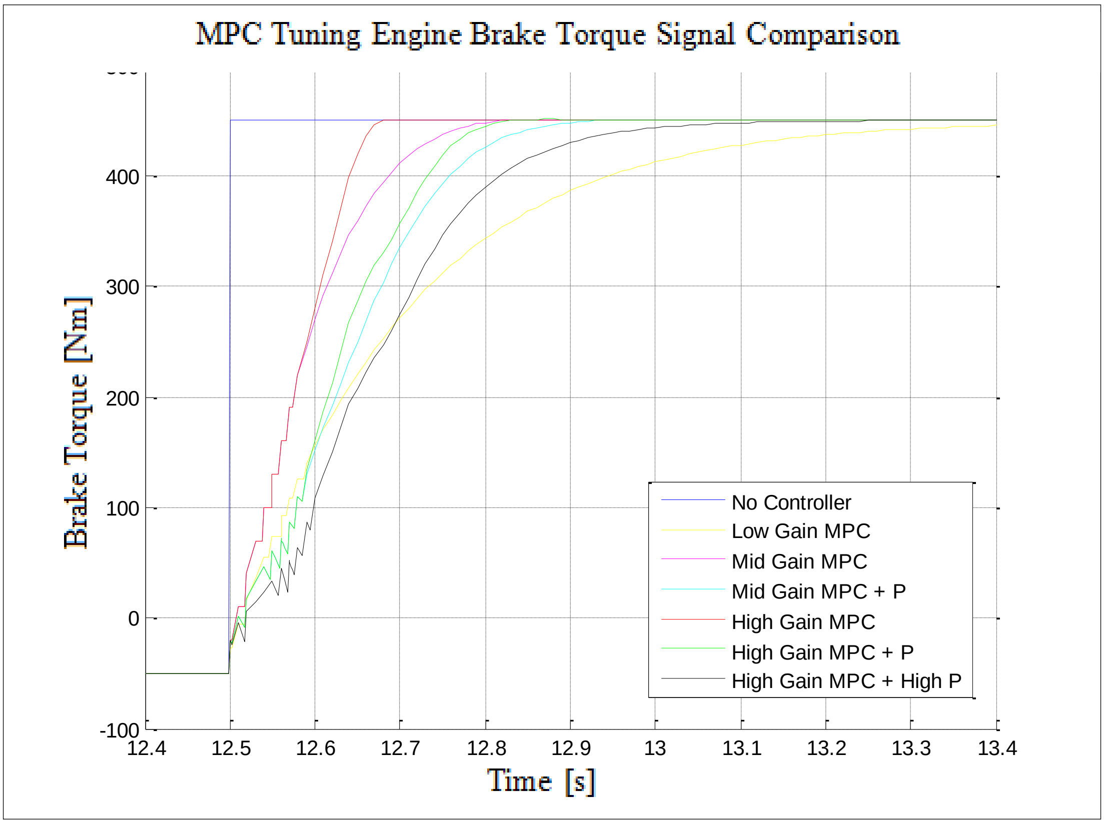

Figure 6.29 : Engine brake torque request for MPC parameters determination (Zoomed view at maximum load change tip-in manoeuvre) for 4th gear.

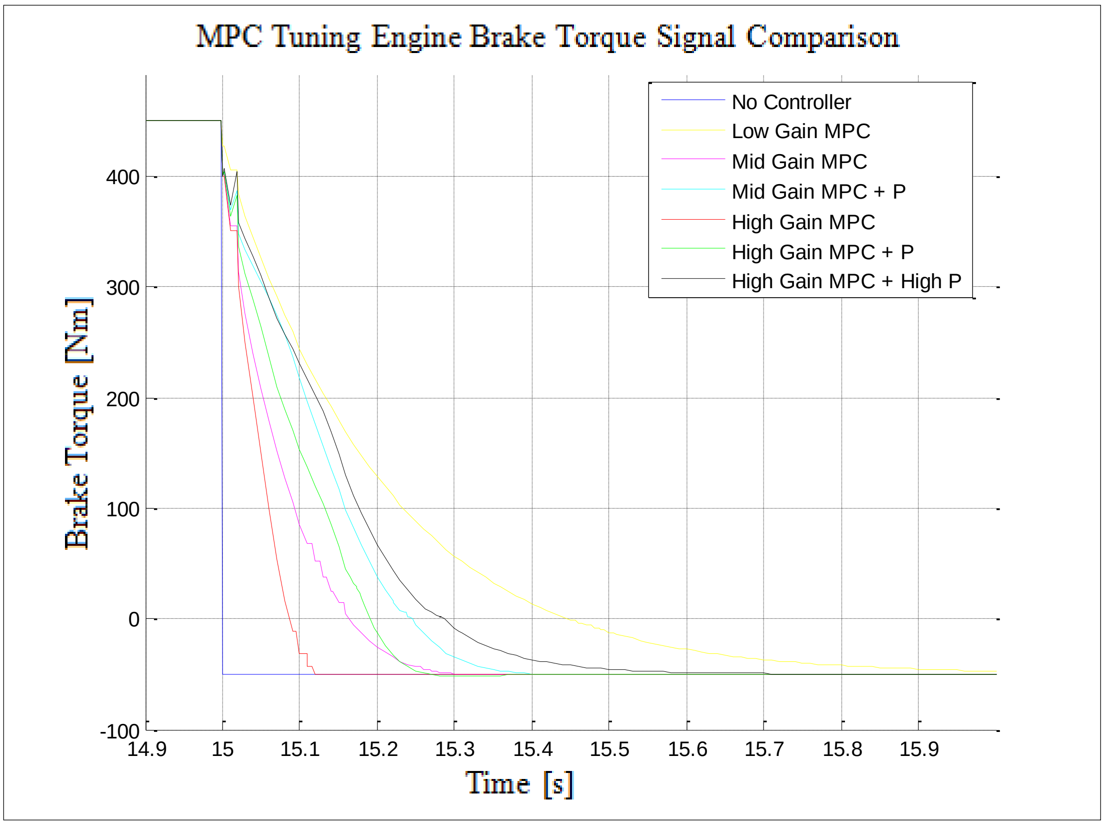

Figure 6.30 : Engine brake torque request for MPC parameters determination (Zoomed view at maximum load change tip-in manoeuvre) for 4th gear.

6.4 2 Mass Vehicle Model Based Controller Results

It was shown at the previous sections that if pedal map based torque request without any driveability corrections applied for a load change manoeuvre, vehicle is subjected to a high amplitude initial kick followed by fading oscillations for both tip-in and tip-out manoeuvres. A 2 mass vehicle model based MPC controller had been utilized in order to actively control the engine brake torque in order to have a smooth vehicle acceleration response without shuffles and compromising from response speed. Modifying weight tuning factor in MPC setting defines system response speed. Increasing the weight rate results with faster response with a compromise from system robustness forming low frequency oscillations. Introduction of the additional P controller based on engine and vehicle speed difference, assists to further reduce the remaining oscillations without renouncing from system response speed. 3rd gear tip-in and tip-out manoeuvres results are showed at figure 6.31. Engine and vehicle speed profiles are very similar for the proposed controllers. Zoomed acceleration graphs in figures 6.32 & 6.33 clearly show that when compared to no controller case both MPC and MPC + P controllers provide smoother vehicle acceleration and deceleration response which will definitely improve comfort characteristics of the vehicle. Additionally system response rate degradation with respect to no controller case is very small. For both controllers initial response delay is lower than 0.04 seconds. Rise time delay of MPC and MPC + P controllers with respect to no controller case is 0.1 seconds for the tip-in manoeuvre. Similarly rise time delay of MPC and MPC + P controllers with respect to no controller case is 0.1 and 0.2 seconds respectively for the tip-out manoeuvre. Figure 6.34 shows the torque request from the engine. For both controllers torque rise rate is slightly lower than the no controller case and additional P controller results with %10 less torque request up to 0.5 seconds from the beginning of tip-in and tip-out manoeuvres.

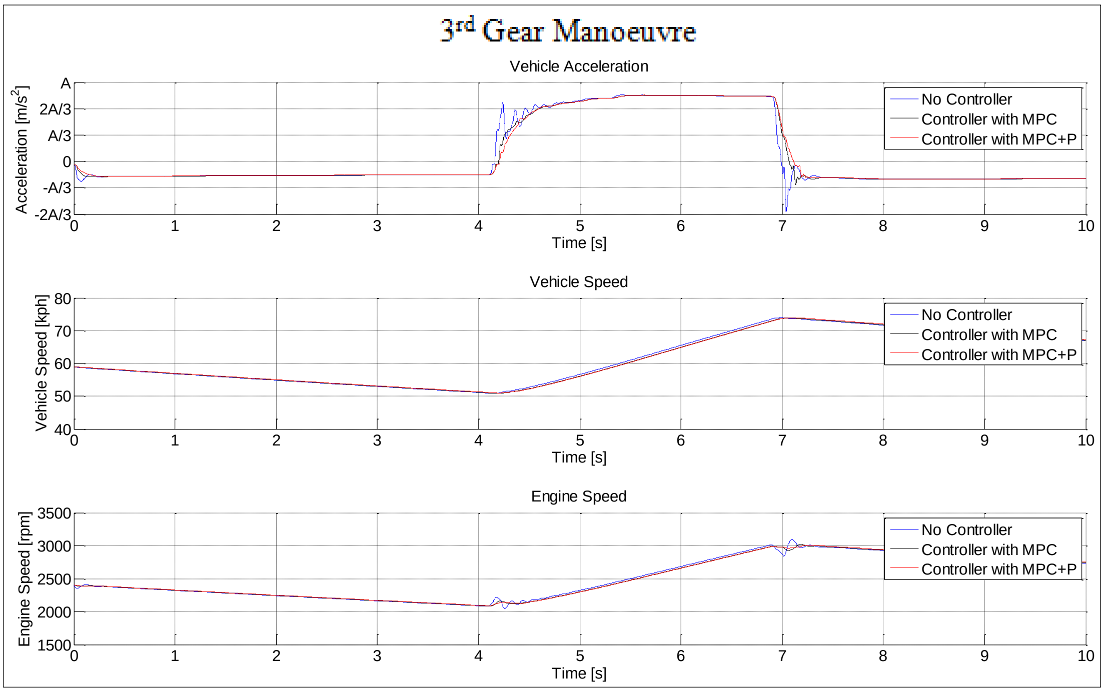

Figure 6.31 : Comparison of simulation results of no-controller, MPC & MPC + P controller for 3rd gear tip-in and tip-out manoeuvre; Top sub-figure: Vehicle longitudinal acceleration measurement, Mid sub-figure: Vehicle speed, Bottom sub-figure: Engine speed.

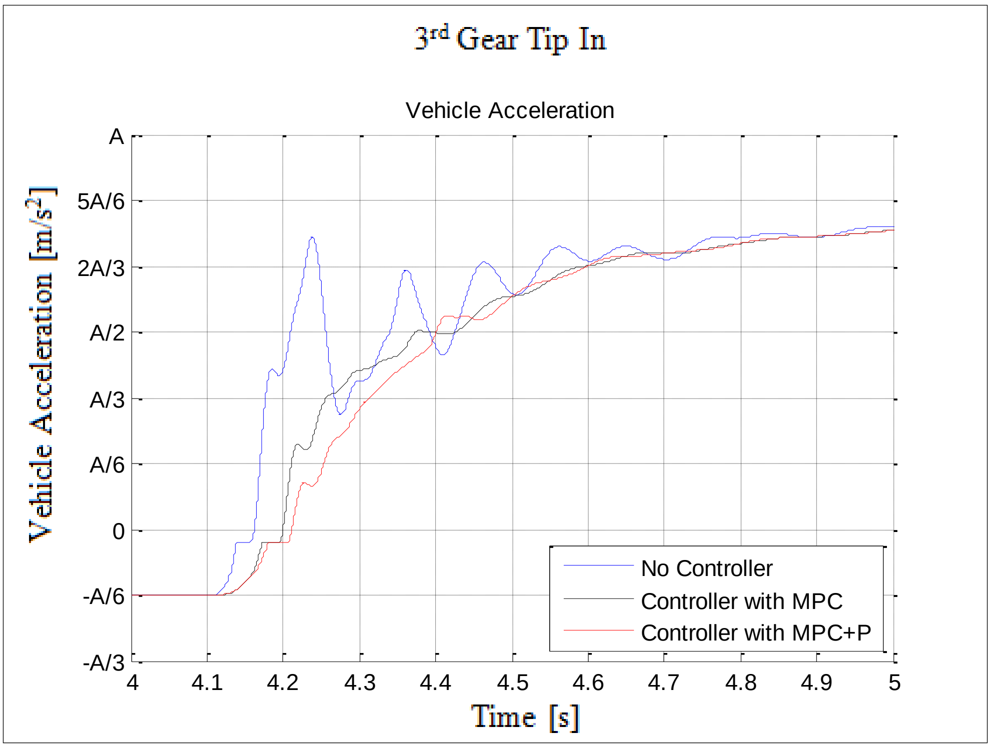

Figure 6.32 : Comparison of simulation results of no-controller, MPC & MPC + P controller for 3rd gear tip-in manoeuvre.

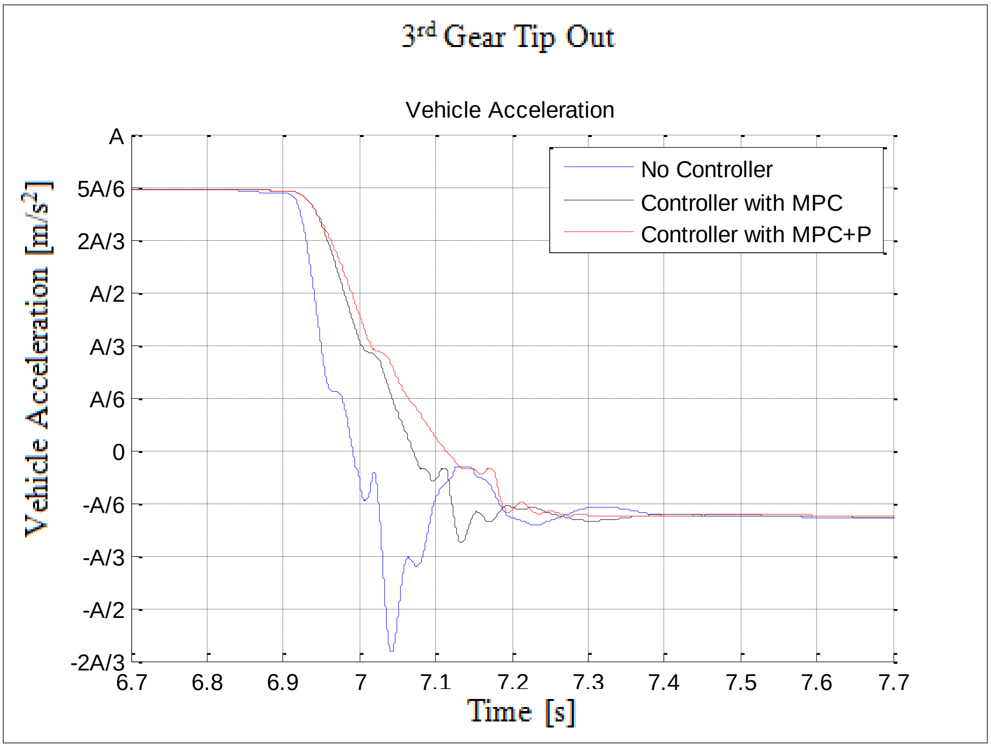

Figure 6.33 : Comparison of simulation results of no-controller, MPC & MPC + P controller for 3rd gear tip-out manoeuvre.

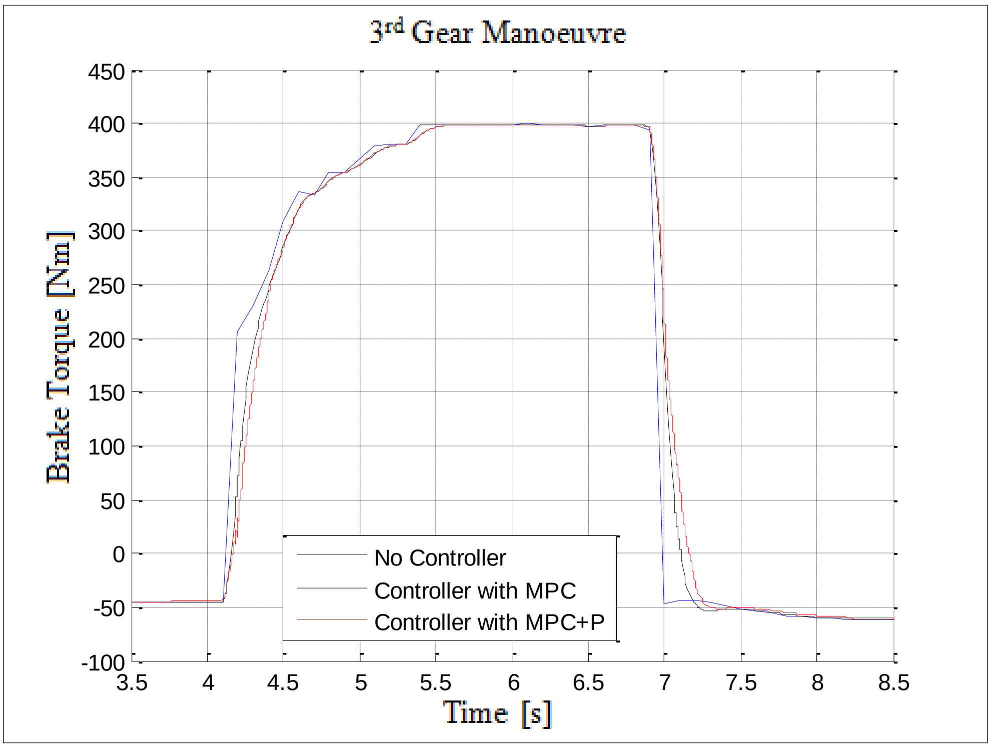

Figure 6.34 : Comparison of engine torque for simulation results of no-controller, MPC & MPC + P controller for 3rd gear tip-in and tip-out manoeuvre.

4th gear tip-in and tip-out manoeuvres' results are shown at figure 6.35. Engine and vehicle speed profiles are very similar for the proposed controllers as in the case with 3rd gear manoeuvres. For both controllers initial response delay is lower than 0.04 seconds (Figure 6.36). Rise time delay of MPC and MPC + P controllers with respect to no controller case is 0.1 seconds for the tip-in manoeuvre. Similarly rise time delay of MPC and MPC + P controllers with respect to no controller case is 0.15 and 0.2 seconds respectively for the tip-out manoeuvre (Figure 6.37). Figure 6.38 shows the torque request from the engine. For both controllers torque rise rate is slightly lower than the no controller case and additional P controller results with %10 less torque results up to 0.3 seconds from the beginning of tip-in and tip-out manoeuvres.

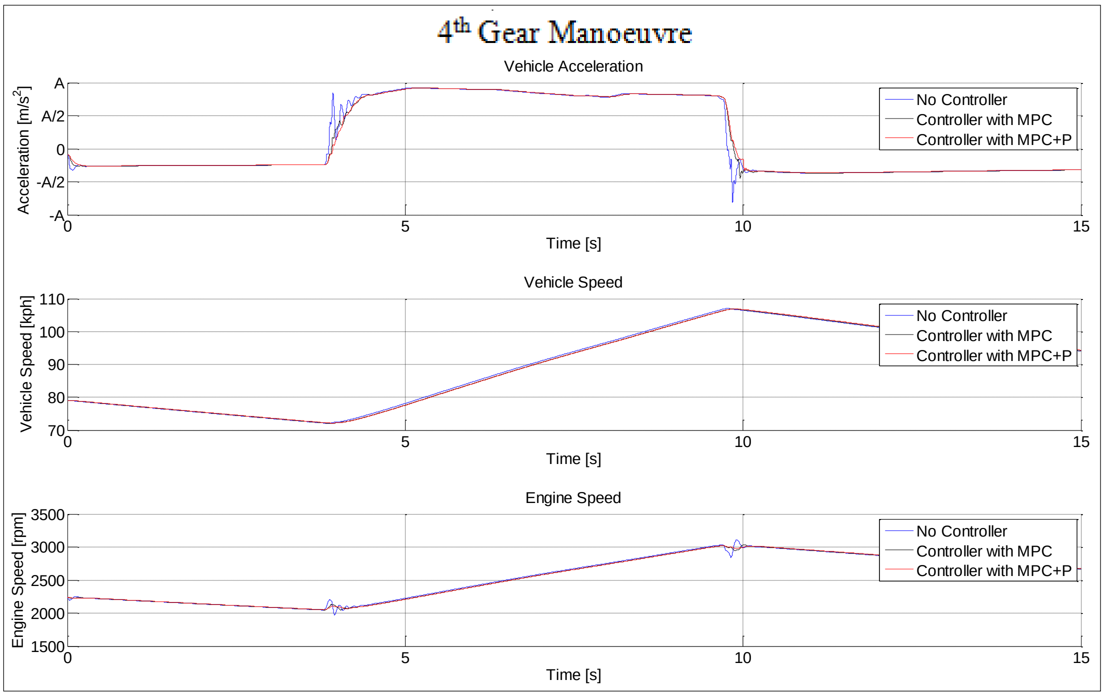

Figure 6.35 : Comparison of simulation results of no-controller, MPC & MPC + P controller for 4th gear tip-in and tip-out manoeuvre; Top sub-figure: Vehicle longitudinal acceleration measurement, Mid sub-figure: Vehicle speed, Bottom sub-figure: Engine speed.

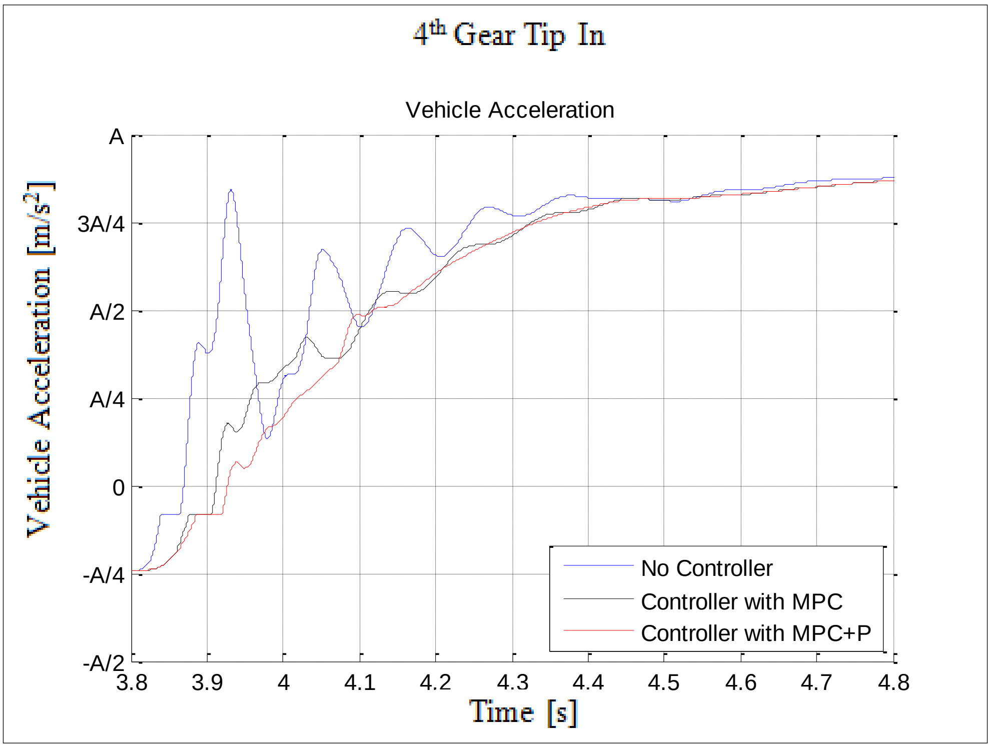

Figure 6.36 : Comparison of simulation results of no-controller, MPC & MPC + P controller for 4th gear tip-in manoeuvre.

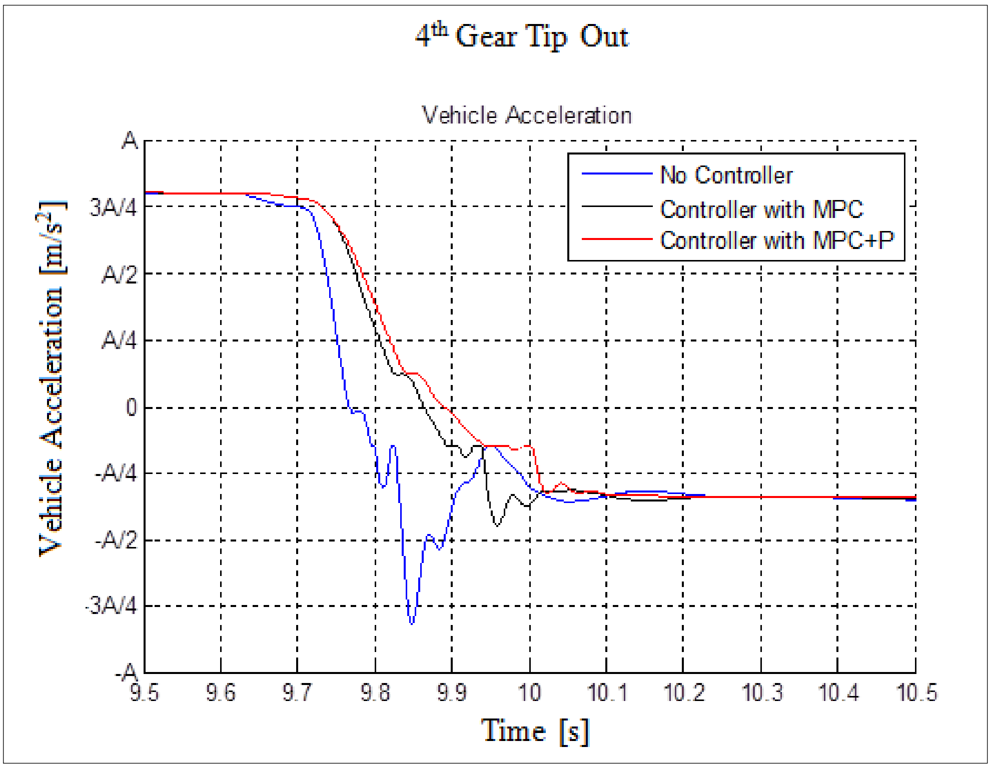

Figure 6.37 : Comparison of simulation results of no-controller, MPC & MPC + P controller for 4th gear tip-out manoeuvre.

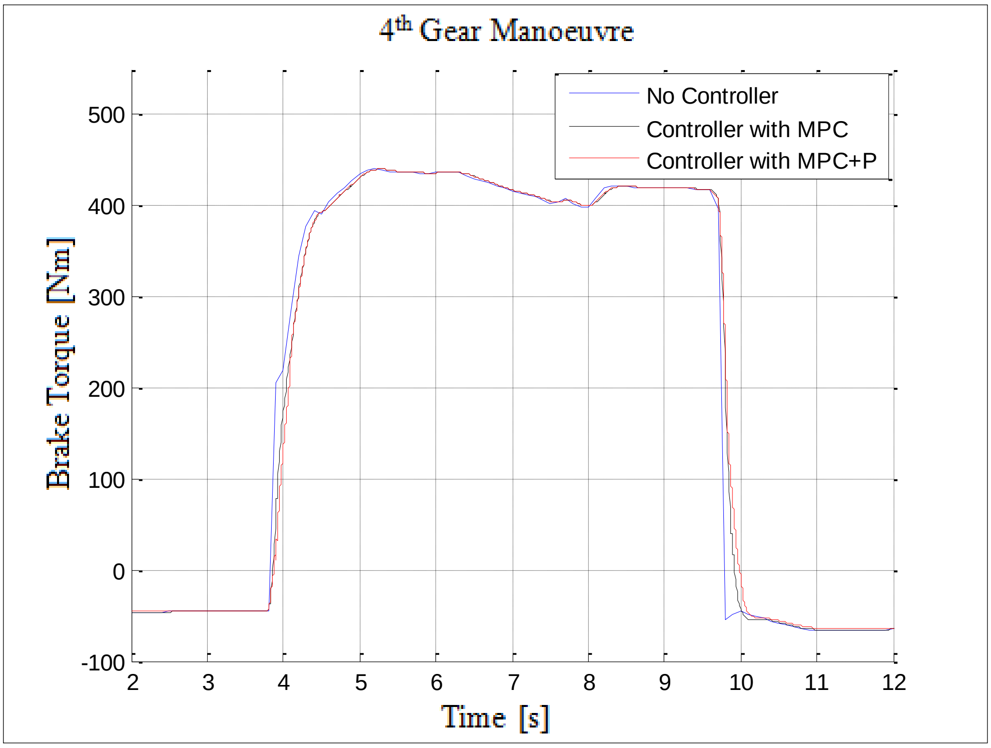

Figure 6.38 : Comparison of engine torque for simulation results of no-controller, MPC & MPC + P controller for 4th gear tip-in and tip-out manoeuvres.

6.5 3 Mass Vehicle Model Based Controller Results

A MPC controller based on a 3 mass vehicle model had been utilized in order to actively control the generated engine brake torque in order to have a smooth vehicle acceleration response without shuffles and compromising from response speed. Modifying weight tuning factor in MPC setting defines system response speed. Increasing weight rate results with faster response with a compromise from system robustness forming low frequency oscillations. Introduction of the additional P controller based on engine and vehicle speed difference, assists to further reduce the remaining oscillations without renouncing from system response speed. 3rd gear tip-in and tip-out manoeuvres results are showed at figure 6.39. Engine and vehicle speed profiles indicate that due to the effect of driveability interventions with the proposed controller algorithms, there forms a delay of 0.2 secs considering vehicle speed reaches no controller case vehicle speed at the end of the stabilized acceleration period. Zoomed acceleration graphs in figures 6.40 & 6.41 clearly show that when compared to no controller case both controllers provide smoother vehicle acceleration and deceleration response which will definitely improve comfort characteristics of the vehicle. Additionally system response speed degradation with respect to no controller case is very minor. For both controllers initial response delay is lower than 0.04 seconds. Rise time delay of both controllers with respect to no controller case is 0.1 and 0.3 seconds for the tip-in and tip-out manoeuvres respectively. Figure 6.42 shows the torque request from the engine. For both controllers torque rise rate is slightly lower than the no controller such that both controller results with %30 and %10 less torque request up to 0.5 seconds from the beginning of tip-in and tip-out manoeuvres respectively.

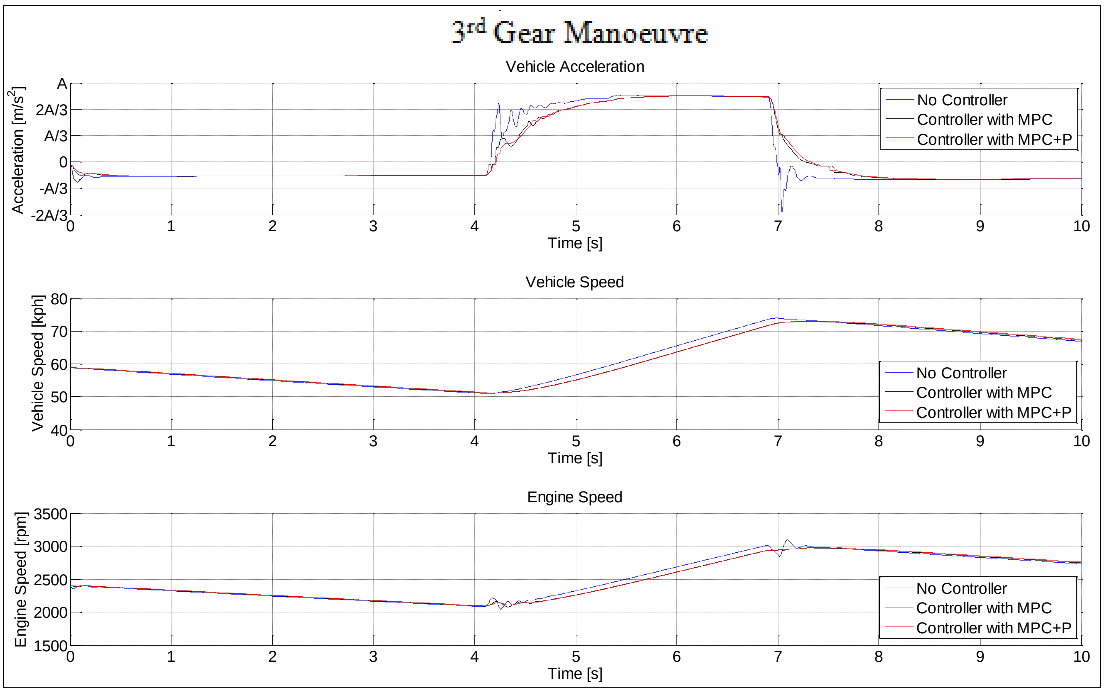

Figure 6.39 : Comparison of simulation results of no controller, MPC & MPC + P controller for 3rd gear tip-in and tip-out manoeuvre; Top sub-figure: Vehicle longitudinal acceleration measurement, Mid sub-figure: Vehicle speed, Bottom sub-figure: Engine speed.

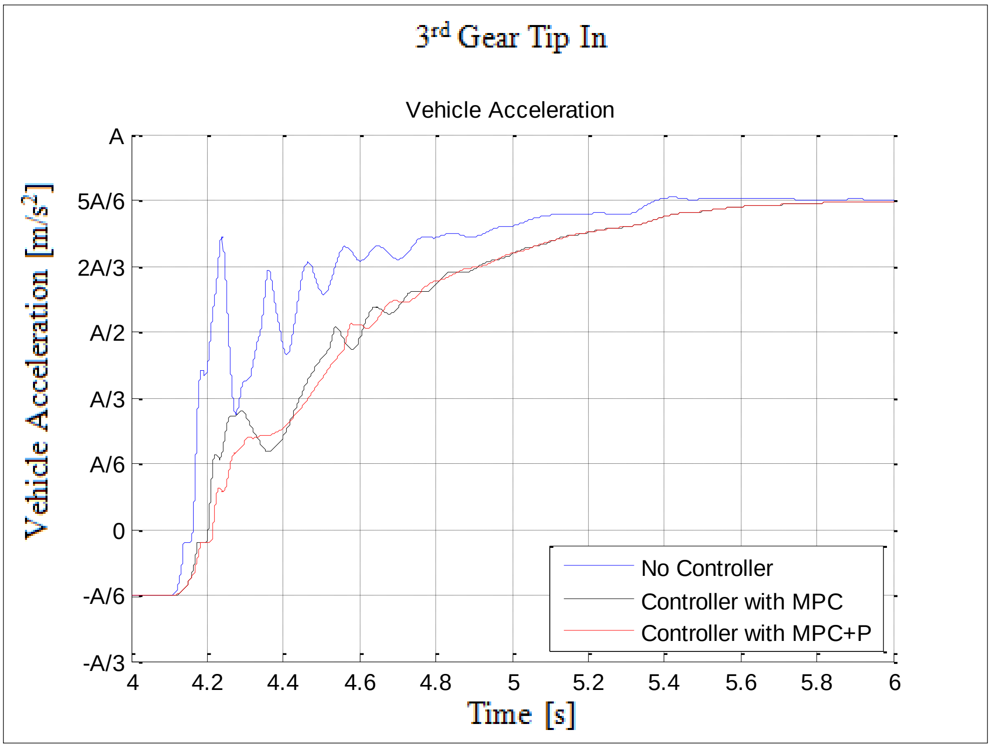

Figure 6.40 : Comparison of simulation results of no controller, MPC & MPC + P controller for 3rd gear tip-in (left) and tip-out manoeuvres (right).

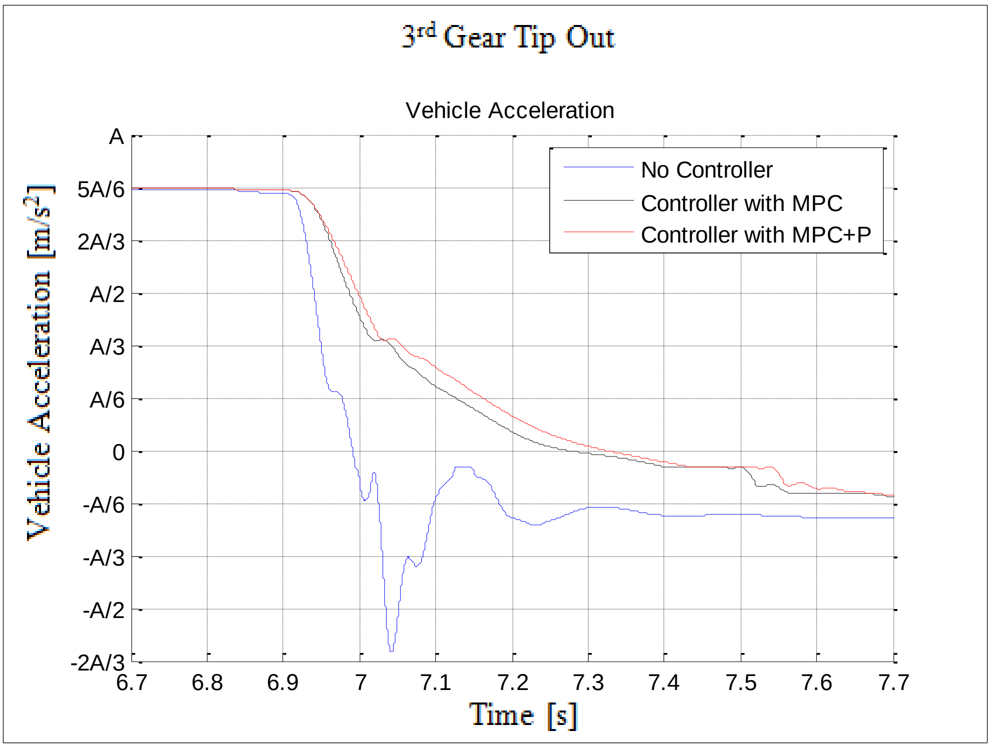

Figure 6.41 : Comparison of simulation results of no controller, MPC & MPC + P controller for 3rd gear tip-out manoeuvre.

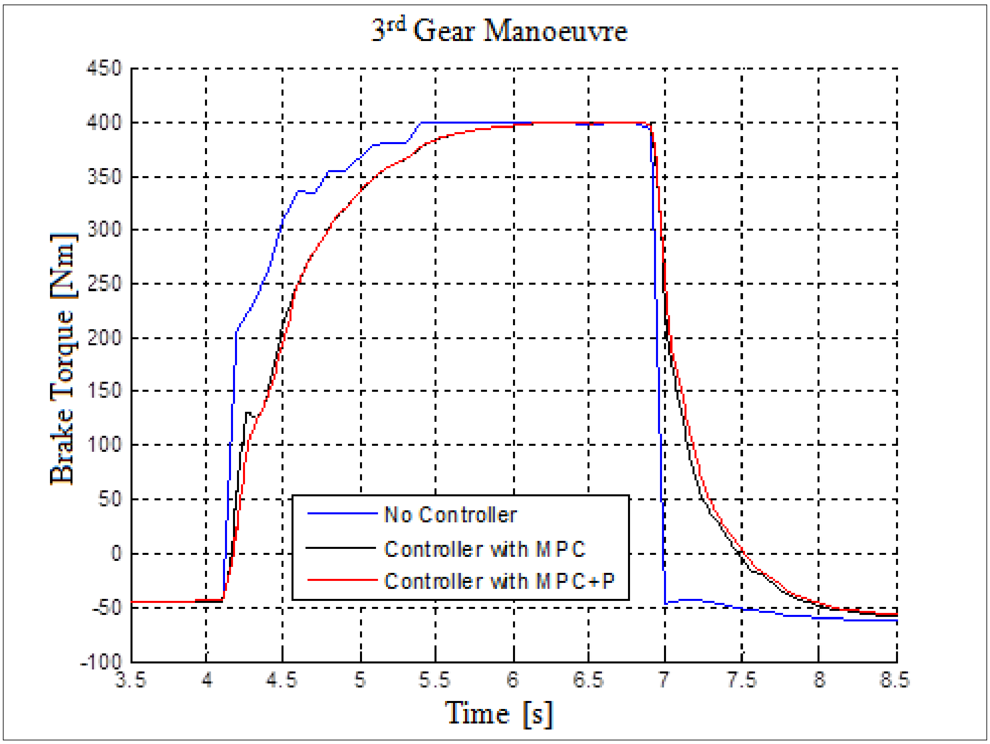

Figure 6.42 : Comparison of engine torque for simulation results of no controller, MPC & MPC + P controller for 3rd gear tip-in and tip-out manoeuvres.

4th gear tip-in and tip-out manoeuvres' results are shown at figure 6.43. Engine and vehicle speed profiles indicate that due to the effect of driveability interventions with the proposed controller algorithms, there forms a delay of 0.2 secs at the instant that vehicle speed reaches no controller case vehicle speed at the end of the stabilized acceleration period as in the case with 3rd gear manoeuvres. For both controllers initial response delay is lower than 0.04 seconds (Figure 6.44). Rise time delay of both controllers with respect to no controller case is 0.1 seconds for the tip-in manoeuvre. Similarly rise time delay of MPC and MPC + P controllers with respect to no controller case is 0.25 and 0.30 seconds respectively for the tip-out manoeuvre (Figure 6.45). Figure 6.46 shows the torque request from the engine. For both controllers torque rise rate is slightly lower than the no controller case and additional P controller results with %25 and %15 less torque results at 0.5 seconds from the beginning of tip-in and tip-out manoeuvres respectively.

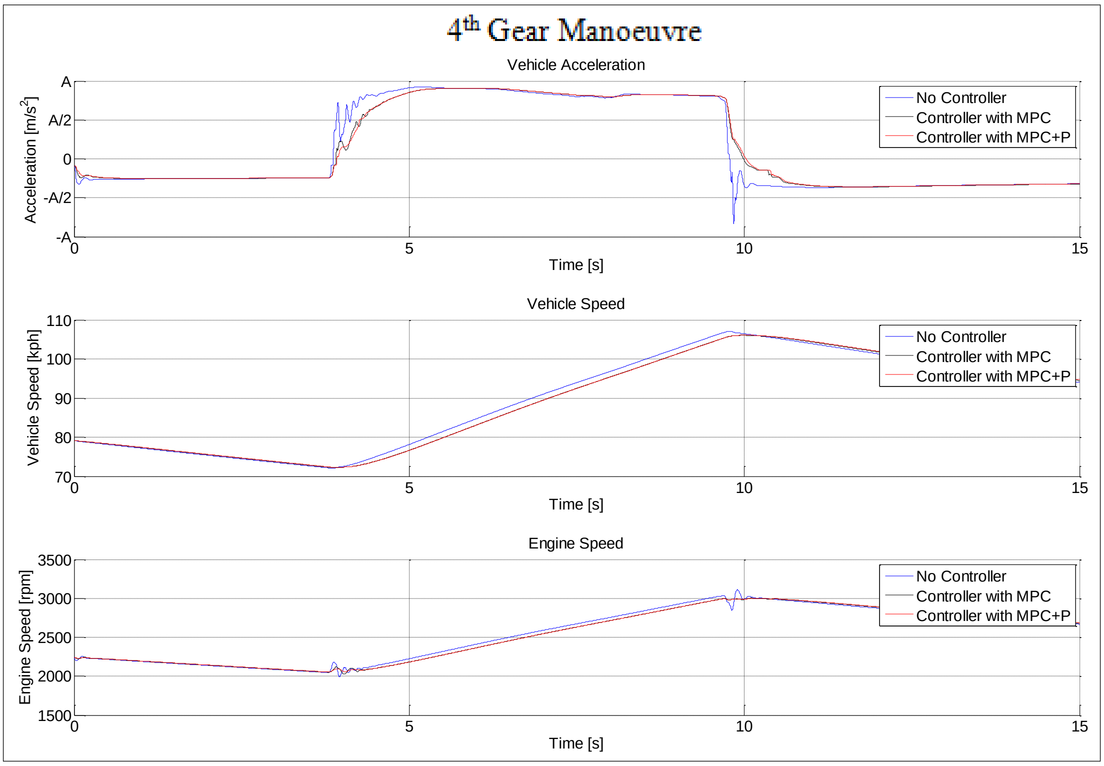

Figure 6.43 : Comparison of simulation results of no-controller, MPC & MPC + P controller for 4th gear tip-in and tip-out manoeuvre; Top sub-figure: Vehicle longitudinal acceleration measurement, Mid sub-figure: Vehicle speed, Bottom sub-figure: Engine speed.

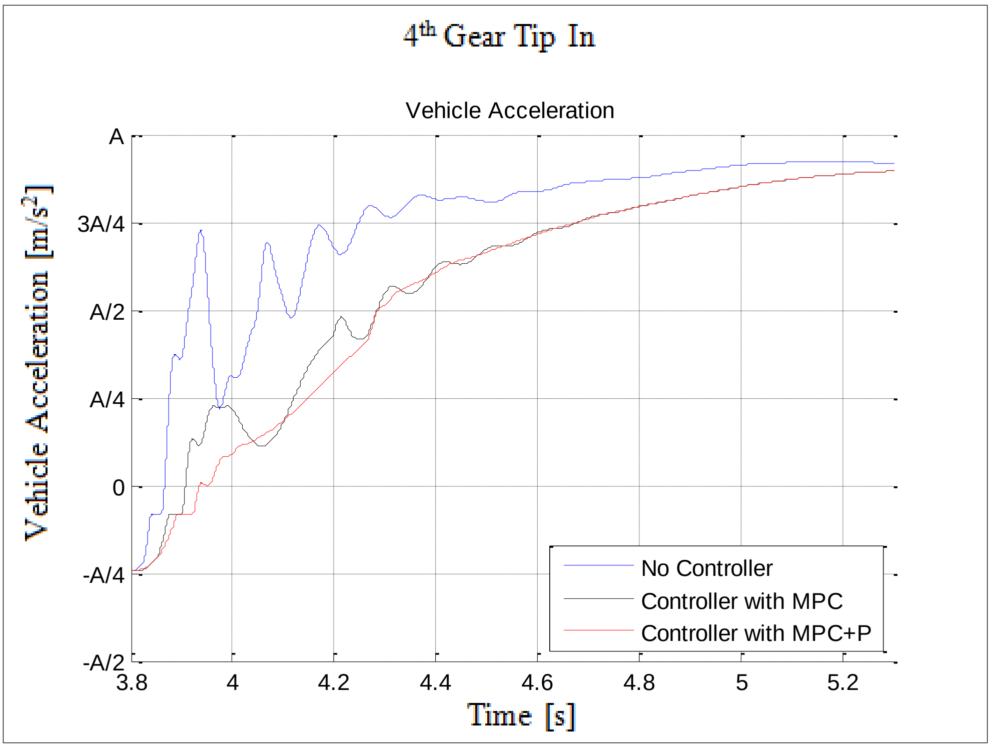

Figure 6.44 : Comparison of simulation results of no-controller, MPC & MPC + P controller for 4th gear tip-in manoeuvre.

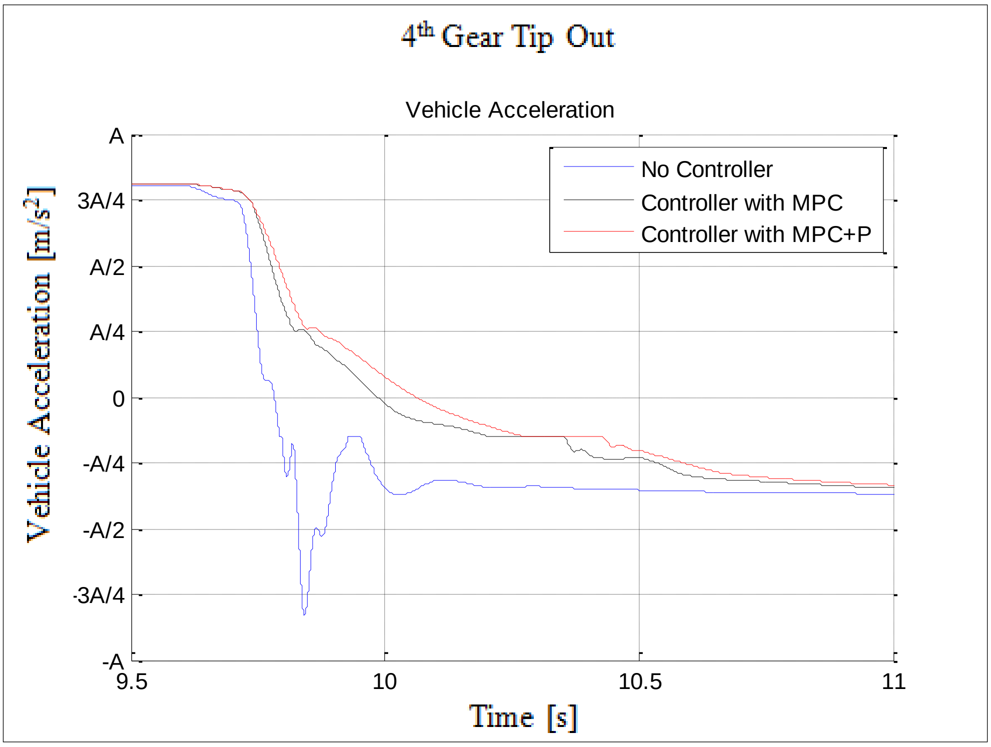

Figure 6.45 : Comparison of simulation results of no-controller, MPC & MPC + P controller for 4th gear tip-out manoeuvre.

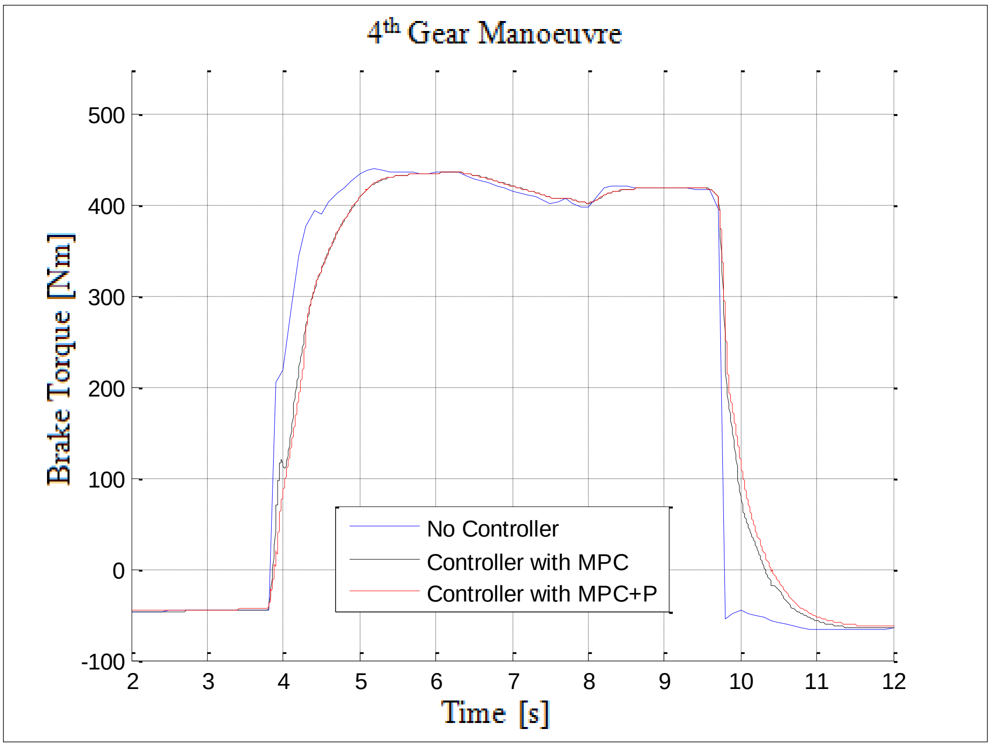

Figure 6.46 : Comparison of engine torque for simulation results of no-controller, MPC & MPC + P controller for 4th gear tip-in and tip-out manoeuvres.

6.6 Conclusion

MPC controller has been employed in order to actively damp the powertrain oscillations. 2 and 3 mass vehicle models are used as the plant models for the MPC controller. MPC controller gives promising results however completely eliminating of the powertrain oscillations is performed using an additional P controller which provides an additional correction torque over the MPC controller engine torque signal. Results show that applying MPC control significantly reduces powertrain oscillations for sudden load change manoeuvres for both 2 and 3 mass models. The additional P controller further smoothens the vehicle acceleration signal for both 2 and 3 mass models. Comparison of the vehicle acceleration and performance metrics between 2 and 3 mass models, 2 mass model provides slight better results.

7. CONCLUSION AND RECOMMEDATIONS

The theme of this dissertation study is engine brake torque control of a vehicle considering longitudinal vehicle dynamics in order to reduce the powertrain first natural frequency related oscillation taking advantage of simulation tools and model based control strategy.

Powertrain components design has a significant contribution on vehicle driveability characteristics, on the other hand due to the complex nature and nonlinear properties of the driveline components eliminating powertrain related oscillations on vehicle longitudinal motion with component parameters optimization is inevitable especially considering load change manoeuvres. The idea of using engine generated brake torque for driveability control is state of the art research topics lead by both automotive manufacturers and academic researchers. Via using model based closed loop control strategies a corrective torque is applied on top of the driver torque request in order to damp the unwanted oscillations and obtain an acceleration / deceleration profile within the automotive manufacturers driveability metrics such as initial delay, rise rate, overshoot/undershoot percentage, and settling time. With the aid of close loop control systems, it is possible to obtain an error free driveability behaviour from a vehicle without any additional system requirements as current vehicle capability provides all the necessary inputs for a close loop driveability control system. Implementation of such systems will not only fulfil customer expectations but also reduce the development time spend on calibrating driveability features on vehicles.

This thesis study “Model Based Optimal Longitudinal Vehicle Control” consists of 4 main sections. In chapter 3, current driveability control strategies in ECU equipped modern vehicles is explained with the introduction of the proposed model based driveability control strategy including engine brake torque modelling aspect. Chapter 4 contains the in cylinder pressure based engine brake torque model. In chapter 5, 3 driveline models with different complexities are proposed. Chapter 6 contains the model based controller development studies and results obtained with the embedded engine and powertrain model based controller.

The model based driveability control algorithm proposed in this thesis is differentiated from the previous studies in the literature within the perspective that, introduced algorithm contains engine brake torque estimation model developed at MATLAB/Simulink modelling environment. In the literature all the known vehicle longitudinal motion control related engine torque control algorithms base on the fact that requested torque will be generated immediately from the diesel engine which is not the case in real life applications due to engine transient response properties. Therefore engine characteristic is either not included or covered with a simple filtering algorithm in conventional vehicle longitudinal motion related engine torque control methodologies. Engine brake torque model combined driveability control algorithm proposed in this thesis works in harmony with the proposed driveability control structure and improves overall vehicle response characteristics.

Within the scope of this study a 4 degree of freedom powertrain model consisting of 4 inertias, 2 set of spring and damper elements with tyre characteristics, is built in MATLAB/Simulink environment. Model validation considering longitudinal vehicle dynamics is performed with employing vehicle level tests using a tip-in followed by a tip-out acceleration pedal signal input load change manoeuvres. Comparison of simulation results and measured vehicle test data shows that proposed model is capable of capturing vehicle acceleration profile revealing unintended error states for the specified input signals.

Considering the driveability control perspective, a Model Predictive Control (MPC) algorithm employed to manipulate the pedal map oriented torque demand signal in order attenuate the powertrain oscillations in longitudinal vehicle motion control. The 4 mass model could not be employed with the MPC algorithm due to very high level of nonlinearity. Therefore two simplified versions of 2 and 3 mass models have been developed. It has been verified that both 2 and 3 mass vehicle models are accurate enough to employ the MPC torque control algorithm. As the aim of this study is to develop a close loop driveability algorithm for real world applications, the 4 mass vehicle model is used as replacement environment for the subjected vehicle in order to employ 2 and 3 mass vehicle model based control algorithm. MPC algorithms via using both models showed good capability, however smoothness of the driving profile with the 2 mass vehicle model is slightly better than the 3 mass model. Additionally due to model simplicity of with the 2 degree of freedom system, computational load requirement is lower than the 3 degree of freedom system. Moreover to further improve the powertrain oscillations without compromising from overall system response speed, an additional anti-shuffle control element, basically a P controller based on the speed difference of engine and vehicle speeds, has been implemented to the MPC control algorithm. Literature review about the engine torque control for improved driveability show that all the researcher use MPC alone. Proposed MPC with additional P controller is a new contribution to the literature in the subjected area of research.

Proposed controller is an optimum control strategy with very minor input requirements. The main prerequisite for the controller algorithm is the knowledge of powertrain parameters which is relatively easy for the automotive manufacturer. Proposed engine brake torque model is based on already available engine control unit measurement variables and contains only a few Wiebe function related tuning parameters which can be easily determined with an engine mapping test with the in cylinder pressure measurement capability which is one of the main signoff tests for engine combustion calibration.

Current approach for driveability calibration is filling the look up based driveability calibration maps with vehicle level subjective evaluation testing. This is a very time consuming process as the current structure is relatively complex containing several maps with at least 8-10 axes for each map and decoupling each map axes reference point is not easy. Besides success ratio is strongly dependant on calibration engineer’s capability. With the proposed methodology is the burden of the driveability calibration is significantly reduced. Once the engine and powertrain models parameters are obtained and related models are tuned, driveability calibration engineer will be able to easily calibrate the MPC + P controller on vehicle as there are only 2 calibration parameters (MPC controller weight parameters and P controller gain value).

It has been showed that proposed engine brake torque estimation model capability added MPC driveability algorithm proves out promising results on vehicle model based simulation environment. However, due to time, project timing and cost constrains proposed strategy has not been implemented within the engine control unit. The suggestion to further improve the applicability of the study is implementation of the proposed model to the current ECU software via rapid prototyping development software strategy and performing validation test initially at HIL environment and afterwards at real life with vehicle level tests.

REFERENCES

[1] **De La Salle, S., Jansz, M.A., Light, D.A.** (1999). Design of a feedback control system for damping of vehicle shuffle, *In Proceedings of the EAEC conference,* Barcelona.

[2] **Cheung, B., Nakashima, A.** (2006). A review on the effects of frequency of oscillation on motion sickness, *Technical Report DRDC TR 2006-229,* Toronto.

[3] ***AVL-Drive Advanced Product Guide.*** (2011). AT2046E, Rev. 20.

[4] **Dorey, R., E., Holmes, C. B.** (1999). Vehicle driveability - its characterization and measurement, *SAE Technical Paper* (No. 1999-01-0949).

[5] **Kiencke, U., Nielsen, L.** (2005). Driveline modelling in automotive control systems: for engine, driveline, and vehicle (2nd ed., pp. 193-221), Springer, 2005.

[6] **Abuasaker S., Sorniotti A.** (2010). Driveability analysis of heavy goods vehicles, SAE Technical Paper (No. 2010-01-1981).

[7] **Sorniotti, A.** (2008). Driveline modelling, experimental validation and evaluation of the influence of the different parameters on the overall system dynamics, *SAE Technical Paper* (No. 2008-01-0632).

[8] **Hayat, O., Lebrun, M., Domingues, E.** (2003). Powertrain driveability evaluation: Analysis and simplification of dynamic models, *SAE Technical Paper* (No. 2003-01-1328).

[9] **Balfour G., Dupraz P., Ramsbottom M.** (2004). Diesel fuel injection control for optimum driveability, *SAE Technical Paper* (No. 2000-01-0265).

[10] **Baumann, J., Swarnakar, A., Kiencke, U., Schlegl, T.** (2005). A robust controller design for anti-jerking, Control Engineering Practice, *SAE Technical Paper* (No. 2005-01-0041)

[11] **Dassen M.,H.,D**. (2003). Modelling and control of automotive clutch systems, *Report Number 2003.73: Technical University of Eindhoven.*

[12] **Serrarens A., Dassen M., Steinbuch M.** (2004). Simulation and control of an automotive dry clutch, *Proceeding of the 2004 American Control Conference,* Boston, (pp. 4078-4083).

[13] **Dolcini P.J., Canudas de Wit C., Bechart H**. (2010). Dry Clutch control for automotive applications, 2010

[14] **Lagerberg, A.** (2004). Control and estimation of automotive powertrains with backlash, *Doctoral dissertation, Chalmers University of Technology.*

[15] **Templin, P.** (2008). Simultaneous estimation of driveline dynamics and backlash size for control design. *Proceedings of 17th IEEE International Conference on Control Applications,* Texas, (pp. 13-18).

[16] **Caruntu C. F., Balau A., E., Lazar C.** (2010). Cascade based control of a drivetrain with backlash, *Proceedings of 12th International Conference on Optimization of Electrical and Electronic Equipment,* (pp. 710-715).

[17] **Berriri, M., Chevrel, P., Lefebvre, D., Yagoubi, M.** (2007). Active damping of automotive powertrain oscillations by a partial torque compensator, *Proceedings of the 2007 American Control Conference*, (pp. 5718-5723).

[18] **Gotoh K., Yakoub R.** (2007). Development of high fidelity combustion-driven vehicle models for driveability using advanced multi-body simulations, *SAE Technical Paper* (No. 2007-01-1634).

[19] **Tiller M., Bowles P., Elmqvist H., Brück D., Mattson S., Möller A., Olsson H., Otter M.** (2000). Detailed vehicle powertrain modelling in modelica, *Proceedings of Modelica Workshop 2000*, (pp. 169-178).

[20] **Powell B. K., Sureshbabu N., Bailey K. E., Dunn M. T.** (1998). HIL Vehicle and Powertrain Analysis and Control Design Issues, *Proceedings of the American Control Conference,* Pennsylvania, (pp. 483-492).

[21] **Brahma I., Sharp M. C., and Frazier T. R.** (2008). Estimation of engine torque from a first law based regression model, *SAE Technical Paper* (No. 2008-01-1014).

[22] **Catania A. E., Finesso R., Spessa E.** (2011). Predictive zero-dimensional combustion model for DI diesel engine feed-forward control, *Journal of Energy Conversion and Management*, (*Vol.* 52, pp. 3159-3175)

[23] **Ponti F., Corti E., Serra G., De Cesare M.** (2007). Common Rail Multi-Jet Diesel Engine Combustion Model Development for Control Purposes, *SAE Technical Paper* (No. 2007-01-0383).

[24] **Filipi Z. S., Assanis D. N.** (2001). A nonlinear, transient, single-cylinder diesel engine simulation for predictions of instantaneous engine speed and torque, *Journal of Engineering for Gas Turbines and Power*, (*Vol.* 123, pp 951-959).

[25] **Katsumata M., Kuroda Y., Ohata A.** (2007). Development of an engine torque estimation model: Integration of physical and statistical combustion model, *SAE Technical Paper* (No. 2007-01-1302).

[26] **Park, K., Lee, J., Park, J.** (2013). Torque control of a vehicle with electronic throttle control using an input shaping method, *International Journal of Automotive Technology*, (*Vol.* 14, No. 2, pp. 189-194).

[27] **Richard, S., Chevrel, P., Maillard, B.** (1999), Active control of future vehicles drivelines, *Proceedings of the 38th IEEE Conference in Decision and Control*, Phoenix, (*Vol.* 4, pp. 3752-3757).

[28] **Lagerberg, A., Egart, B.** (2002). Evaluation of control strategies for automotive powertrains with backlash, *Proceedings of 6th International Symposium on Advanced Vehicle Control*, Hiroshima, (pp. 517-522).

[29] **Fredriksson, J., Weiefors, H., Egardt, B.** (2002). Powertrain control for active damping of driveline oscillations, *Vehicle System Dynamics*, (*Vol.* 37, No.5, pp. 359-376).

[30] **Bruce, M., Egardt, B., Petterson S.** (2005). On powertrain oscillations damping using feedforward and LQ feedback control, *Proceedings of the 2005 IEEE Conference on Control Applications*, Toronto, (pp. 1414-1420).

[31] **Baumann, J., Torkzadeh, D.D., Ramstein, A., Kiencke, U., Schlegl, T.** (2006). Model-based predictive anti-jerk control, *Control Engineering Practice*, (*Vol.* 14, No. 3, pp.259-266).

[32] **Pettersson, M. and Nielsen, L.** (2003). Diesel engine speed control with handling of driveline resonances, *Control Engineering Practice*, (*Vol.* 11, No. 3, pp. 319-328).

[33] **Webersinke, L., Augenstein, L., Kiencke, U., Hertweck, M.** (2008). Adaptive linear quadratic control for high dynamical and comfortable behaviour of a heavy truck, *SAE Technical Paper* (No. 2008-01-0534).

[34] **Templin, P., Egardt, B.** (2009). An LQR torque compensator for driveline oscillation damping, *Proceedings of 18th IEE International Conference on Control Applications,* Saint Petersburg, (pp. 352-356).

[35] **Templin, P., Egardt, B.** (2011). A powertrain LQR-Torque compensator with backlash handling, *Oil & Gas Science and Technology – Rev. IFP Energies nouvelles,* (*Vol.* 66, No.4, pp. 645-654).

[36] **He, L., Li, L., Yu, L., Mao, E., Song, J.** (2012). A torque-based nonlinear predictive control approach of automotive powertrain by iterative optimization, *Journal of Automobile Engineering*, (*Vol.* 226(8), pp 1016-1025).

[37] **Fang, C., Cao, Z., Ektesabi, M. M., Kapoor, A., Sayem, A. H. M.** (2014). Model reference control for active driveability improvement, *Proceedings of 2014 International Conference on Modelling, Identification and Control, Melbourne*, (pp. 202-206).

[38] **Lagerberg, A., Egardt, B.** (2005) Model predictive control of automotive powertrains with backlash, *Proceedings of in 16th IFAC World Congress*, Prague, (pp. 1887-1887).

[39] **Xiaohui, L., Hong, C., Huayu, Z., Ping, W.and Bingzhao, G.** (2011). Design of model predictive controller for anti-jerk during tip-in/out process of vehicles. *Proceedings of 30th Chinese Control Conference*, Yantai, (pp. 3395-3400).

[40] **Yoon, Y., An, Y., Park, Y. and Kim, H. J.** (2010). Model predictive control for driveability enhancement with input dead-segment, *Proceedings of International Conference on Control Automation and Systems (ICCAS),* Gyeonggi-do, (pp. 916-921).

[41] **Balau, A., Lazar, C.** (2011). One step ahead MPC for an automotive control application, *Proceedings of 2nd Eastern European Regional Conference on the Engineering of Computer Based Systems*, Bratislava, (pp. 61-70).

[42] **Url-1** <https://www.avl.com/combustion-measurement1>, date retrieved 12. 04. 2016

[43] **Pacejka, H., B.** (2006). *Tyre and Vehicle Dynamics*, 2nd Edition, Butterworth-Heinemann.

[44] **Dorf, R., C., Bishop, R., H.** (2005). *Modern Control Systems*, 10th Edition, Pearson Education & Prentice Hall.

[45] **Url-2** <https://en.wikipedia.org/wiki/ PID_controller>, date retrieved 14. 05. 2016

[46] **Url-3** <https://en.wikipedia.org/wiki/H-infinity_methods_in_control_theory>, date retrieved 16. 05. 2016

[47] **Url-4** <https://en.wikipedia.org/wiki/LTI_system_theory>, date retrieved 19. 05. 2016

[48] **Url-5** <https://en.wikipedia.org/wiki/Linear-quadratic_regulator>, date retrieved 20. 05. 2016

[49] **Camacho, E. F., Bordons, C.** (2000). *Model Predictive Control*, Springer.

APPENDICES

APPENDIX A : Indices.

APPENDIX B : Test vehicle specifications.

APPENDIX C : Vehicle model parameters.

APPENDIX D : MPC tuning parameters.

APPENDIX A: Indices

1 : Equivalent node for engine, flywheel, clutch primary side (4 mass model), Equivalent node for engine, flywheel, clutch primary & secondary sides, final drive (2 mass model)
2 : Equivalent node for clutch secondary side, transmission, final drive (4 Mass Model) Equivalent node for wheels, tyres and vehicle (2 mass model)
3 : Equivalent node for wheels and tyres, equivalent node for wheels, tyres and vehicle (3 mass model)
4 : Equivalent node for vehicle
e : Engine
rl : Road Load
air : Air
aero : Aerodynamic
charge : Combustion charge
coolant : Engine coolant
cp : Clutch primary side
cs : Clutch secondary side
egr : Exhaust gas recirculation
egrcooler : Exhaust gas recirculation cooler
exh : Exhaust
rr : Rolling resistance
g : Gravitational
fw : Flywheel
maf : Mass air flow
t : Reduction ratio of the selected gear
f : Reduction ratio of the final gear
w : Wheel
v : Vehicle
tot : All driveline components and vehicle

APPENDIX B : Test Vehicle Specifications.

Table B.1 : Test Vehicle Specifications.

Feature	**Value**	**Unit**
Engine Displacement	2.0	lt
Number of Cylinder	4	-
Rated Power	210	PS
Rated Power Speed	3750	rpm
Rated Torque	450	Nm
Rated Torque Speed Range	2000-2500	rpm
Transmission	6 Speed Automatic	-
Torque Truncation at 3rd Gear	400	Nm
Drive Wheel Configuration	Front Wheel Drive	-
Final Drive Ratio	3.55	-
Tire Dimensions	245/50R17	-
Test Weight	2125	-

APPENDIX C : Vehicle model parameters.

Table C.1 : Driveline model parameters.

Feature	**Value**	**Unit**
Engine Inertia	0.2860	kg/m^2
Double Mass Flywheel Primary Side Inertia	0.1210	kg/m^2
Double Mass Flywheel Secondary Side Inertia	0.051	kg/m^2
Clutch Primary Side Inertia	0.0503	kg/m^2
Clutch Secondary Side Inertia	0.0064	kg/m^2
3rd Gear Transmission Inertia	0.0127	kg/m^2
4th Gear Transmission Inertia	0.0185	kg/m^2
Left Driveshaft Inertia	0.0003	kg/m^2
Right Driveshaft Inertia	0.00043	kg/m^2
Wheel Inertia	0.975	kg/m^2
Transmission Ratio 3rd Gear	1.194	–
Transmission Ratio 4th Gear	0.829	–
Final Drive Ratio	4.36	–
Tyre Size	205/55/R17	–
Air Density	1.3	kg/m^3
Coefficient of Drag	0.273	-
Frontal Area Projection	2.35	m^2

APPENDIX D : MPC tuning parameters.

Table D.1 : Summary of MPC and P controller gain parameters for 3rd gear 3 mass model.

Controller Type	**MPC Gain Input Rate Weight**	**MPC Gain Output Weight**	**P Controller Gain**
Low Gain MPC	1.2214	0.081872	0
Medium Gain MPC	1.8221	0.05488	0
Medium Gain MPC + P Controller	1.8221	0.05488	10
High Gain MPC	3.3201	0.030119	0
High Gain MPC + P Controller	3.3201	0.030119	10
High Gain MPC + P Controller High Gain	3.3201	0.030119	15

Table D.2 : Summary of MPC and P controller gain parameters for 4th gear 3 mass model.

Controller Type	**MPC Gain Input Rate Weight**	**MPC Gain Output Weight**	**P Controller Gain**
Low Gain MPC	0.081872	1.2214	0
Medium Gain MPC	0.036787	2.7183	0
Medium Gain MPC + P Controller	0.036787	2.7183	10
High Gain MPC	0.01324	4.5341	0
High Gain MPC + P Controller	0.01324	4.5341	10
High Gain MPC + P Controller High Gain	0.01324	4.5341	20

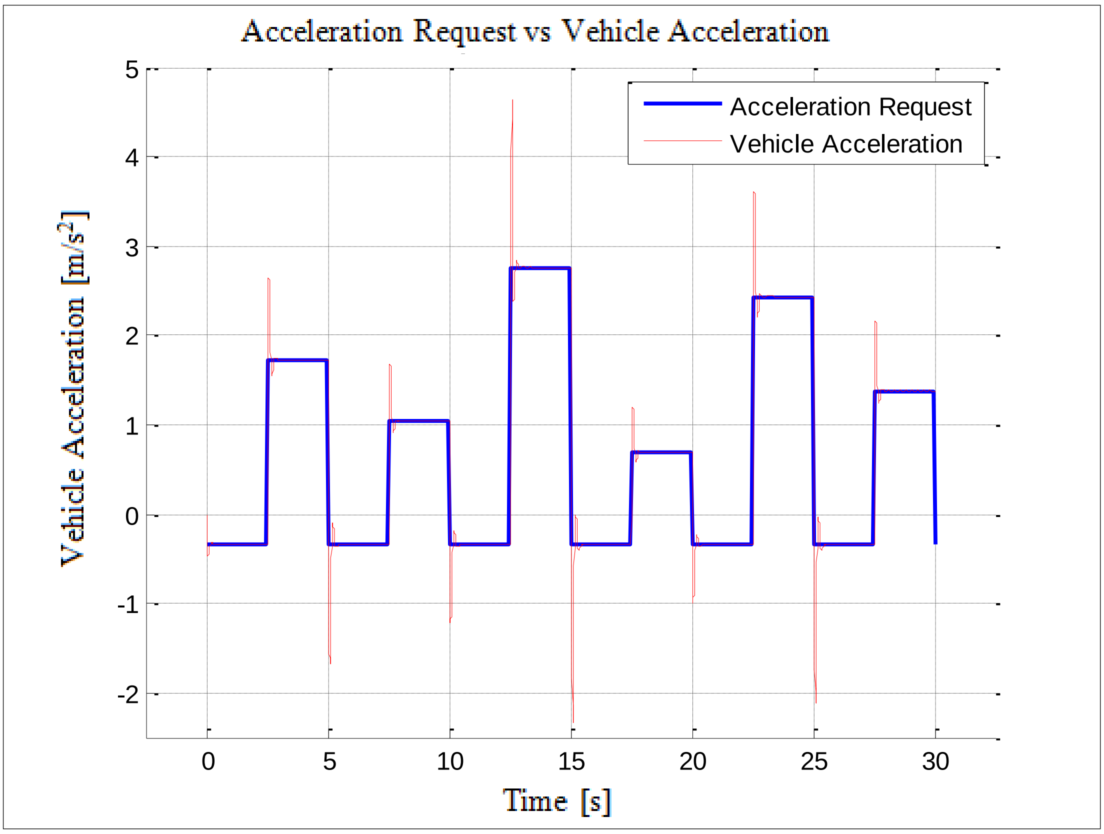

Figure D.1 : 3 mass model vehicle acceleration response for no controller case for 4th gear.

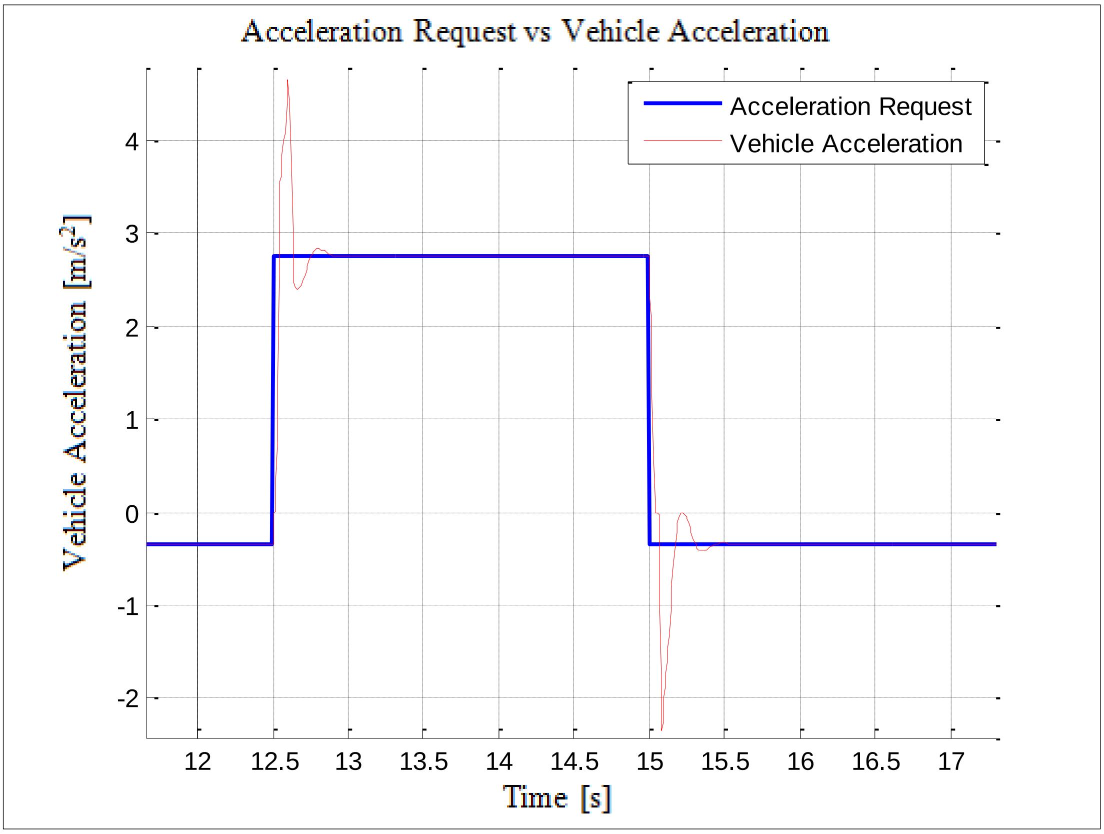

Figure D.2 : 3 mass model vehicle acceleration response for no controller case (Zoomed view at maximum load change manoeuvre) for 4th gear.

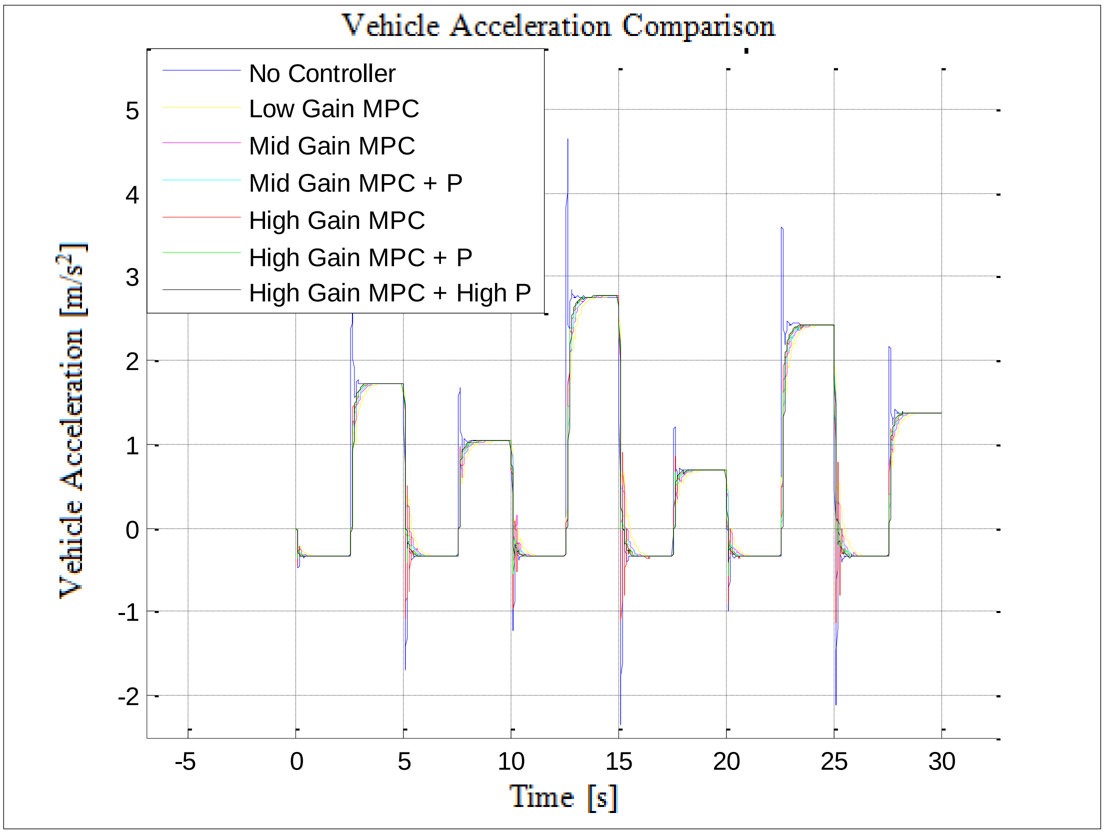

Figure D.3 : 3 mass model vehicle acceleration response for MPC parameters determination for 3rd gear.

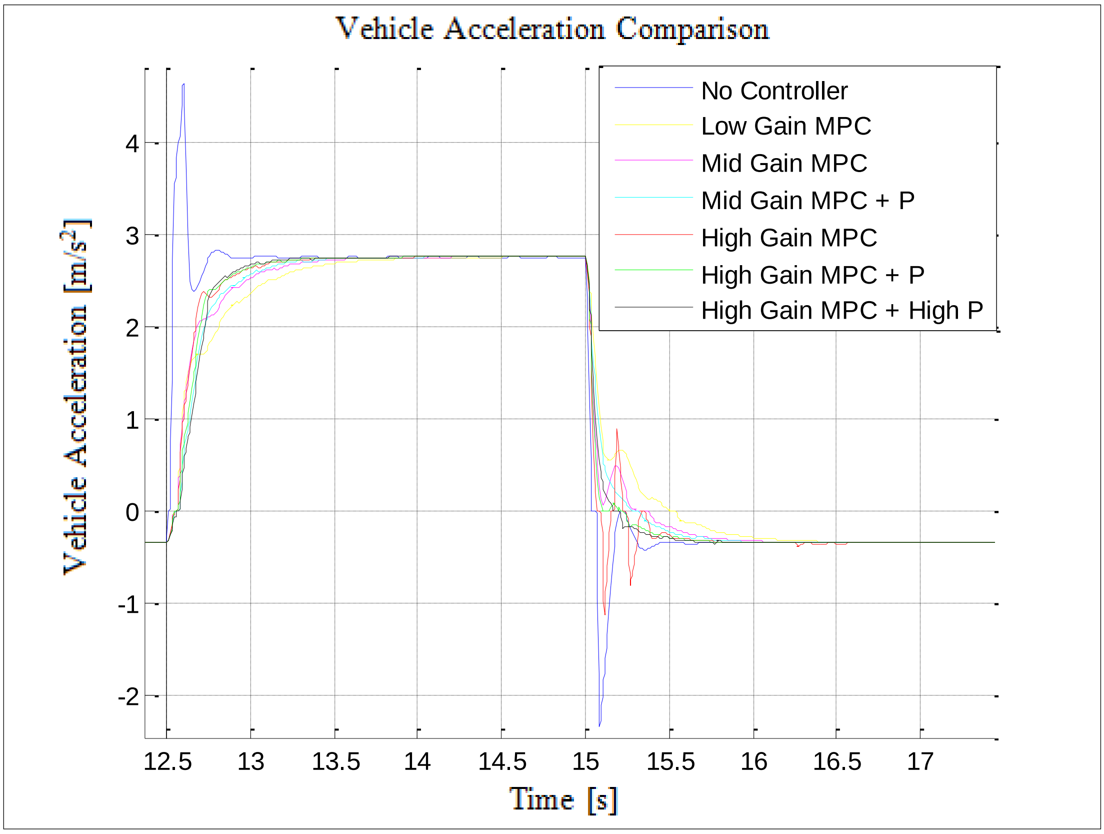

Figure D.4 : 3 mass model vehicle acceleration response for no controller case (Zoomed view at maximum load change manoeuvre) for 3rd gear.

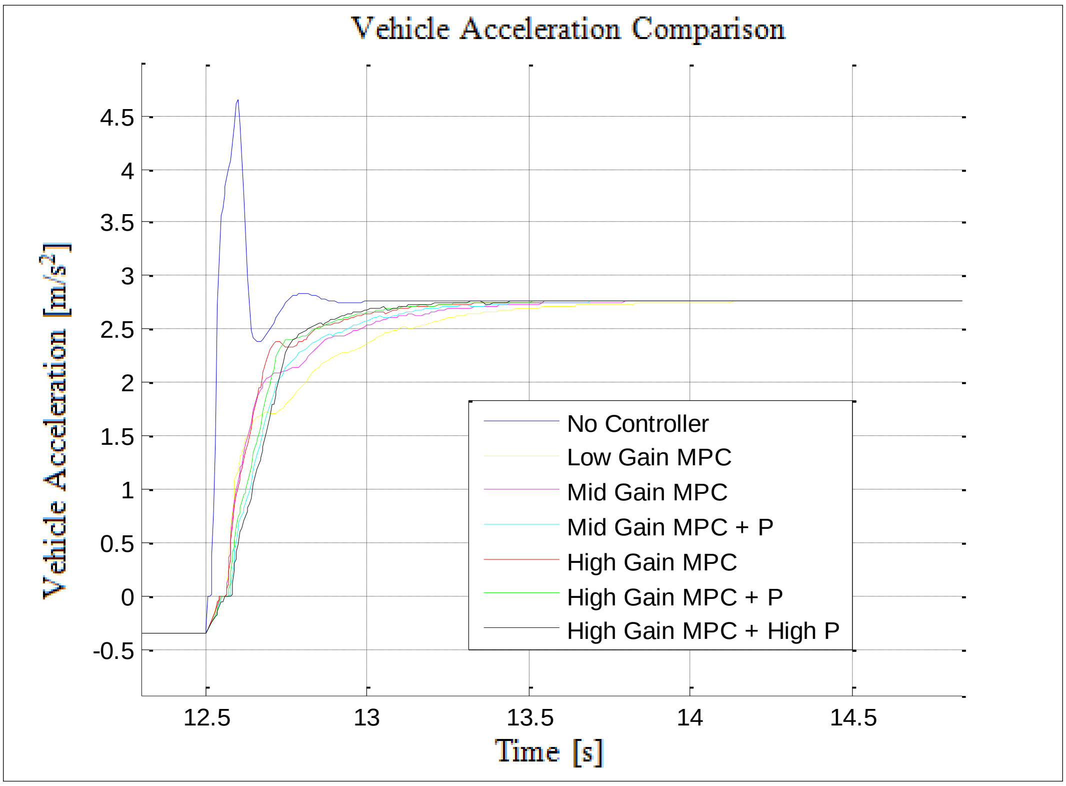

Figure D.5 : 3 mass model vehicle acceleration response for MPC parameters determination (Zoomed view at maximum load change tip-in manoeuvre) for 3rd gear.

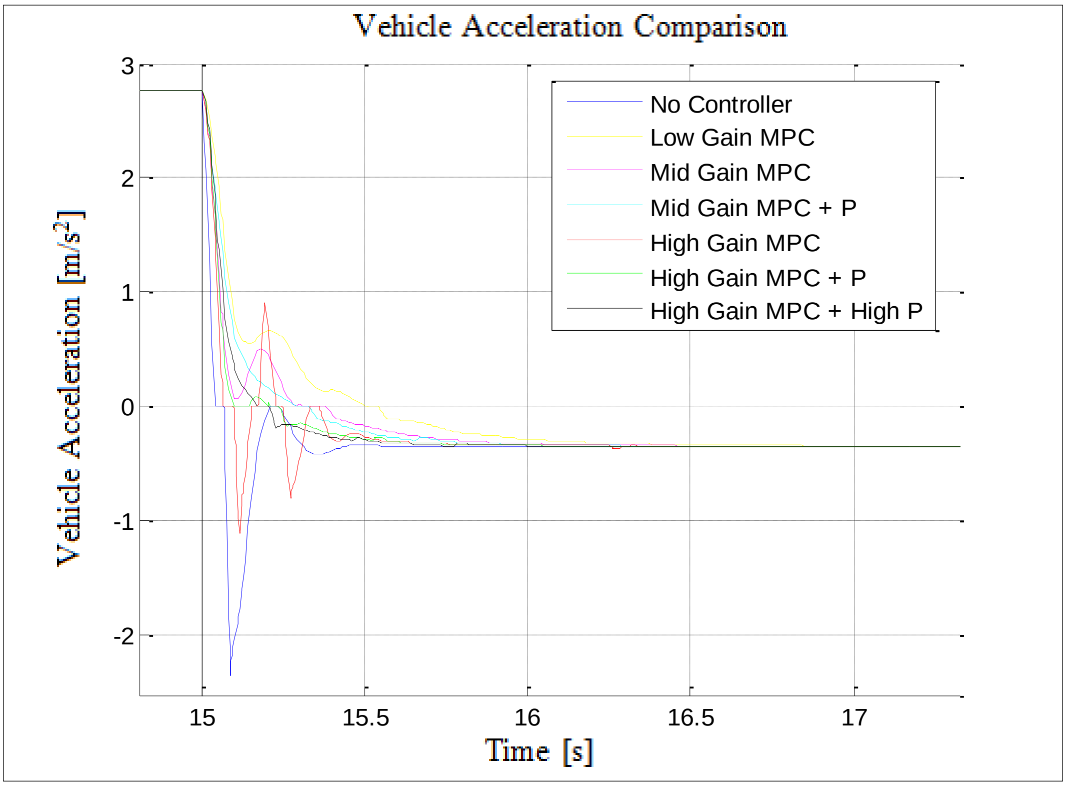

Figure D.6 : 3 mass model vehicle acceleration response for MPC parameters determination (Zoomed view at maximum load change tip-out manoeuvre) for 3rd gear.

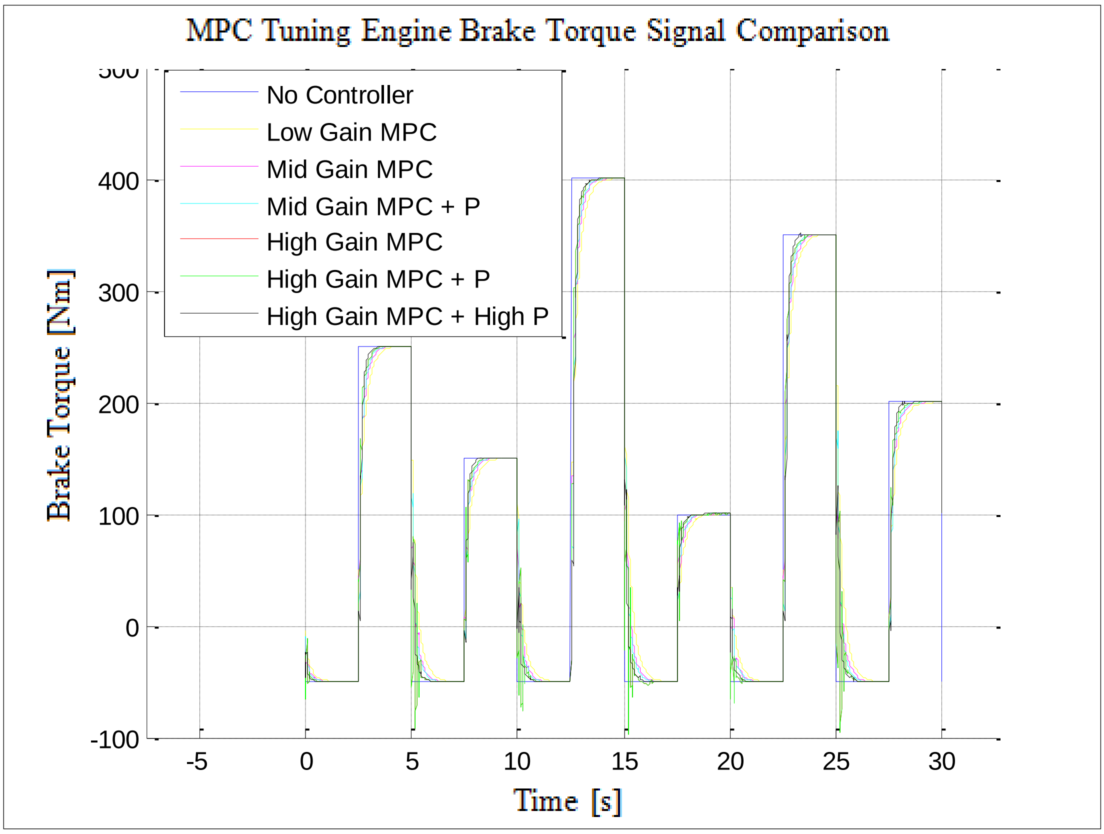

Figure D.7 : 3 mass model engine brake torque request for MPC parameters determination for 3rd gear.

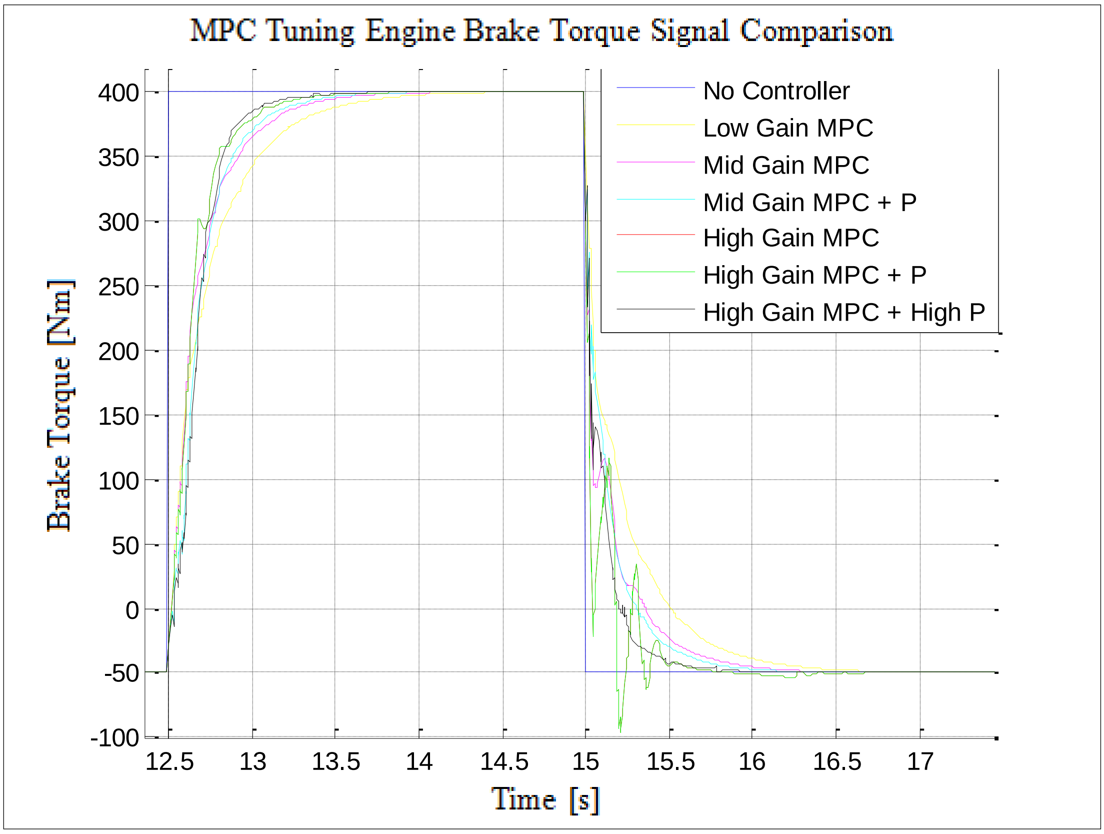

Figure D.8 : 3 mass model engine brake torque request for MPC parameters determination (Zoomed view at maximum load change manoeuvre) for 3rd gear.

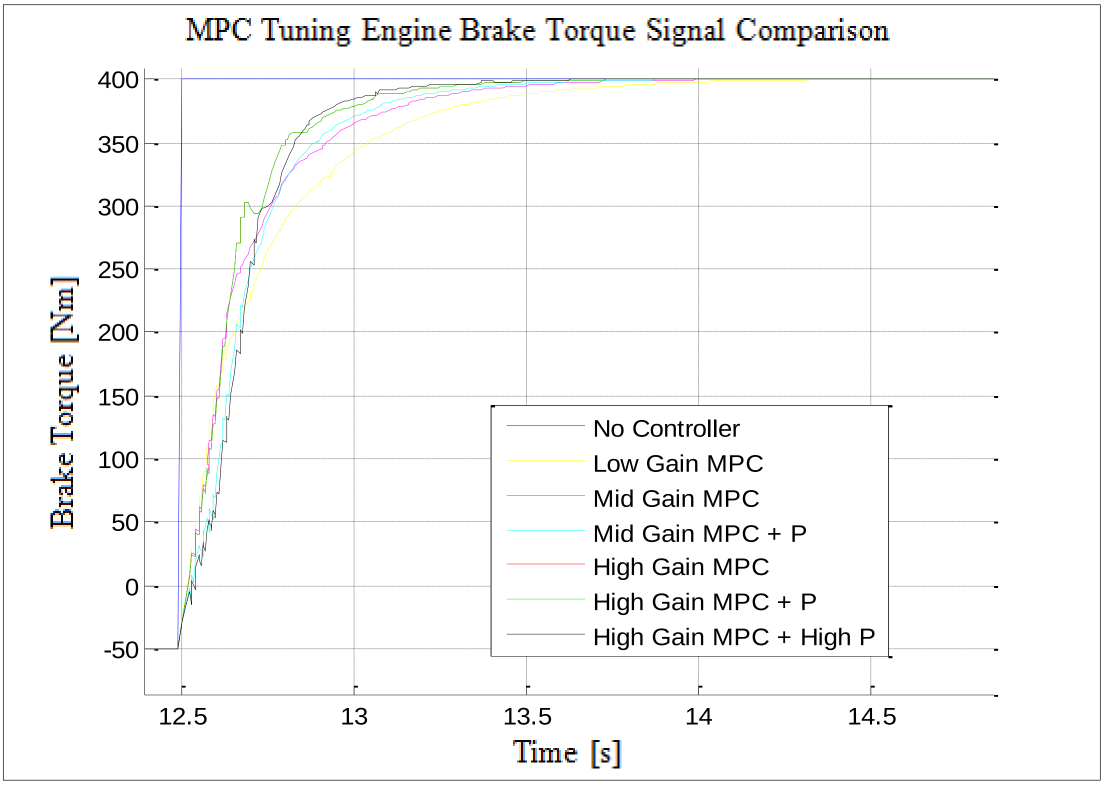

Figure D.9 : 3 mass model engine brake torque request for MPC parameters determination (Zoomed view at maximum load change tip-in manoeuvre) for 3rd gear.

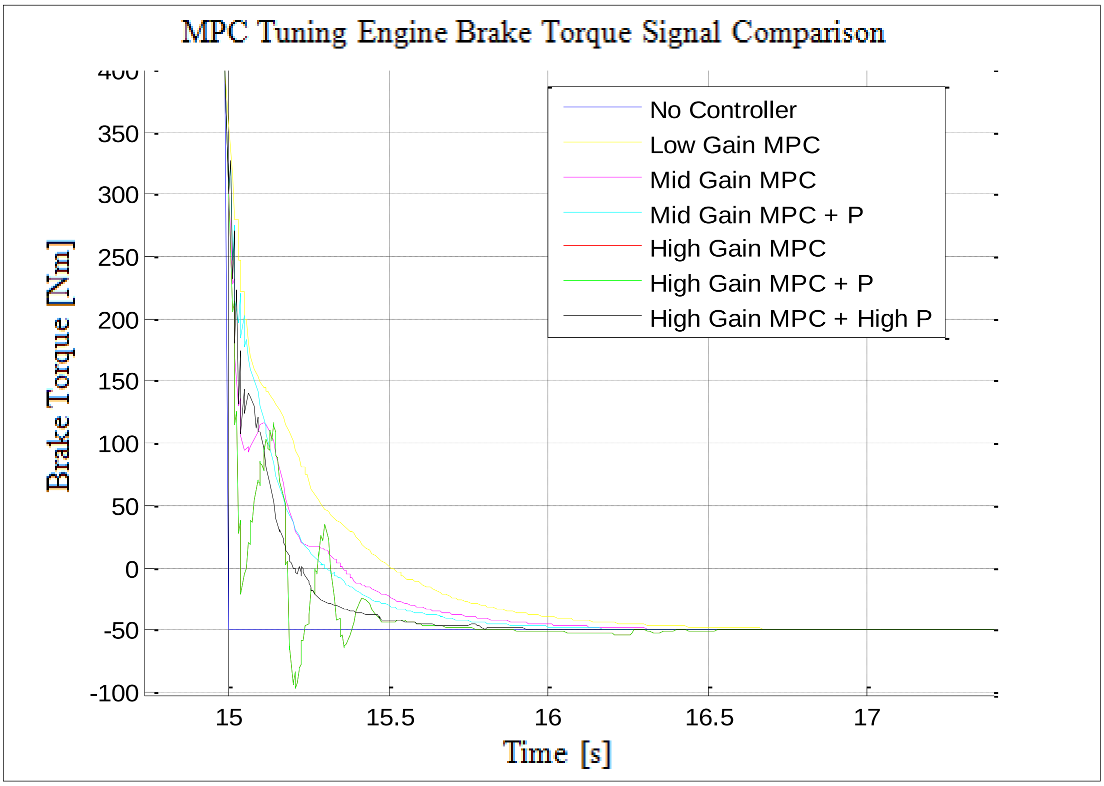

Figure D.10 : 3 mass model engine brake torque request for MPC parameters determination (Zoomed view at maximum load change tip-in manoeuvre) for 3rd gear.

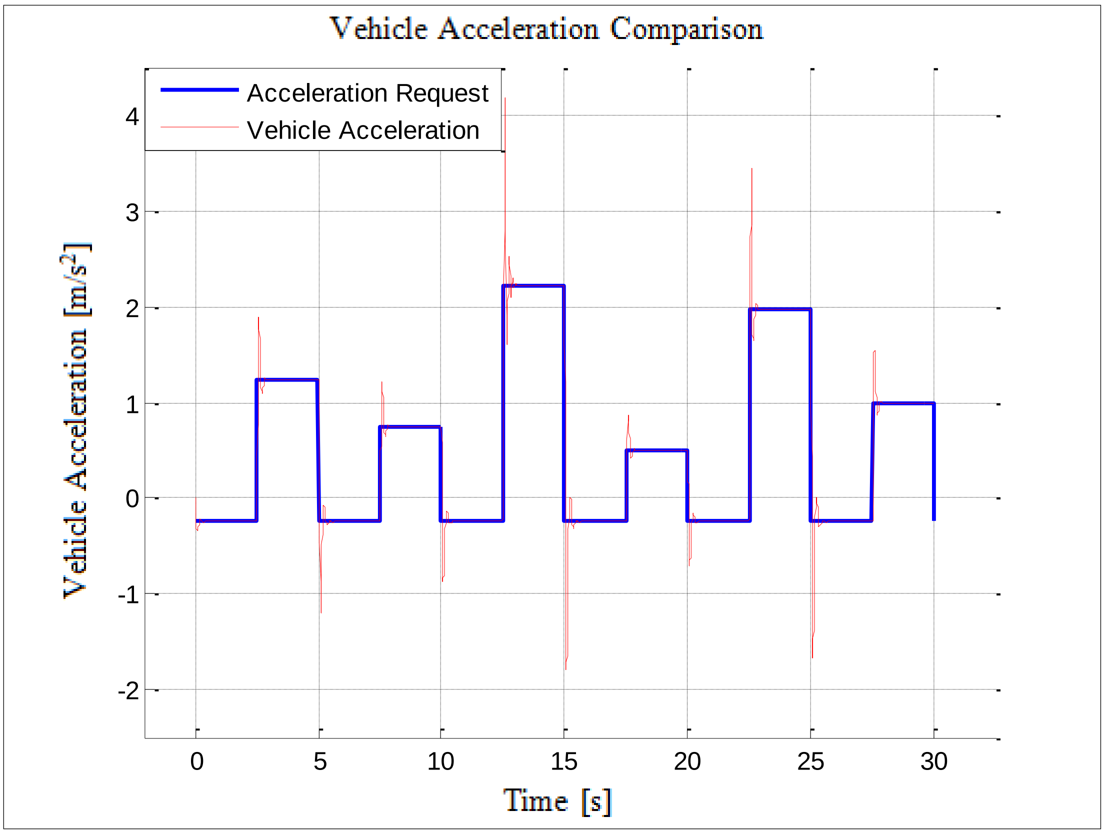

Figure D.11 : 3 mass model vehicle acceleration response for no controller case for 4th gear.

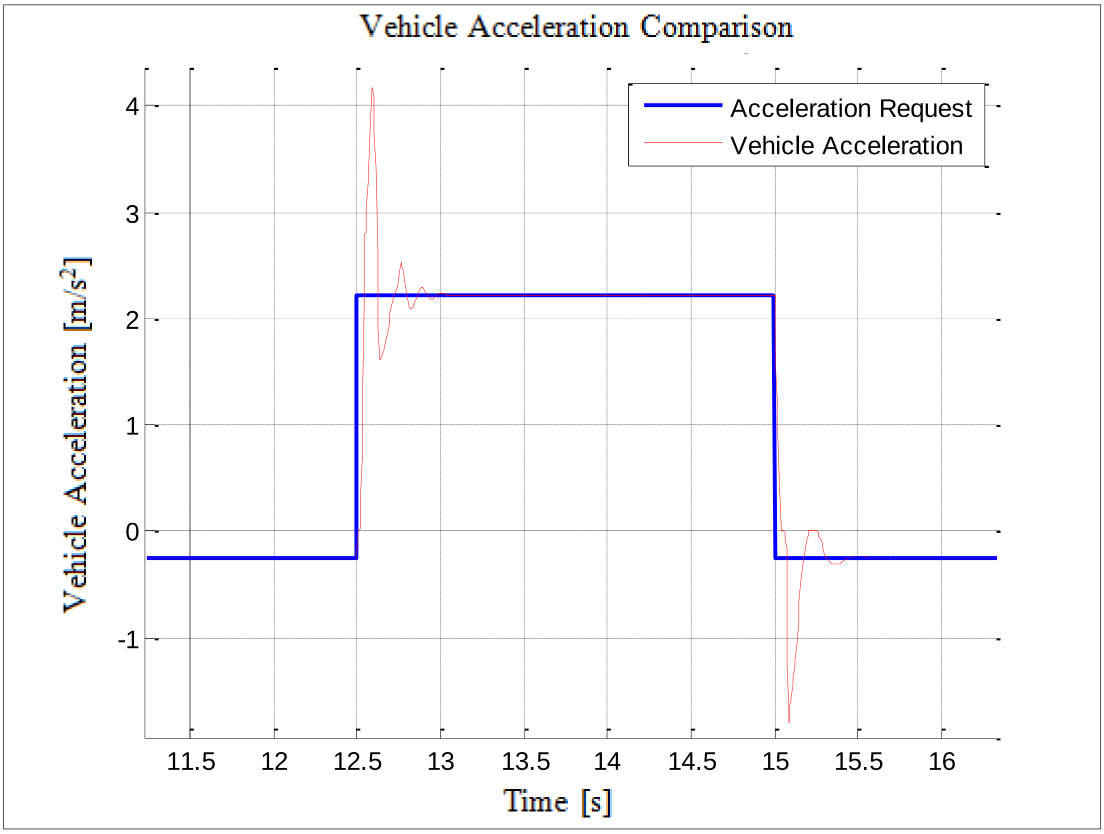

Figure D.12 : 3 mass model vehicle acceleration response for no controller case (Zoomed view at maximum load change manoeuvre) for 4th gear.

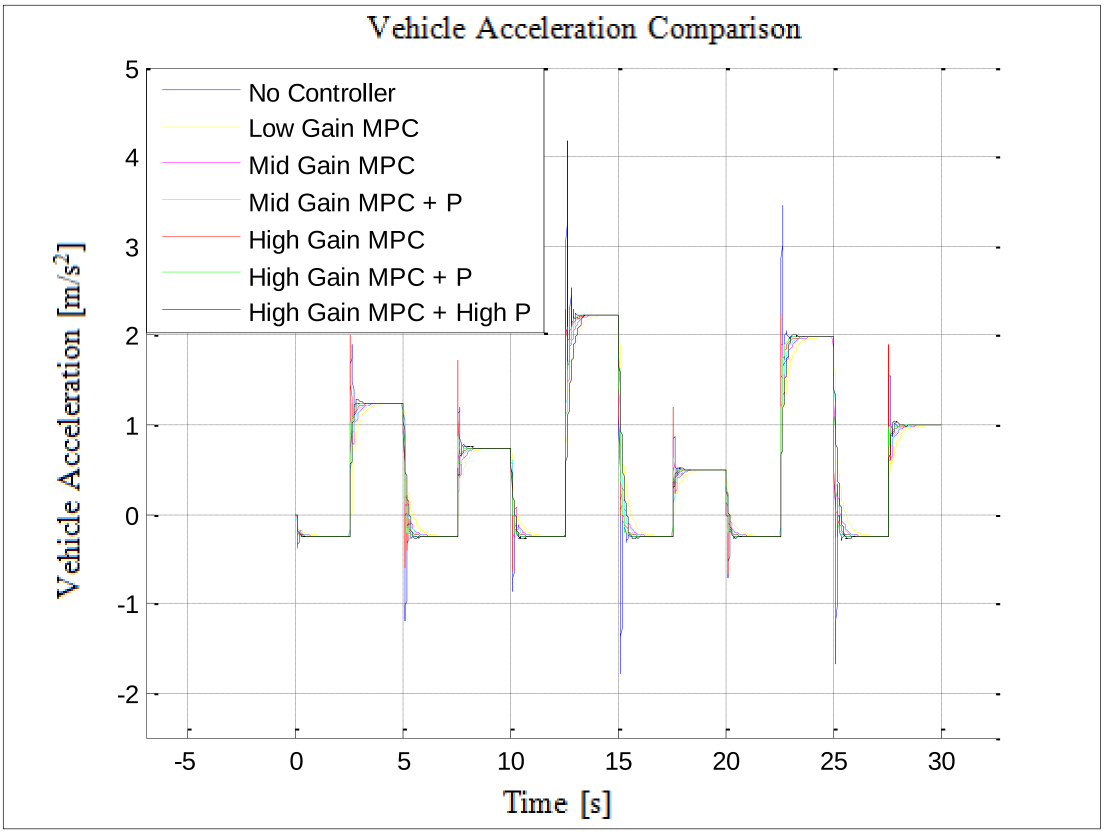

Figure D.13 : 3 mass model vehicle acceleration response for MPC parameters determination for 4th gear.

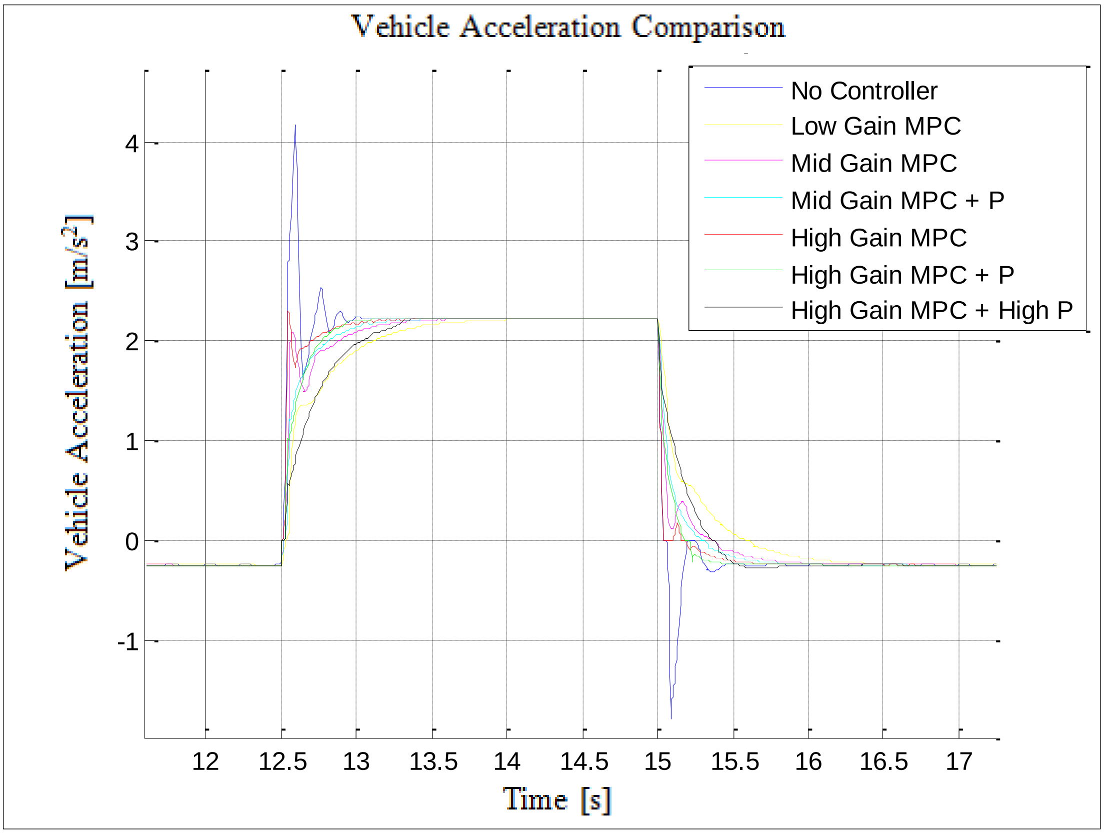

Figure D.14 : 3 mass model vehicle acceleration response for MPC parameters determination (Zoomed view at maximum load change manoeuvre) for 4th gear.

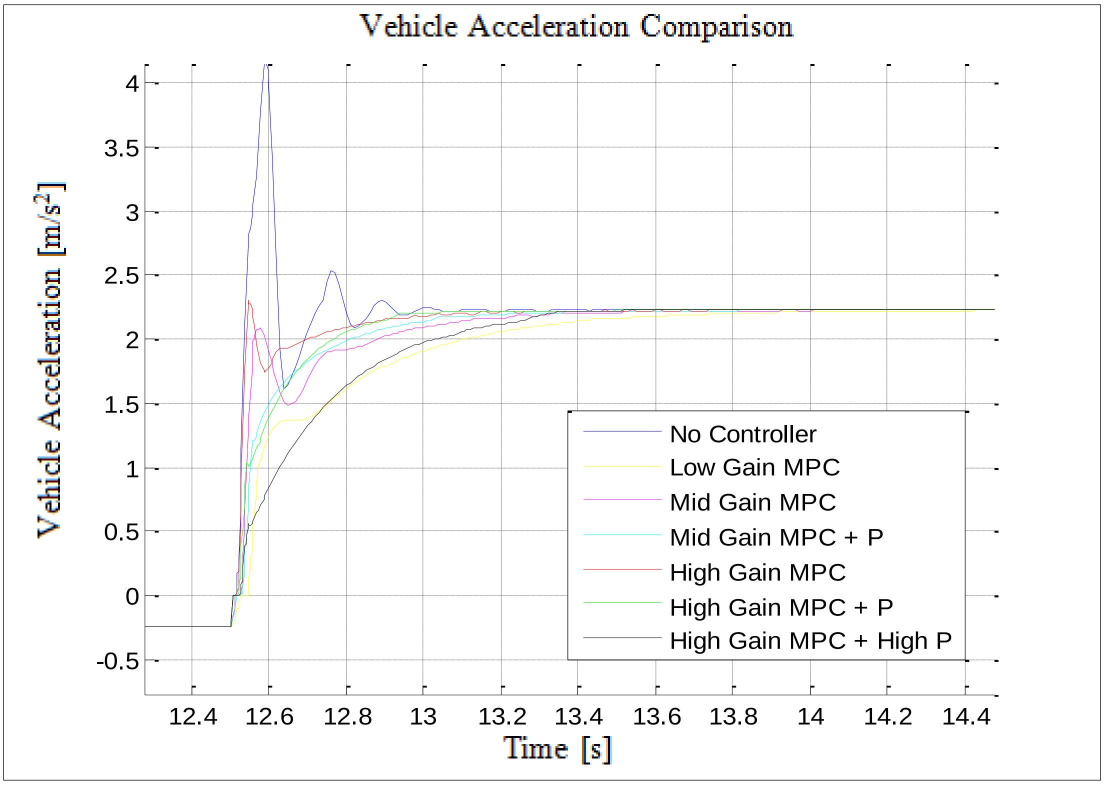

Figure D.15 : 3 mass model vehicle acceleration response for MPC parameters determination (Zoomed view at maximum load change tip-in manoeuvre) for 4th gear.

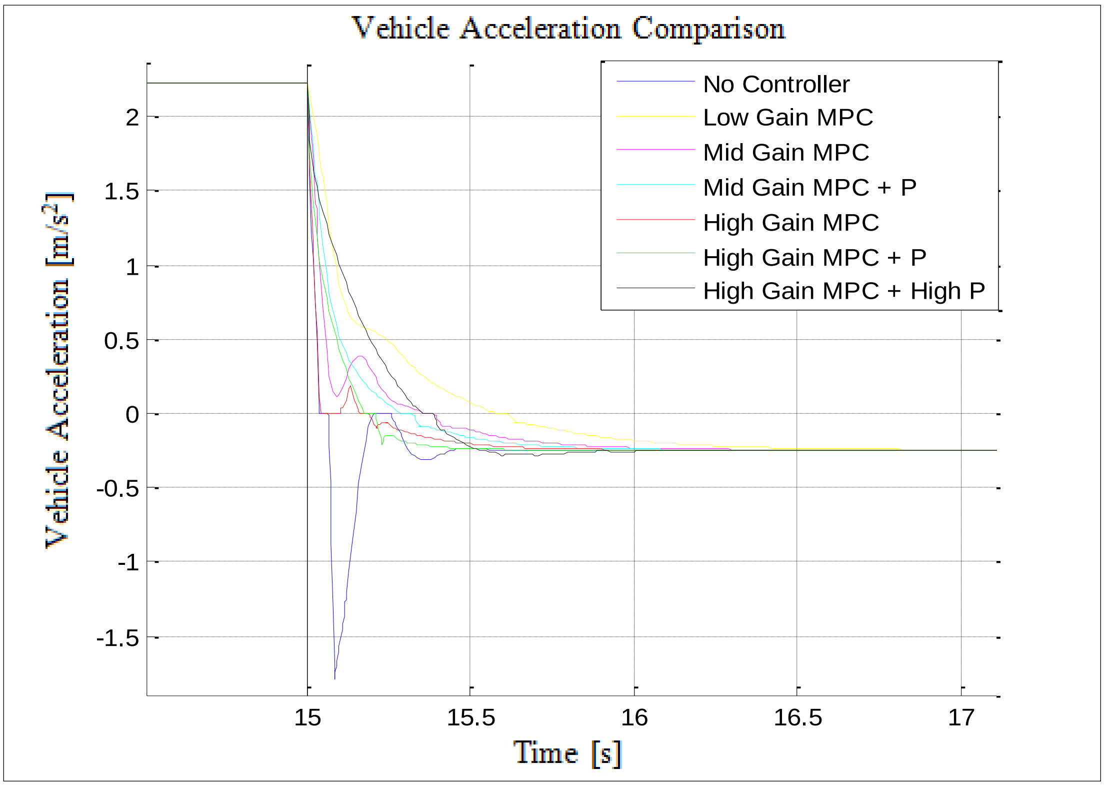

Figure D.16 : 3 mass model vehicle acceleration response for MPC parameters determination (Zoomed view at maximum load change tip-out manoeuvre) for 4th gear.

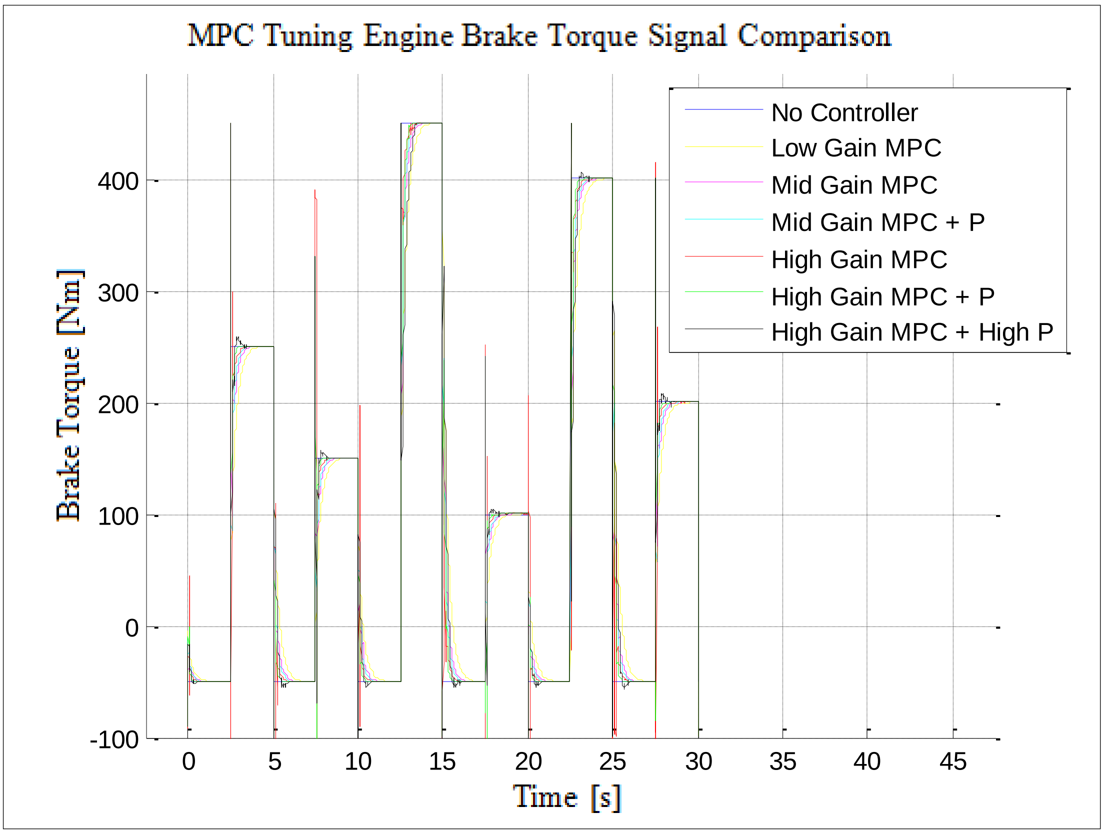

Figure D.17 : 3 mass model engine brake torque request for MPC parameters determination for 4th gear.

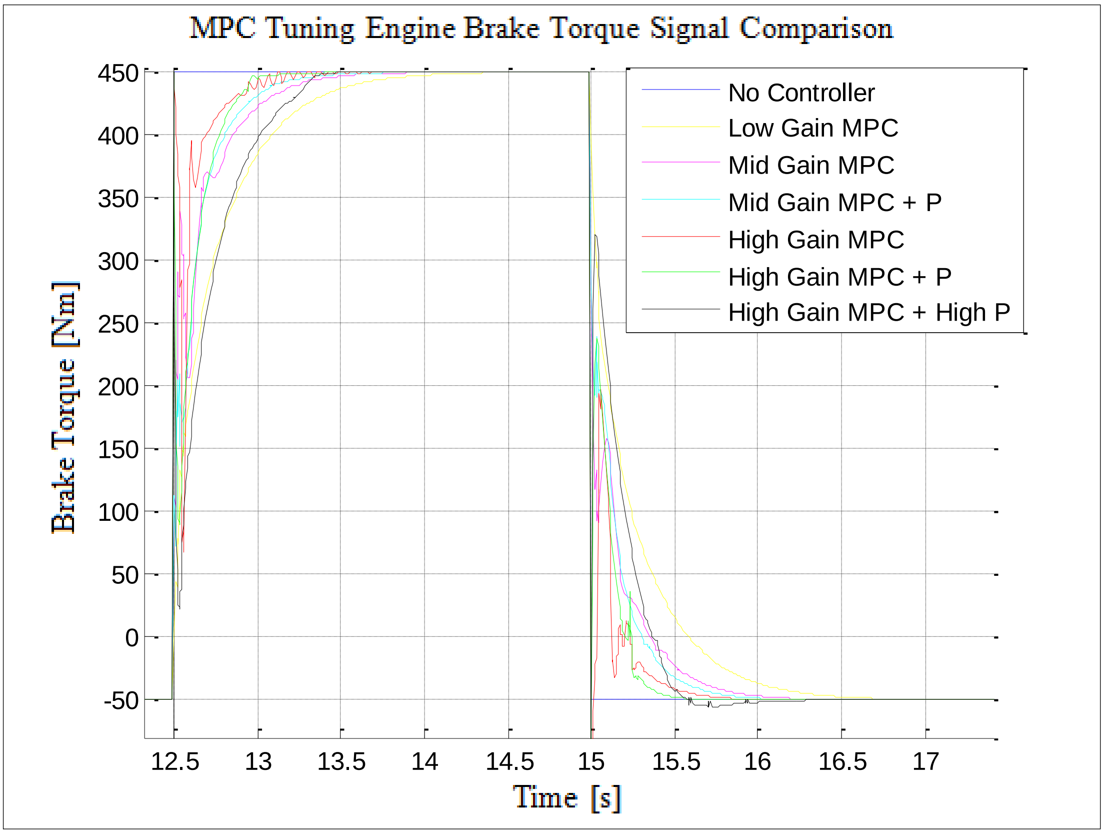

Figure D.18 : 3 mass model engine brake torque request for MPC parameters determination (Zoomed view at maximum load change manoeuvre) for 4th gear.

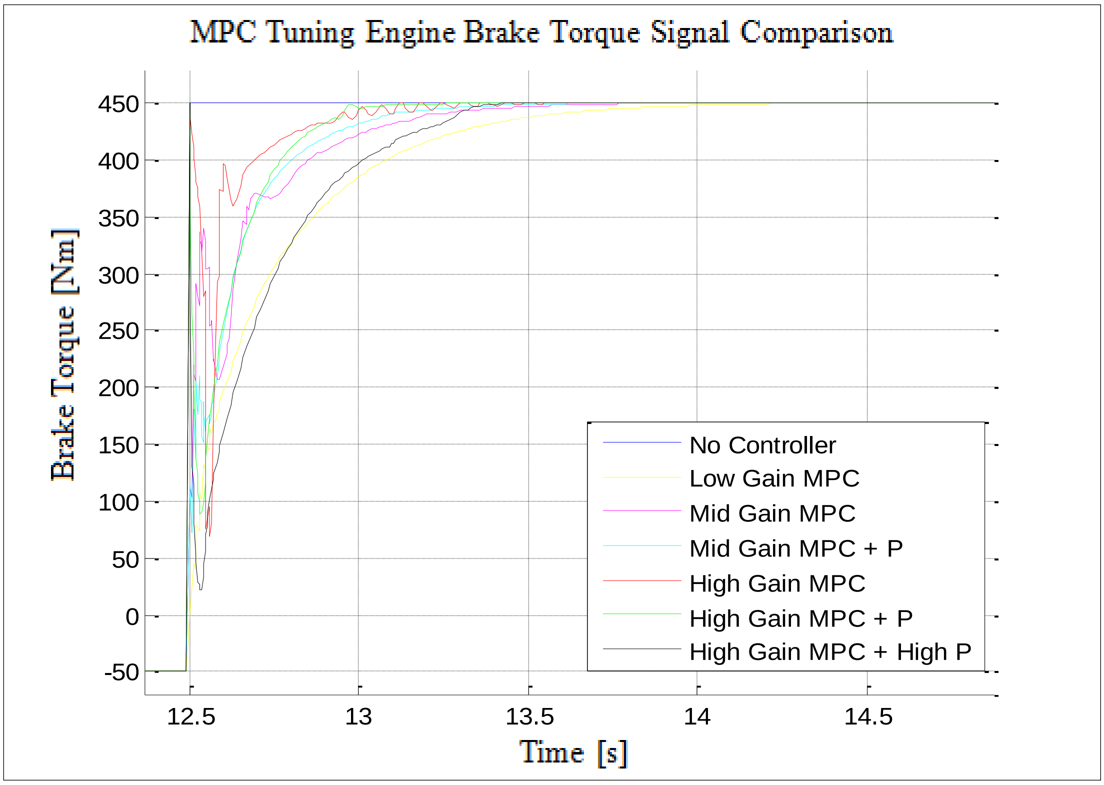

Figure D.19 : 3 mass model engine brake torque request for MPC parameters determination (Zoomed view at maximum load change tip-in manoeuvre) for 4th gear.

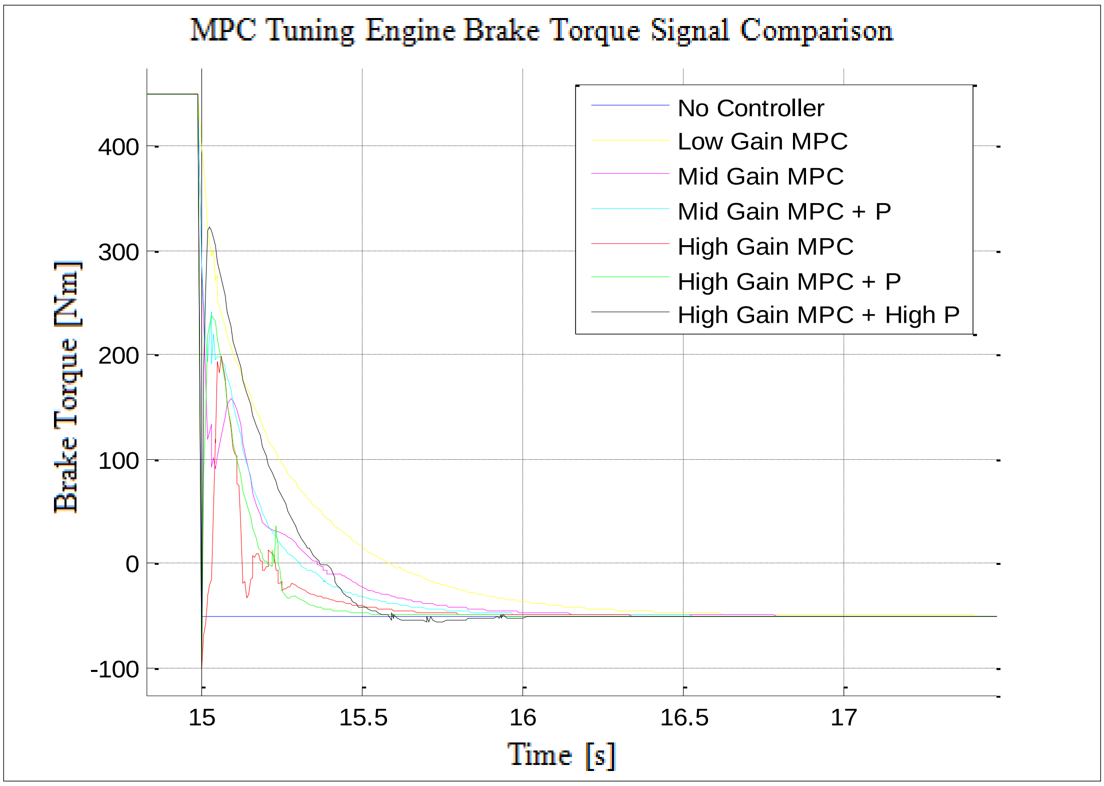

Figure D.20 : 3 mass model engine brake torque request for MPC parameters determination (Zoomed view at maximum load change tip-in manoeuvre) for 4th gear.

CURRICULUM VITAE

Name Surname **:** Murat Ötkür

Place and Date of Birth **:** Konya, 22.01.1981

E-Mail **:** otkurmur@hotmail.com

EDUCATION **:**

B.Sc. **:** 2004, İstanbul Technical University, Mechanical Engineering Faculty, Mechanical Engineering

M.Sc. **:** 2006, Koç University, Engineering Faculty, Mechanical Engineering

PUBLICATIONS, PRESENTATIONS AND PATENTS ON THE THESIS:

- **Otkur, M.,** Atabay, O., Ereke, M**.** (2013). In Cylinder Pressure Based Brake Torque Model for Diesel Engines, *Automotive and Vehicle Technologies: AVTECH '13 Conference Proceedings*, October 3-4, 2013 Yildiz Technical University.
- **Otkur, M.,** Atabay, O., Ereke, M. (2016). Model Based Predictive Torque Control of a Passenger Vehicle for Improved Driveability, *Gazi Üniversitesi Politeknik Dergisi,* Accepted on 29th April 2016.

OTHER PUBLICATIONS, PRESENTATIONS:

- **Otkur, M.,** Lazoglu , İ. (2007). Trochoidal Milling, *International Journal of Machine Tools and Manufacture*, (V. 47, I. 9, pp. 1324-1332).
- **Otkur, M.,** Lazoglu, İ**.** (2007). Tool Wear in Trochoidal Hard Milling, *4th International Conference and Exhibition on Design and Production of Machines and Dies/Molds*, İzmir.
- **Otkur, M.,** Lazoglu, İ. (2006). Trochoidal Milling, *CIRP - 2nd International Conference on High Performance Cutting*, Vancouver.